

DYNAMIC MODELING OF HUMAN CARDIOVASCULAR
SYSTEM AND AN AXIAL HEART PUMP

by
Selim Bozkurt

Submitted to the Institute of Graduate Studies in
Science and Engineering in partial fulfillment of
the requirements for the degree of
Master of Science
in
Mechanical Engineering

Yeditepe University
2009


DYNAMIC MODELING OF HUMAN CARDIOVASCULAR
SYSTEM AND AN AXIAL HEART PUMP

APPROVED BY:

Asst. Prof. Koray K. Şafak
(Thesis Supervisor)

..........

Asst. Prof. Esra Sorgüven

..........

Assoc. Prof. İsmail Lazoğlu

..........

DATE OF APPROVAL: 06/11/2009

ACKNOWLEDGMENTS

I want to thank to my advisor Koray K. Şafak for his continuous support and patience during the study. Also I would like to thank to my family for their encouragement.

ABSTRACT

DYNAMIC MODELING OF HUMAN CARDIOVASCULAR SYSTEM AND AN AXIAL HEART PUMP

Engineering applications are widely used in modern medicine with the progress of technology. Heart pumps are an example to those engineering applications which is used for treatment of cardiovascular system diseases. In this thesis a numerical human cardiovascular system model that includes heart chambers, heart valves, systemic arteries, systemic veins, pulmonary arteries and pulmonary veins was developed. Diseased human cardiovascular system model was obtained by adjusting the parameters of the healthy cardiovascular system model. Numerical models were developed for two types of heart pumps (Heart Turcica axial and Heart Turcica centrifugal). Heart Turcica axial model includes the dc motor dynamics. These models were integrated to diseased human cardiovascular system. Simulations were performed to assess the boundary operating speeds of heart pumps which causes different physiologically significant pumping states. Also pulsatility indexes were defined for pressure difference across the pump, pump flow rate and motor current. These pulsatility indexes are calculated for increasing operating speeds. Studies on control of the pressure difference across the pump and control of pump flow rate were also done.

Based on the findings it has been concluded that Heart Turcica axial and Heart Turcica centrifugal may provide sufficient pressure and flow required for the perfusion blood for the tissues.

ÖZET

İNSAN DOLAŞIM SİSTEMİ İLE EKSENEL BİR KALP POMPASININ DİNAMİK MODELLEMESİ

Teknolojinin ilerlemesi modern tıpta mühendislik uygulamalarının önemli ölçüde kullanılmasına neden olmuştur. Yapay kalp pompaları da mühendislik konularının tıptaki uygulamalarından biridir. Bu tezde geliştirilmekte olan iki farklı tipte (Heart Turcica eksenel ve Heart Turcica merkezci) yapay kalp pompasının simülasyonlarını yapmak için kalp odacıklarını, kalp kapakçıklarını, büyük dolaşım atardamarlarını, büyük dolaşım toplardamarlarını, küçük dolaşım atardamarlarını ve küçük dolaşım toplardamarlarını içeren sayısal bir insan dolaşım sistemi oluşturulmuştur. Bu modelin parametre değerleri kullanılarak hasta dolaşım sistemi modeli elde edilmiştir. Her iki yapay kalp pompası için de sayısal modeller geliştirilmiştir. Heart Turcica eksenel için geliştirilen model motor dinamiklerini de içermektedir. Hasta dolaşım sistemi modeli ve yapay kalp pompası modelleri kullanılarak insan vücudunda ortaya çıkacak fizyolojik durumlara bakılmış ve yapay kalp pompalarının hangi devir sayısı aralıklarında çalışmaları gerektiği belirlenmiştir. Ortaya çıkan sonuçlara göre pompa giriş ve çıkış arasındaki basınç farkı, pompa akışı ve motor akımı için pulsatile indeksleri tanımlanmış ve devir sayısının değişimine göre pulsatile indekslerinin değişimleri de hesaplanmıştır. Yapılan modelleme ve simülasyon çalışmalarına ek olarak Heart Turcica eksenel için pompa giriş ve çıkışında basınç farkı kontrolü ve pompa akış kontrolü çalışmaları yapılmış ve ortaya çıkan sonuçlar karşılaştırılmıştır.

Yapılan simülasyonlar sonucunda Heart Turcica eksenel ve Heart Turcica merkezci pompalarının hastalık durumunda dokulara yeterli miktarda kan pompalayabileceği görülmektedir.

TABLE OF CONTENTS

ACKNOWLEDGEMENTS	iii
ABSTRACT.....	iv
ÖZET	v
TABLE OF CONTENTS.....	vi
LIST OF FIGURES	ix
LIST OF TABLES	xxii
LIST OF SYMBOLS/ABBREVIATIONS.....	xxiv
1. INTRODUCTION	1
2. MODELING OF THE HUMAN CARDIOVASCULAR SYSTEM	6
2.1. THE HUMAN CARDIOVASCULAR SYSTEM	6
2.1.1. Cardiac Cycle.....	7
2.1.2. Vascular System.....	10
2.1.3. Heart Failure	11
2.2. MODELING OF THE HUMAN CARDIOVASCULAR SYSTEM.....	12
2.2.1. Ventricles	13
2.2.2. Atria	15
2.2.3. Heart Valves.....	16
2.2.4. Vascular System.....	16
2.2.5. Simulation Results	19
2.3. MODELING OF THE DISEASED CARDIOVASCULAR SYSTEM	24
2.3.1. Simulation Results	25
2.4. DISCUSSION	29
3. MODELLING OF THE LEFT VENTRICULAR ASSIST DEVICES.....	31
3.1. THE LEFT VENTRICULAR ASSIST DEVICES	31
3.2. MODELING OF HEART TURCICA AXIAL	32
3.3. MODELING OF HEART TURCICA CENTRIFUGAL.....	39
3.4. DISCUSSION	43
4. COMBINED MODEL OF CVS AND HEART PUMPS.....	44
4.1. PHYSIOLOGICALLY SIGNIFICANT PUMPING STATES IN LVADS	44
4.2. COMBINED MODEL OF CARDIOVASCULAR SYSTEM AND LVADS ..	45

4.3. COMBINED MODEL OF CARDIOVASCULAR SYSTEM AND HEART	
TURCICA AXIAL.....	46
4.3.1. Simulation Results at 7000 rpm Operating Speed	47
4.3.2. Simulation Results at 7565 rpm Operating Speed	50
4.3.3. Simulation Results at 8000 rpm Operating Speed	54
4.3.4. Simulation Results at 9000 rpm Operating Speed	57
4.3.5. Simulation Results at 9250 rpm Operating Speed	60
4.3.6. Simulation Results at 10000 rpm Operating Speed	64
4.3.7. Simulation Results at 11000 rpm Operating Speed	67
4.3.8. Simulation Results at 12000 rpm Operating Speed	70
4.3.9. Simulation Results at 13000 rpm Operating Speed	74
4.4. COMBINED MODEL OF CARDIOVASCULAR SYSTEM AND HEART	
TURCICA CENTRIFUGAL	82
4.4.1. Simulation Results at 1250 rpm Operating Speed	82
4.4.2. Simulation Results at 1380 rpm Operating Speed	85
4.4.3. Simulation Results at 1500 rpm Operating Speed	88
4.4.4. Simulation Results at 1638 rpm Operating Speed	90
4.4.5. Simulation Results at 1900 rpm Operating Speed	94
4.4.6. Simulation Results at 2140 rpm Operating Speed	96
4.4.7. Simulation Results at 2350 rpm Operating Speed	99
4.4.8. Simulation Results at 2542 rpm Operating Speed	102
4.4.9. Simulation Results at 2600 rpm Operating Speed	105
4.5. DISCUSSION	112
5. CONTROL STUDIES OF HEART TURCICA AXIAL.....	114
5.1. CONTROL OF PRESSURE DIFFERENCE ACROSS THE PUMP	114
5.1.1. Simulation results for 65 mmHg reference pressure difference	115
5.1.2. Simulation results for 75 mmHg reference pressure difference	119
5.1.3. Simulation results for 85 mmHg reference pressure difference	123
5.1.4. Simulation results for 95 mmHg reference pressure difference	127
5.2. CONTROL OF PUMP FLOW RATE	132
5.2.1. Simulation results for 50 ml/s reference flow rate.....	133
5.2.2. Simulation results for 60 ml/s reference flow rate.....	137
5.3. DISCUSSION	143

6. CONCLUSION AND FUTURE WORK	144
REFERENCES	146
REFERENCES NOT CITED	153

LIST OF FIGURES

Figure 2.1. The heart and circulatory system.....	7
Figure 2.2. The pressure and volume change in the left heart chamber during a cardiac cycle	8
Figure 2.3. Pressure – volume diagram of the left ventricle.....	9
Figure 2.4. Block diagram of the human cardiovascular system model.....	13
Figure 2.5. Elastance function of left ventricle (continuous line) and right ventricle (dashed line) in a cardiac cycle duration	14
Figure 2.6. Simulation results for left ventricular pressure (continuous line), left atrial pressure (chain line), the pressure of the systemic arteries (dashed line) and the pressure of the systemic veins (dotted line)	20
Figure 2.7. Simulation results for right ventricular pressure (continuous line), right atrial pressure (chain line), the pressure of the pulmonary arteries (dashed line) and the pressure of the pulmonary veins (dotted line).....	21
Figure 2.8. Volume of the heart chambers, left ventricular volume (continuous line), right ventricular volume (chain line), left atrial volume (dotted line), right atrial volume (dashed line).....	22
Figure 2.9. Flow rate of the mitral valve (dashed line), flow rate of the aortic valve (continuous line), flow rate of the systemic arteries (chain line), flow rate of the systemic veins (dotted line)	22
Figure 2.10. Flow rate of the tricuspid valve (dashed line), flow rate of the pulmonary valve (continuous line), flow rate of the pulmonary arteries (chain line),	

flow rate of the pulmonary veins (dotted line).....	23
Figure 2.11. Pressure – volume loop of the left ventricle (blue line) and right ventricle (red line)	24
Figure 2.12. Simulation results for left ventricular pressure (continuous line), left atrial pressure (chain line), the pressure of the systemic arteries (dashed line) and the pressure of the systemic veins (dotted line)	25
Figure 2.13. Simulation results for right ventricular pressure (continuous line), right atrial pressure (chain line), the pressure of the pulmonary arteries (dashed line) and the pressure of the pulmonary veins (dotted line).....	26
Figure 2.14. Volume of the heart chambers, left ventricular volume (continuous line), right ventricular volume (chain line), left atrial volume (dotted line), right atrial volume (dashed line).....	27
Figure 2.15. Flow rate of the mitral valve (dashed line), flow rate of the aortic valve (continuous line), flow rate of the systemic arteries (chain line), flow rate of the systemic veins (dotted line).....	27
Figure 2.16. Flow rate of the tricuspid valve (dashed line), flow rate of the pulmonary valve (continuous line), flow rate of the pulmonary arteries (chain line), flow rate of the pulmonary veins (dotted line).....	28
Figure 2.17. Pressure – volume loop of the diseased left ventricle (blue line) and right ventricle (red line).....	29
Figure 3.1. Pressure – flow rate diagram of the Heart Turcica axial	33
Figure 3.2. Load torque – rotation speed diagram of the Heart Turcica axial.....	36
Figure 3.3. Pressure – flow rate diagram of the Heart Turcica centrifugal	40

Figure 4.1. Block diagram of the human cardiovascular system model and heart pump	46
Figure 4.2. Pressure difference across the pump (continuous line), left atrial pressure (dotted line), left ventricular pressure (dashed line) and aortic pressure (chain line) at 7000 rpm operating speed	47
Figure 4.3. Left ventricular volume (continuous line) and left atrial volume (dashed line) at 7000 rpm pump operating speed	48
Figure 4.4. Pump flow rate (continuous line), mitral valve flow rate (chain line) and aortic valve flow rate (dashed line) at 7000 rpm operating speed.....	49
Figure 4.5. Motor current at 7000 rpm operating speed	49
Figure 4.6. Pressure difference across the pump (continuous line), left atrial pressure (dotted line), left ventricular pressure (dashed line) and aortic pressure (chain line) at 7565 rpm operating speed	50
Figure 4.7. Left ventricular pressure (continuous line), aortic pressure (dashed line) at 7565 rpm operating speed.....	51
Figure 4.8. Left ventricular volume (continuous line) and left atrial volume (dashed line) at 7565 rpm pump operating speed	52
Figure 4.9. Pump flow rate (continuous line), mitral valve flow rate (chain line) and aortic valve flow rate (dashed line) at 7565 rpm operating speed.....	52
Figure 4.10. Motor current at 7565 rpm operating speed	53
Figure 4.11. Pressure difference across the pump (continuous line), left atrial pressure (dotted line), left ventricular pressure (dashed line) and aortic pressure (chain line) at 8000 rpm operating speed	54

Figure 4.12. Left ventricular volume (continuous line) and left atrial volume (dashed line) at 8000 rpm pump operating speed	55
Figure 4.13. Pump flow rate (continuous line), mitral valve flow rate (chain line) and aortic valve flow rate (dashed line) at 8000 rpm operating speed.....	56
Figure 4.14. Motor current at 8000 rpm operating speed	56
Figure 4.15. Pressure difference across the pump (continuous line), left atrial pressure (dotted line), left ventricular pressure (dashed line) and aortic pressure (chain line) at 9000 rpm operating speed	57
Figure 4.16. Left ventricular volume (continuous line) and left atrial volume (dashed line) at 9000 rpm pump operating speed	58
Figure 4.17. Pump flow rate (continuous line), mitral valve flow rate (chain line) and aortic valve flow rate (dashed line) at 9000 rpm operating speed.....	59
Figure 4.18. Motor current at 9000 rpm operating speed	59
Figure 4.19. Pressure difference across the pump (continuous line), left atrial pressure (dotted line), left ventricular pressure (dashed line) and aortic pressure (chain line) at 8000 rpm operating speed.....	60
Figure 4.20. Left ventricular volume (continuous line) and left atrial volume (dashed line) at 9250 rpm pump operating speed	61
Figure 4.21. Pump flow rate (continuous line), mitral valve flow rate (chain line) and aortic valve flow rate (dashed line) at 9250 rpm operating speed.....	62
Figure 4.22. Pump Flow rate at 9250 rpm operating speed.....	62
Figure 4.23. Motor current at 9250 rpm operating speed	63

Figure 4.24. Pressure difference across the pump (continuous line), left atrial pressure (dotted line), left ventricular pressure (dashed line) and aortic pressure (chain line) at 10000 rpm operating speed.....	64
Figure 4.25 Left ventricular volume (continuous line) and left atrial volume (dashed line) at 10000 rpm pump operating speed	65
Figure 4.26. Pump flow rate (continuous line), mitral valve flow rate (chain line) and aortic valve flow rate (dashed line) at 10000 rpm operating speed.....	66
Figure 4.27. Motor current at 10000 rpm operating speed	66
Figure 4.28. Pressure difference across the pump (continuous line), left atrial pressure (dotted line), left ventricular pressure (dashed line) and aortic pressure (chain line) at 11000 rpm operating speed.....	68
Figure 4.29 Left ventricular volume (continuous line) and left atrial volume (dashed line) at 11000 rpm pump operating speed	68
Figure 4.30. Pump flow rate (continuous line), mitral valve flow rate (chain line) and aortic valve flow rate (dashed line) at 11000 rpm operating speed.....	69
Figure 4.31. Motor current at 11000 rpm operating speed	70
Figure 4.32. Left ventricular pressure (continuous line), left atrial pressure (chain line), pump inlet pressure (dashed line) at 12000 rpm operating speed.....	71
Figure 4.33. Pressure difference across the pump (continuous line), aortic pressure (dashed line) at 12000 rpm operating speed.....	71
Figure 4.34. Left ventricular volume (continuous line) and left atrial volume (dashed line) at 12000 rpm pump operating speed	72

Figure 4.35. Pump flow rate (continuous line), mitral valve flow rate (chain line) and aortic valve flow rate (dashed line) at 12000 rpm operating speed.....	73
Figure 4.36. Motor current at 12000 rpm operating speed	73
Figure 4.37. Left ventricular pressure (continuous line) and left atrial pressure (dashed line) at 13000 rpm operating speed.....	74
Figure 4.38. Pump inlet pressure at 13000 rpm pump operating speed.....	75
Figure 4.39. Pressure difference across the pump (continuous line), aortic pressure (dashed line) at 13000 rpm operating speed.....	76
Figure 4.40. Left ventricular volume (continuous line) and left atrial volume (dashed line) at 13000 rpm pump operating speed	76
Figure 4.41. Pump flow rate (continuous line), mitral valve flow rate (chain line) and aortic valve flow rate (dashed line) at 13000 rpm operating speed.....	77
Figure 4.42. Motor current at 13000 rpm operating speed	78
Figure 4.43. Left ventricular pressure – volume loops from 7000 rpm to 13000 rpm with 1000 rpm increase	79
Figure 4.44. Heart Turcica axial pressure – flow rate diagram from 7000 rpm to 13000 rpm with 1000 rpm increments.....	80
Figure 4.45. Heart Turcica axial pressure pulsatility index from 7000 rpm to 13000 rpm with 1000 rpm increments.....	80
Figure 4.46. Heart Turcica axial flow pulsatility index from 7000 rpm to 13000 rpm with 1000 rpm increments	81

Figure 4.47. Heart Turcica axial current pulsatility index from 7000 rpm to 13000 rpm with 1000 rpm increments.....	81
Figure 4.48. Pressure difference across the pump (continuous line), left atrial pressure (dotted line), left ventricular pressure (dashed line) and aortic pressure (chain line) at 1250 rpm operating speed.....	83
Figure 4.49. Left ventricular volume (continuous line) and left atrial volume (dashed line) at 1250 rpm pump operating speed	83
Figure 4.50. Pump flow rate (continuous line), mitral valve flow rate (chain line) and aortic valve flow rate (dashed line) at 1250 rpm operating speed.....	84
Figure 4.51. Pressure difference across the pump (continuous line), left atrial pressure (dotted line), left ventricular pressure (dashed line) and aortic pressure (chain line) at 1380 rpm operating speed.....	85
Figure 4.52 Left ventricular volume (continuous line) and left atrial volume (dashed line) at 1380 rpm pump operating speed	86
Figure 4.53. Pump flow rate (continuous line), mitral valve flow rate (chain line) and aortic valve flow rate (dashed line) at 1380 rpm operating speed.....	87
Figure 4.54. Pump flow rate at 1380 rpm operating speed.....	87
Figure 4.55. Pressure difference across the pump (continuous line), left atrial pressure (dotted line), left ventricular pressure (dashed line) and aortic pressure (chain line) at 1500 rpm operating speed.....	89
Figure 4.56. Left ventricular volume (continuous line) and left atrial volume (dashed line) at 1500 rpm pump operating speed	89
Figure 4.57. Pump flow rate (continuous line), mitral valve flow rate (chain line) and	

aortic valve flow rate (dashed line) at 1500 rpm operating speed.....	90
Figure 4.58. Pressure difference across the pump (continuous line), left atrial pressure (dotted line), left ventricular pressure (dashed line) and aortic pressure (chain line) at 1638 rpm operating speed.....	91
Figure 4.59. Left ventricular pressure (continuous line), aortic pressure (dashed line) at 1638 rpm operating speed.....	92
Figure 4.60. Left ventricular volume (continuous line) and left atrial volume (dashed line) at 1638 rpm pump operating speed	92
Figure 4.61. Pump flow rate (continuous line), mitral valve flow rate (chain line) and aortic valve flow rate (dashed line) at 1638 rpm operating speed.....	93
Figure 4.62. Pressure difference across the pump (continuous line), left atrial pressure (dotted line), left ventricular pressure (dashed line) and aortic pressure (chain line) at 1900 rpm operating speed.....	94
Figure 4.63 Left ventricular volume (continuous line) and left atrial volume (dashed line) at 1900 rpm pump operating speed	95
Figure 4.64. Pump flow rate (continuous line), mitral valve flow rate (chain line) and aortic valve flow rate (dashed line) at 1900 rpm operating speed.....	96
Figure 4.65. Pressure difference across the pump (continuous line), left atrial pressure (dotted line), left ventricular pressure (dashed line) and aortic pressure (chain line) at 2140 rpm operating speed.....	97
Figure 4.66. Left ventricular volume (continuous line) and left atrial volume (dashed line) at 2140 rpm pump operating speed	98
Figure 4.67. Pump flow rate (continuous line), mitral valve flow rate (chain line) and	

aortic valve flow rate (dashed line) at 2140 rpm operating speed.....	98
Figure 4.68. Pressure difference across the pump (continuous line), left atrial pressure (dotted line), left ventricular pressure (dashed line) and aortic pressure (chain line) at 2350 rpm operating speed.....	100
Figure 4.69 Left ventricular volume (continuous line) and left atrial volume (dashed line) at 2350 rpm pump operating speed	100
Figure 4.70. Pump flow rate (continuous line), mitral valve flow rate (chain line) and aortic valve flow rate (dashed line) at 2350 rpm operating speed.....	101
Figure 4.71. Pressure difference across the pump (continuous line), left atrial pressure (dotted line), left ventricular pressure (dashed line) and aortic pressure (chain line) at 2542 rpm operating speed.....	102
Figure 4.72. Left ventricular volume (continuous line) and left atrial volume (dashed line) at 2542 rpm pump operating speed	103
Figure 4.73. Pump flow rate (continuous line), mitral valve flow rate (chain line) and aortic valve flow rate (dashed line) at 2542 rpm operating speed.....	104
Figure 4.77. Left ventricular pressure (continuous line), left atrial pressure (dashed line) at 2600 rpm operating speed	105
Figure 4.78. Pump inlet pressure at 2600 rpm pump operating speed.....	106
Figure 4.79. Pressure difference across the pump (continuous line), aortic pressure (dashed line) at 2600 rpm operating speed.....	106
Figure 4.80. Left ventricular volume (continuous line) and left atrial volume (dashed line) at 2600 rpm pump operating speed	107

Figure 4.81. Pump flow rate (continuous line), mitral valve flow rate (chain line) and aortic valve flow rate (dashed line) at 2600 rpm operating speed.....	108
Figure 4.82. Left ventricular pressure – volume loops from 1250 rpm to 2600 rpm	109
Figure 4.83. Heart Turcica centrifugal V13 pressure–flow rate diagram from 1250 rpm to 2600 rpm	110
Figure 4.84. Heart Turcica centrifugal V13 pressure pulsatility index from 1250 rpm to 2600 rpm.....	111
Figure 4.85. Heart Turcica centrifugal V13 flow pulsatility index from 1250 rpm to 2600 rpm.....	111
Figure 5.1. Block diagram of the pressure difference control across Heart Turcica axial	114
Figure 5.2. Pressure difference across the pump (continuous line), left atrial pressure (dotted line), left ventricular pressure (dashed line) and aortic pressure (chain line) for 65 mmHg reference pressure difference value....	115
Figure 5.3. Left ventricular volume (continuous line), left atrial volume (dashed line) for 65 mmHg reference pressure difference value	116
Figure 5.4. Pump flow rate (continuous line), mitral valve flow rate (chain line) and aortic valve flow rate (dashed line) for 65 mmHg reference pressure difference value	117
Figure 5.5. Rotation speed for 65 mmHg reference pressure difference value	117
Figure 5.6. Motor current for 65 mmHg reference pressure difference value.....	118
Figure 5.7. Pressure difference across the pump (continuous line), left atrial	

pressure (dotted line), left ventricular pressure (dashed line) and aortic pressure (chain line) for 75 mmHg reference pressure difference value....	119
Figure 5.8. Left ventricular volume (continuous line), left atrial volume (dashed line) for 75 mmHg reference pressure difference value	120
Figure 5.9. Pump flow rate (continuous line), mitral valve flow rate (chain line) and aortic valve flow rate (dashed line) for 75 mmHg reference pressure difference value	121
Figure 5.10. Rotation speed for 75 mmHg reference pressure difference value	121
Figure 5.11. Motor current for 75 mmHg reference pressure difference value.....	122
Figure 5.12. Pressure difference across the pump (continuous line), left atrial pressure (dotted line), left ventricular pressure (dashed line) and aortic pressure (chain line) for 85 mmHg reference pressure value.....	123
Figure 5.13. Left ventricular volume (continuous line), left atrial volume (dashed line) for 85 mmHg reference pressure difference value	124
Figure 5.14. Pump flow rate (continuous line), mitral valve flow rate (chain line) and aortic valve flow rate (dashed line) for 85 mmHg reference pressure difference value	125
Figure 5.15. Rotation speed for 85 mmHg reference pressure difference value	125
Figure 5.16. Motor current for 85 mmHg reference pressure difference value.....	126
Figure 5.17. Pressure difference across the pump (continuous line), left atrial pressure (dotted line), left ventricular pressure (dashed line) and aortic pressure (chain line) for 95 mmHg reference pressure difference value....	127

Figure 5.18. Left ventricular volume (continuous line), left atrial volume (dashed line) for 95 mmHg reference pressure difference value	128
Figure 5.19. Pump flow rate (continuous line), mitral valve flow rate (chain line) and aortic valve flow rate (dashed line) for 95 mmHg reference pressure difference value	129
Figure 5.20. Rotation speed for 95 mmHg reference pressure difference value	129
Figure 5.21. Motor current for 95 mmHg reference pressure difference value.....	130
Figure 5.22. Left ventricular pressure – volume loops from 65 mmHg to 95 mmHg with 10 mmHg increments	131
Figure 5.23. Heart Turcica Axial pressure–flow rate diagram from 65 mmHg to 95 mmHg reference pressure difference with 10 mmHg increments.....	132
Figure 5.24. Block diagram of the flow rate control through Heart Turcica Axial.....	133
Figure 5.25. Pressure difference across the pump (continuous line), left atrial pressure (dotted line), left ventricular pressure (dashed line) and aortic pressure (chain line) for 50 ml/s reference pump flow rate value	134
Figure 5.26. Left ventricular volume (continuous line), left atrial volume (dashed line) for 50 ml/s reference pump flow rate value	135
Figure 5.27. Pump flow rate (continuous line), mitral valve flow rate (chain line) and aortic valve flow rate (dashed line) for 50 ml/s reference pump flow rate value	135
Figure 5.28. Rotation speed for 50 ml reference pump flow rate value	136
Figure 5.29. Motor current 50 ml/s reference pump flow rate value.....	137

Figure 5.30. Pressure difference across the pump (continuous line), left atrial pressure (dotted line), left ventricular pressure (dashed line) and aortic pressure (chain line) for 60 ml/s ml reference pump flow rate value.....	138
Figure 5.31. Left ventricular volume (continuous line), left atrial volume (dashed line) for 60 ml/s reference pump flow rate value	139
Figure 5.32. Pump flow rate (continuous line), mitral valve flow rate (chain line) and aortic valve flow rate (dashed line) for 60 ml/s reference pump flow rate value	139
Figure 5.33. Rotation speed for 60 ml reference pump flow rate value	140
Figure 5.34. Motor current for 60 ml/s reference pump flow rate value	141
Figure 5.35. Left ventricular pressure–volume loops of 50 ml reference pump flow rate and 60 ml reference pump flow rate.....	142
Figure 5.36. Heart Turcica Axial pressure–flow rate diagram of 50 ml reference pump flow rate and 60 ml reference pump flow rate	143

LIST OF TABLES

Table 2.1. The analogy between electrical systems and fluid systems.....	12
Table 2.2. The parameters used in numerical human cardiovascular system model.....	18
Table 2.3. The parameters used in ventricular modeling.....	19
Table 2.4. Simulation results of human cardiovascular system model.....	24
Table 2.5. Simulation results of diseased human cardiovascular system model	30
Table 3.1. The least square fit data and errors	35
Table 3.2. The least square fit data and errors	38
Table 3.3. Values of the parameters in Eq. 3.2 and Eq. 3.3.....	39
Table 3.4. The least square fit data and errors	42
Table 4.1. Simulation results for 7000 rpm operating speed	50
Table 4.2. Simulation results for 7565 rpm operating speed	53
Table 4.3. Simulation results for 8000 rpm operating speed	57
Table 4.4. Simulation results for 9000 rpm operating speed	60
Table 4.5. Simulation results for 9250 rpm operating speed	63
Table 4.6. Simulation results for 10000 rpm operating speed	67
Table 4.7. Simulation results for 11000 rpm operating speed	70
Table 4.8. Simulation results for 12000 rpm operating speed	74
Table 4.9. Simulation results for 13000 rpm operating speed	78

Table 4.10. Simulation results for 1250 rpm operating speed	84
Table 4.11. Simulation results for 1380 rpm operating speed	88
Table 4.12. Simulation results for 1500 rpm operating speed	90
Table 4.13. Simulation results for 1638 rpm operating speed	93
Table 4.14. Simulation results for 1900 rpm operating speed	97
Table 4.15. Simulation results for 2140 rpm operating speed	99
Table 4.16. Simulation results for 2350 rpm operating speed	101
Table 4.17. Simulation results for 2542 rpm operating speed	104
Table 4.18. Simulation results for 2600 rpm operating speed	108
Table 5.1. Simulation results for 65 mmHg reference pressure difference value	118
Table 5.2. Simulation results for 75 mmHg reference pressure difference value	122
Table 5.3. Simulation results for 85 mmHg reference pressure difference value	126
Table 5.4. Simulation results for 95 mmHg reference pressure difference value	130
Table 5.6. Simulation results for 50 ml/s reference pump flow rate value.....	137
Table 5.7. Simulation results for 60 ml/s reference pump flow rate value.....	141

LIST OF SYMBOLS / ABBREVIATIONS

<i>AV</i>	Aortic Valve
<i>BP</i>	Beat Period
<i>BSA</i>	Body Surface Area
<i>C</i>	Compliance, Capacitance
<i>C₀</i>	Static Friction Torque
<i>C₁</i>	Empirically Determined Coefficient
<i>C₂</i>	Empirically Determined Coefficient
<i>CI</i>	Cardiac Index
<i>CI</i>	Current Index
<i>C_{max}</i>	Maximum Motor Current
<i>C_{min}</i>	Minimum Motor Current
<i>CO</i>	Cardiac Output
<i>C_{pa}</i>	Pulmonary Arterial Compliance
<i>C_{pv}</i>	Pulmonary Veins Compliance
<i>C_{sa}</i>	Systemic Arterial Compliance
<i>C_{sv}</i>	Systemic Veins Compliance
<i>C_v</i>	Viscous damping Factor
<i>DP</i>	Diastolic Pressure
<i>e</i>	Activation Function
<i>E</i>	Elastance
<i>E_{dias}</i>	Diastolic Elastance
<i>EDV</i>	End Diastolic Volume
<i>E_f</i>	Ejection Fraction
<i>E_{lv}</i>	Left Ventricular Elastance
<i>E_{rv}</i>	Right Ventricular Elastance
<i>ESV</i>	End Systolic Volume
<i>E_{sys}</i>	Systolic Elastance
<i>HR</i>	Heart Rate
<i>I</i>	Current

J	Rotor Inertia
K_1	Empirically Determined Coefficient
K_2	Empirically Determined Coefficient
K_3	Empirically Determined Coefficient
k_m	Torque Constant
L	Inertance, Inductance
L_1	Empirically Determined Coefficient
L_2	Empirically Determined Coefficient
L_3	Empirically Determined Coefficient
L_{pa}	Pulmonary Arterial Inertance
L_{sa}	Systemic Arterial Inertance
MAP	Mean Aortic Pressure
PI	Pressure Index
P_{lv}	Left Ventricular Pressure
P_{pa}	Pulmonary Arterial Pressure
P_{pv}	Pulmonary Veins Pressure
P_{rv}	Right Ventricular Pressure
P_{sa}	Systemic Arterial Pressure
P_{sv}	Systemic Veins Pressure
P_{th}	Threshold Pressure Value
Q	Flow Rate
q	Electrical Charge
Q_{ao}	Aortic Valve Flow Rate
QI	Flow Rate Index
$Q_{lv,i}$	Left ventricle inlet flow rate
$Q_{lv,o}$	Left ventricle outlet flow rate
Q_{max}	Maximum Pump Flow Rate
Q_{mi}	Mitral Valve Flow Rate
Q_{min}	Minimum Pump Flow Rate
Q_p	Pump Flow Rate
Q_{pa}	Pulmonary Arterial Flow Rate
Q_{pu}	Pulmonary Valve Flow Rate
Q_{pv}	Pulmonary Veins Flow Rate

$Q_{rv,i}$	Right ventricle inlet flow rate
$Q_{rv,o}$	Right ventricle outlet flow rate
Q_{sa}	Systemic Arterial Flow Rate
Q_{sv}	Systemic Veins Flow Rate
Q_{ti}	Tricuspid Valve Flow Rate
R	Fluid Resistance, Electrical resistance
R_{ao}	Aortic Valve Flow Resistance
R_{mi}	Mitral Valve Flow Resistance
R_{pa}	Pulmonary Arterial Resistance
R_{po}	Pulmonary Valve Flow Resistance
R_{pv}	Pulmonary Veins Resistance
R_{sa}	Systemic Arterial Resistance
R_{suc}	Suction Resistance
R_{sv}	Systemic Veins Resistance
R_{ti}	Tricuspid Valve Flow Resistance
SP	Systolic Pressure
SV	Stroke Volume
t	Time
T_1	Systolic Peak Time
T_2	End of Diastolic Time
T_e	Motor Torque
T_p	Load Torque
V	Volume
V_{la}	Left Atrial Volume
V_{lv}	Left Ventricular Volume
$V_{lv,0}$	Left Ventricular Zero Pressure Filling Volume
V_{ra}	Right Atrial Volume
V_{rv}	Right Ventricular Volume
$V_{rv,0}$	Right Ventricular Zero Pressure Filling Volume
V_{tot}	Total Blood Volume
V_u	Unstressed Blood Volume
ΔP	Pressure Difference

ΔP_{max}	Maximum Pressure Difference Across the Pump
ΔP_{min}	Minimum Pressure Difference Across the Pump
ω	Rotation Speed
AV	Aortic Valve
EDPVR	End Diastolic Pressure Volume Relationship
ESPVR	End Systolic Pressure Volume Relationship
LA	Left Atrium
LV	Left Ventricle
MV	Mitral Valve
PV	Pulmonary Valve
RA	Right Atrium
RV	Right Ventricle
TV	Tricuspid Valve

1. INTRODUCTION

Congestive heart failure is a serious health problem that affects many people in the world [1]. For example in USA prevalence of the congestive heart failure is 4.8 million people every year. This is the 1.76 per cent of population. There are several pharmacological treatment methods to treat congestive heart failure. If these methods fail, mechanical devices called ventricular assist devices (heart pumps) are used to support heart [1, 2]. However, heart pumps cannot be used as a treatment method. Heart pumps support the diseased heart until a heart is transplanted to the patient.

Heart pumps can be classified as pulsatile pumps and rotary pumps [3]. Rotary blood pumps reduce the myocardial work by unloading the ventricle [2]. But rotary blood pumps can cause deleterious effects at high operating speeds in the ventricles such as suction effect. Also regurgitant pump flow may occur at low speeds, because rotary blood pumps are preload insensitive devices [4]. Suction effect can cause damage in ventricles, tissue damage and pain in the chest [3, 5].

Various numerical cardiovascular models were developed for different purposes. The first numerical cardiovascular system model is Grodins' model [6]. Generally, blood vessels are expressed as an electric circuit. Sungawa and Sagawa proposed a time varying capacitor numerical heart model and this approach has been used by many researches in the following years [6].

In simple models the atrial contraction and the dynamics of the heart valves are ignored and blood vessel compartments are lumped into one compartment. But more detailed numerical cardiovascular system models were also developed. For example, Muro Ursino modeled the carotid baroregulation in pulsating conditions [7, 8]. Lu et al. modeled the cardiopulmonary system with the analysis of the valsalava maneuver [9]. Heldt et al. modeled the cardiovascular response to the orthostatic stress [10].

Numerical cardiovascular system models are also used for simulating cardiovascular system diseases. For example Podnar et al. modeled the short term control mechanisms in

cardiovascular physiology and made simulations for different conditions such as exercise, hemorrhage etc. [11]. Smith et al. modeled the cardiovascular system diseases by including autonomic nervous system [12]. In Smith's another study hemodynamic system was modeled by including ventricular interaction and valve dynamics [13].

Danielsen and Ottesen modeled ventricular contraction for the different conditions and proposed a new model for pumping heart [14, 15].

Korakianitis and Shi modeled the cardiovascular system that includes atrioventricular interaction and heart valve dynamics [16]. Shi et al. made simulations with different types of heart pumps by using this model [17].

Different heart pump models and control strategies were developed by many researchers. Li et al. developed an empirical model to simulate Hemopump that is a left ventricular assist device [18]. He et al. studied optimum control of the hemopump by using this empirical model [19].

Nishida proposed a linear model that includes pressure difference, flow rate and rotation speed terms to simulate heart pumps [20].

Choi et al. used a dynamic pump model that includes difference, flow rate, derivative of flow rate with respect to time and rotation speed. In this study motor dynamics were also modeled [21].

By conducting experiments and using numerical models physiologically significant pumping states in implantable rotary blood pumps were indentified. For example Ayre et al. identified physiologically significant pumping states in implantable rotary blood pumps by using a mock up circulatory loop [22]. Karantonis et al. made studies to identify and classify the physiologically significant pumping states in implantable rotary blood pumps [23-26].

Choi et al. used pulsatility index, diminishing returns index and harmonic index of current to detect suction which is a physiologically significant pumping state in

implantable rotary blood pumps [27]. In another study Choi used data fusion approach to detect suction [28]. In suction conditions flow rate of pump and pressure difference between outlet and inlet of the pump exhibit a unique property. By using this property Choi et al. presented a control index to detect suction [29]. Choi et al. used fuzzy logic control method based on pulsatility ratio to detect suction [30, 31].

Chen et al. made physiological control of left ventricular assist devices based on gradient flow. In this study Chen et al. made comparison between extremum seeking algorithm and gradient method [32].

Vollkron et al. made simulations with a refined computer model of human cardiovascular system and a left ventricular assist device [33]. In other studies they defined several criteria for suction detection from patient data and developed a multidimensional optimization process to prevent suction [34-36].

Giridharan et al. developed physiological control strategies to maintain physiological perfusion and prevent suction. They proposed that control of the pressure difference between outlet and inlet of the pump or pressure difference between aorta and pulmonary veins maintain physiological perfusion and prevent suction [37-39]. Unfortunately sensor technology has not been improved yet to measure directly pressures in the blood vessels and heart chambers.

Oshikawa et al. examined by acute animal experiments to change the left ventricular contractility or left ventricular end diastolic pressure [40]. Index of motor current amplitude and motor current waveform was used to estimate pulsatility of pump without any sensor in this study.

Motor current waveform was used by Ohuchi et al. to determine the optimum pump rotation speed [41]. Power spectral density of motor current waveform was calculated and amplitude of motor current waveform used to detect suction.

Iijima et al. used fast Fourier transform and power spectral density of motor current was used to detect suction in another study [42].

Kikugawa suggested that there is fairly good correlation between left ventricular pressure and motor current [43]. Therefore left ventricular pressure can be estimated by using motor current.

Arndt et al. made physiological control of a rotary pump. They used gradient of pulsatility index with respect to pump speed. In this study regurgitant pump flow and ventricular suction were detected by using gradient of pulsatility index [44].

Fu et al. made computer simulations for a sensorless fuzzy control to assure normal physiology by using electric motor current and speed [45].

Casas et al. made a physiological fuzzy logic control by using empirical relation between pump flow rate, pressure difference outlet and inlet of the heart pump and pump rotation speed [46, 47].

The studies in this dissertation were done in the scope of a TÜBİTAK funded project entitled ‘Design, Analysis and Prototype Production of a Miniature Implantable Rotary Blood Pump.’ An axial heart pump called Heart Turcica axial is developed by Yeditepe University Mechanical Engineering Department and a centrifugal heart pump called Heart Turcica centrifugal is developed by Koç University Mechanical Engineering Department in the scope of this project.

This dissertation is organized as follows. In chapter two, short background information on human cardiovascular system and heart failure are reviewed. The developed numerical models of human cardiovascular system and diseased human cardiovascular system are explained. Also simulation results of the numerical models are shown and discussed in chapter two.

In chapter three, the procedure for derivation of a pump model is explained for Heart Turcica axial and Heart Turcica centrifugal.

In chapter four, physiologically significant pumping states in implantable rotary blood pumps were reviewed. The combined model of left ventricular assist devices and

human cardiovascular system are explained. The boundary operating speeds of heart pumps, which cause different physiologically significant pumping states are determined.

In chapter five different control strategies for Heart Turcica axial including variable pump operating speeds were proposed. The proposed control strategies in this section are control of pressure difference control across the pump and control of pump flow.

In chapter six conclusions are drawn and future works are discussed.

2. MODELING OF THE HUMAN CARDIOVASCULAR SYSTEM

2.1. THE HUMAN CARDIOVASCULAR SYSTEM

The human cardiovascular system delivers nutrients, oxygen, to tissues and removes wastes and carbon dioxide from tissues. The cardiovascular system consists of two primary components: heart and blood vessels [48].

The heart can be thought as two working pumps. Left heart pumps blood into the systemic circulation and right heart pumps blood into the pulmonary circulation [48]. The heart mainly consists of four chambers and four valves. Left heart includes left atrium, mitral valve, left ventricle, aortic valve. The oxygenated blood that comes from pulmonary veins flows into the left atrium. Left ventricular blood pressure decreases with left ventricle relaxation and oxygenated blood passes through the mitral valve and flows into the left ventricle. Left ventricular blood pressure increases with left ventricle contraction and aortic valve opens. Blood passes through the aortic valve and flows into the systemic arteries [48].

Right heart includes right atrium, tricuspid valve, right ventricle and pulmonary valve. The de-oxygenated blood that comes from systemic veins flows into the right atrium. Right ventricular blood pressure decreases with right ventricle relaxation and de-oxygenated blood passes through the tricuspid valve and flows into the right ventricle. Right ventricular blood pressure increases with right ventricle contraction and pulmonary valve opens. Blood passes through the pulmonary valve and flows into the pulmonary arteries [48].

The circulatory system includes systemic circulation that carries oxygenated blood to the tissues and pulmonary circulation carries de-oxygenated blood to the lungs to be oxygenated. Both systemic and pulmonary circulation include three main kinds of blood vessels: arteries, veins and capillaries [48].

Systemic arteries take blood from the left heart and bring the oxygenated blood from

the left heart and to the tissues. Oxygen and nutrients diffuse to the cells from the systemic capillaries and carbon dioxide diffuses into the blood. The de – oxygenated blood flows into the right heart from the systemic veins [48].

Pulmonary arteries take the de – oxygenated blood from the right heart and bring to the lungs. Blood is oxygenated in the lungs and pulmonary veins bring blood back to the left heart. Carbon dioxide diffuses in the alveoli from the pulmonary capillaries and oxygen diffuses into the pulmonary capillaries from the alveoli [48]. The heart and circulatory system are shown in Figure 2.1.

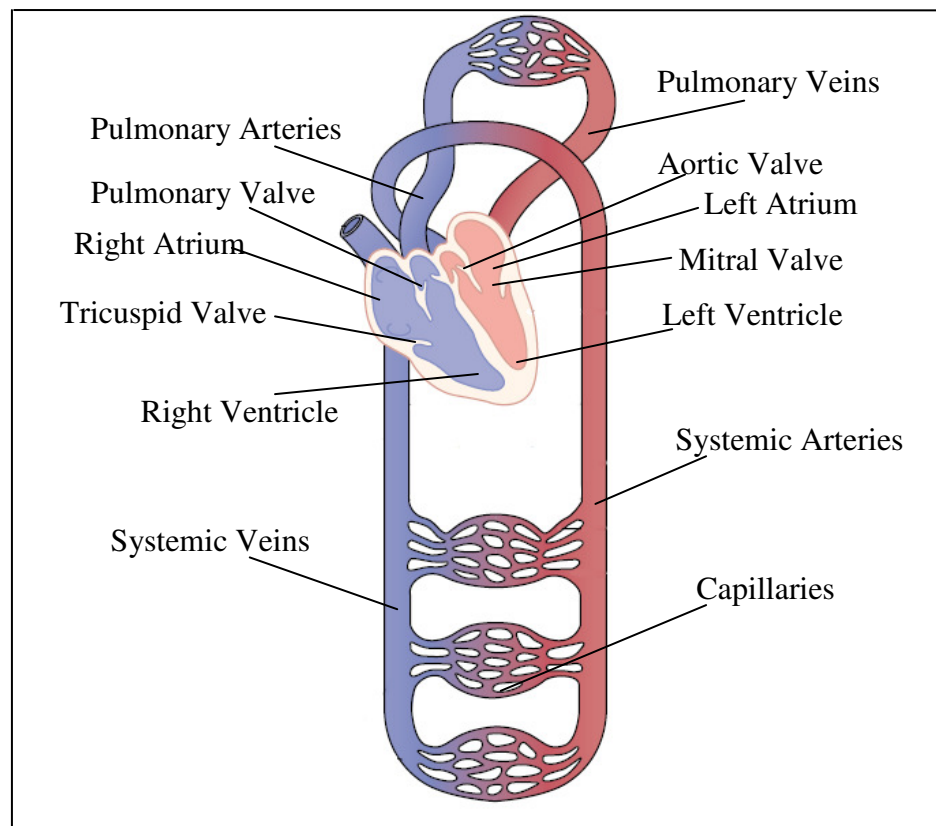


Figure 2.1. The heart and circulatory system [49]

2.1.1. Cardiac Cycle

Cardiac cycle is the events that occur in a heartbeat period. The cardiac cycle consist of two phases which are called diastole (a period of relaxation) and systole (a period of contraction) [49].

Normally blood flow from veins to the atria is continuous. At the end of the ventricular systole intra-ventricular pressure drops rapidly and blood flows into the ventricles through the atrioventricular valves. With atrial contraction (atrial systole) additional blood flows into the ventricles. The atrial contraction contributes 20 per cent of ventricular filling. Atrioventricular valves close with the beginning of the ventricular systole. With the beginning of the ventricular systole ventricular pressure rise rapidly. In the additional 0.02 – 0.03 seconds ventricles do not pump blood because of relatively low pressure in the ventricles to open the semilunar valves. This period is called "isovolumic contraction". The ventricles start to pump blood after ventricular pressure slightly exceeds the arterial pressure. When the ventricular pressure slightly exceeds the arterial pressure semilunar valves open and blood flows into the arteries. This period is called "ejection period". At the end of the systolic period ventricular pressure decreases rapidly and semilunar valves close. At this period ventricles relax and all the valves remain closed. This period is called "isovolumic relaxation". After the isovolumic relaxation period atrioventricular valves open and blood from atria flows into the ventricles [49]. The pressure and volume change in the left heart chamber during a cardiac cycle are shown in Figure 2.2.

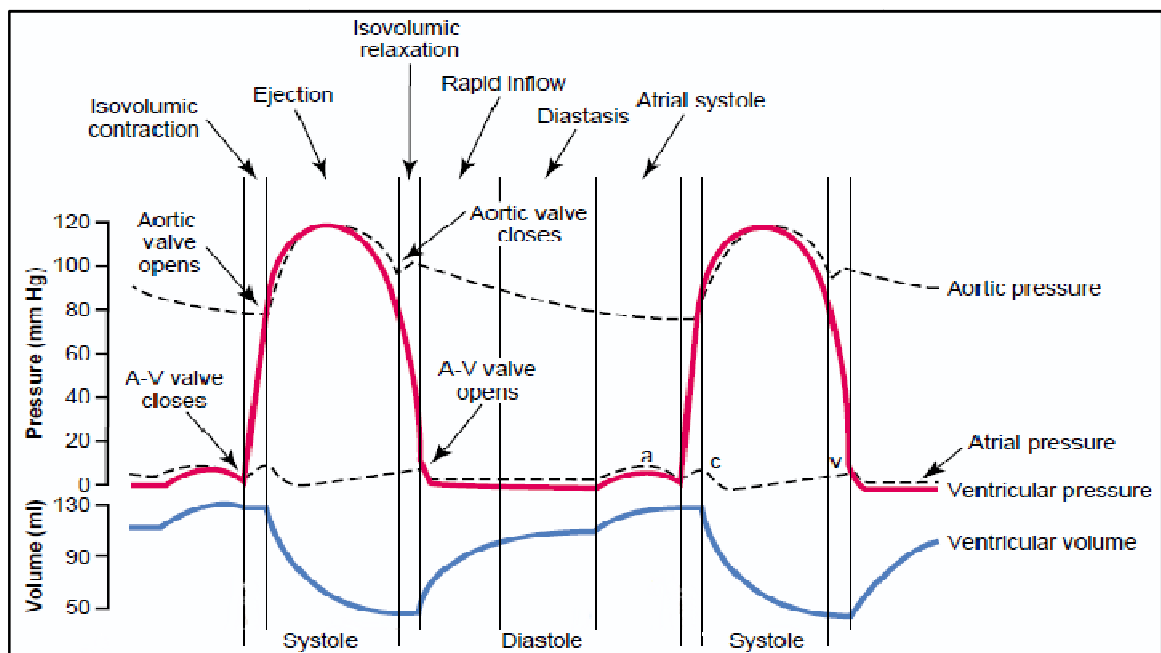


Figure 2.2. The pressure and volume change in the left heart chamber during a cardiac cycle [49]

As shown in Figure 2.2 in normal conditions end diastolic left ventricular volume (EDV) is about 120 ml and end systolic left ventricular volume (ESV) is about 50 ml. The difference between the end diastolic left ventricular volume and end systolic left ventricular volume is called the “stroke volume”. In normal conditions stroke volume of the left ventricle is 70 ml [48].

$$SV = EDV - ESV \quad (2.1)$$

Pressure-volume loop of the ventricles are useful to understand the pumping mechanism of ventricles [49]. As shown in Figure 2.3 filling period and ejection period occur at the first and third phases respectively. Figure 2.3 shows that isovolumic contraction and isovolumic relaxation occur at the second and fourth phases of pressure-volume loop of the left ventricle respectively. ESPVR and EDPVR represent the end systolic pressure volume relationship and end diastolic pressure volume relationship in Figure 2.3. Opening and closing phases of aortic and mitral valves are also shown in Figure 2.3.

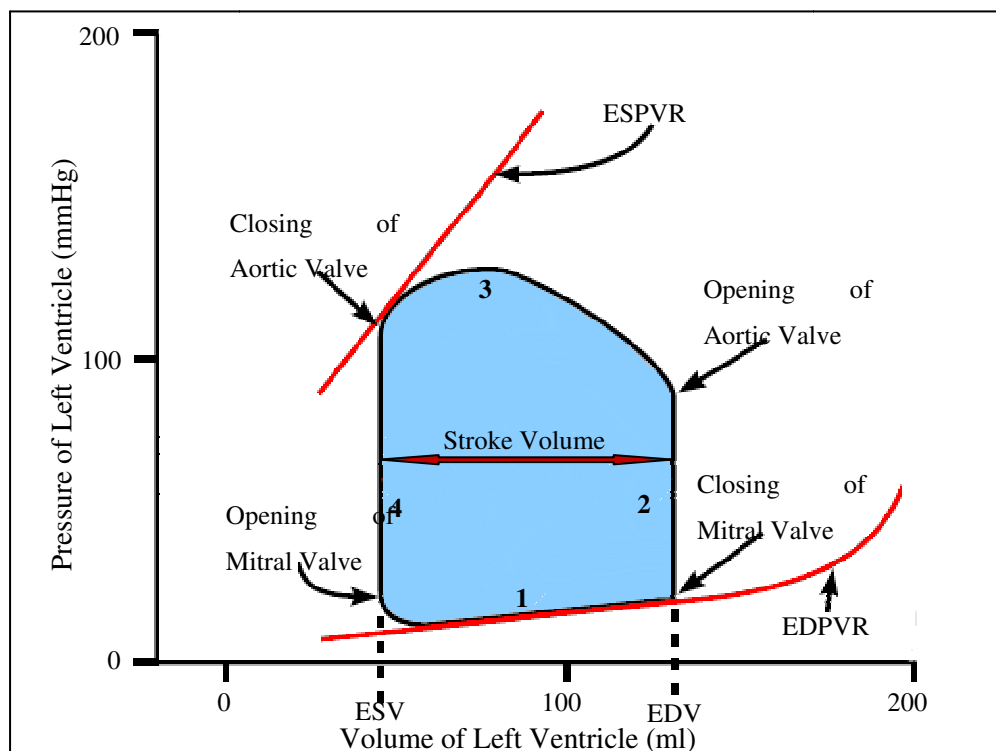


Figure 2.3. Pressure – volume diagram of the left ventricle [48]

Another important concept is the “heart rate (HR)”. Heart rate is the number of heart beats per unit of time [48]. Generally heart rate is expressed in beats per minute. Also in this thesis heart rate was expressed in beats per minute.

Cardiac output (CO) is the blood volume that is pumped by the heart to the circulation system [48]. In normal conditions average cardiac output is five or six liters per minute. Cardiac output is calculated by multiplying stroke volume and heart rate as shown below.

$$CO = SV \times HR \quad (2.2)$$

The stroke volume divided by the end diastolic volume is called the “ejection fraction” (E_f). Normally ejection fraction is greater than 55 per cent. Ejection fraction is calculated as shown below.

$$E_f = \frac{SV}{EDV} \quad (2.3)$$

The heart performance to size of the body is called the “cardiac index (CI)”. To calculate the cardiac index the body surface area (BSA) must be determined. For men average body surface area is nearly 1.9 m^2 and for women average body surface area is nearly 1.6 m^2 . Normally cardiac index varies between 2.6 l/min/m^2 and 4.2 l/min/m^2 . Cardiac index can be calculated as shown below.

$$CI = \frac{CO}{BSA} \quad (2.4)$$

2.1.2. Vascular System

The vascular system mainly consists of aorta, arteries, arterioles, capillaries, venules, veins and vena cava [48, 49]. The left ventricle ejects the blood into the aorta and blood passes through the circulation system and flows back to the heart. Before the left ventricular contraction aortic pressure falls nearly 80 mmHg that is the lowest pressure value in the aorta. This value is called the “diastolic pressure (DP)”. During the left

ventricular contraction the pressure in the aorta reaches its maximum value that is nearly 120 mmHg. This value is called the “systolic pressure (SP)” The mean arterial blood pressure (MAP) is the average pressure in the arteries. Mean arterial blood pressure is summation of 60 per cent of diastolic pressure and 40 per cent of systolic pressure as shown below [49].

$$MAP = 0.6 DP + 0.4 SP \quad (2.5)$$

The blood flows through the blood vessels with pressure difference (ΔP) that pushes the blood. Blood flow (Q) is also depends on the resistance effects of the blood vessels. Vascular resistance is the resistance flow must overcome to eject the blood through the circulation system. According to the Ohm’s Law blood flow is calculated as below [49].

$$Q = \frac{\Delta P}{R} \quad (2.6)$$

Blood vessels also have an elastic property that is called “compliance”. Compliance describes the change of change of volume (ΔV) divided by change of pressure (ΔP) [49].

$$C = \frac{\Delta V}{\Delta P} \quad (2.7)$$

2.1.3. Heart Failure

Heart failure is a condition that occurs when the heart cannot pump enough blood through the body. In other words cardiac output decreases and strain in heart increases. Heart failure is a serious health problem which causes to death or disabling.

In a heart failure condition a certain number of changes occur in cardiovascular system. Some of the changes are listed below

- Contractility reduces
- Stroke volume reduces
- Ventricles get enlarged

- Heart rate increases to pump more blood through the body
- Blood pressure in the arteries falls

Heart failure affects many organs of the body. As a result heart continues to work but efficiency of the heart reduces. Therefore people with heart failure feel tired and breathe frequently.

In a heart failure condition left ventricular assist devices can be used to support partially or completely the failing heart. Ventricular assist devices can support left ventricle, right ventricle or both of them. Ventricular assist devices reduce myocardial work and maintain the output of the ventricles. Ventricular assist devices are used if the patient's cardiac index is less than two $l/min/m^2$, systolic blood pressure is less than 90 mmHg, atrial pressure is greater than 20 mmHg and systemic vascular resistance greater than $1.57 \text{ mmHg}\cdot\text{s}^2/\text{ml}$ [2].

2.2. MODELING OF THE HUMAN CARDIOVASCULAR SYSTEM

There are similarities between the electrical and fluid systems. In other words fluid systems can be represented as electrical circuits. Therefore human cardiovascular system was modeled as an electrical system that includes resistance, capacitance and inductance elements. The analogy between electrical systems and fluid systems is shown below.

Table 2.1. The analogy between electrical systems and fluid systems

Electrical Systems	Fluid Systems
Electrical charge (q)	Fluid volume (V)
Current (I)	Flow rate (Q)
Potential difference (V)	Pressure Difference (ΔP)
Electrical Resistance (R)	Fluid resistance (R)
Capacitance (C)	Compliance (C)
Inductance (L)	Fluid inertance (L)

The numerical model of human cardiovascular system includes heart chambers, heart

valves, systemic arteries, systemic veins, pulmonary arteries, pulmonary veins. The human cardiovascular system model does not include capillary blood vessels for the sake of simplicity. Systemic arteries and aorta are combined into one segment. Also systemic veins and vena cava are combined into one segment for the sake of simplicity. Block diagram of the human cardiovascular system model is shown in Figure 2.4.

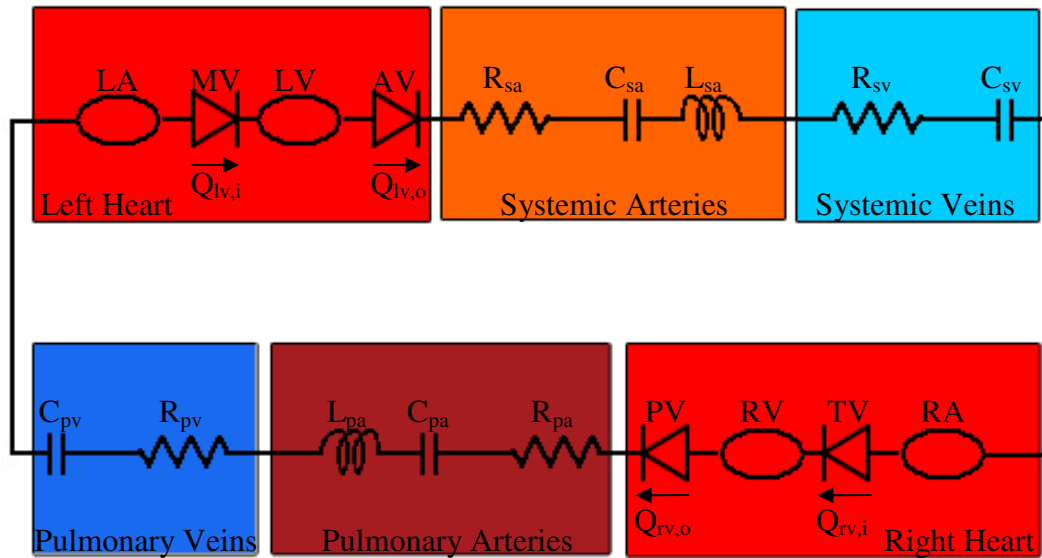


Figure 2.4. Block diagram of the human cardiovascular system model

2.2.1. Ventricles

Ventricles in the cardiovascular system model are described as time varying elastance. To define elastance a commonly used activation function is adopted to the cardiovascular system model [10].

$$e = \begin{cases} 1 - \cos\left(\frac{t}{T_1}\pi\right) & 0 \leq t \leq T_1 \\ 1 + \cos\left(\frac{t - T_1}{T_2 - T_1}\pi\right) & T_1 \leq t \leq T_2 \\ 0 & T_2 \leq t \leq BP \end{cases} \quad (2.8)$$

Activation function defines the changes in the ventricle during the systole and diastole. Elastance change is defined by using the activation function. Elastance change is shown below.

$$E = E_{dias} + \frac{E_{sys} - E_{dias}}{2} e \quad (2.9)$$

Elastance function describes the relation between ventricular volume and pressure. Models of both ventricle elastance functions are identical but the parameter values are different. The change of elastance function in a cardiac cycle is shown in Figure 2.5.

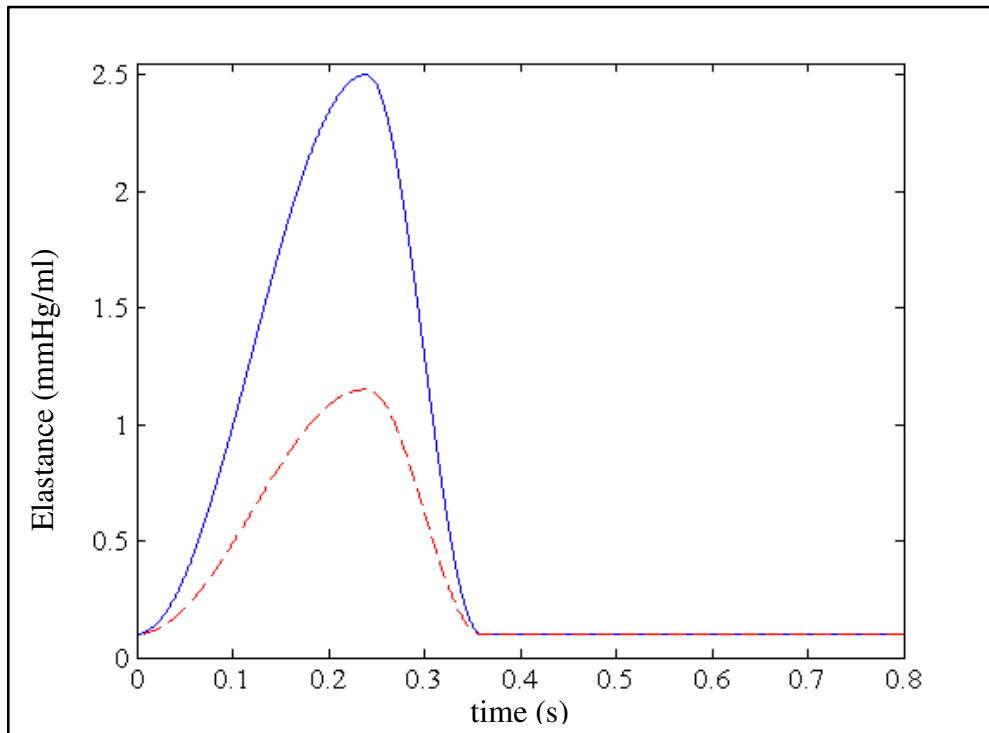


Figure 2.5. Elastance function of left ventricle (continuous line) and right ventricle (dashed line) in a cardiac cycle duration

Volume changes of the ventricles are described as the difference between instantaneous inflow and outflow of the ventricles. The volume change of the left ventricle and right ventricle is shown below.

$$\frac{dV_{lv}}{dt} = Q_{lv,i} - Q_{lv,o} \quad (2.10)$$

$$\frac{dV_{rv}}{dt} = Q_{rv,i} - Q_{rv,o} \quad (2.11)$$

V_{lv} , V_{rv} , $Q_{lv,i}$, $Q_{lv,o}$, $Q_{rv,i}$, $Q_{rv,o}$ are left ventricular and right ventricular volume, left ventricular inlet and outlet flow rates, right ventricular inlet and outlet flow rates respectively in the equations shown above. The ventricular pressures are defined as the product of instantaneous ventricular volumes and elastances. The left and right ventricular pressure changes are shown below.

$$P_{lv} = E_{lv} (V_{lv} - V_{lv,0}) \quad (2.12)$$

$$P_{rv} = E_{rv} (V_{rv} - V_{rv,0}) \quad (2.13)$$

P_{lv} , P_{rv} , $V_{lv,0}$ and $V_{rv,0}$ are left and right ventricular pressure and left and right ventricular zero pressure filling volume respectively in the equations shown above.

2.2.2. Atria

Atrial contraction is very low in comparison to ventricular contraction. In normal conditions atrial contraction contributes 20 per cent to ventricular filling [49]. Blood passively flows from veins into the atria and then into the ventricles through the mitral valve and tricuspid valve. Therefore atria are described with constant elastance values [16]. The change of blood volume in the atria is very similar to ventricles. Therefore atrial volume change is described as difference between flow rate of veins and inflow of ventricles. The change of blood volume in the atria is defined below.

$$\frac{dV_{la}}{dt} = Q_{pv} - Q_{lv,i} \quad (2.14)$$

$$\frac{dV_{ra}}{dt} = Q_{sv} - Q_{rv,i} \quad (2.15)$$

V_{la} , V_{ra} , Q_{pv} , Q_{sv} are left and right atrial volume, flow rate of pulmonary veins and flow rate of systemic veins respectively in the equations shown above.

2.2.3. Heart Valves

In the developed cardiovascular system model heart valves are described as diodes [50]. Blood flow in the heart valves are assumed to be only one way. Regurgitant blood flow is ignored. Governing blood flow equations of heart valves are shown below. Model of the blood flow through the heart valves is the same but the parameter values are different.

$$Q_{mi} = \frac{P_{la} - P_{lv}}{R_{mi}} \quad (2.16)$$

$$Q_{ao} = \frac{P_{lv} - P_{sa}}{R_{ao}} \quad (2.17)$$

$$Q_{ti} = \frac{P_{ra} - P_{rv}}{R_{ti}} \quad (2.18)$$

$$Q_{pu} = \frac{P_{rv} - P_{pa}}{R_{po}} \quad (2.19)$$

Q_{mi} , Q_{ao} , Q_{ti} , Q_{pu} are flow rates that flows through the mitral, aortic, tricuspid and pulmonary valves respectively. P_{la} , P_{lv} , P_{sa} , P_{ra} , P_{rv} , P_{pa} denote left atrial pressure, left ventricular pressure, systemic arterial pressure, right atrial pressure, right ventricular pressure, pulmonary arterial pressure respectively. R_{mi} , R_{ao} , R_{ti} , R_{po} denote flow resistance of mitral, aortic, tricuspid and pulmonary valves respectively.

2.2.4. Vascular System

In the cardiovascular system model resistance effects, compliance effects and inertance effects are considered. In modeling of systemic arteries and pulmonary arteries these three elements are included. Change of pressure and flow rate of the arteries are defined below.

$$\frac{dP_{sa}}{dt} = \frac{Q_{ao} - Q_{sa}}{C_{sa}} \quad (2.20)$$

$$\frac{dQ_{sa}}{dt} = \frac{P_{sa} - P_{sv} - Q_{sa}R_{sa}}{L_{sa}} \quad (2.21)$$

$$\frac{dP_{pa}}{dt} = \frac{Q_{pu} - Q_{pa}}{C_{pa}} \quad (2.22)$$

$$\frac{dQ_{pa}}{dt} = \frac{P_{pa} - P_{pv} - Q_{pa}R_{pa}}{L_{pa}} \quad (2.23)$$

Q_{sa} , Q_{pa} , P_{sv} , P_{pv} denote flow rate of systemic arteries, flow rate of pulmonary arteries, pressure of systemic veins, pressure of pulmonary veins respectively. C_{sa} , R_{sa} , L_{sa} , C_{pa} , R_{pa} , L_{pa} denote systemic arteries compliance, flow resistance, inertance and pulmonary arteries compliance, flow resistance, inertance respectively in the equations shown above.

Systemic veins and pulmonary veins do not include the inertance effect. Therefore flow rates through the veins are expressed as algebraic equations. Flow rates and the pressures of the veins are defined below.

$$\frac{dP_{sv}}{dt} = \frac{Q_{sa} - Q_{sv}}{C_{sv}} \quad (2.24)$$

$$Q_{sv} = \frac{P_{sv} - P_{ra}}{R_{sv}} \quad (2.25)$$

$$P_{pv} = \frac{1}{C_{pv}} (V_{tot} - P_{sa}C_{sa} - P_{sv}C_{sv} - P_{pa}C_{pa} - V_{la} - V_{lv} - V_{ra} - V_{rv} - V_u) \quad (2.26)$$

$$Q_{pv} = \frac{P_{pv} - P_{la}}{R_{pv}} \quad (2.27)$$

C_{sv} , C_{pv} , R_{sv} , R_{pv} denote compliance of systemic veins, compliance of pulmonary veins, flow resistance of systemic veins, flow resistance of pulmonary veins respectively in

the equations shown above. V_{tot} and V_u denote total blood volume and unstressed blood volume in the human body respectively in the equations shown above.

The parameters used in numerical human cardiovascular system model are taken from the literature. Compliance of the left and right atrium, systemic arterial resistance, pulmonary arterial resistance, compliance of systemic veins, compliance of pulmonary arteries and veins, inertance of systemic arteries and pulmonary arteries are taken from [51]. The resistances of heart valves and systemic arterial compliance values are taken from [52]. Resistance of systemic veins value is taken from [16]. Resistance of pulmonary veins value is taken from [53]. The parameters used in numerical human cardiovascular system model are shown in Table 2.2.

Table 2.2. The parameters used in numerical human cardiovascular system model

	R (mmHg s / ml)	C (ml / mmHg)	L (mmHg s ² / ml)
Left Atrium	-	5	-
Right Atrium	-	5	-
Mitral Valve	0.005	-	-
Aortic Valve	0.001	-	-
Tricuspid Valve	0.005	-	-
Pulmonary Valve	0.001	-	-
Systemic Arteries	0.97	1.3	0.00001
Systemic Veins	0.075	82.5	-
Pulmonary Arteries	0.106	4.8	0.00001
Pulmonary Veins	0.005	5	-

The parameters used for modeling activation function and elastance function are taken from [16]. The value of zero pressure filling volume of the left ventricle is taken from [5]. The value of zero pressure filling volume of the right ventricle is taken from [54]. The parameters used in ventricular modeling are shown in Table 2.3.

Table 2.3. The parameters used in ventricular modeling

	E_{sys} (mmHg/ml)	E_{dias} (mmHg/ml)	V_0 (ml)
Left Ventricle	2.5	0.1	5
Right Ventricle	1.15	0.1	5

For simulations total blood volume was set to 5700 ml [10] and unstressed blood volume for vascular compartments of the human cardiovascular system model was set to 3800 ml [55].

2.2.5. Simulation Results

The cardiovascular system model was built in Matlab and Simulink. Simulations were performed by using ode15s solver and maximum step size was adjusted to 0.0001 s. Heart rate was adjusted to 75 beat/min thus one heart beat period is 0.8 s.

According to the simulation results the maximum and minimum left ventricular pressure is nearly 121 mmHg and 7 mmHg respectively. Left atrial maximum pressure is nearly 15 mmHg and the minimum pressure is nearly 10 mmHg. Systolic pressure of the systemic arteries is nearly 121 mmHg and diastolic pressure is 79 mmHg. The pressure of systemic veins is nearly 16 mmHg. The pressure of the left heart chambers and the systemic circulation are shown in Figure 2.6.

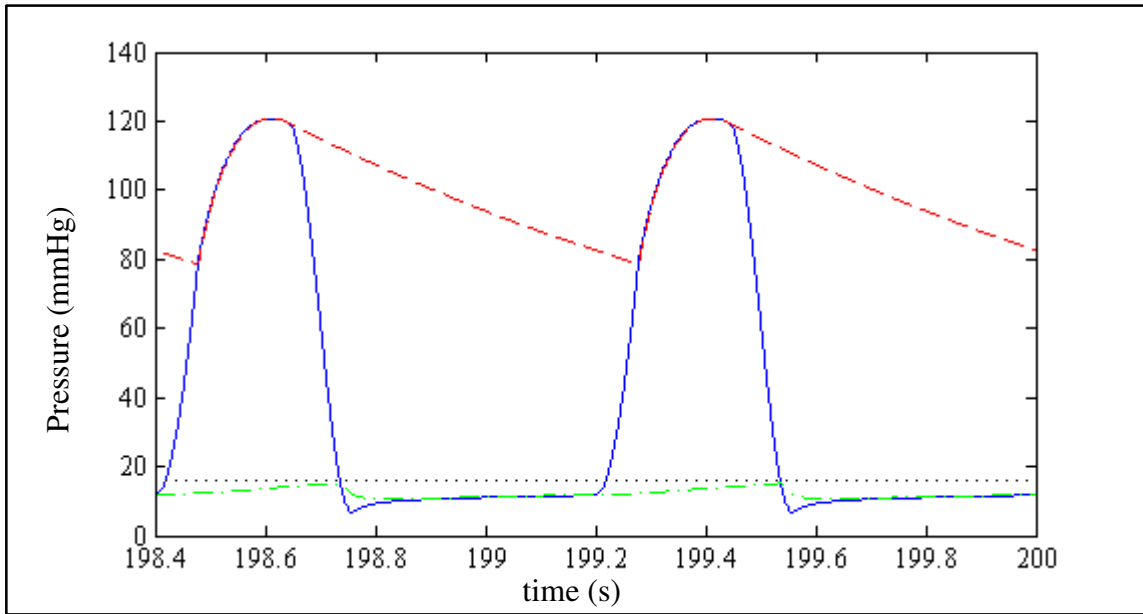


Figure 2.6. Simulation results for left ventricular pressure (continuous line), left atrial pressure (chain line), the pressure of the systemic arteries (dashed line) and the pressure of the systemic veins (dotted line)

Right ventricular maximum and minimum pressure is nearly 27 mmHg and 5 mmHg respectively. Right atrial maximum pressure is nearly 13 mmHg and minimum pressure is 7 mmHg. Maximum pressure of the pulmonary arteries is nearly 27 mmHg and minimum pressure of the pulmonary arteries is 17 mmHg. Maximum pressure of the pulmonary veins is nearly 15 mmHg and minimum pressure of the pulmonary veins is 11 mmHg. The pressure of the right heart chambers and the pulmonary circulation are shown in Figure 2.7.

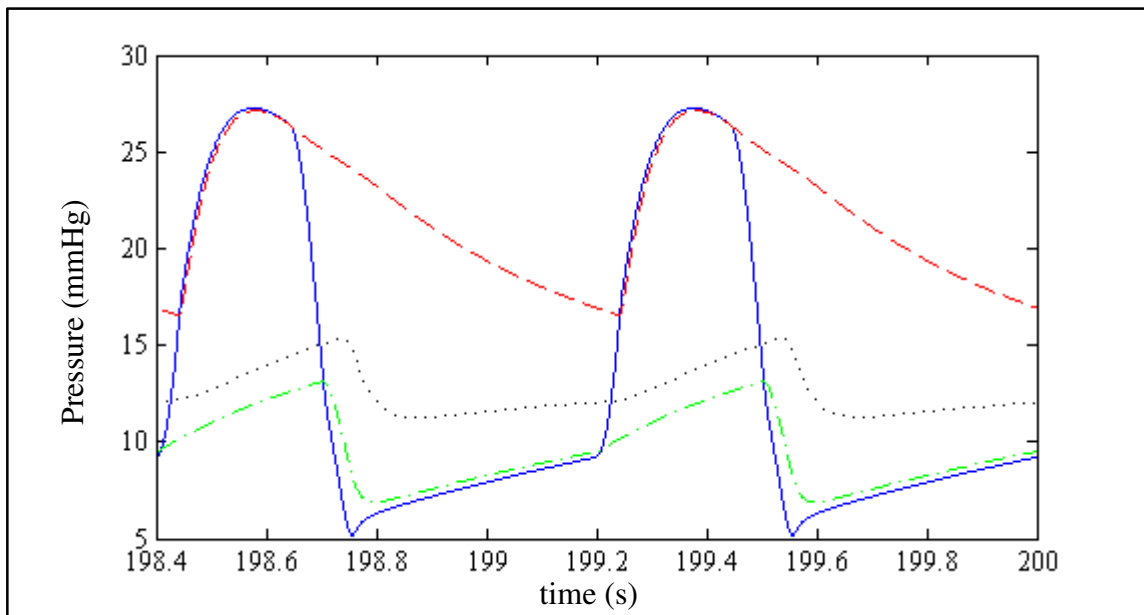


Figure 2.7. Simulation results for right ventricular pressure (continuous line), right atrial pressure (chain line), the pressure of the pulmonary arteries (dashed line) and the pressure of the pulmonary veins (dotted line)

Maximum left ventricular volume is nearly 122.2 ml and minimum left ventricular volume is nearly 52.9 ml. According to these results stroke volume of the left ventricle is 69.3 ml. Maximum right ventricular volume is nearly 97.3 ml and minimum right ventricular volume is nearly 28 ml. Stroke volume of the right ventricle is calculated as 69.3 ml according to these results. The left atrial maximum volume is nearly 76 ml and minimum volume is nearly 53 ml. The right atrial maximum volume is nearly 66 ml and minimum volume is nearly 34 ml. The volume of the heart chambers are shown in Figure 2.8.

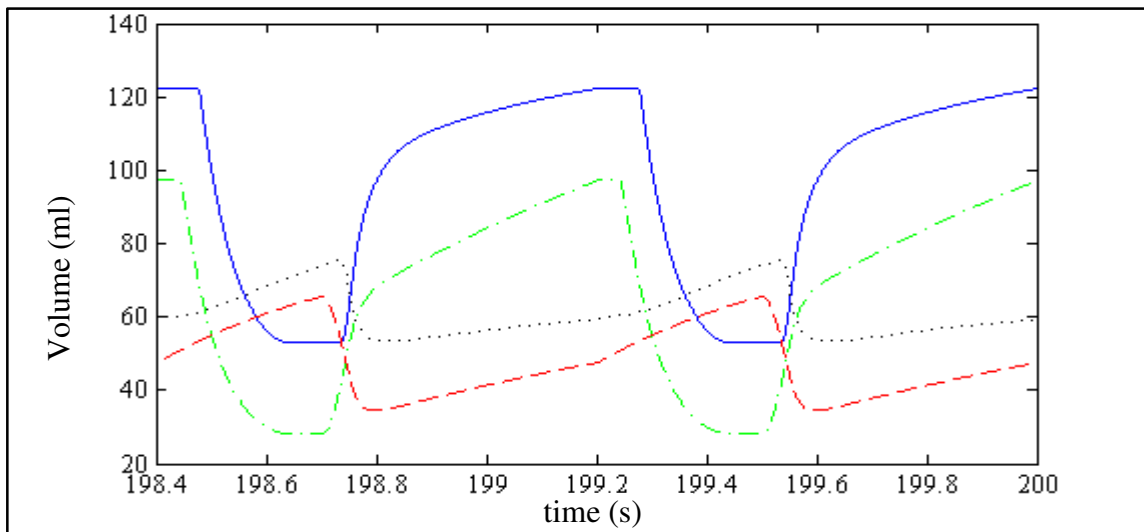


Figure 2.8. Volume of the heart chambers, left ventricular volume (continuous line), right ventricular volume (chain line), left atrial volume (dotted line), right atrial volume (dashed line)

Periodic peak flow occurs in the mitral valve and aortic valve flow rates. Average blood flow is nearly 5.2 l/min. The flow rates of the left heart valves and systemic blood vessels are shown in Figure 2.9.

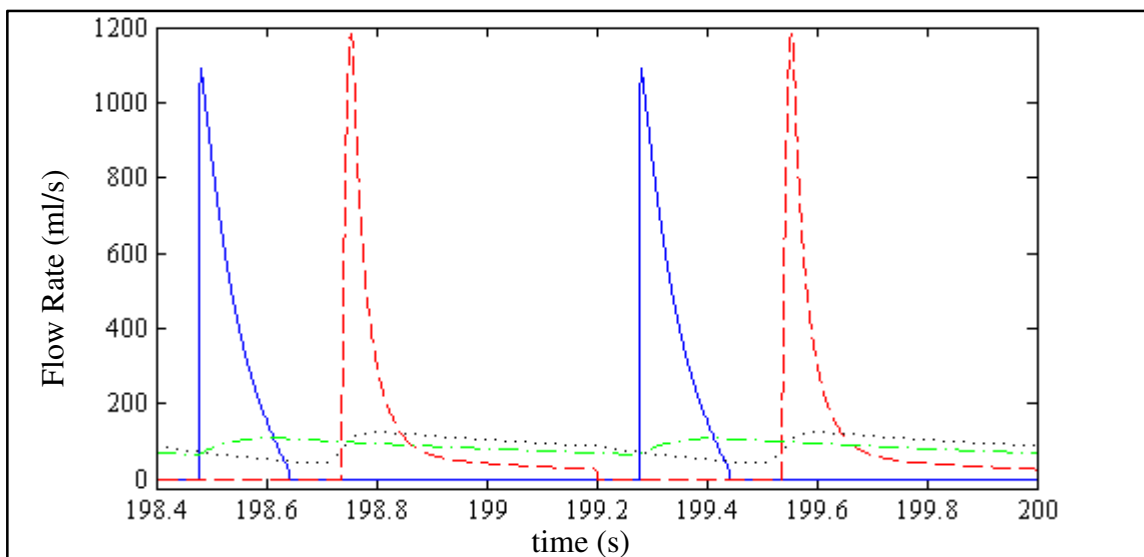


Figure 2.9. Flow rate of the mitral valve (dashed line), flow rate of the aortic valve (continuous line), flow rate of the systemic arteries (chain line), flow rate of the systemic veins (dotted line)

Periodic peak flow occurs in the tricuspid valve, pulmonary valve and pulmonary vein flow rates. The flow rates of the right heart valves and pulmonary blood vessels are shown in Figure 2.10.

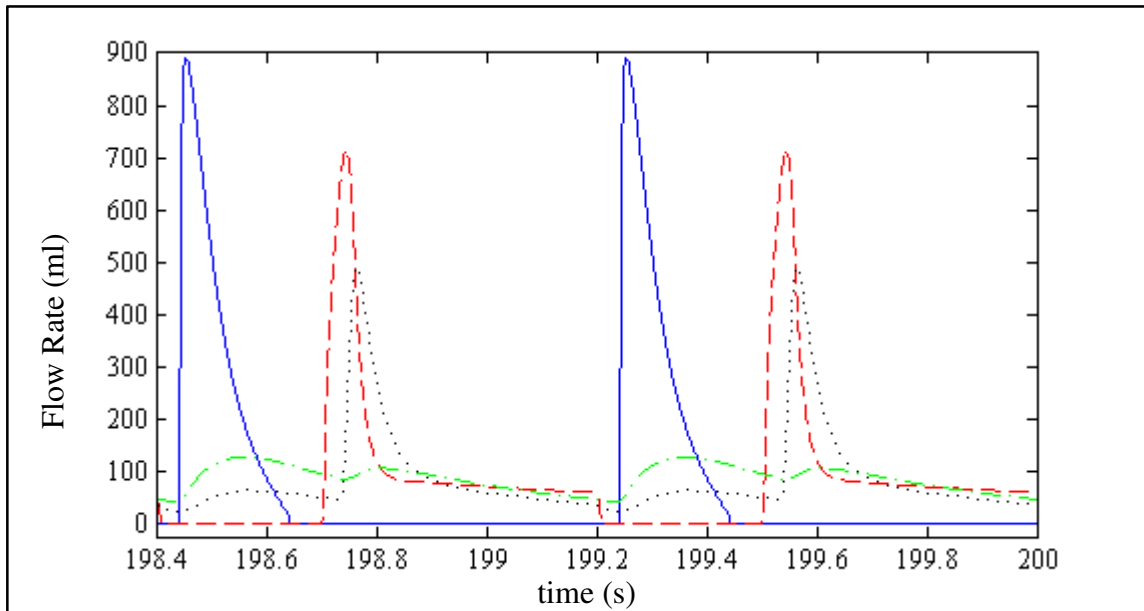


Figure 2.10. Flow rate of the tricuspid valve (dashed line), flow rate of the pulmonary valve (continuous line), flow rate of the pulmonary arteries (chain line), flow rate of the pulmonary veins (dotted line)

Pressure – volume loops that show the external work of the ventricles are useful to understand pumping mechanism. Pressure – volume loops of the developed human cardiovascular system model are shown in Figure 2.11.

By using these results cardiac output is calculated as 5200 ml/min. Mean arterial blood pressure is 95.8 mmHg. The ejection fraction of the left ventricle is 0.567. Body surface area is assumed to be 1.90 m^2 (180 cm tall, 72 kg weight healthy man). By using these results cardiac index is calculated as 2.74 l/min/m^2 . Simulation results are shown in Table 2.4.

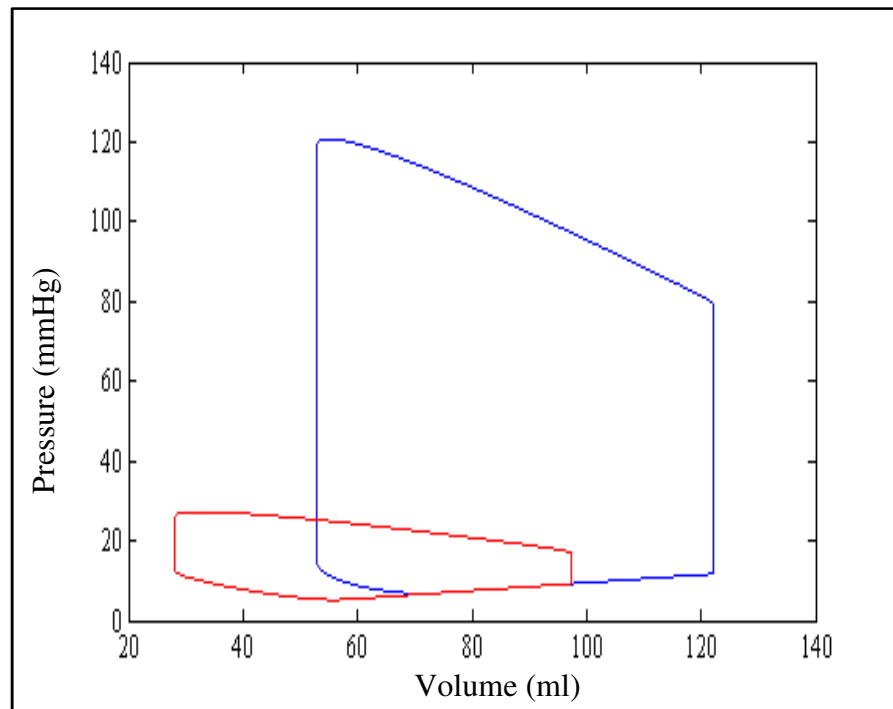


Figure 2.11. Pressure-volume loop of the left ventricle (blue line) and right ventricle (red line)

Table 2.4. Simulation results of human cardiovascular system model

Parameter	Max. Value	Min. Value	Parameter	Max. Value	Min. Value
P_{la} (mmHg)	15	10	P_{ra} (mmHg)	13	7
P_{lv} (mmHg)	121	7	P_{rv} (mmHg)	27	5
P_{sa} (mmHg)	121	79	P_{pa} (mmHg)	27	17
P_{sv} (mmHg)	16	16	P_{pv} (mmHg)	15	11
V_{la} (ml)	76	53	V_{ra} (ml)	66	34
V_{lv} (ml)	122.2	52.9	V_{rv} (ml)	97.3	28

2.3. MODELING OF THE DISEASED CARDIOVASCULAR SYSTEM

To obtain the pathological conditions mentioned in 2.1.3 the left ventricular maximum elastance was reduced to 0.7 mmHg/ml from 2.5 mmHg/ml, right ventricular maximum elastance was reduced to 0.3 mmHg/ml from 1.15 mmHg/ml. Also left

ventricular zero pressure filling volume was increased to 15 ml from 5 ml [56].

2.3.1. Simulation Results

Simulations were performed by using ode15s solver and maximum step size was adjusted to 0.0001 s, which are the same as the healthy cardiovascular system simulations.

According to the simulation results the maximum and minimum left ventricular pressure is nearly 74 mmHg and 11.5 mmHg respectively. Left atrial maximum pressure is nearly 16 mmHg and the minimum pressure is nearly 14 mmHg. Systolic pressure of the systemic arteries is nearly 74 mmHg and diastolic pressure is 50 mmHg. The pressure of systemic veins is nearly 15.5 mmHg. The pressure of the left heart chambers and the systemic circulation are shown in Figure 2.12.

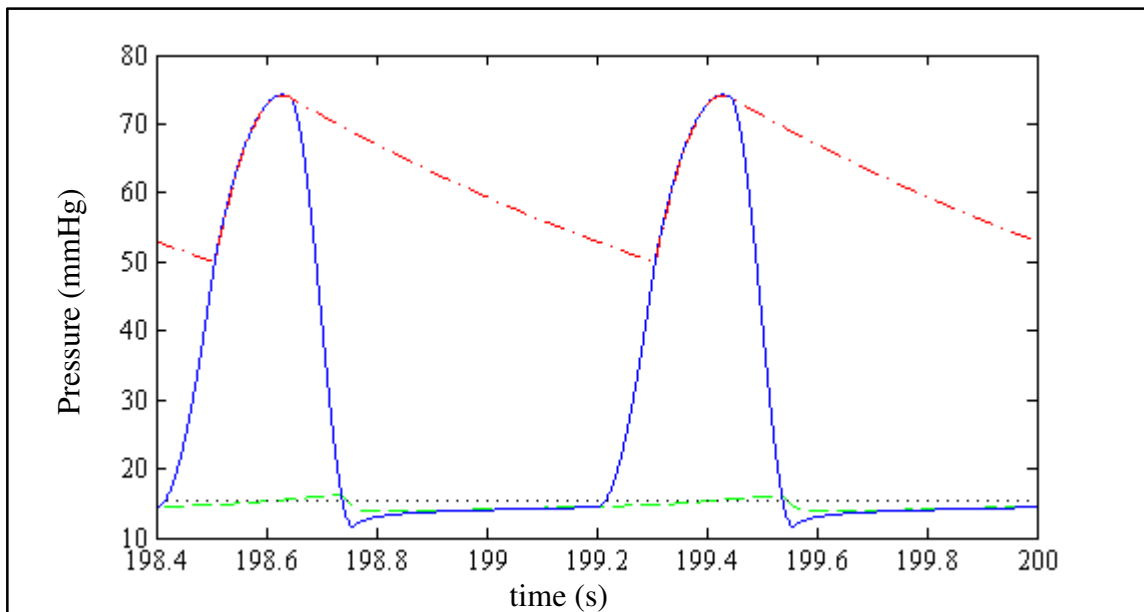


Figure 2.12. Simulation results for left ventricular pressure (continuous line), left atrial pressure (chain line), the pressure of the systemic arteries (dashed line) and the pressure of the systemic veins (dotted line)

Right ventricular maximum and minimum pressure is nearly 23 mmHg and 9 mmHg respectively. Right atrial maximum pressure is nearly 14 mmHg and minimum pressure is 10 mmHg. Maximum pressure of the pulmonary arteries is nearly 23 mmHg and minimum

pressure of the pulmonary arteries is 17 mmHg. Maximum pressure of the pulmonary veins is nearly 16 mmHg and minimum pressure of the pulmonary veins is 14 mmHg. The pressure of the right heart chambers and the pulmonary circulation are shown in Figure 2.13.

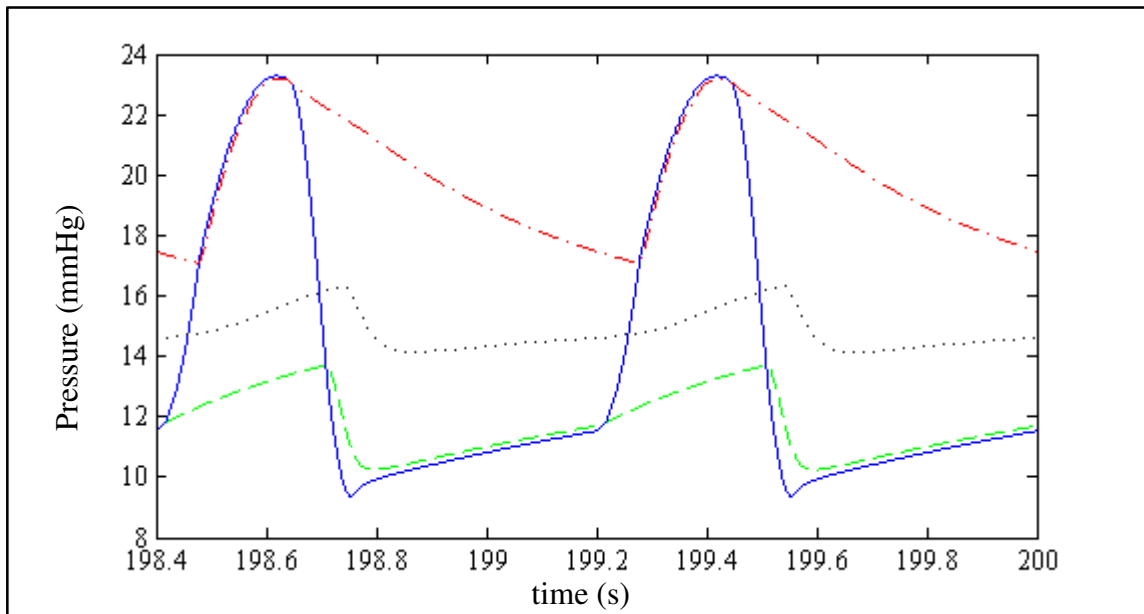


Figure 2.13. Simulation results for right ventricular pressure (continuous line), right atrial pressure (chain line), the pressure of the pulmonary arteries (dashed line) and the pressure of the pulmonary veins (dotted line)

Maximum left ventricular volume is nearly 159.2 ml and minimum left ventricular volume is nearly 120.8 ml. According to these results stroke volume of the left ventricle is 38.4 ml. Maximum right ventricular volume is nearly 120.6 ml and minimum right ventricular volume is nearly 82.2 ml. Stroke volume of the right ventricle is calculated as 38.4 ml based on these results. The left atrial maximum volume is nearly 81 ml and minimum volume is nearly 69 ml. The right atrial maximum volume is nearly 69 ml and minimum volume is nearly 51 ml. The volume of the heart chambers are shown in Figure 2.14.

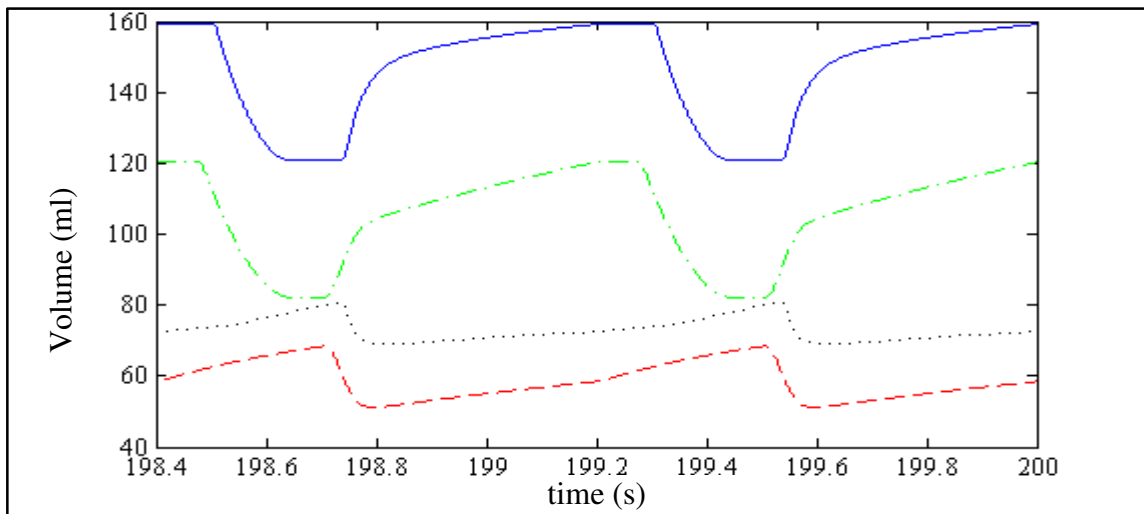


Figure 2.14. Volume of the heart chambers, left ventricular volume (continuous line), right ventricular volume (chain line), left atrial volume (dotted line), right atrial volume (dashed line)

Periodic peak flow occurs in the mitral valve and aortic valve flow rates, which are the same as the healthy cardiovascular system model simulation results. Average blood flow is nearly 2.88 l/min. The flow rates of the left heart valves and systemic blood vessels are shown in Figure 2.15.

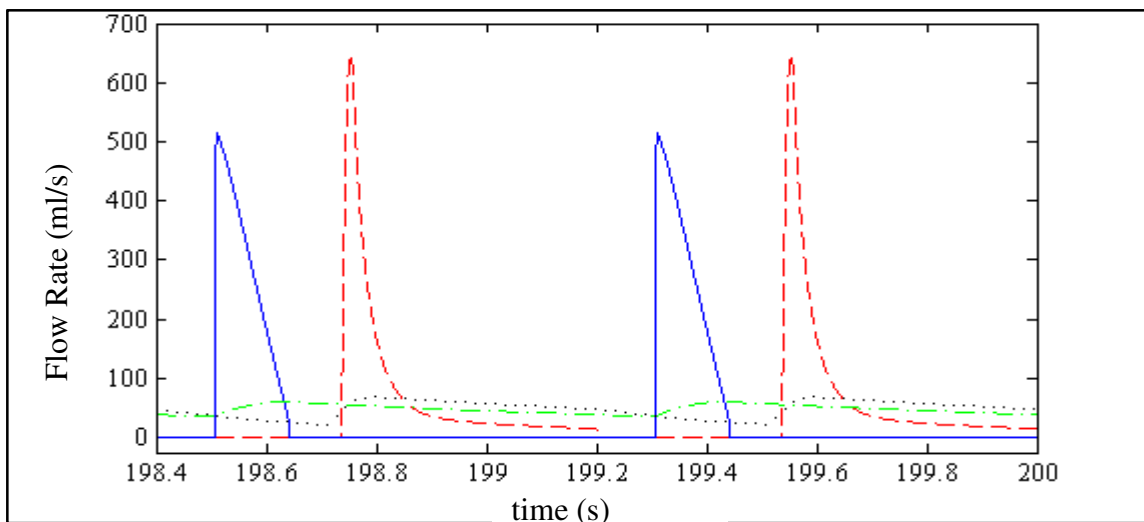


Figure 2.15. Flow rate of the mitral valve (dashed line), flow rate of the aortic valve (continuous line), flow rate of the systemic arteries (chain line), flow rate of the systemic veins (dotted line)

Periodic peak flow occurs in the tricuspid valve, pulmonary valve and pulmonary vein flow rates which is same as the healthy cardiovascular system model simulation results. The flow rates of the right heart valves and pulmonary blood vessels are shown in Figure 2.16.

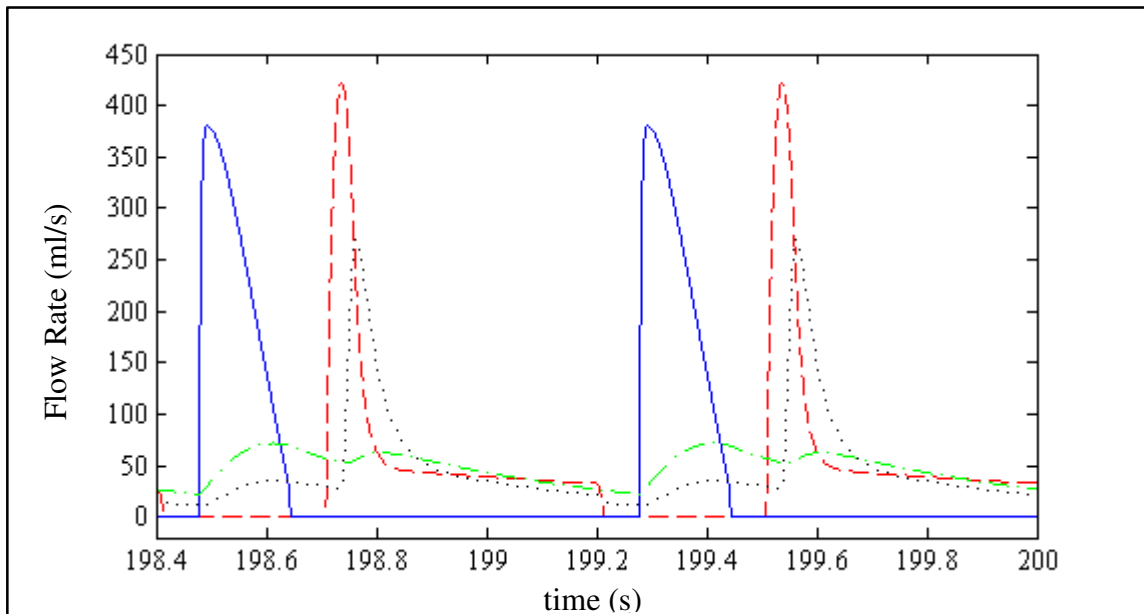


Figure 2.16. Flow rate of the tricuspid valve (dashed line), flow rate of the pulmonary valve (continuous line), flow rate of the pulmonary arteries (chain line), flow rate of the pulmonary veins (dotted line)

Ventricular pressure-volume loops of the diseased human cardiovascular system model are shown in Figure 2.17.

By using these results cardiac output is calculated as 2880 ml/min. Mean arterial blood pressure is 59.6 mmHg. The ejection fraction of the left ventricle is 0.241. Body surface area is assumed to be 1.90 m². By using these results cardiac index is calculated as 1.52 l/min/m². Simulation results are shown in Table 2.5.

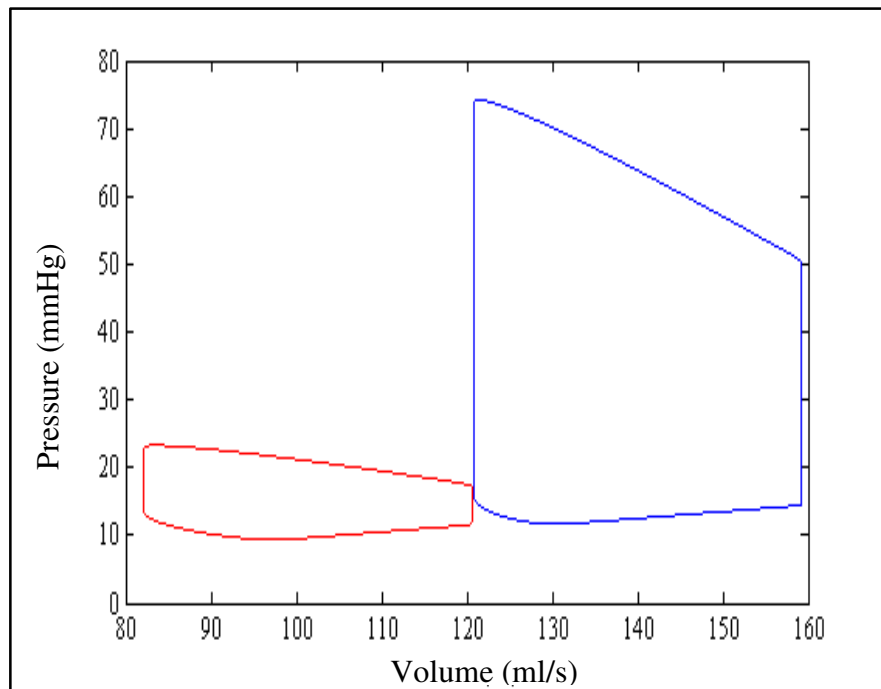


Figure 2.17. Pressure – volume loop of the diseased left ventricle (blue line) and right ventricle (red line)

Table 2.5. Simulation results of diseased human cardiovascular system model

Parameter	Max. Value	Min. Value	Parameter	Max. Value	Min. Value
P_{la} (mmHg)	16	15	P_{ra} (mmHg)	14	10
P_{lv} (mmHg)	74	11.5	P_{rv} (mmHg)	23	9
P_{sa} (mmHg)	74	50	P_{pa} (mmHg)	23	17
P_{sv} (mmHg)	15.5	15.5	P_{pv} (mmHg)	16	14
V_{la} (ml)	81	69	V_{ra} (ml)	69	51
V_{lv} (ml)	150.2	120.8	V_{rv} (ml)	120.6	82.2

2.4. DISCUSSION

In this chapter a numerical human cardiovascular system model was developed that will be used for LVAD simulations. The developed cardiovascular system model is a simple model which does not include the capillary blood vessels. The atrial contraction

was neglected in this model. Also the regurgitant blood flow through the aortic valve and pulmonary valve was not modeled. Simulation results of the simple healthy cardiovascular system are in an acceptable range [44].

The pathological condition was obtained by decreasing the maximum ventricular elastance function values and increasing the left ventricular zero pressure filling volume value. These changes provide a systolic left ventricular pressure which is under 90 mmHg as mentioned in section 2.1.3.

As it is seen in the simulation results, decreasing maximum values of elastance functions cause a decrease in ventricular systolic pressure values and an increase in ventricular volume values as expected. Due to decrease in left ventricular pressure, arterial pressure decreases. This decrease causes the mean arterial pressure to drop from 95.8 mmHg to 59.6 mmHg. Also a considerable decrement occurs in ventricular stroke volume values. Decrease in ventricular stroke volume causes a decrease in cardiac output. Cardiac output decreases from 5.2 l/min to 2.88 l/min in diseased cardiovascular model simulations as expected. Instantaneous peak flow rate values of heart valves decrease considerably. Cardiac index value decreases from 2.74 l/min/m² to 1.52 l/min/m² and ejection fraction value decreases from 0.567 to 0.241.

Under these conditions LVAD assistance can be recommended as described in section 2.1.3.

3. MODELING OF THE LEFT VENTRICULAR ASSIST DEVICES

Empirical models were developed by using static pressure-flow rate diagrams. In this chapter development of a numerical pump model was explained for Heart Turcica axial and Heart Turcica centrifugal V13.

3.1. THE LEFT VENTRICULAR ASSIST DEVICES

The left ventricular assist devices (LVADs) are devices that partially or completely support the failing left ventricle. In a failing left ventricle systolic left ventricular pressure and systolic aortic pressure drops. LVADs support left ventricle with a rotating impeller by increasing the pressure difference between aorta and left ventricle [2]. In other words rotating impeller cause a pressure difference between outlet and inlet of an LVAD. LVADs are used as bridge to recovery and bridge to transplantation because they do not require removal of the heart [1].

A short literature survey of the ventricular assist devices is shown in this section of the thesis.

Micomed DeBakey ventricular assist device is an axial flow pump that can pump 10 l/min. It is inserted between the apex of the heart and the aorta. This pump consists of an inducer, an impeller and a diffuser. Also it includes a flowmeter to measure the pump flow [2].

Jarvik 2000 is an axial flow pump which produces 7 l/min flow. It operates at 8000 to 12000 rpm. This pump is inserted in the ventricle and has an outflow cannula that anastomosed to the ascending aorta [2].

Heartmate is a pulsatile left ventricular assist device. This left ventricular assist device has 9 l/min pumping capacity. The stroke volume is 83 ml in this flow rate. To use this device in patient, patient's body surface area has to be greater than 1.5 m² [2].

Heartmate II is an axial flow pump that and produce flow rate greater than 10 l/min speeds at greater than 10000 rpm. This pump is inserted between the apex of the heart and the aorta like Micomed DeBakey ventricular assist device [2].

Novacor is a pulsatile left ventricular assist device as Heartmate. This pump is placed in the left upper abdominal quadrant and the inflow tract is connected to the left ventricular apex [2].

Arrow Lionheart LVD-2000 is a totally implantable pulsatile device. Maximum pump flow is 8 l/min with 64 ml stroke volume in this device [2].

3.2. MODELING OF HEART TURCICA AXIAL

An empirical numerical model which was developed by using CFD analysis data were used for the Heart Turcica axial [20]. The empirical model is shown below.

$$\Delta P = C_1 Q_p + C_2 \omega^2 \quad (3.1)$$

Here C_1 and C_2 are empirically determined coefficients, Q_p is the pump flow rate, ω is rotation speed of the impeller and ΔP is the pressure difference between outlet and inlet of the pump.

A commonly used model was adopted for the mechanical part of the heart pump [21].

$$J \frac{d\omega}{dt} = T_e - (C_0 + C_v \omega) - T_p \quad (3.2)$$

Where J is the rotor inertia, T_e is motor torque, C_0 is static friction torque, C_v is viscous damping factor of the motor used in the experiments. T_p is the load torque on the pump. The used electric motor in the experiments is Faulhaber 2057 S 024 B K1155 brushless DC servomotor.

The T_e term in the equation 3.2 is expressed as shown below.

$$T_e = k_m I \quad (3.3)$$

In Equation 3.3 k_m denotes torque constant and I denotes current. For load torque on the pump an empirical expression was developed that contains the rotation speed of the impeller and flow rate of the pump. The developed empirical expression is shown below.

$$T_p = K_1 \omega^2 + K_2 Q_p \omega + K_3 Q_p \quad (3.4)$$

In the equation 3.4 K_1 , K_2 , K_3 are empirically determined coefficients and Q_p is the flow rate of the pump.

To determine the C_1 and C_2 coefficients the data shown in Figure 3.1 are fitted to a line by using least squares method. Figure 3.1 shows the pressure vs. flow rate data of Heart Turcica axial that is obtained from CFD analysis.

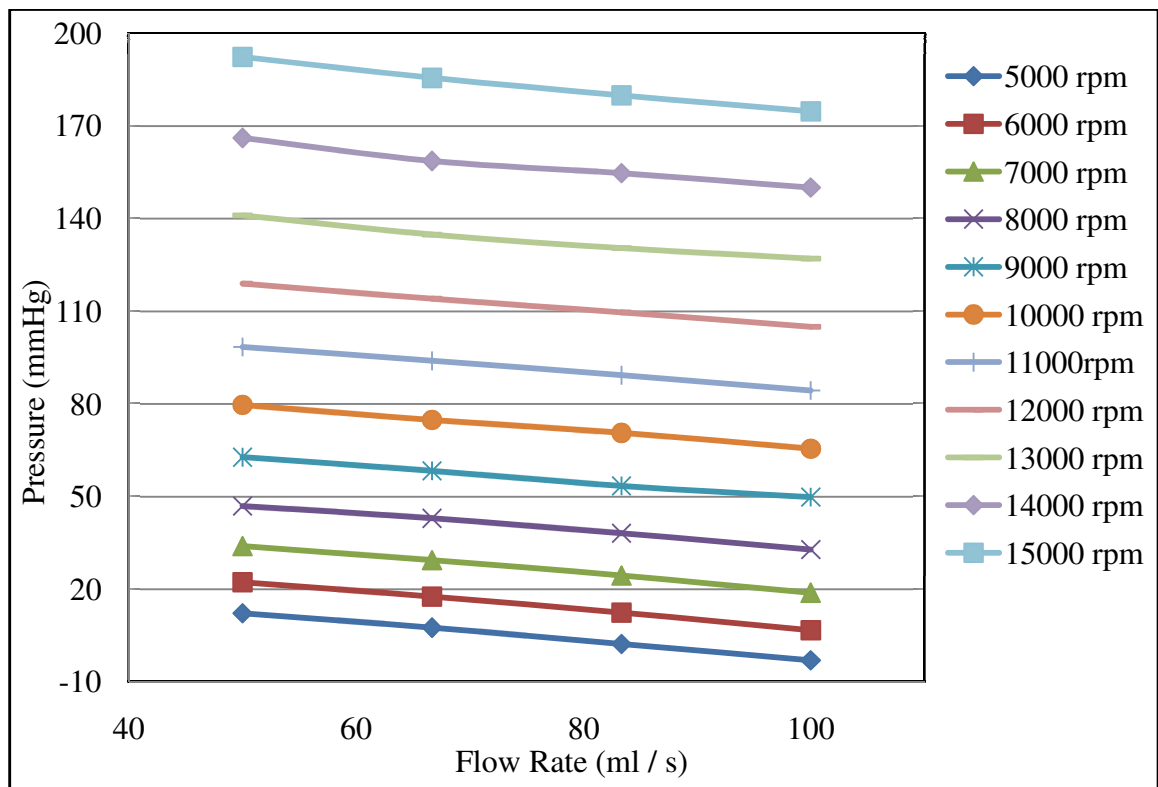


Figure 3.1. Pressure – flow rate diagram of the Heart Turcica axial

A least square fit operation was conducted to determine the C_1 and C_2 coefficients.

At first, a 44×1 matrix which contains the pressure data was created. This matrix is shown below.

$$\mathbf{A} = \begin{bmatrix} 12.42 \\ 7.33 \\ \cdot \\ \cdot \\ \cdot \\ 180.21 \\ 174.35 \end{bmatrix}_{44 \times 1} \quad (3.5)$$

A 44×2 matrix which contains flow rate data at its first column and square of the rotation speed data at its second column was created. Although unit of the rotation speed data is 'rpm' in table '1/s' was used for calculations. This matrix is shown below.

$$\mathbf{B} = \begin{bmatrix} 50 & 6944.44 \\ 66.67 & 6944.44 \\ \cdot & \cdot \\ \cdot & \cdot \\ \cdot & \cdot \\ \cdot & \cdot \\ 83.33 & 62500 \\ 100 & 62500 \end{bmatrix}_{44 \times 2} \quad (3.6)$$

The coefficients of the equation are the elements of a matrix which is a 2×1 matrix. This matrix is shown below.

$$\mathbf{C} = \begin{bmatrix} C_1 \\ C_2 \end{bmatrix}_{2 \times 1} \quad (3.7)$$

Coefficients C_1 and C_2 are calculated by using equations shown below.

$$\mathbf{A} = \mathbf{B} \mathbf{C} \quad (3.8)$$

$$\mathbf{C} = (\mathbf{B}^T \mathbf{B})^{-1} (\mathbf{B}^T \mathbf{A}) \quad (3.9)$$

C_1 and C_2 are calculated as -0.23779 mmHg/ml/s and 0.00323 mmHg/s² respectively. According to these results final form of the Equation 3.1 is shown below.

$$\Delta P = -0.23779 Q + 0.00323 \omega^2 \quad (3.10)$$

The least square fit data and errors are shown in Table 3.1.

Table 3.1. The least square fit data and errors

ω (rpm)	Q (ml/s)	ΔP (mmHg), CFD Analysis Data	ΔP (mmHg), Least Squares Fit Data	Error (mmHg)
5000	50.00	12.24	10.54	1.70
	66.67	7.54	6.58	0.96
	83.33	2.35	2.61	-0.27
	100.00	-3.00	-1.35	-1.65
6000	50.00	22.29	20.41	1.88
	66.67	17.64	16,45	1,19
	83.33	12.48	12,48	0,00
	100.00	6.80	8,52	-1,73
7000	50.00	34.04	32,07	1,96
	66.67	29.48	28,11	1,36
	83.33	24.50	24,15	0,35
	100.00	18.86	20,18	-1,33
8000	50.00	46.98	45.53	1.44
	66.67	42.99	41.57	1.42
	83.33	38.16	37.61	0.55
	100.00	32.85	33.64	-0.79
9000	50.00	62.77	60.79	1.98
	66.67	58.41	56.82	1.58
	83.33	53.49	52.86	0.62
	100.00	49.86	48.90	0.96
10000	50.00	79.72	77.83	1.88
	66.67	74.86	73.87	0.98
	83.33	70.67	69.91	0.76
	100.00	65.53	65.94	-0.42
11000	50.00	98.46	96.67	1.78
	66.67	93.95	92.71	1.23
	83.33	89.32	88.75	0.56
	100.00	84.37	84.78	-0.42
12000	50.00	118.93	117.31	1.61
	66.67	114.06	113.35	0.71
	83.33	109.61	109.38	0.21
	100.00	104.99	105.42	-0.44

Table 3.1. The least square fit data and errors (continued)

13000	50.00	141.07	139.74	1.32
	66.67	134.87	135.78	-0.92
	83.33	130.44	131.81	-1.38
	100.00	127.05	127.85	-0.81
14000	50.00	166.09	163.97	2.11
	66.67	158.65	160.00	-1.37
	83.33	154.73	156.04	-1.32
	100.00	150.06	152.08	-2.02
15000	50.00	192.34	189.99	2.34
	66.67	185.59	186.02	-0.45
	83.33	179.91	182.06	-2.16
	100.00	174.71	178.10	-3.40

To determine K_1 , K_2 , K_3 coefficients the data shown in Figure 3.2 are fitted to a second order polynomial. Figure 3.2 shows the torque vs. rotation speed data of Heart Turcica axial that obtained from CFD analysis.

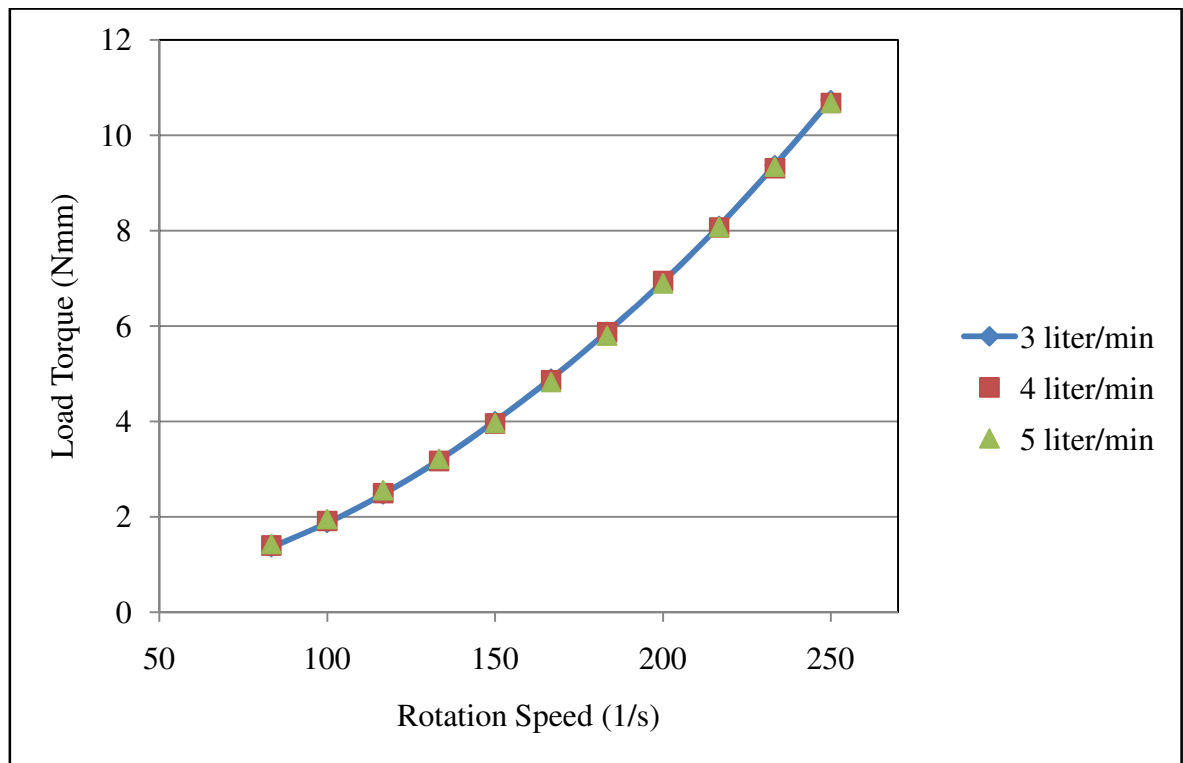


Figure 3.2. Load torque – rotation speed diagram of the Heart Turcica axial

A least square fit operation was conducted to determine the K_1 and K_2 and K_3 coefficients. At first a 33×1 matrix which contains the load torque data was created. This matrix is shown below.

$$D = \begin{bmatrix} 1.3652 \\ 1.869 \\ \cdot \\ \cdot \\ 9.316 \\ 10.6725 \end{bmatrix}_{33 \times 1} \quad (3.11)$$

A 33×3 matrix which contains square of rotation speed data at its first column, multiplication of rotation speed and pump flow rate at its second column and pump flow rate data at its third column was created. Although unit of the rotation speed data is 'rpm' and flow rate data is 'l/min' in the table '1/s' and 'ml/s' were used respectively for calculations. This matrix is shown below.

$$E = \begin{bmatrix} 6944.44 & 4166.67 & 50.00 \\ 10000.00 & 5000.00 & 50.00 \\ \cdot & \cdot & \cdot \\ \cdot & \cdot & \cdot \\ 54444.44 & 11666.67 & 83.33 \\ 62500.00 & 12500.00 & 83.33 \end{bmatrix}_{33 \times 3} \quad (3.12)$$

The coefficients of the equation are the elements of a matrix which is a 3×1 matrix. This matrix is shown below.

$$K = \begin{bmatrix} K_1 \\ K_2 \\ K_3 \end{bmatrix}_{3 \times 1} \quad (3.13)$$

Coefficients K_1 , K_2 and K_3 are calculated by using equations shown below.

$$D = E K \quad (3.14)$$

$$K = (E^T E)^{-1} (E^T D) \quad (3.15)$$

K_1 , K_2 and K_3 are calculated as 0.00017 Nmm/s^2 , $-3.45511 \times 10^{-5} \text{ Nmm/ml}$ and 0.00596 Nmm/ml/s respectively. According to these results final form of the equation 3.4 is shown below.

$$T_p = 0.00017 \omega^2 - 3.45511 \times 10^{-5} Q_p \omega + 0.00596 Q_p \quad (3.16)$$

The least square fit data and errors are shown in Table 3.2.

Table 3.2. The least square fit data and errors

Q (l/min)	ω (rpm)	Torque (N mm) CFD Analysis Data	Torque (N mm) Least Squares Fit Data	Error
3	5000	1.365	1.365	0
	6000	1.874	1.869	0.005
	7000	2.475	2.469	0.006
	8000	3.188	3.167	0.021
	9000	4.008	3.961	0.047
	10000	4.901	4.852	0.049
	11000	5.880	5.841	0.039
	12000	6.936	6.925	0.010
	13000	8.102	8.107	-0.005
	14000	9.380	9.386	-0.006
	15000	10.739	10.761	-0.022
4	5000	1.400	1.416	-0.016
	6000	1.913	1.910	0.003
	7000	2.498	2.501	-0.003
	8000	3.173	3.189	-0.017
	9000	3.957	3.974	-0.017
	10000	4.864	4.856	0.008
	11000	5.871	5.834	0.037
	12000	6.944	6.910	0.034
	13000	8.069	8.082	-0.013
	14000	9.311	9.351	-0.040
	15000	10.681	10.717	-0.036
5	5000	1.433	1.467	-0.035
	6000	1.955	1.952	0.003
	7000	2.554	2.534	0.020
	8000	3.217	3.212	0.005
	9000	3.970	3.987	-0.017
	10000	4.828	4.859	-0.031
	11000	5.799	5.828	-0.029

Table 3.2. The least square fit data and errors (continued)

12000	6.891	6.894	-0.003
13000	8.073	8.056	0.016
14000	9.342	9.316	0.027
15000	10.676	10.672	0.004

Rotor inertia, torque constant, static friction torque and viscous damping factor values are taken from [57]. These values are shown in Table 3.3.

Table 3.3. Values of the Parameters in Eq. 3.2 and Eq. 3.3

J (g cm ²)	k _m (N mm/A)	C ₀ (N mm)	C _v (N mm/rpm)
3.95	8.56	0.28	3.7×10 ⁻⁵

3.3. MODELING OF HEART TURCICA CENTRIFUGAL

A second order numerical model was developed for Heart Turcica Centrifugal V13 by using experimental results. This numerical model is shown below.

$$\Delta P = L_1 Q_p^2 + L_2 Q_p + L_3 \omega^2 \quad (3.17)$$

In the equation 3.17 L_1 , L_2 and L_3 are empirically determined coefficients. Only pressure – flow rate relation was considered in the Heart Turcica centrifugal model. A mechanical model was not developed for Heart Turcica centrifugal. The pressure–flow rate diagram of Heart Turcica centrifugal is shown in Figure 3.3.

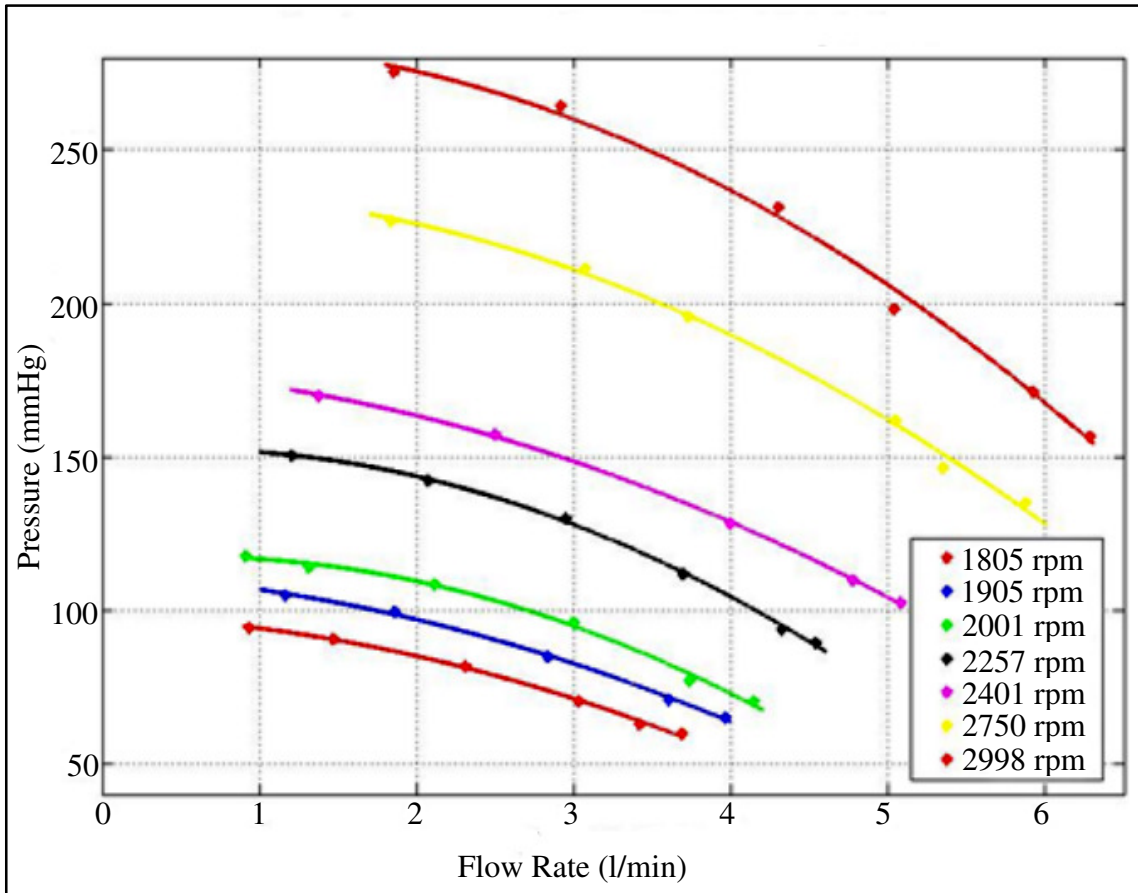


Figure 3.3. Pressure – flow rate diagram of the Heart Turcica centrifugal

To determine L_1 , L_2 , L_3 coefficients the data shown in the Figure 3.3 are fitted to a second order polynomial by using least squares method.

A least square fit operation was conducted. At first a 42×1 matrix which contains the pressure difference data was created. This matrix is shown below.

$$F = \begin{bmatrix} 94.37 \\ 90.12 \\ \cdot \\ \cdot \\ \cdot \\ \cdot \\ 170.15 \\ 154.63 \end{bmatrix}_{42 \times 1} \quad (3.18)$$

A 42×3 matrix which contains square of pump flow rate data at its first column, pump flow rate data at its second column and square of the rotation speed data at its third column was created. Although unit of the rotation speed data is 'rpm' in the table '1/s' was used for calculations. This matrix is shown below.

$$\mathbf{G} = \begin{bmatrix} 15.61 & 243.67 & 905.01 \\ 24.63 & 606.64 & 905.01 \\ \cdot & \cdot & \cdot \\ \cdot & \cdot & \cdot \\ \cdot & \cdot & \cdot \\ \cdot & \cdot & \cdot \\ 98.91 & 9783.19 & 2496.67 \\ 104.92 & 11008.21 & 2496.67 \end{bmatrix}_{42 \times 3} \quad (3.19)$$

The coefficients of the equation are the elements of a 3×1 matrix. It is shown below.

$$\mathbf{L} = \begin{bmatrix} L_1 \\ L_2 \\ L_3 \end{bmatrix}_{3 \times 1} \quad (3.20)$$

Coefficients L_1 , L_2 and L_3 are calculated by using equations shown below.

$$\mathbf{F} = \mathbf{G} \mathbf{L} \quad (3.21)$$

$$\mathbf{L} = (\mathbf{G}^T \mathbf{G})^{-1} (\mathbf{G}^T \mathbf{F}) \quad (3.22)$$

L_1 , L_2 and L_3 are calculated as $-0.00955 \text{ mmHg/ml}^2/\text{s}^2$, -0.18338 mmHg/s and 0.11446 mmHg/s^2 respectively. According to these results final form of the equation 3.17 is shown below.

$$\Delta P = -0.00955 Q_p^2 - 0.18338 Q_p + 0.11446 \omega^2 \quad (3.23)$$

The least square fit data and errors are shown in Table 3.4.

Table 3.4. The least square fit data and errors

ω (rpm)	Q (ml/s)	ΔP (mmHg), Experimental Data	ΔP (mmHg), Least Squares Fit Data	Error (mmHg)
1805	15.61	94.12	98.40	-4.28
	24.63	90.29	93.28	-2.99
	38.74	81.47	82.15	-0.68
	50.57	70.00	69.89	0.11
	57.04	62.06	62.06	0.00
	61.50	60.00	56.20	3.81
1905	19.53	104.41	108.16	-3.75
	31.00	98.83	100.52	-1.70
	40.10	91.47	92.67	-1.20
	47.20	85.00	85.45	-0.45
	60.13	70.29	69.83	0.47
	65.96	65.00	61.74	3.26
2001	15.16	117.65	122.33	-4.68
	21.89	114.12	118.71	-4.59
	35.37	107.94	108.87	-0.93
	50.02	95.88	94.23	1.65
	62.41	77.06	78.67	-1.61
	68.96	69.71	69.24	0.46
2257	20.26	150.30	154.33	-4.03
	34.28	142.06	144.46	-2.39
	49.02	129.12	130.02	-0.90
	61.59	112.06	114.45	-2.38
	72.06	93.83	99.16	-5.34
	75.79	88.53	93.21	-4.68
2401	22.99	169.42	174.03	-4.61
	41.65	156.18	159.08	-2.90
	52.30	145.59	147.57	-1.98
	66.68	128.24	128.59	-0.36
	79.61	109.71	108.16	1.55
	84.62	102.36	99.39	2.97
2750	30.82	226.48	225.73	0.75
	51.21	210.59	206.01	4.58
	62.22	195.59	192.06	3.53
	84.07	161.18	157.53	3.65
	89.26	145.59	147.98	-2.39
	97.91	134.71	130.94	3.77
2998	30.91	274.70	270.98	3.72
	48.75	263.54	254.13	9.40
	71.78	230.89	223.40	7.49
	84.16	197.65	202.69	-5.03
	98.91	170.59	174.20	-3.61
	104.92	156.47	161.40	-4.93

3.4. DISCUSSION

In this chapter, numerical models for Heart Turcica axial and Heart Turcica centrifugal were developed.

A linear empirical model was developed for Heart Turcica axial by using CFD analysis results. The mechanical model of the pump includes motor torque, friction torque and load torque terms. Also an empirical model for load torque term which is a second order polynomial was developed by using CFD analysis results. The differences between CFD analysis results and least square fit operation results are very low in these models. Therefore these models are acceptable for using in the simulations. Rotor inertia, torque constant, static friction torque and viscous damping factor values are taken from catalogue of the motor manufacturer.

The empirical model developed for Heart Turcica centrifugal is for the 13th version of Heart Turcica centrifugal. Data of the other versions are not available. The mechanical engineering department of the Koç University will decide which version will be used as a cardiac assist device.

4. COMBINED MODEL OF CVS AND HEART PUMPS

Before talking about the combined model of cardiovascular system and the left ventricular assist devices, the physiologically significant pumping states must be explained. Five significant pumping states occur in consequence of varying pumping speed. These pumping states are regurgitant pump flow, ventricular ejection, non-opening aortic valve over the cardiac cycle, intermittent collapse of ventricle wall and continuous collapse of ventricle wall. Details about significant pumping states can be found in [22-26]. In the following section these pumping states are explained briefly.

4.1. PHYSIOLOGICALLY SIGNIFICANT PUMPING STATES IN LVADS

The regurgitant pump flow state occurs at relatively low pumping speeds. Pressure difference between the outlet and inlet of the pump is higher than the pressure difference created by the heart pump. Hence the pump flow regurgitates during every cardiac cycle. Usually negative pump flow is observed at the diastolic phase.

The heart pump and the left ventricle pump blood together at the ventricular ejection state. The heart pump provides a continuous blood flow and the left ventricle pumps blood at systolic phase. Therefore pumping together occurs at the systolic phase.

The aortic valve does not open because of relatively high aortic pressure at the non-opening aortic valve over the cardiac cycle state. Only heart pump operates at this state. The pressure in the left ventricle is not sufficient to open the aortic valve.

Increasing pump rotation speed causes pressure decrease in the left ventricle. If the rotation speed of the pump increases too much, pressure in the left ventricle decreases too much and mitral valve remains open [52]. In this state pulsatility of the pump flow is very small. If the pressure in the left ventricle drops near zero the ventricle walls are sucked by the heart pump. This phenomenon is called the ventricular suction and provides harmful effects to the heart. Collapse of ventricle wall occurs at the relatively higher rotation

speeds in comparison to the other states. At this state pulsatility in pump flow and pressure difference across the pump can be observed.

4.2. COMBINED MODEL OF CARDIOVASCULAR SYSTEM AND LVADS

The pump models are connected between left ventricle and systemic arteries. Equations 2.14 and 2.20 were changed as shown below [56].

$$\frac{dV_{lv}}{dt} = Q_{lv,i} - Q_{lv,o} - Q_p \quad (4.1)$$

$$\frac{dP_{sa}}{dt} = \frac{Q_{ao} + Q_p - Q_{sa}}{C_{sa}} \quad (4.2)$$

ΔP term in the heart pump models denotes pressure difference between the outlet and inlet of the heart pumps. In other words ΔP is the pressure difference between aorta and left ventricle. Therefore these terms are used in equation 3.1 and equation 3.17 while implementing the pump models into the human cardiovascular system model.

To simulate the suction phenomenon more accurately and realistically the resistance at the inlet of the heart pump must be increased in suction condition. Therefore a variable resistance which is called suction resistance was defined at the inlet of the heart pump models [5]. The suction resistance is defined below.

$$R_{suc} = \begin{cases} 0, & P_{lv} > P_{th} \\ -3.5P_{lv} + 3.5P_{th}, & P_{lv} \leq P_{th} \end{cases} \quad (4.3)$$

P_{th} denotes threshold pressure value for suction condition in the equation 4.3. In the simulations 1 mmHg was used for P_{th} [5]. The block diagram of combined model of the human cardiovascular system model and heart pump is shown in Figure 4.1.

To assess the increasing rotation speed pressure pulsatility index, flow pulsatility index and current pulsatility index were defined. pressure pulsatility index, flow pulsatility index and current pulsatility index are shown below.

$$PI = \frac{\Delta P_{max} - \Delta P_{min}}{(\Delta P_{max} + \Delta P_{min})/2} \quad (4.4)$$

$$QI = \frac{Q_{max} - Q_{min}}{(Q_{max} + Q_{min})/2} \quad (4.5)$$

$$CI = \frac{C_{max} - C_{min}}{(C_{max} + C_{min})/2} \quad (4.6)$$

PI denotes pressure pulsatility index across the pump. ΔP_{max} and ΔP_{min} denote maximum pressure difference and minimum pressure difference across the pump respectively. QI denotes flow pulsatility index of the pump flow. ΔQ_{max} and ΔQ_{min} denote maximum pump flow and minimum pump flow that flow through the pump respectively. CI denotes current pulsatility index. C_{max} and C_{min} denote maximum motor current and minimum motor current respectively.

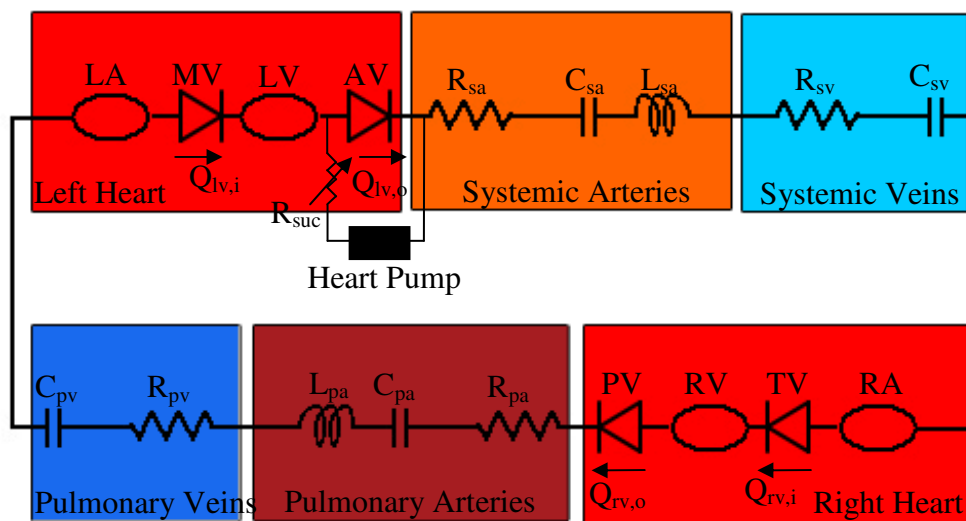


Figure 4.1. Block diagram of the human cardiovascular system model and heart pump

4.3. COMBINED MODEL OF CARDIOVASCULAR SYSTEM AND HEART TURCICA AXIAL

Heart Turcica axial model was implemented to diseased cardiovascular system model and simulations were performed to assess rotation speeds at which different

physiologically significant pumping states occur. Simulations were performed at operating speeds from 7000 rpm to 13000 rpm with 1000 rpm intervals. The hemodynamic variables are shown at these operating speeds in this part. (PI control was applied to rotation speed during simulations. Proportional and integral gain values are set to be one). Simulation results indicate PI control provides sufficiently stable speed response.

The used solver was ode15s and maximum step size was adjusted to 0.0001 s in the simulations. Steady results obtained after 60 heart beats.

4.3.1. Simulation Results at 7000 rpm Operating Speed

Operating speed of Heart Turcica axial was adjusted to 7000 rpm and simulations were performed at this constant operating speed. Pressure difference across the pump, left atrial pressure, left ventricular pressure and aortic pressure are shown in Figure 4.2.

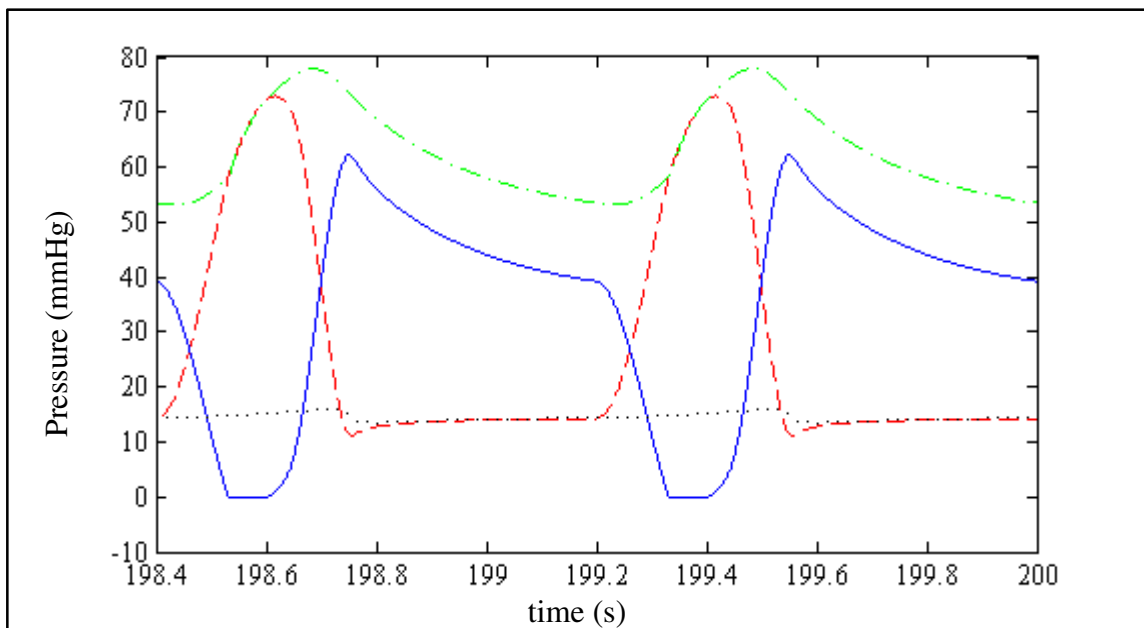


Figure 4.2. Pressure difference across the pump (continuous line), left atrial pressure (dotted line), left ventricular pressure (dashed line) and aortic pressure (chain line) at 7000 rpm operating speed

Maximum pressure difference across the pump is 62.1 mmHg and minimum pressure difference across the pump is -0.2 mmHg. Maximum left atrial pressure is 16.1 mmHg and minimum left atrial pressure is 13.5 mmHg. Maximum left ventricular pressure is 72.9 mmHg and minimum left ventricular pressure is 11.1 mmHg. Left ventricular pressure is above the threshold suction resistance value is defined in Equation 4.3. Therefore pump inlet pressure is same as the left ventricular pressure. Maximum aortic pressure is 77.9 mmHg and minimum aortic pressure is 53.1 mmHg at 7000 rpm pump operating speed.

Left ventricular and left atrial volumes are shown in Figure 4.3 at 7000 rpm operating speed.

End diastolic volume of left ventricle is 147.3 ml, end systolic volume of left ventricle is 100.8 ml and stroke volume of left ventricle is 46.5 ml. Maximum volume of left atrium is 80.3 ml and minimum volume at left atrium is 67.6 ml at 7000 rpm operating speed.

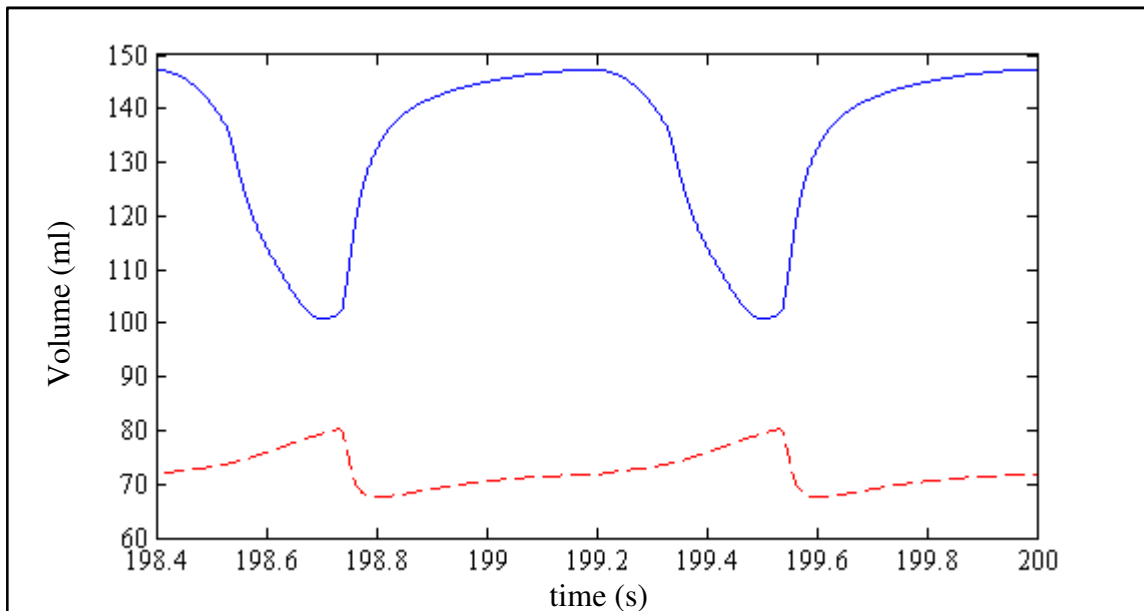


Figure 4.3 Left ventricular volume (continuous line) and left atrial volume (dashed line) at 7000 rpm pump operating speed

Pump flow rate, mitral valve flow rate and aortic valve flow rate at 7000 rpm operating speed are shown in Figure 4.4.

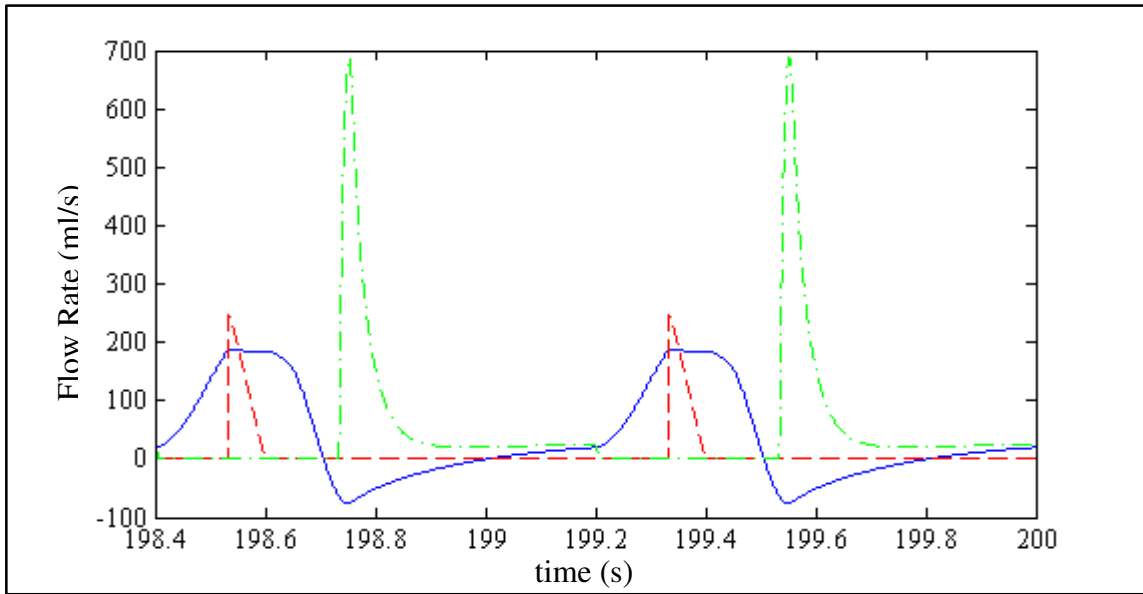


Figure 4.4. Pump flow rate (continuous line), mitral valve flow rate (chain line) and aortic valve flow rate (dashed line) at 7000 rpm operating speed

At 7000 rpm operating speed heart and Heart Turcica axial are operating together. Also pump flow regurgitates due to relatively high aortic pressure in diastolic phase.

Motor current at 7000 rpm operating speed is shown Figure 4.5.

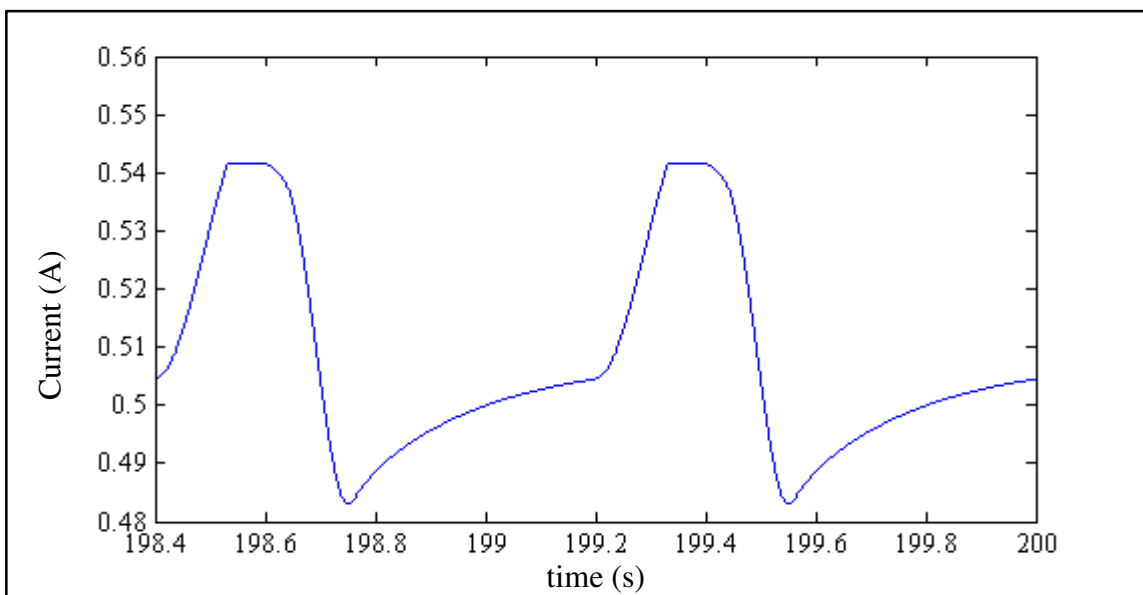


Figure 4.5. Motor current at 7000 rpm operating speed

Motor current varies between 0.542 A and 0.483 A at 7000 rpm operating speed. Total cardiac output is 2.93 l/min at 7000 rpm operating speed. Pressure pulsatility index is 2.01, flow pulsatility index is 4.78 and current pulsatility index is 0.115 at this speed. Results that are explained above are shown in Table 4.1.

Table 4.1. Simulation results for 7000 rpm operating speed

Parameter	Max. Value	Min. Value	Parameter	Max. Value	Min. Value
ΔP_{pump} (mmHg)	62.1	-0.2	V_{la} (ml)	80.3	67.6
P_{in} (mmHg)	72.9	11.1	V_{lv} (ml)	147.3	100.8
P_{la} (mmHg)	16.1	13.5	Stroke V_{lv} (ml)	46.5	
P_{lv} (mmHg)	72.9	11.1	I_{motor} (A)	0.542	0.483
P_{ao} (mmHg)	77.9	53.1	CO (l/min)	2.93	

4.3.2. Simulation Results at 7565 rpm Operating Speed

At 7565 rpm operating speed flow through aortic valve disappears. Therefore simulations are performed at 7565 rpm constant operating speed. Pressure difference across the pump, left atrial pressure, left ventricular pressure and aortic pressure at 7565 rpm operating speed is shown in Figure 4.6.

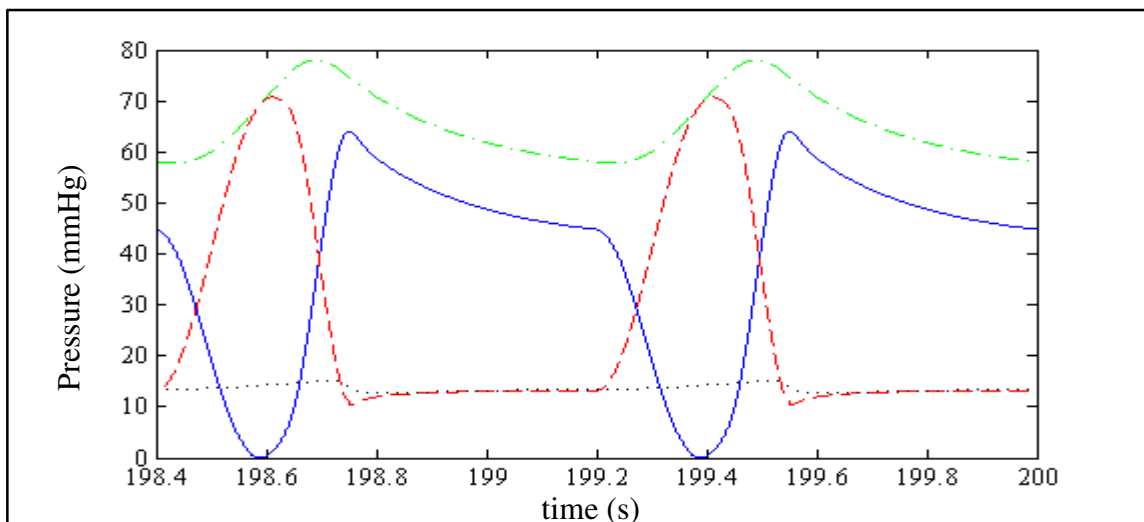


Figure 4.6. Pressure difference across the pump (continuous line), left atrial pressure (dotted line), left ventricular pressure (dashed line) and aortic pressure (chain line) at 7565 rpm operating speed

Maximum pressure difference across the pump is 64 mmHg and minimum pressure difference across the pump is zero. Maximum left atrial pressure is 15.2 mmHg and minimum left atrial pressure is 12.7 mmHg. Maximum left ventricular pressure is 70.7 mmHg and minimum left ventricular pressure is 10.5 mmHg. Left ventricular pressure is above the threshold suction resistance value that defined in Equation 4.3. Therefore pump inlet pressure is the same as left ventricular pressure. Maximum aortic pressure is 78 mmHg and minimum aortic pressure is 57.8 mmHg at 7565 rpm pump operating speed.

At 7565 rpm operating speed, flow through aortic valve disappears. In other words left ventricular pressure is not sufficient to open the aortic valve. Therefore 7565 rpm is accepted as boundary operating speed between ventricular ejection state and aortic valve non – opening state. The comparison of left ventricular pressure and aortic pressure at 7565 rpm is shown in Figure 4.7.

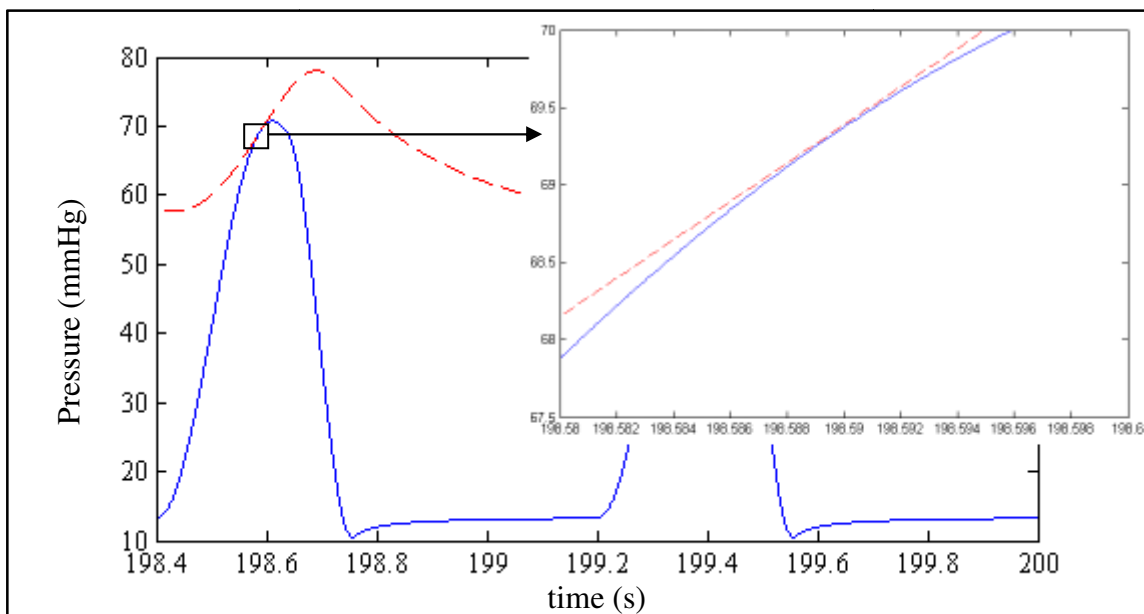


Figure 4.7. Left ventricular pressure (continuous line), aortic pressure (dashed line) at 7565 rpm operating speed

Left ventricular and left atrial volumes are shown in Figure 4.8 at 7565 rpm operating speed.

End diastolic volume of left ventricle is 137.2 ml, end systolic volume of left ventricle is 95.5 ml and stroke volume of left ventricle is 41.7 ml. Maximum volume of left atrium is 76 ml and minimum volume at left atrium is 63.7 ml at 7565 rpm operating speed.

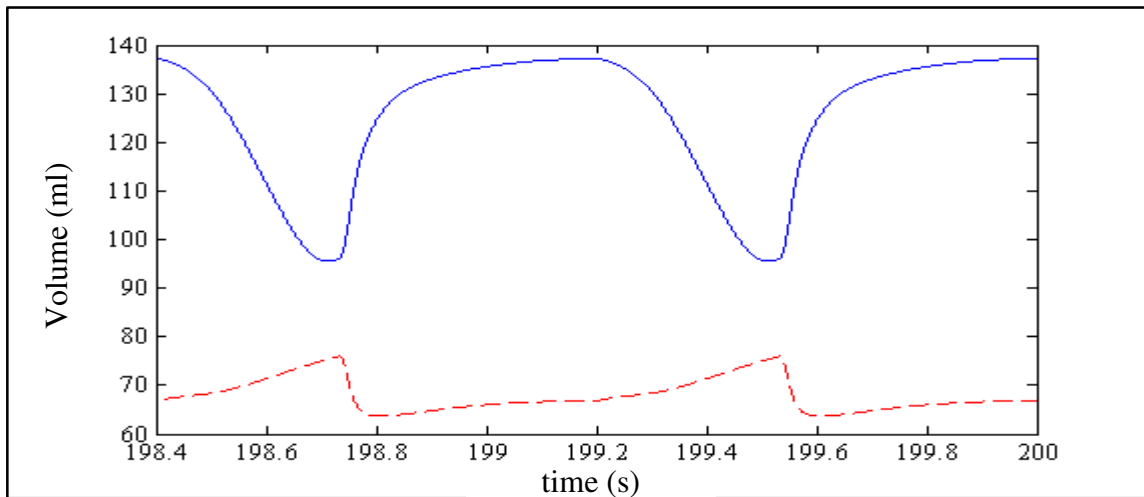


Figure 4.8 Left ventricular volume (continuous line) and left atrial volume (dashed line) at 7565 rpm pump operating speed

Pump flow rate, mitral valve flow rate and aortic valve flow rate at 7565 rpm operating speed are shown in Figure 4.9.

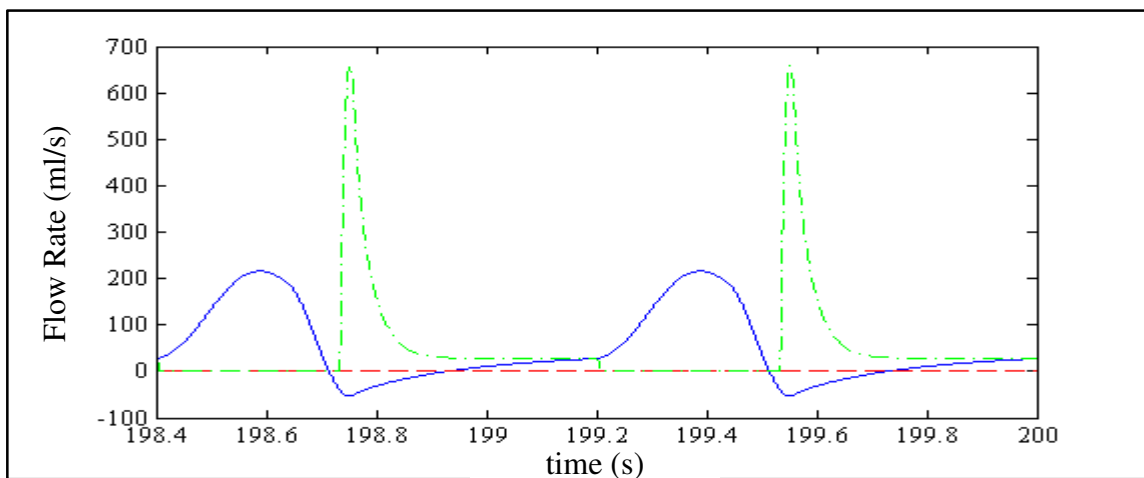


Figure 4.9. Pump flow rate (continuous line), mitral valve flow rate (chain line) and aortic valve flow rate (dashed line) at 7565 rpm operating speed

At 7565 rpm operating speed heart and Heart Turcica axial are not operating together due to relatively low pressure in left ventricle. Pump flow regurgitates due to relatively high aortic pressure in diastolic phase.

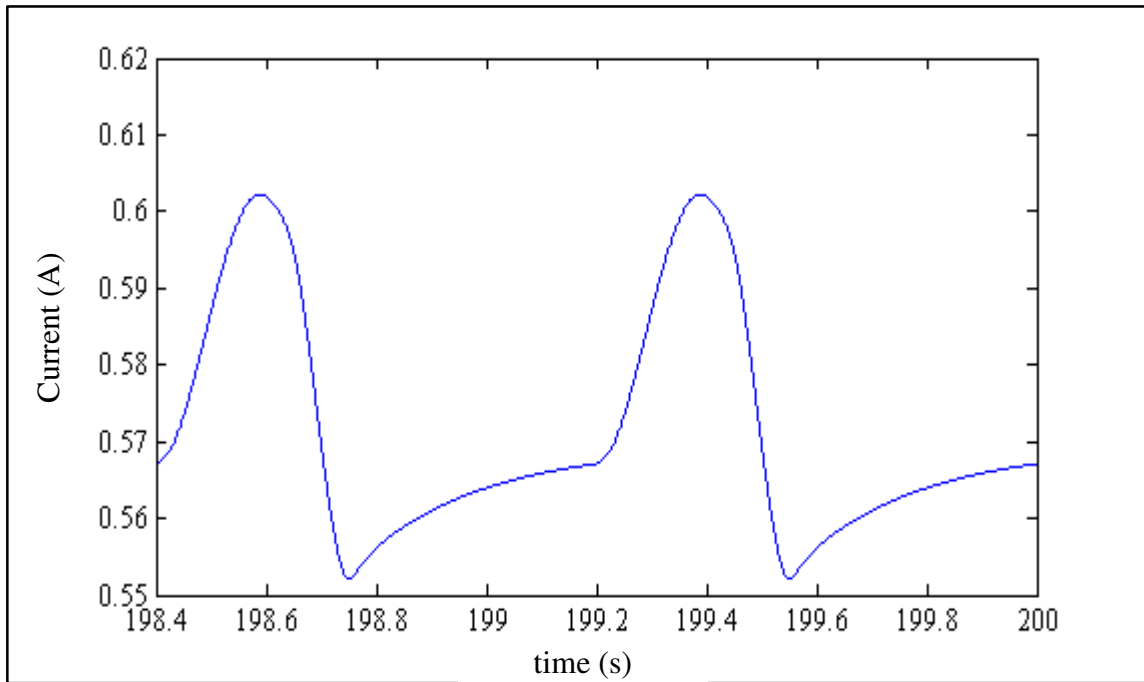


Figure 4.10. Motor current at 7565 rpm operating speed

Motor current varies between 0.602 A and 0.552 A at 7565 rpm operating speed. Total cardiac output is 3.08 l/min at 7565 rpm operating speed. Pressure pulsatility index is 2, flow pulsatility index is 3.30 and current pulsatility index is 0.087 at this speed. Results that are explained above are shown in Table 4.2.

Table 4.2. Simulation results for 7565 rpm operating speed

Parameter	Max. Value	Min. Value	Parameter	Max. Value	Min. Value
ΔP_{pump} (mmHg)	64	0	V_{la} (ml)	76	63.7
P_{in} (mmHg)	70.7	10.5	V_{lv} (ml)	137.2	95.5
P_{la} (mmHg)	15.2	12.7	Stroke V_{lv} (ml)	41.7	
P_{lv} (mmHg)	70.7	10.5	I_{motor} (A)	0.602	0.552
P_{ao} (mmHg)	78	57.8	CO (l/min)	3.08	

4.3.3. Simulation Results at 8000 rpm Operating Speed

Operating speed of Heart Turcica axial was adjusted to 8000 rpm and simulations were performed at this constant operating speed. Pressure difference across the pump, left atrial pressure, left ventricular pressure and aortic pressure are shown in Figure 4.11.

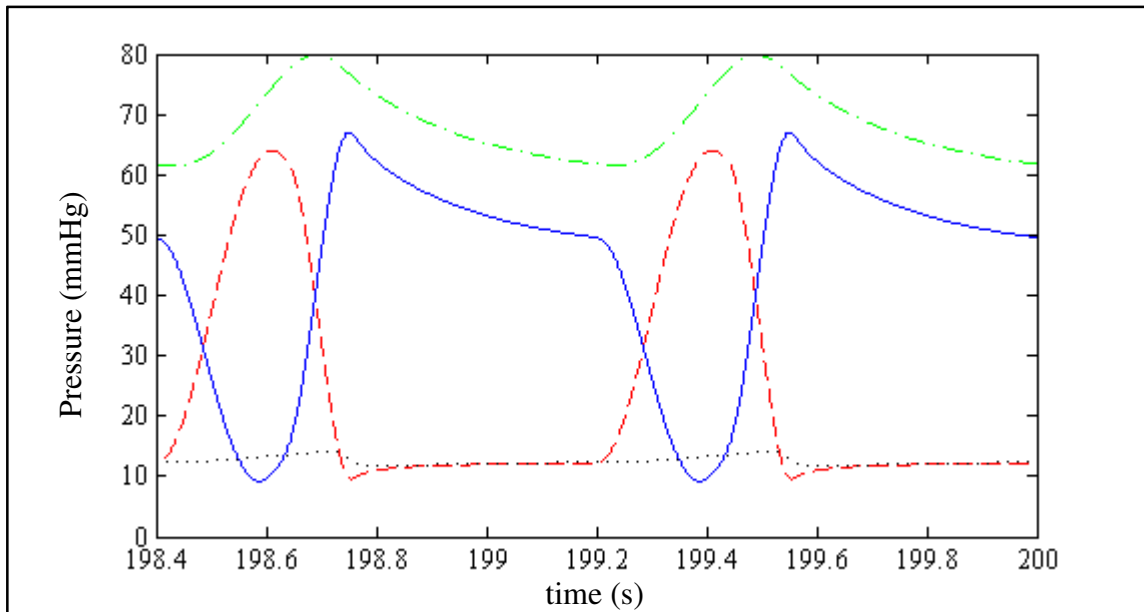


Figure 4.11. Pressure difference across the pump (continuous line), left atrial pressure (dotted line), left ventricular pressure (dashed line) and aortic pressure (chain line) at 8000 rpm operating speed

Maximum pressure difference across the pump is 67 mmHg and minimum pressure difference across the pump is 9.2 mmHg. Maximum left atrial pressure is 14.2 mmHg and minimum left atrial pressure is 11.8 mmHg. Maximum left ventricular pressure is 64 mmHg and minimum left ventricular pressure is 9.5 mmHg. Left ventricular pressure is above the threshold suction resistance value defined in Equation 4.3. Therefore pump inlet pressure is the same as left ventricular pressure. Maximum aortic pressure is 79.8 mmHg and minimum aortic pressure is 61.5 mmHg at 8000 rpm pump operating speed.

Left ventricular and left atrial volumes are shown in Figure 4.12 at 8000 rpm operating speed.

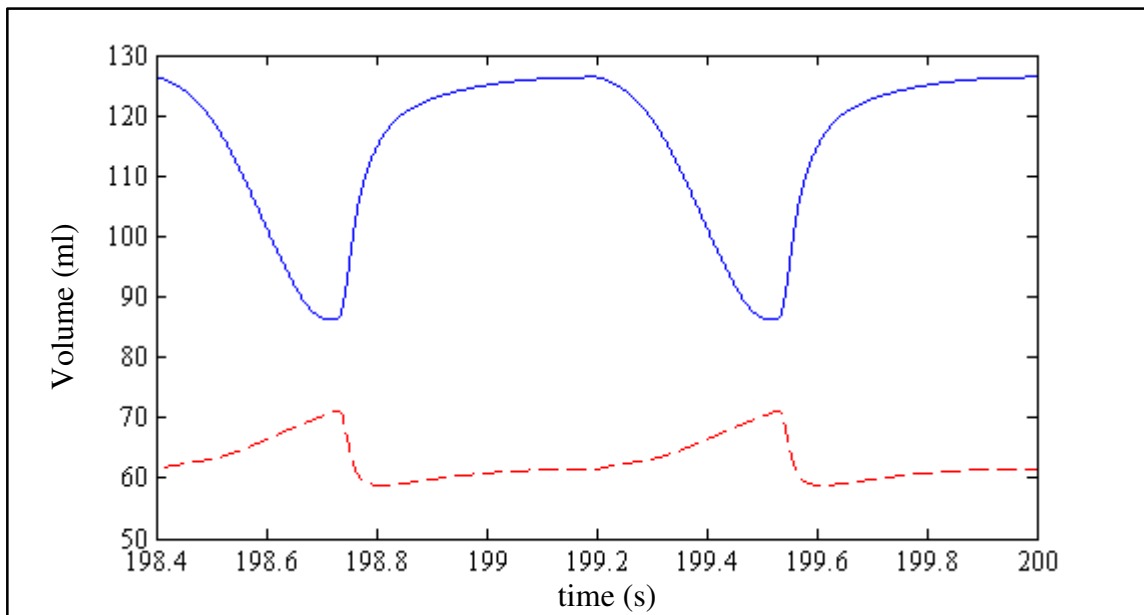


Figure 4.12 Left ventricular volume (continuous line) and left atrial volume (dashed line) at 8000 rpm pump operating speed

End diastolic volume of left ventricle is 126.3 ml end systolic volume of left ventricle is 86.3 ml and stroke volume of left ventricle is 40 ml. Maximum volume of left atrium is 71.2 and minimum volume at left atrium is 58.8 at 8000 rpm operating speed.

Pump flow rate, mitral valve flow rate and aortic valve flow rate at 8000 rpm operating speed are shown in Figure 4.13.

At 8000 rpm operating speed heart and Heart Turcica axial are not operating together. In other words blood flow through aortic valve disappears due to aortic valve closure. Also pump flow regurgitates due to relatively high aortic pressure in diastolic phase.

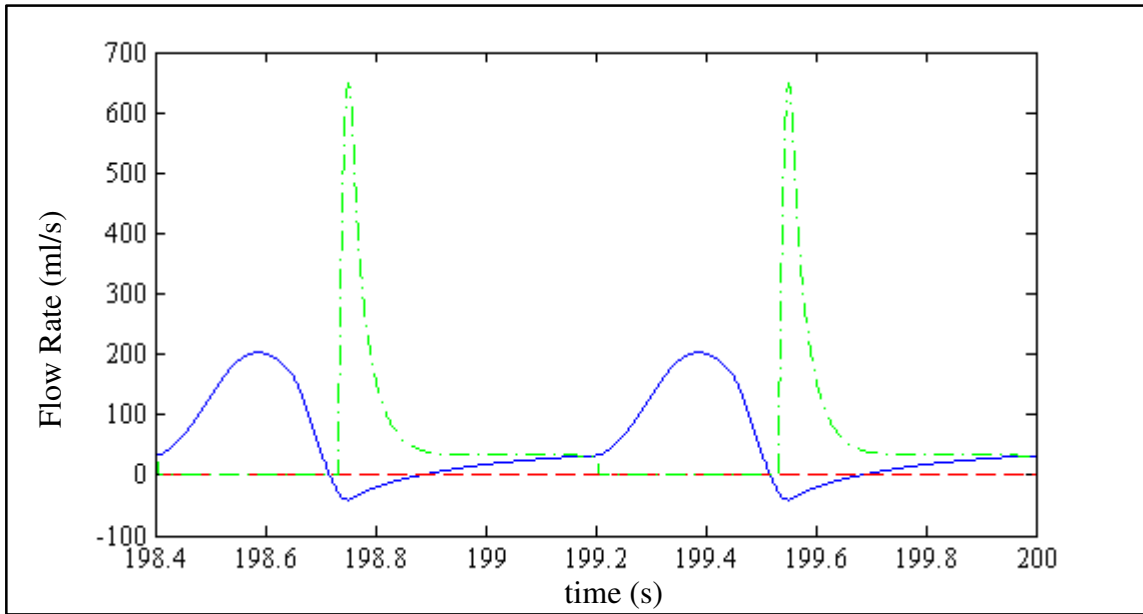


Figure 4.13. Pump flow rate (continuous line), mitral valve flow rate (chain line) and aortic valve flow rate (dashed line) at 8000 rpm operating speed

Motor current at 8000 rpm operating speed is shown Figure 4.14.

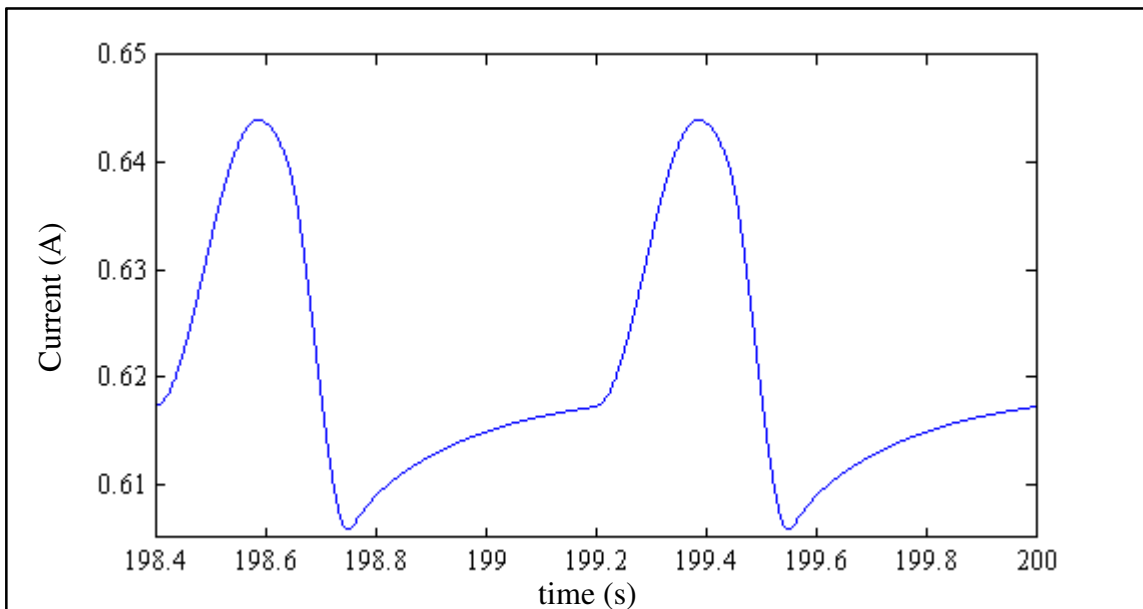


Figure 4.14. Motor current at 8000 rpm operating speed

Motor current varies between 0.644 A and 0.606 A at 8000 rpm operating speed.

Total cardiac output is 3.25 l/min at 8000 rpm operating speed. Pressure pulsatility index is 1.52, flow pulsatility index is 2.99 and current pulsatility index is 0.061 at this speed. Results that are explained above are shown in Table 4.3.

Table 4.3. Simulation results for 8000 rpm operating speed

Parameter	Max. Value	Min. Value	Parameter	Max. Value	Min. Value
ΔP_{pump} (mmHg)	67	9.2	V_{la} (ml)	71.2	58.8
P_{in} (mmHg)	64	9.5	V_{lv} (ml)	126.3	86.3
P_{la} (mmHg)	14.2	11.8	Stroke V_{lv} (ml)	40	
P_{lv} (mmHg)	70.7	10.5	I_{motor} (A)	0.644	0.606
P_{ao} (mmHg)	79.8	61.5	CO (l/min)	3.25	

4.3.4. Simulation Results at 9000 rpm Operating Speed

Operating speed of Heart Turcica axial was adjusted to 9000 rpm and simulations were performed at this constant speed. Pressure difference across the pump, left atrial pressure, left ventricular pressure and aortic pressure are shown in Figure 4.15.

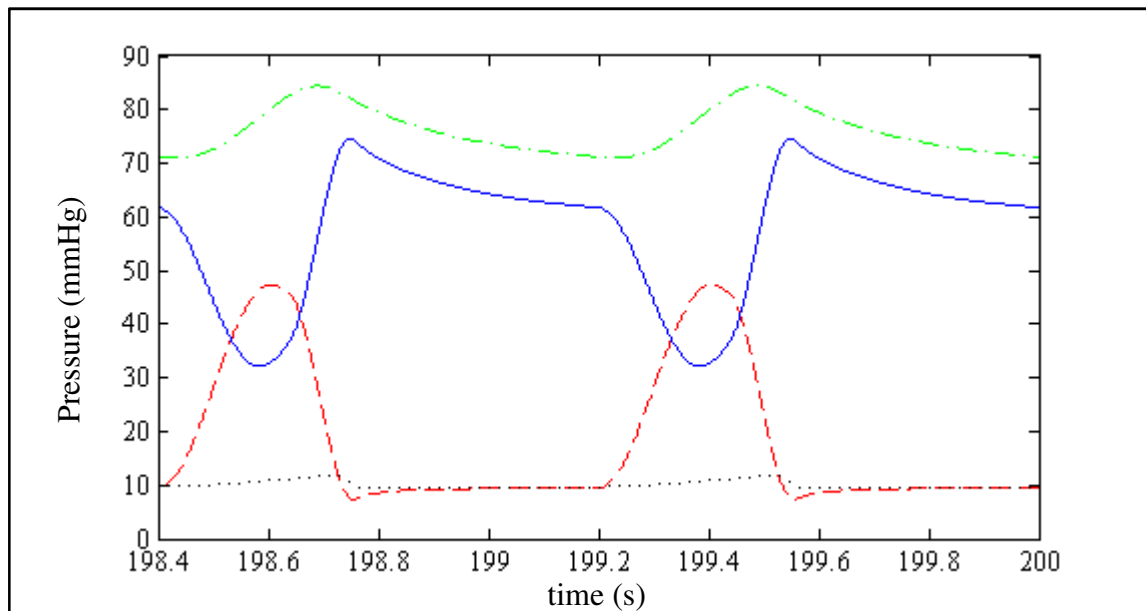


Figure 4.15. Pressure difference across the pump (continuous line), left atrial pressure (dotted line), left ventricular pressure (dashed line) and aortic pressure (chain line) at 9000 rpm operating speed

Maximum pressure difference across the pump is 74.7 mmHg and minimum pressure difference across the pump is 32.1 mmHg. Maximum left atrial pressure is 11.9 mmHg and minimum left atrial pressure is 9.3 mmHg. Maximum left ventricular pressure is 47.3 mmHg and minimum left ventricular pressure is 7.3 mmHg. Left ventricular pressure is above the threshold suction resistance value that defined in Equation 4.3. Therefore pump inlet pressure is the same as left ventricular pressure. Maximum aortic pressure is 84.4 mmHg and minimum aortic pressure is 71.1 mmHg at 9000 rpm pump operating speed.

Left ventricular and left atrial volumes are shown in Figure 4.16 at 9000 rpm operating speed.

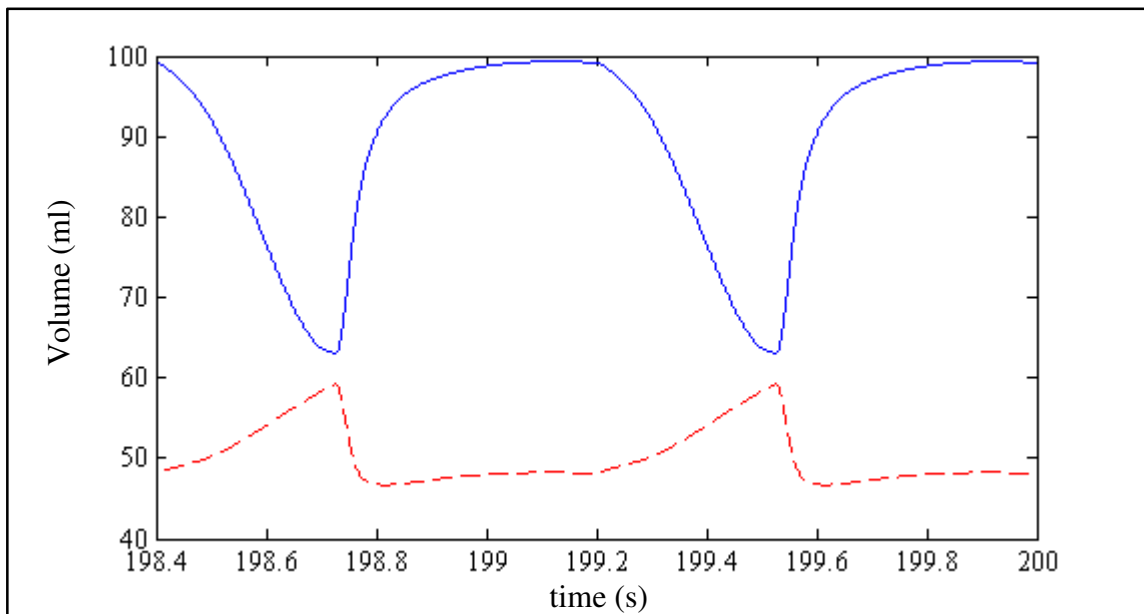


Figure 4.16 Left ventricular volume (continuous line) and left atrial volume (dashed line) at 9000 rpm pump operating speed

End diastolic volume of left ventricle is 99.3 ml, end systolic volume of left ventricle is 63.1 ml and stroke volume of left ventricle is 36.2 ml. Maximum volume of left atrium is 59.2 ml and minimum volume at left atrium is 46.7 ml at 9000 rpm operating speed.

Pump flow rate, mitral valve flow rate and aortic valve flow rate at 9000 rpm operating speed are shown in Figure 4.17.

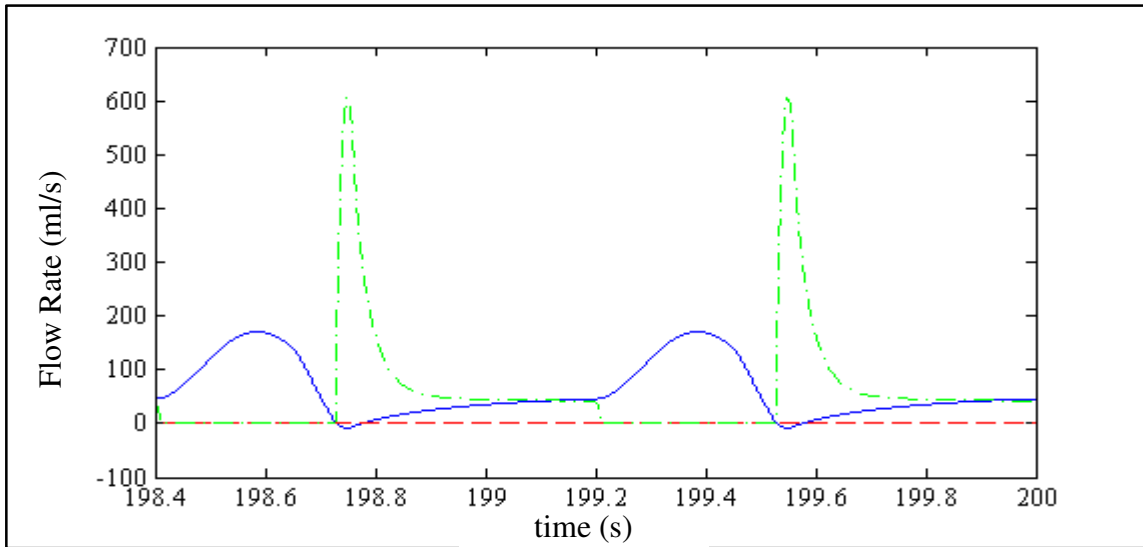


Figure 4.17. Pump flow rate (continuous line), mitral valve flow rate (chain line) and aortic valve flow rate (dashed line) at 9000 rpm operating speed

At 9000 rpm operating speed heart and Heart Turcica axial are not operating together. In other words blood flow through aortic valve disappears due to aortic valve closure. Also pump flow regurgitates due to relatively high aortic pressure in diastolic phase.

Motor current at 9000 rpm operating speed is shown Figure 4.18.

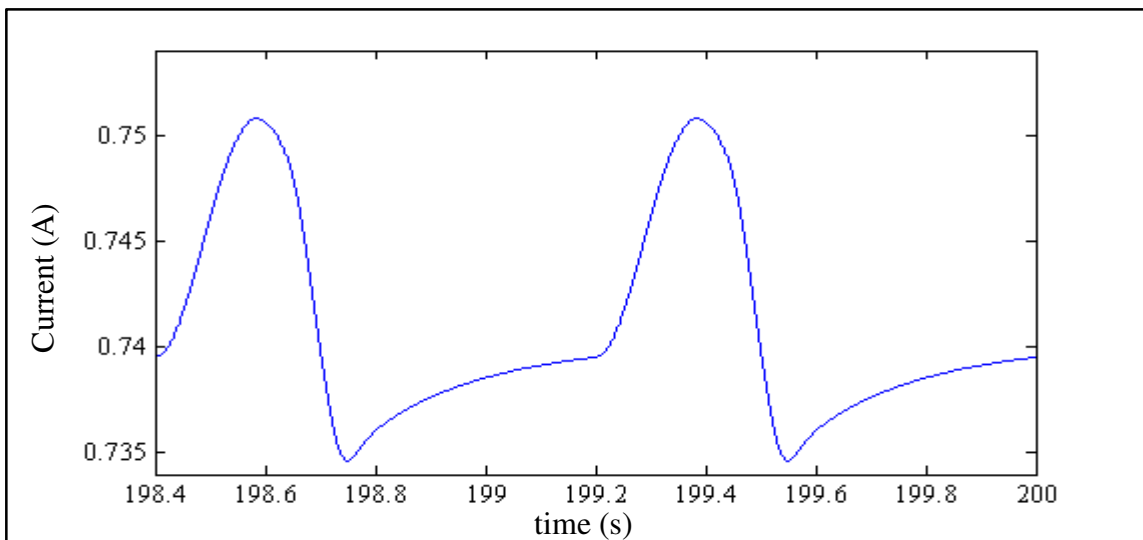


Figure 4.18. Motor current at 9000 rpm operating speed

Motor current varies between 0.751 A and 0.734 A at 9000 rpm operating speed. Total cardiac output is 3.69 l/min at 9000 rpm operating speed. Pressure pulsatility index is 0.79, flow pulsatility index is 2.20 and current pulsatility index is 0.022 at this speed. Results that are explained above are shown in Table 4.4.

Table 4.4. Simulation results for 9000 rpm operating speed

Parameter	Max. Value	Min. Value	Parameter	Max. Value	Min. Value
ΔP_{pump} (mmHg)	74.7	32.1	V_{la} (ml)	59.2	46.7
P_{in} (mmHg)	47.3	7.3	V_{lv} (ml)	99.2	63.1
P_{la} (mmHg)	11.9	9.3	Stroke V_{lv} (ml)	36.2	
P_{lv} (mmHg)	47.3	7.3	I_{motor} (A)	0.751	0.734
P_{ao} (mmHg)	84.4	71.1	CO (l/min)	3.69	

4.3.5. Simulation Results at 9250 rpm Operating Speed

At 9250 rpm operating speed regurgitant pump flow disappears. Therefore simulations are performed at this constant operating speed. Pressure difference across the pump, left atrial pressure, left ventricular pressure and aortic pressure at 9250 rpm operating speed are shown in Figure 4.19.

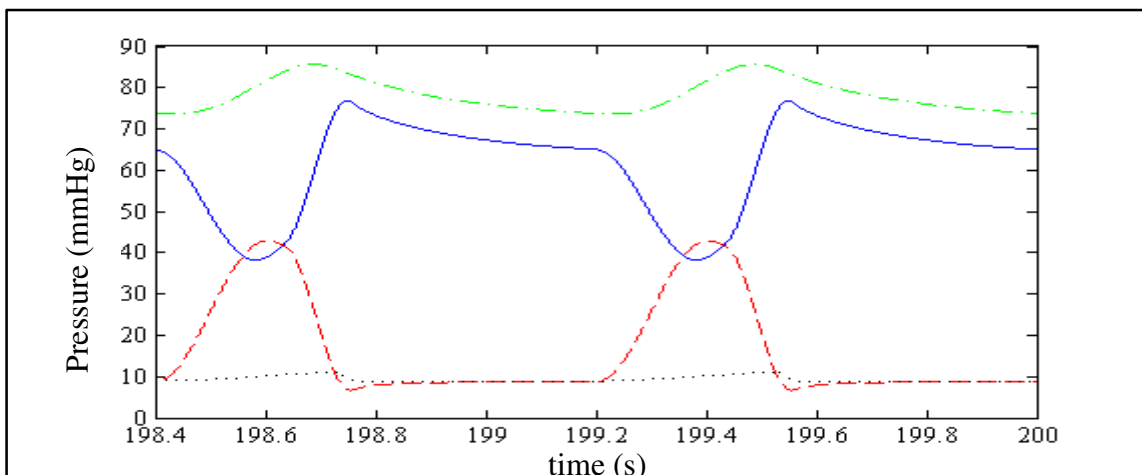


Figure 4.19. Pressure difference across the pump (continuous line), left atrial pressure (dotted line), left ventricular pressure (dashed line) and aortic pressure (chain line) at 8000 rpm operating speed

Maximum pressure difference across the pump is 76.7 mmHg and minimum pressure difference across the pump is 38.2 mmHg. Maximum left atrial pressure is 11.2 mmHg and minimum left atrial pressure is 8.7 mmHg. Maximum left ventricular pressure is 42.9 mmHg and minimum left ventricular pressure is 6.7 mmHg. Left ventricular pressure is above the threshold suction resistance value defined in Equation 4.3. Therefore pump inlet pressure is the same as left ventricular pressure. Maximum aortic pressure is 85.7 mmHg and minimum aortic pressure is 73.6 mmHg at 9250 rpm pump operating speed.

Left ventricular and left atrial volumes are shown in Figure 4.20 at 9250 rpm operating speed.

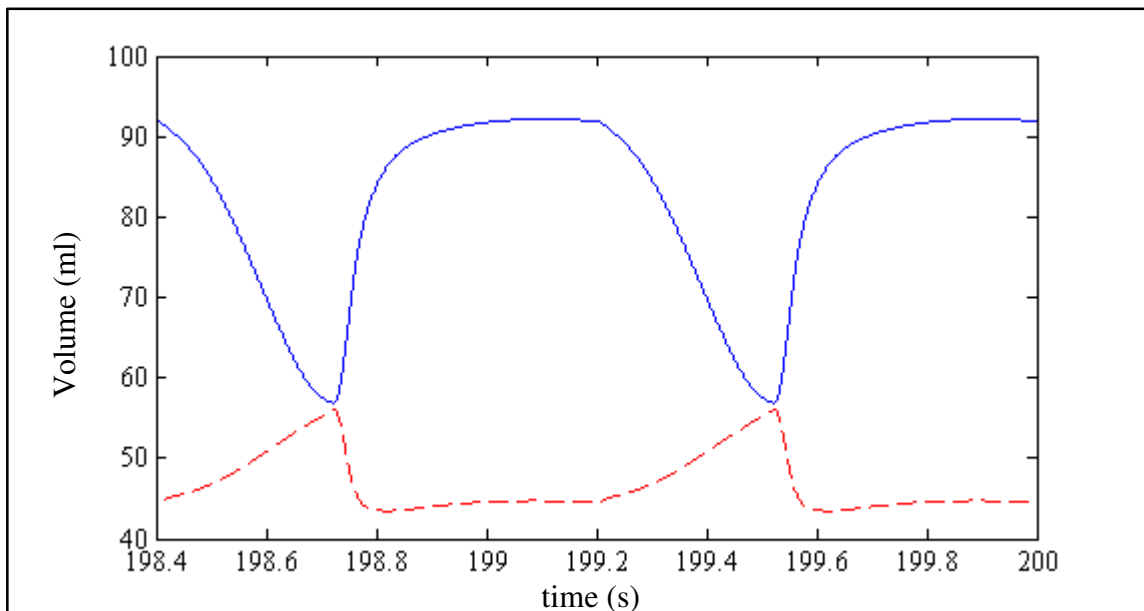


Figure 4.20 Left ventricular volume (continuous line) and left atrial volume (dashed line) at 9250 rpm pump operating speed

End diastolic volume of left ventricle is 92.2 ml, end systolic volume of left ventricle is 56.9 ml and stroke volume of left ventricle is 35.3 ml. Maximum volume of left atrium is 56 ml and minimum volume at left atrium is 43.5 ml at 9250 rpm operating speed.

Pump flow rate, mitral valve flow rate and aortic valve flow rate at 9250 rpm operating speed are shown in Figure 4.21.

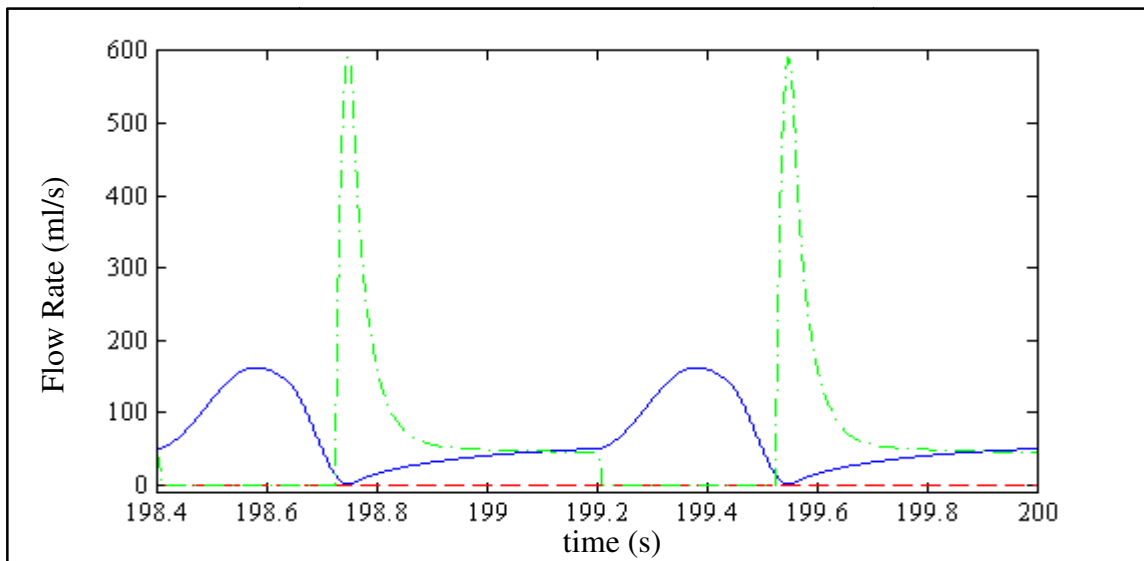


Figure 4.21. Pump flow rate (continuous line), mitral valve flow rate (chain line) and aortic valve flow rate (dashed line) at 9250 rpm operating speed

At 9250 rpm operating speed heart and Heart Turcica axial are not operating together. Regurgitation of pump flow is disappeared. In other words aortic pressure is not higher than the pressure difference across the pump over a cardiac cycle. The lowest value of pump flow is shown in Figure 4.22.

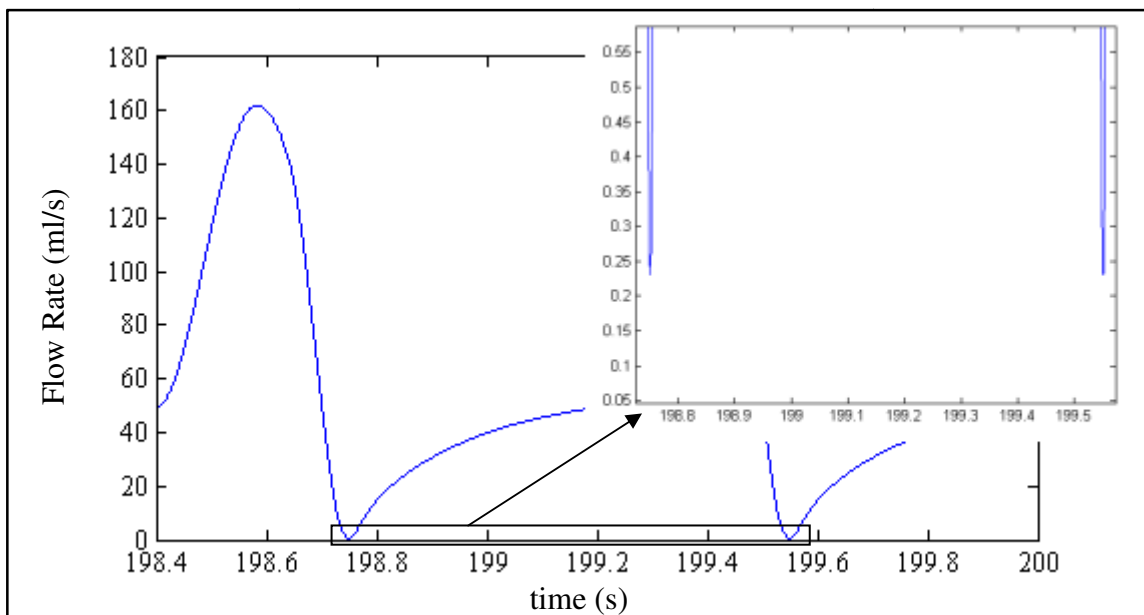


Figure 4.22. Pump Flow rate at 9250 rpm operating speed

As shown in Figure 4.22 the lowest value of pump flow is very close to zero. If the rotation speed of the pump is decreased slightly, regurgitation in pump flow will occur again.

Motor current at 9250 rpm operating speed is shown Figure 4.23.

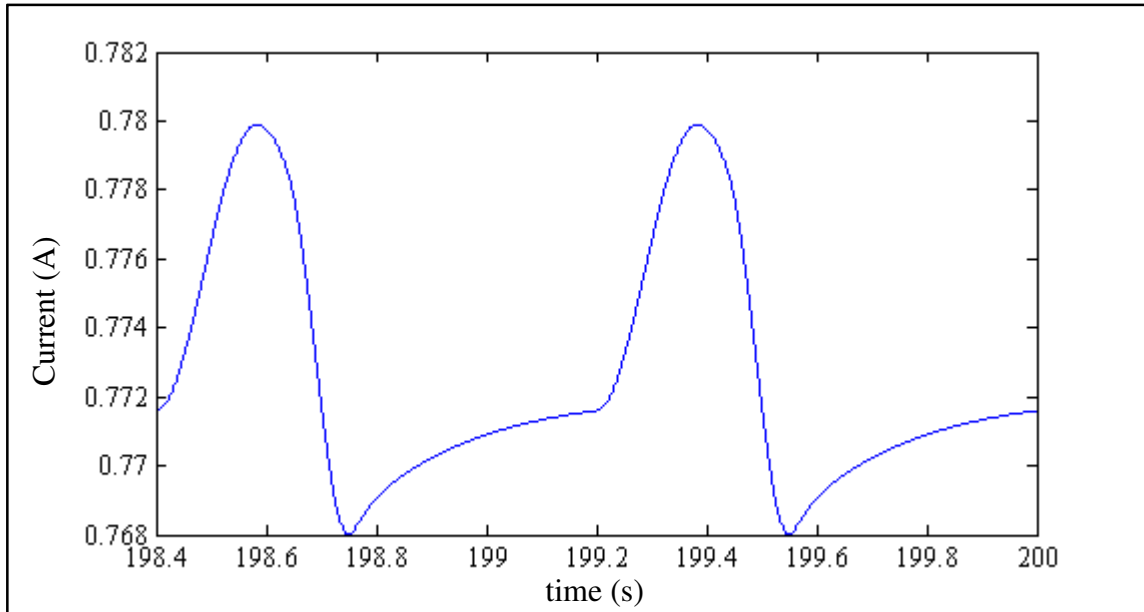


Figure 4.23. Motor current at 9250 rpm operating speed

Motor current varies between 0.780 A and 0.768 A at 9250 rpm operating speed. Total cardiac output is 3.80 l/min at 9250 rpm operating speed. Pressure pulsatility index is 0.67, flow pulsatility index is 1.99 and current pulsatility index is 0.015 at this speed. Results that are explained above are shown in Table 4.5.

Table 4.5. Simulation results for 9250 rpm operating speed

Parameter	Max. Value	Min. Value	Parameter	Max. Value	Min. Value
ΔP_{pump} (mmHg)	76.7	38.2	V_{la} (ml)	56	43.5
P_{in} (mmHg)	42.9	6.7	V_{lv} (ml)	92.2	56.9
P_{la} (mmHg)	11.2	8.7	Stroke V_{lv} (ml)	35.3	
P_{lv} (mmHg)	42.9	6.7	I_{motor} (A)	0.780	0.768
P_{ao} (mmHg)	85.7	73.6	CO (l/min)	3.80	

4.3.6. Simulation Results at 10000 rpm Operating Speed

Operating speed of Heart Turcica axial was adjusted to 10000 rpm and simulations were performed at this constant operating speed. Pressure difference across the pump, left atrial pressure, left ventricular pressure and aortic pressure are shown in Figure 4.24.

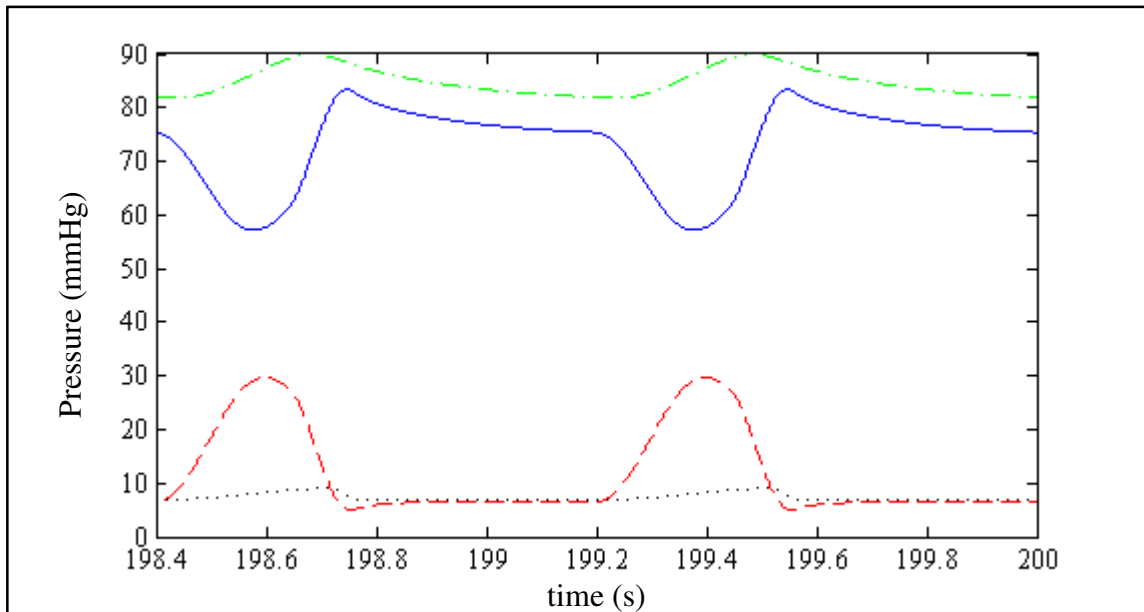


Figure 4.24. Pressure difference across the pump (continuous line), left atrial pressure (dotted line), left ventricular pressure (dashed line) and aortic pressure (chain line) at 10000 rpm operating speed

Maximum pressure difference across the pump is 83.3 mmHg and minimum pressure difference across the pump is 57.2 mmHg. Maximum left atrial pressure is 9.3 mmHg and minimum left atrial pressure is 6.7 mmHg. Maximum left ventricular pressure is 29.6 mmHg and minimum left ventricular pressure is 4.9 mmHg. Left ventricular pressure is above the threshold suction resistance value defined in Equation 4.3. Therefore pump inlet pressure is the same as left ventricular pressure. Maximum aortic pressure is 89.9 and minimum aortic pressure is 81.8 at 10000 rpm pump operating speed.

Left ventricular and left atrial volumes are shown in Figure 4.25 at 10000 rpm operating speed.

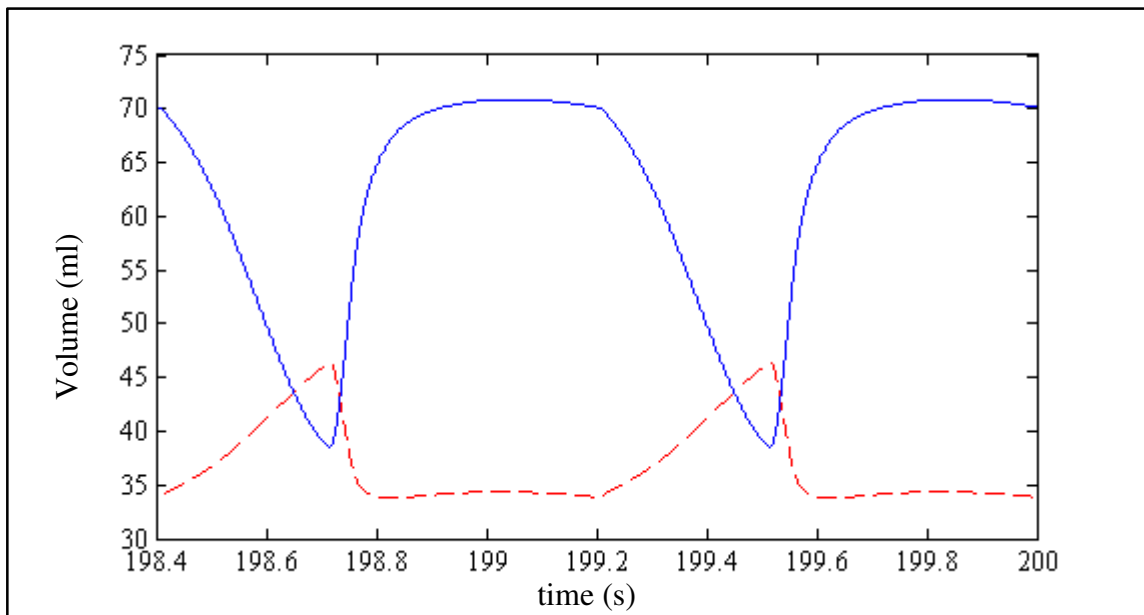


Figure 4.25 Left ventricular volume (continuous line) and left atrial volume (dashed line) at 10000 rpm pump operating speed

End diastolic volume of left ventricle is 70.9 ml, end systolic volume of left ventricle is 38.5 ml and stroke volume of the left ventricle is 32.4 ml. Maximum volume of left atrium is 46.4 and minimum volume at left atrium is 33.8 at 10000 rpm operating speed.

Pump flow rate, mitral valve flow rate and aortic valve flow rate at 10000 rpm operating speed are shown in Figure 4.26.

At 10000 rpm operating speed heart and Heart Turcica axial are not operating together. Also regurgitant pump flow does not occur at 10000 rpm operating speed.

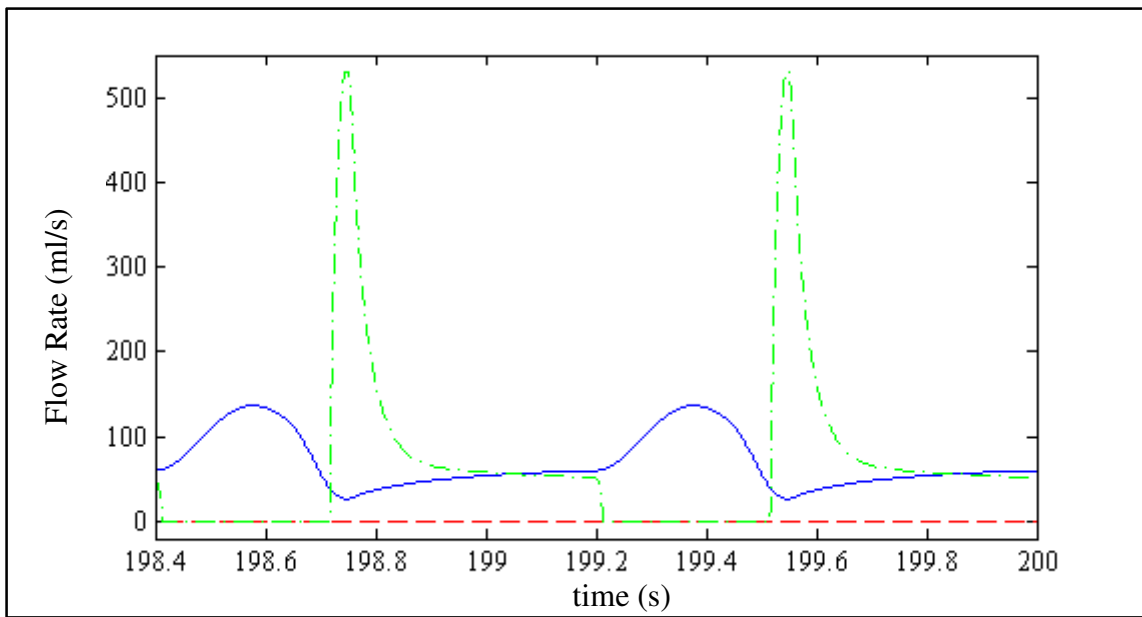


Figure 4.26. Pump flow rate (continuous line), mitral valve flow rate (chain line) and aortic valve flow rate (dashed line) at 10000 rpm operating speed

Motor current at 10000 rpm operating speed is shown in Figure 4.27.

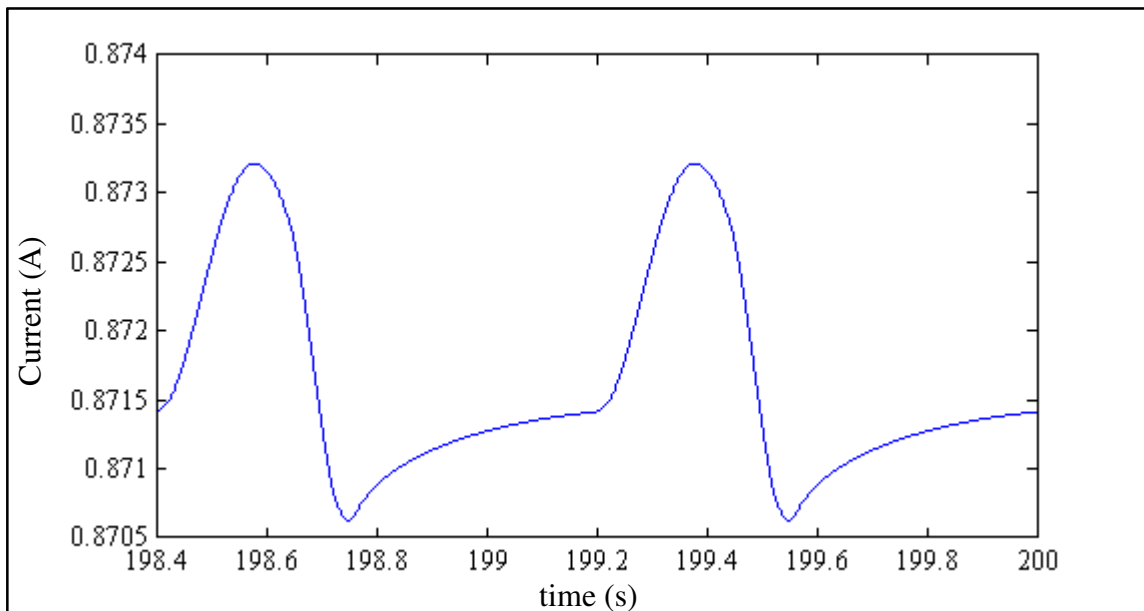


Figure 4.27. Motor current at 10000 rpm operating speed

Motor current varies between 0.873 A and 0.870 A at 10000 rpm operating speed.

Total cardiac output is 4.19 l/min at 10000 rpm operating speed. At this speed total cardiac output reaches minimum acceptable cardiac output level. Also maximum aortic pressure is 89.9 mmHg which is a sufficient value to provide perfusion. According to these results 10000 rpm rotation speed is the minimum operating speed for a Heart Turcica axial implanted cardiovascular system. Pressure pulsatility index is 0.37, flow pulsatility index is 1.34 and current pulsatility index is 0.003 at this speed. Results that are explained above are shown in Table 4.6.

Table 4.6. Simulation results for 10000 rpm operating speed

Parameter	Max. Value	Min. Value	Parameter	Max. Value	Min. Value
ΔP_{pump} (mmHg)	83.3	57.2	V_{la} (ml)	46.4	33.8
P_{in} (mmHg)	29.6	4.9	V_{lv} (ml)	70.9	38.5
P_{la} (mmHg)	9.3	6.7	Stroke V_{lv} (ml)	32.4	
P_{lv} (mmHg)	29.6	4.9	I_{motor} (A)	0.873	0.870
P_{ao} (mmHg)	89.9	81.8	CO (l/min)	4.19	

4.3.7. Simulation Results at 11000 rpm Operating Speed

Operating speed of Heart Turcica axial was further measured to 11000 rpm and simulations were performed at this constant operating speed. Pressure difference across the pump, left atrial pressure, left ventricular pressure and aortic pressure are shown in Figure 4.28.

Maximum pressure difference across the pump is 93.8 mmHg and minimum pressure difference across the pump is 82.6 mmHg. Maximum left atrial pressure is 6.7 mmHg and minimum left atrial pressure is 4.2 mmHg. Maximum left ventricular pressure is 13.6 mmHg and minimum left ventricular pressure is 2.9 mmHg. Left ventricular pressure is above the threshold suction resistance value defined in Equation 4.3. Therefore pump inlet pressure is the same as left ventricular pressure. Maximum aortic pressure is 97.5 mmHg and minimum aortic pressure is 94.2 mmHg at 11000 rpm pump operating speed.

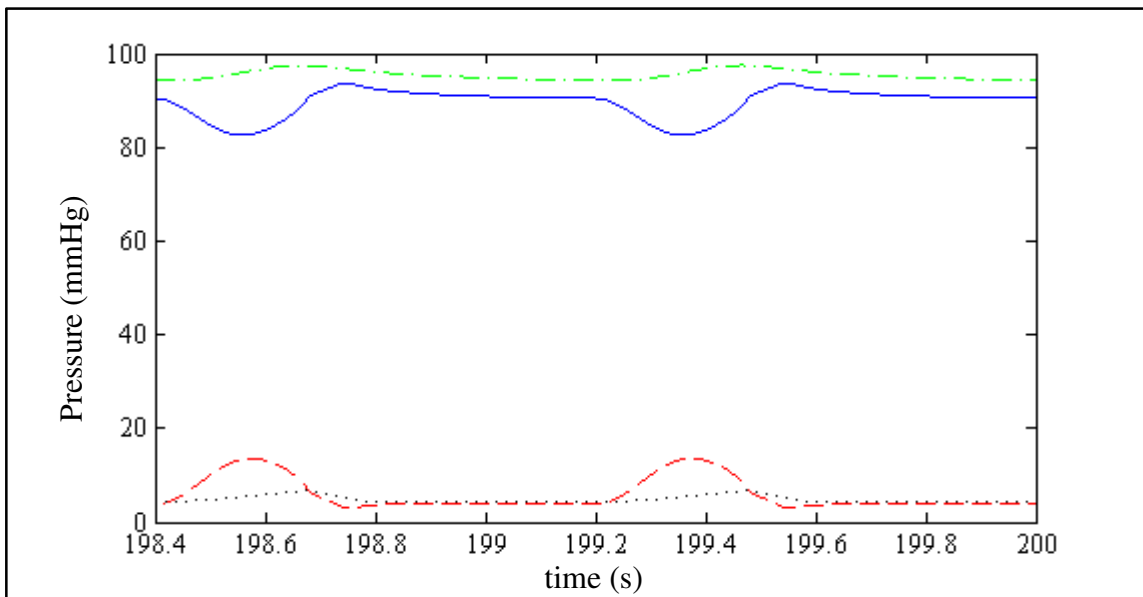


Figure 4.28. Pressure difference across the pump (continuous line), left atrial pressure (dotted line), left ventricular pressure (dashed line) and aortic pressure (chain line) at 11000 rpm operating speed

Left ventricular and left atrial volumes are shown in Figure 4.29 at 11000 rpm operating speed.

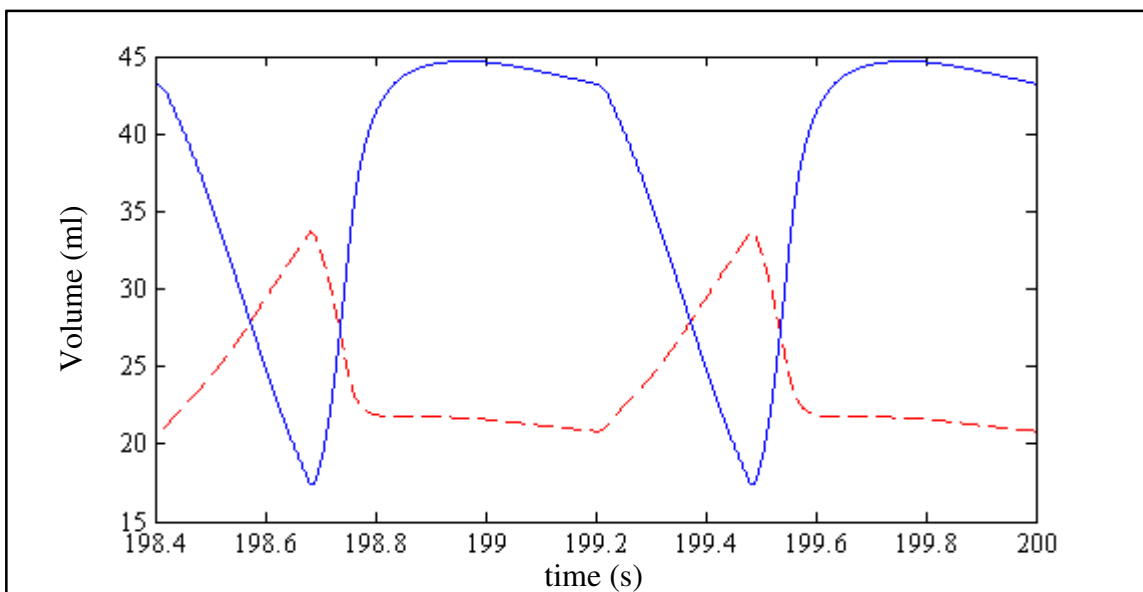


Figure 4.29 Left ventricular volume (continuous line) and left atrial volume (dashed line) at 11000 rpm pump operating speed

End diastolic volume of left ventricle is 44.7 ml, end systolic volume of left ventricle is 17.3 ml and stroke volume of left ventricle is 27.4 ml Maximum volume of left atrium is 33.7 ml and minimum volume at left atrium is 20.8 ml at 11000 rpm operating speed.

Pump flow rate, mitral valve flow rate and aortic valve flow rate at 11000 rpm operating speed are shown in Figure 4.30.

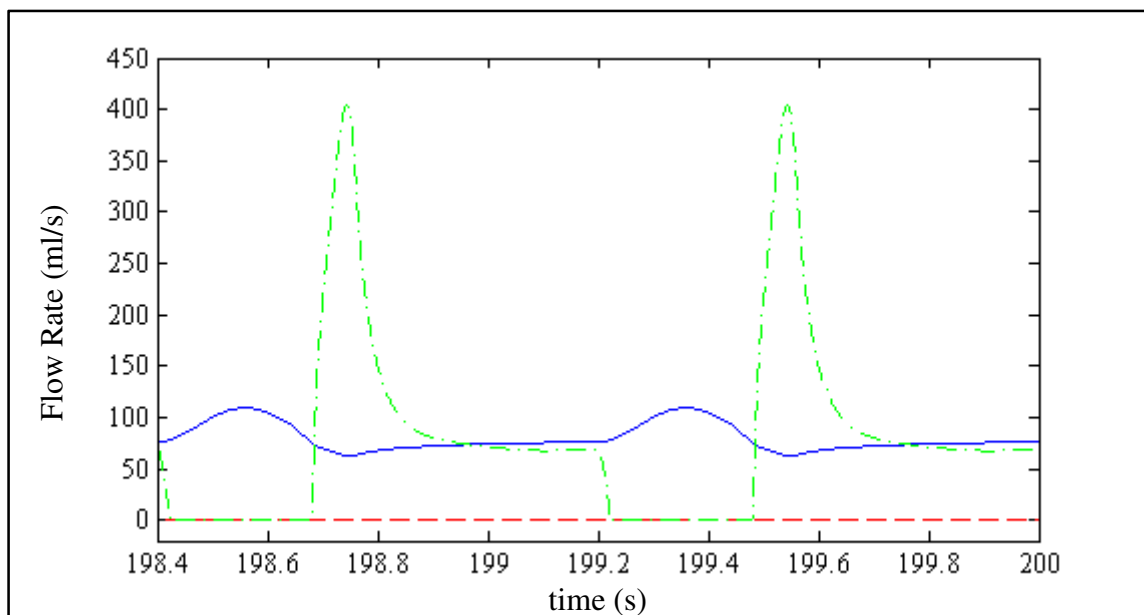


Figure 4.30. Pump flow rate (continuous line), mitral valve flow rate (chain line) and aortic valve flow rate (dashed line) at 11000 rpm operating speed

At 11000 rpm operating speed heart and Heart Turcica axial are not operating together. Also regurgitant pump flow does not occur at 11000 rpm operating speed.

Motor current at 11000 rpm operating speed is shown Figure 4.31.

Motor current varies between 1.013 A and 1.011 A at 11000 rpm operating speed. Total cardiac output is 4.80 l/min at 11000 rpm operating speed. Pressure pulsatility index is 0.12, flow pulsatility index is 0.54 and current pulsatility index is 0.002 at this speed. Results that are explained above are shown in Table 4.7.

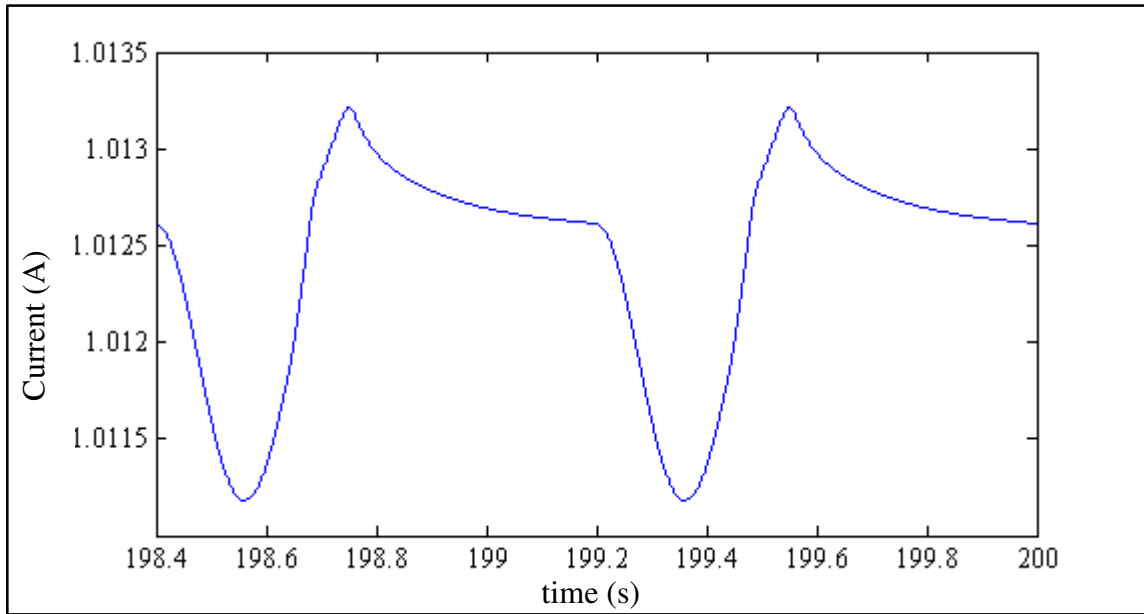


Figure 4.31. Motor current at 11000 rpm operating speed

Table 4.7. Simulation results for 11000 rpm operating speed

Parameter	Max. Value	Min. Value	Parameter	Max. Value	Min. Value
ΔP_{pump} (mmHg)	93.8	82.6	V_{la} (ml)	33.7	20.8
P_{in} (mmHg)	13.6	2.9	V_{lv} (ml)	44.7	14.3
P_{la} (mmHg)	6.7	4.2	Stroke V_{lv} (ml)	27.3	
P_{lv} (mmHg)	13.6	2.9	I_{motor} (A)	1.013	1.011
P_{ao} (mmHg)	97.5	94.2	CO (l/min)	4.80	

4.3.8. Simulation Results at 12000 rpm Operating Speed

Operating speed of Heart Turcica axial was adjusted to 12000 rpm and simulations were performed at 12000 rpm constant operating speed. Left atrial pressure, left ventricular pressure and pump inlet pressure are shown in Figure 4.32.

Maximum left atrial pressure is 2.6 mmHg and minimum left atrial pressure is 1.5 mmHg. Maximum left ventricular pressure is 2.1 mmHg and minimum left ventricular pressure is 0.99 mmHg. Minimum value of the left ventricular pressure is below the threshold pressure of suction resistance defined in Equation 4.3. Therefore pump inlet pressure is not equal to the left ventricular pressure over a cardiac cycle.

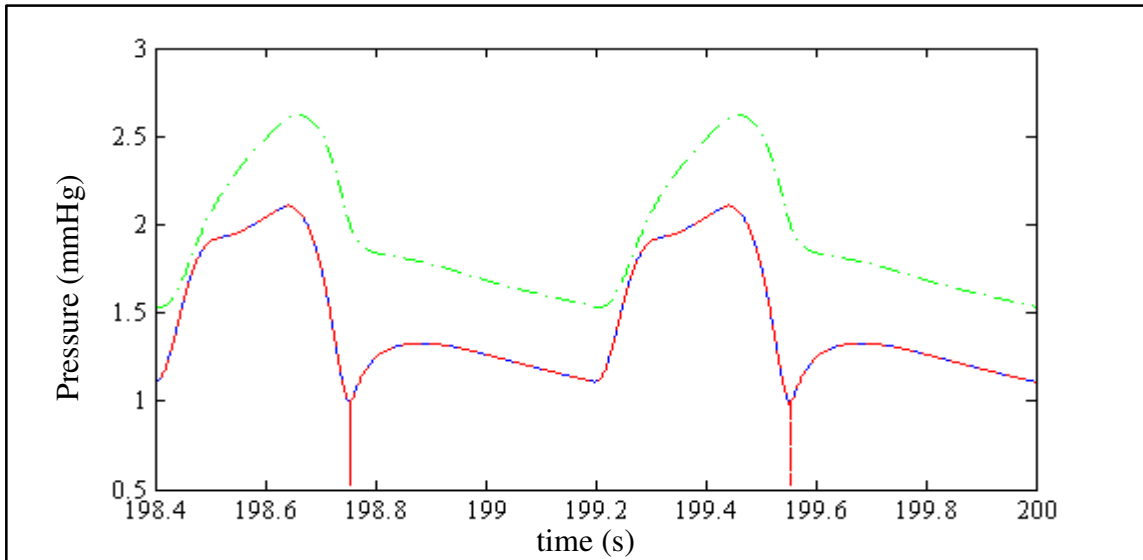


Figure 4.32. Left ventricular pressure (continuous line), left atrial pressure (chain line), pump inlet pressure (dashed line) at 12000 rpm operating speed

Pressure difference across the pump and aortic pressure is in Figure 4.33.

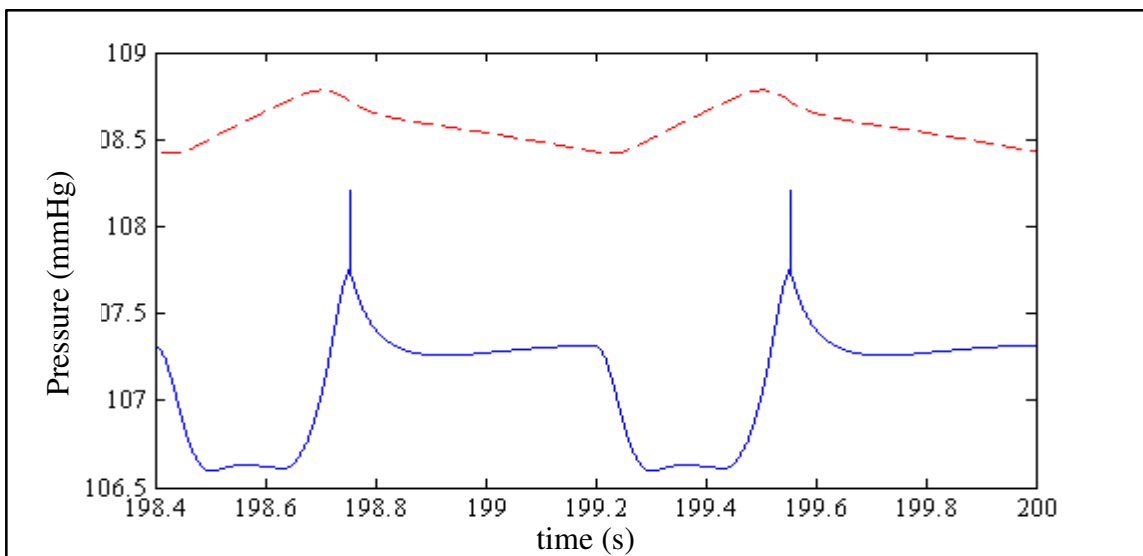


Figure 4.33. Pressure difference across the pump (continuous line), aortic pressure (dashed line) at 12000 rpm operating speed

Maximum pressure difference across the pump is 108.2 mmHg and minimum pressure difference across the pump is 106.6 mmHg. Maximum aortic pressure is 108.8

mmHg and minimum aortic pressure is 108.4 mmHg at 12000 rpm pump operating speed.

According results shown in Figure 4.32 if the operating speed is slightly increased above 12000 rpm, pump inlet pressure will drop below zero. In other words ventricular suction which is a harmful condition to left ventricle and heart occurs. Hence these results indicate that operating speed for Heart Turcica Axial should be set below 12000 rpm.

Left ventricular and left atrial volumes are shown in Figure 4.34 at 12000 rpm operating speed.

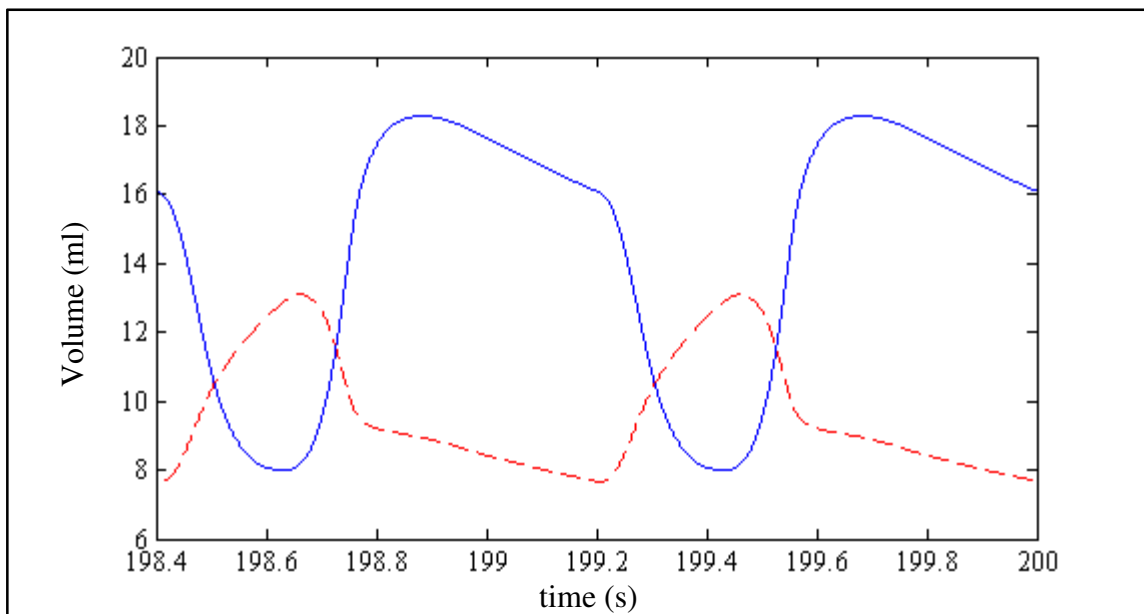


Figure 4.34. Left ventricular volume (continuous line) and left atrial volume (dashed line) at 12000 rpm pump operating speed

End diastolic volume of left ventricle is 18.3 ml, end systolic volume of left ventricle is 8 ml and stroke volume of left ventricle is 10.3 ml. Maximum volume of left atrium is 13.1 ml and minimum volume at left atrium is 7.6 ml at 12000 rpm operating speed.

Pump flow rate, mitral valve flow rate and aortic valve flow rate at 12000 rpm operating speed are shown in Figure 4.35.

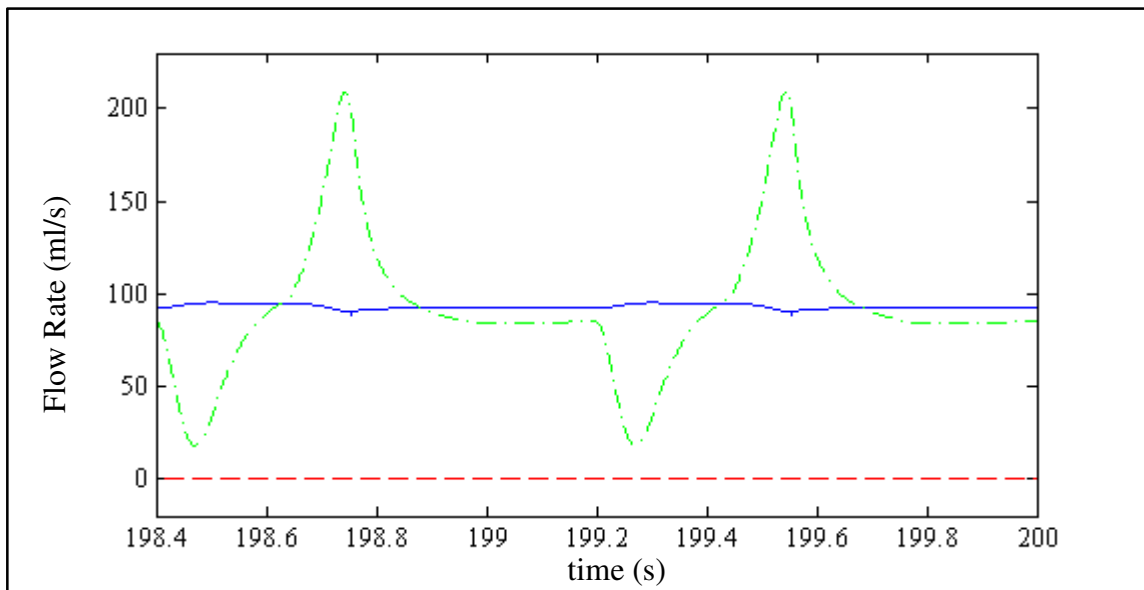


Figure 4.35. Pump flow rate (continuous line), mitral valve flow rate (chain line) and aortic valve flow rate (dashed line) at 12000 rpm operating speed

At 12000 rpm operating speed mitral valve remains open due to relatively lower pressure in left ventricle. In other words pressure in left ventricle is lower than left atrial pressure over a cardiac cycle.

Motor current at 12000 rpm operating speed is shown in Figure 4.36.

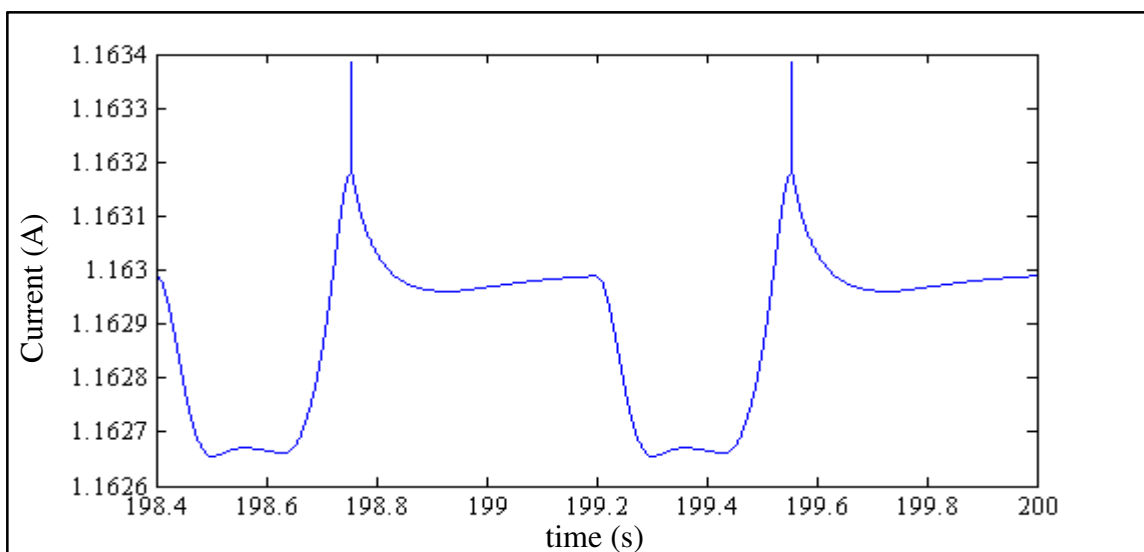


Figure 4.36. Motor current at 12000 rpm operating speed

Motor current varies between 1.163 A and 1.162 A at 12000 rpm operating speed. Peaks in the motor current indicate the pre-suction condition. Total cardiac output is 5.58 l/min at 12000 rpm operating speed. Pressure pulsatility index is 0.01, flow pulsatility index is 0.07 and current pulsatility index is 0.0006 at this speed. Results that are explained above are shown in Table 4.8.

Table 4.8. Simulation results for 12000 rpm operating speed

Parameter	Max. Value	Min. Value	Parameter	Max. Value	Min. Value
ΔP_{pump} (mmHg)	108.2	106.6	V_{la} (ml)	13.1	7.6
P_{in} (mmHg)	2.1	0.52	V_{lv} (ml)	18.3	8
P_{la} (mmHg)	2.6	1.5	Stroke V_{lv} (ml)	10.3	
P_{lv} (mmHg)	2.1	0.99	I_{motor} (A)	1.163	1.162
P_{ao} (mmHg)	108.8	108.4	CO (l/min)	5.58	

4.3.9. Simulation Results at 13000 rpm Operating Speed

Operating speed of Heart Turcica axial was adjusted to 13000 rpm and simulations were performed at 13000 rpm constant operating speed. Left atrial pressure, left ventricular pressure and pump inlet pressure are shown in Figure 4.37.

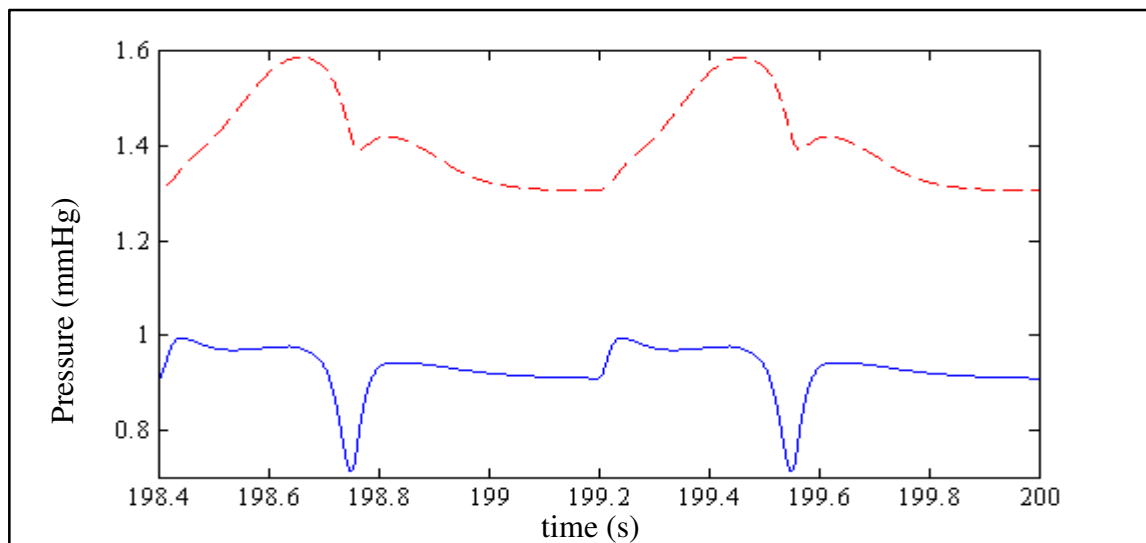


Figure 4.37. Left ventricular pressure (continuous line) and left atrial pressure (dashed line) at 13000 rpm operating speed

Left atrial maximum pressure is 1.6 mmHg and left atrial minimum pressure is 1.3 mmHg. Left ventricular maximum pressure is 0.99 mmHg and left ventricular minimum pressure is 0.71 mmHg at 13000 rpm operating speed.

Pump inlet pressure at 13000 rpm operating speed is shown in Figure 4.38.

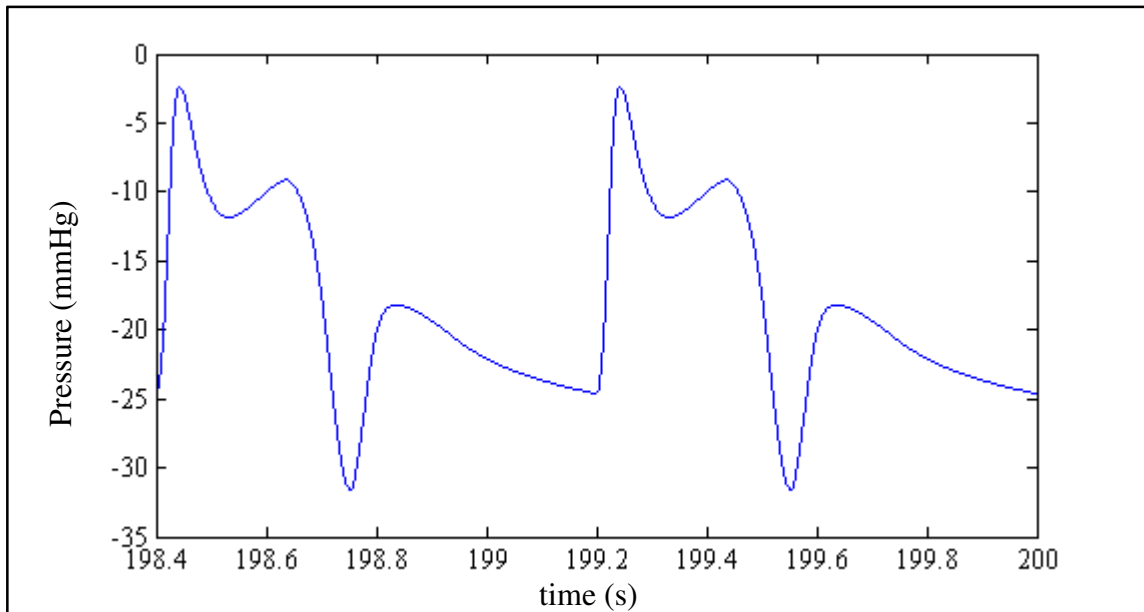


Figure 4.38. Pump inlet pressure at 13000 rpm pump operating speed

Maximum pump inlet pressure is -2.3 mmHg and minimum pump inlet pressure is -31.6 mmHg. Pump inlet pressure is negative over a cardiac cycle. These results show that ventricular suction occurs in left ventricle.

Pressure difference across the pump and aortic pressure are shown in Figure 4.39.

Maximum pressure difference across the pump is 144 mmHg and minimum pressure difference across the pump is 111.5 mmHg. Maximum aortic pressure is 114.3 mmHg and 108 mmHg.

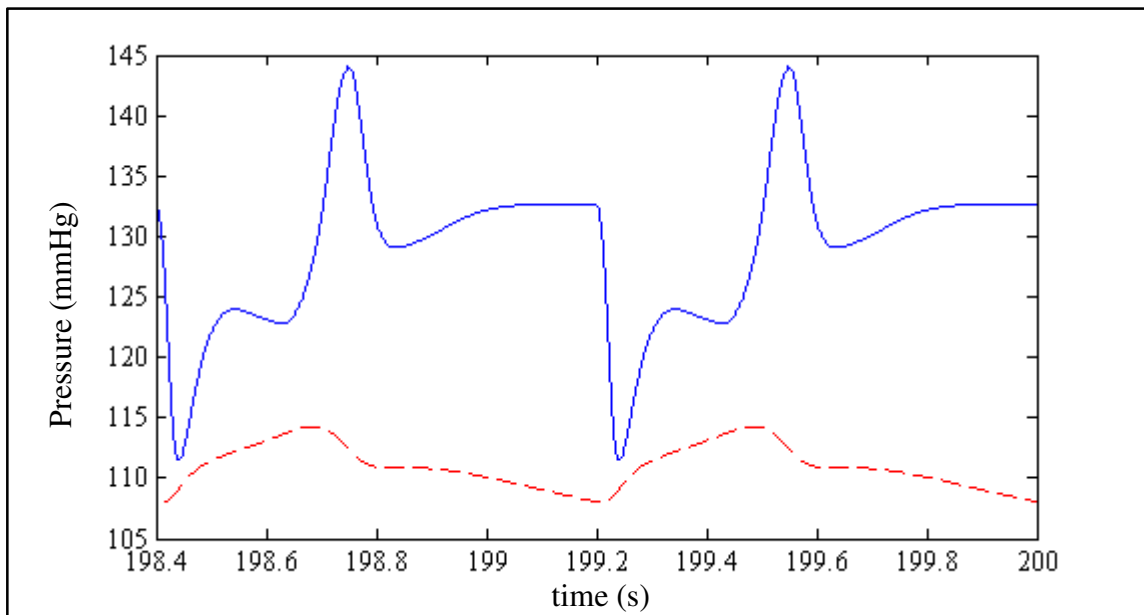


Figure 4.39. Pressure difference across the pump (continuous line), aortic pressure (dashed line) at 13000 rpm operating speed

Left ventricular and left atrial volumes are shown in Figure 4.40 at 13000 rpm operating speed.

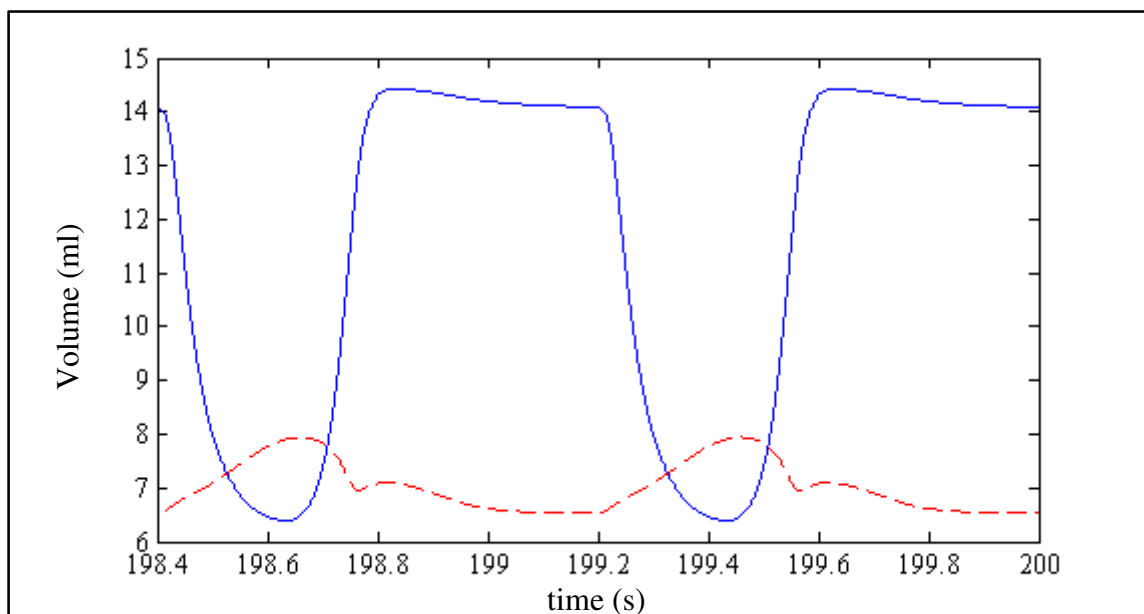


Figure 4.40. Left ventricular volume (continuous line) and left atrial volume (dashed line) at 13000 rpm pump operating speed

End diastolic volume of left ventricle is 14.4 ml, end systolic volume of left ventricle is 6.4 ml and stroke volume of left ventricle is 8 ml. Maximum volume of left atrium is 7.9 ml and minimum volume at left atrium is 6.5 ml at 13000 rpm operating speed.

Pump flow rate, mitral valve flow rate and aortic valve flow rate at 13000 rpm operating speed are shown in Figure 4.41.

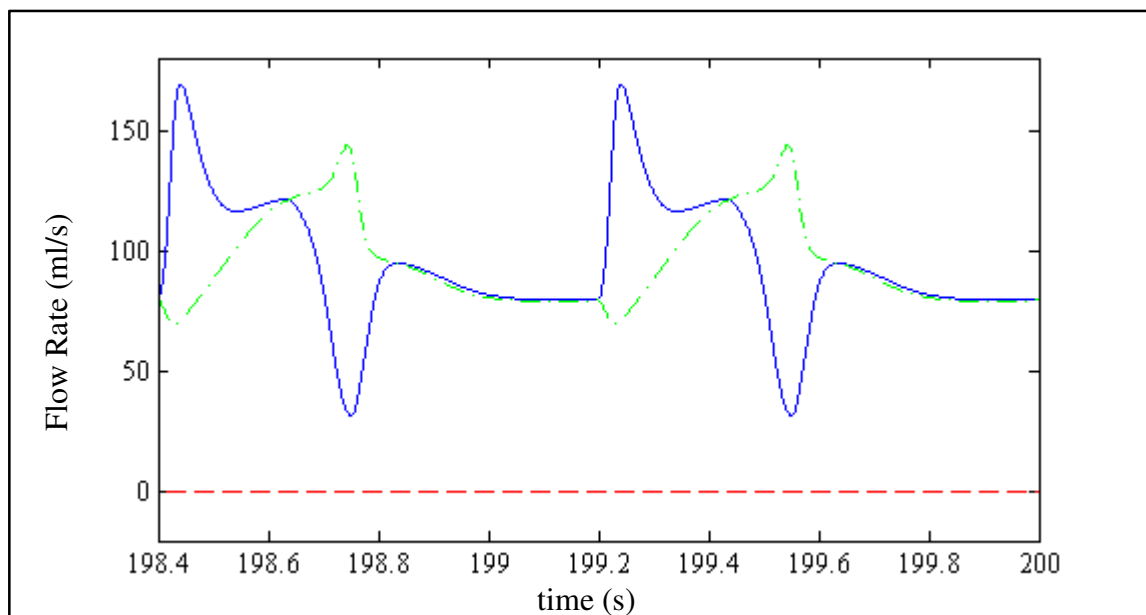


Figure 4.41. Pump flow rate (continuous line), mitral valve flow rate (chain line) and aortic valve flow rate (dashed line) at 13000 rpm operating speed

At 13000 rpm operating speed mitral valve remains open due to relatively low pressure in left ventricle. In other words pressure in left ventricle is lower than left atrial pressure over a cardiac cycle.

Motor current at 13000 rpm operating speed is shown Figure 4.42.

Motor current varies between 1.336 A and 1.312 A at 13000 rpm operating speed. Total cardiac output is 5.72 l/min at 13000 rpm operating speed. Pressure pulsatility index is 0.25, flow pulsatility index is 1.36 and current pulsatility index is 0.018 at this speed. Results that are explained above are shown in Table 4.9.

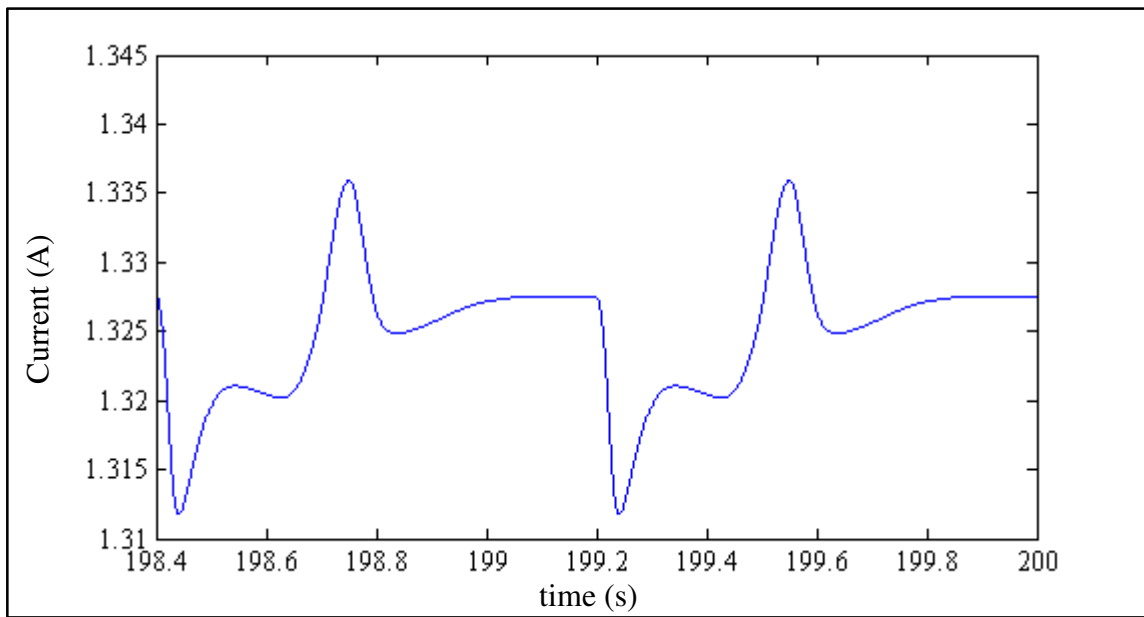


Figure 4.42. Motor current at 13000 rpm operating speed

Table 4.9. Simulation results for 13000 rpm operating speed

Parameter	Max. Value	Min. Value	Parameter	Max. Value	Min. Value
ΔP_{pump} (mmHg)	144	111.5	V_{la} (ml)	7.9	6.5
P_{in} (mmHg)	-2.3	-31.6	V_{lv} (ml)	14.4	6.4
P_{la} (mmHg)	1.6	1.3	Stroke V_{lv} (ml)	8	
P_{lv} (mmHg)	0.99	0.7	I_{motor} (A)	1.336	1.312
P_{ao} (mmHg)	114.4	108	CO (l/min)	5.72	

As shown in the figures during suction condition, the shape of pump flow, pressure difference across the pump, motor current change over a cardiac cycle. In other words distortion occurs due to suction. Also pulsatility appears again that disappeared with increasing operating speed.

Left ventricular pressure – volume loops are good indicators to explain the help of the left ventricular assist devices to left ventricle. Left ventricular pressure-volume loops from 7000 rpm to 13000 rpm with 1000 rpm increments are shown in Figure 4.43.

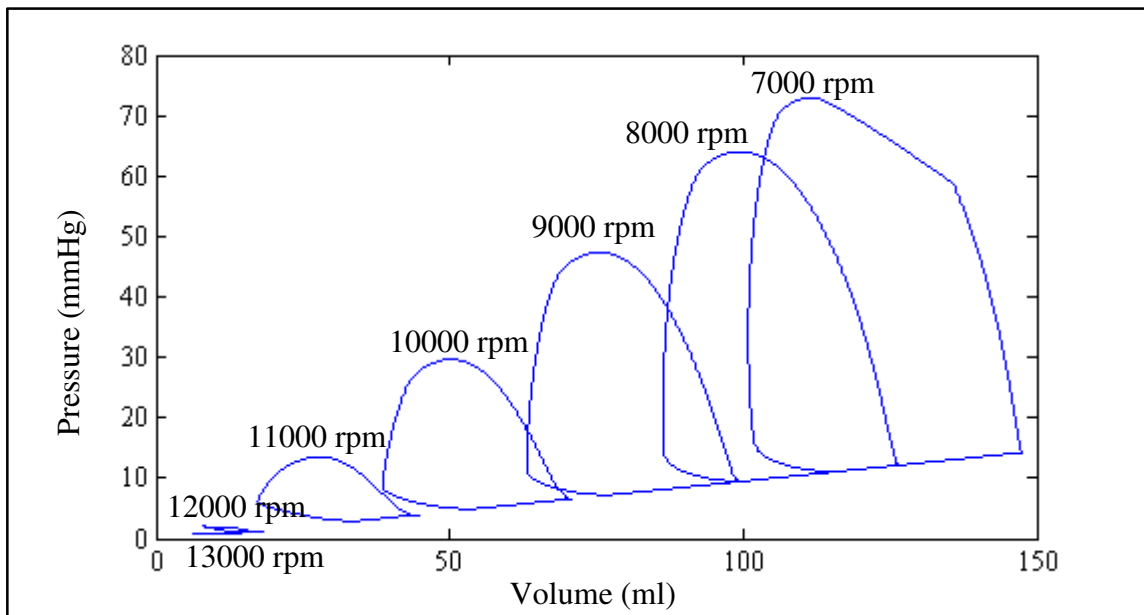


Figure 4.43. Left ventricular pressure – volume loops from 7000 rpm to 13000 rpm with 1000 rpm increase

According to the results, area of the left ventricular pressure – volume loop is getting smaller with increasing pump operating speed. In other words external work of the left ventricle is decreasing.

Also pressure – flow rate diagram of Heart Turcica axial shows the effect of increasing pump operating speed. Pressure – flow rate diagram of Heart Turcica axial from 7000 rpm to 13000 rpm with 1000 rpm increments is shown in Figure 4.44.

As mentioned above increasing pump operating speed causes to disappear pulsatility in pump flow rate and pressure difference across the pump. After suction occurrence pulsatility appears again in these variables. In other words increasing pump operating speed provides shorter pressure – flow rate curves in non – suction conditions. But in suction conditions longer pressure – flow rate curves are obtained again.

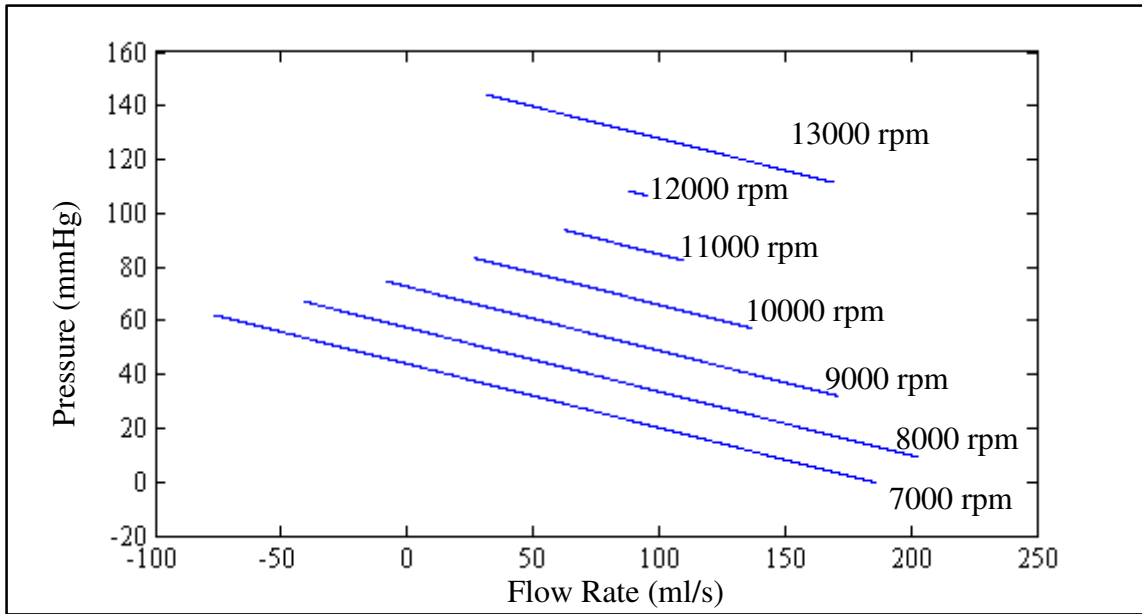


Figure 4.44. Heart Turcica axial pressure – flow rate diagram from 7000 rpm to 13000 rpm with 1000 rpm increments

Pulsatility indexes are also good indicators of increasing operating speed. Pressure pulsatility index, flow pulsatility index and current pulsatility index with respect pump rotation speed are shown in Figure 4.45, 4.46 and 4.47 respectively.

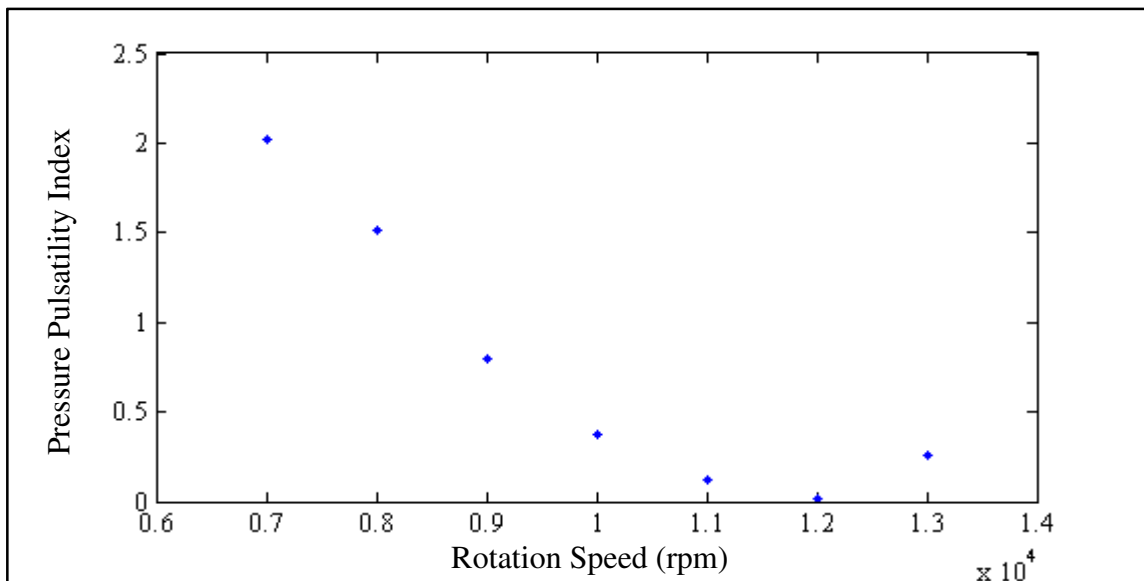


Figure 4.45. Heart Turcica axial pressure pulsatility index from 7000 rpm to 13000 rpm with 1000 rpm increments

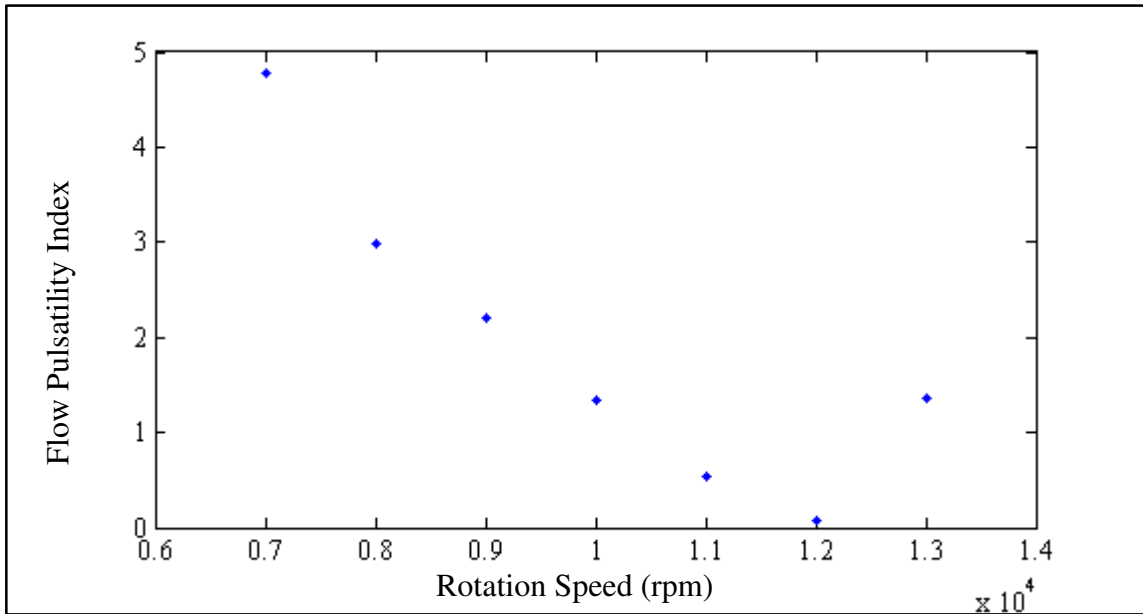


Figure 4.46. Heart Turcica axial flow pulsatility index from 7000 rpm to 13000 rpm with 1000 rpm increments

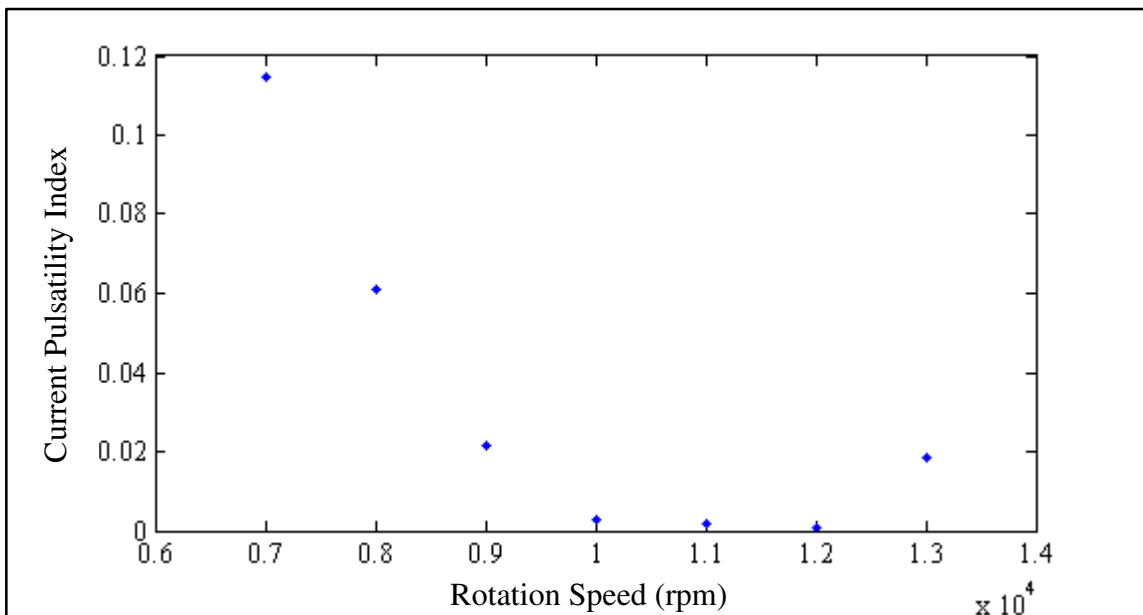


Figure 4.47. Heart Turcica axial current pulsatility index from 7000 rpm to 13000 rpm with 1000 rpm increments

As shown in the results pressure pulsatility index, flow pulsatility index and current pulsatility index decrease with increasing pump rotation speed. Suction initiation makes

increase the pulsatility indexes again.

4.4. COMBINED MODEL OF CARDIOVASCULAR SYSTEM AND HEART TURCICA CENTRIFUGAL

Heart Turcica centrifugal V13 model was implemented to diseased cardiovascular system model and simulations were performed to assess rotation speeds which induces different physiologically significant pumping states. Also simulations were performed from 1250 rpm operating speed to 2600 rpm operating speed with variable speed intervals. The hemodynamic variables are shown at these operating speeds in this part.

The used solver is ode15s and maximum step size was adjusted to 0.00025 s in the simulations. Simulations were performed 100 s because of long simulation time. It takes to complete simulations nearly 20 minutes by using AMD Turion dual core 1.83 GHz processor and 2 GB memory.

4.4.1. Simulation Results at 1250 rpm Operating Speed

Operating speed of Heart Turcica centrifugal V13 was adjusted to 1250 rpm and simulations were performed at that constant speed. Pressure difference across the pump, left atrial pressure, left ventricular pressure and aortic pressure are shown in Figure 4.48.

Maximum pressure difference across the pump is 59.7 mmHg and minimum pressure difference across the pump is -0.4 mmHg. Maximum left atrial pressure is 15.8 mmHg and minimum left atrial pressure is 13.4 mmHg. Maximum left ventricular pressure is 73.7 mmHg and minimum left ventricular pressure is 11.3 mmHg. Left ventricular pressure is above the threshold suction resistance value defined in Equation 4.3. Therefore pump inlet pressure is the same as left ventricular pressure. Maximum aortic pressure is 73.7 mmHg and minimum aortic pressure is 55.5 mmHg at 1250 rpm pump operating speed.

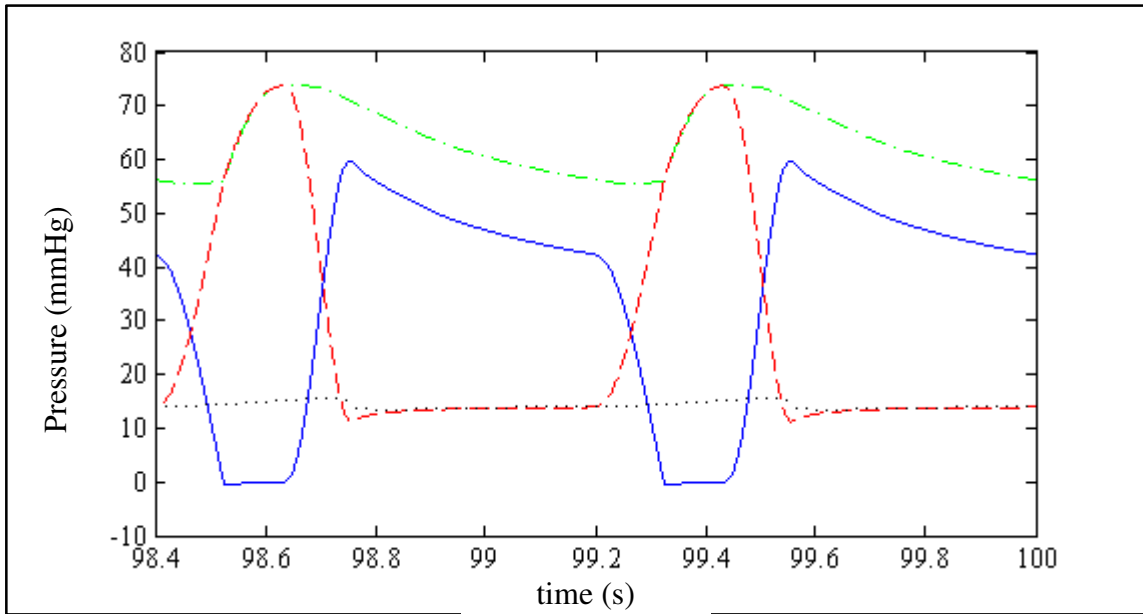


Figure 4.48. Pressure difference across the pump (continuous line), left atrial pressure (dotted line), left ventricular pressure (dashed line) and aortic pressure (chain line) at 1250 rpm operating speed

Left ventricular and left atrial volumes are shown in Figure 4.49 at 1250 rpm operating speed.

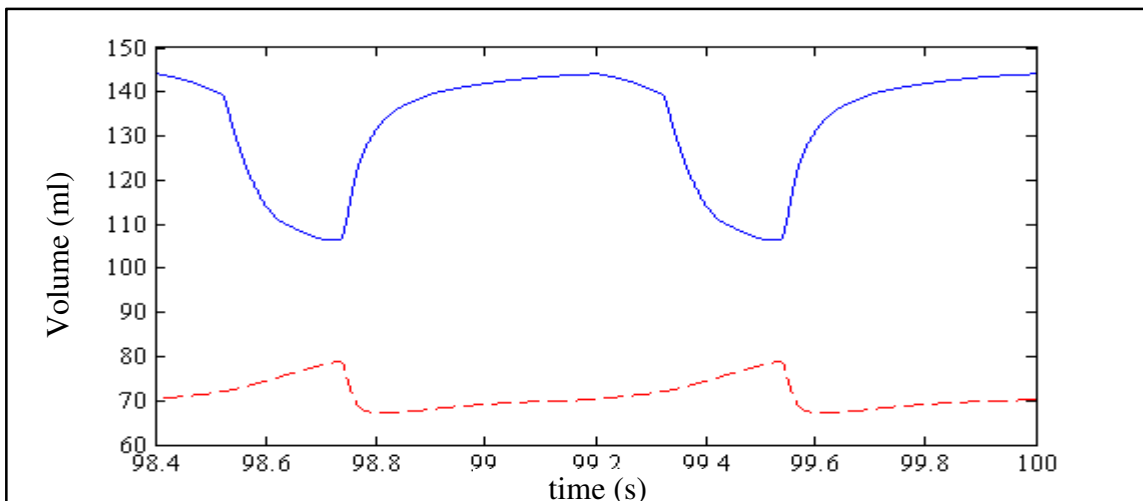


Figure 4.49 Left ventricular volume (continuous line) and left atrial volume (dashed line) at 1250 rpm pump operating speed

End diastolic volume of left ventricle is 144 ml, end systolic volume of left ventricle is 106.3 ml and stroke volume of left ventricle is 37.7 ml. Maximum volume of left atrium is 79 ml and minimum volume at left atrium is 67.1 ml at 1250 rpm operating speed.

Pump flow rate, mitral valve flow rate and aortic valve flow rate at 1250 rpm operating speed are shown in Figure 4.50.

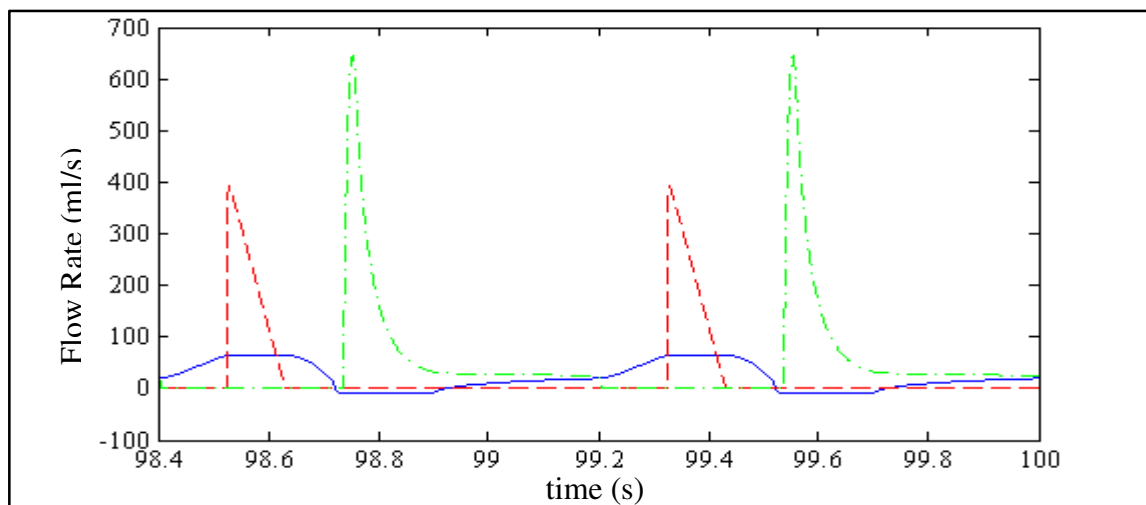


Figure 4.50. Pump flow rate (continuous line), mitral valve flow rate (chain line) and aortic valve flow rate (dashed line) at 1250 rpm operating speed

At 1250 rpm operating speed heart and Heart Turcica centrifugal V13 are operating together. Also pump flow regurgitates due to relatively high aortic pressure in diastolic phase. Cardiac output is 2.97 l/min at 1250 rpm operating speed. Pressure pulsatility index is 2.02 and flow pulsatility index is 2.69 at this speed. Results that are explained above are shown in Table 4.10.

Table 4.10. Simulation results for 1250 rpm operating speed

Parameter	Max. Value	Min. Value	Parameter	Max. Value	Min. Value
ΔP_{pump} (mmHg)	59.7	-0.4	V_{la} (ml)	79	67.1
P_{in} (mmHg)	73.7	11.3	V_{lv} (ml)	144	106.3
P_{la} (mmHg)	15.8	13.3	Stroke V_{lv} (ml)	37.7	
P_{lv} (mmHg)	73.7	11.3	CO (l/min)	2.97	
P_{ao} (mmHg)	73.7	55.5			

4.4.2. Simulation Results at 1380 rpm Operating Speed

Operating speed of Heart Turcica centrifugal V13 was adjusted to 1380 rpm and simulations were performed at 1380 rpm constant operating speed. Regurgitant pump flow disappears at 1380 rpm operating speed. Pressure difference across the pump, left atrial pressure, left ventricular pressure and aortic pressure are shown in Figure 4.51.

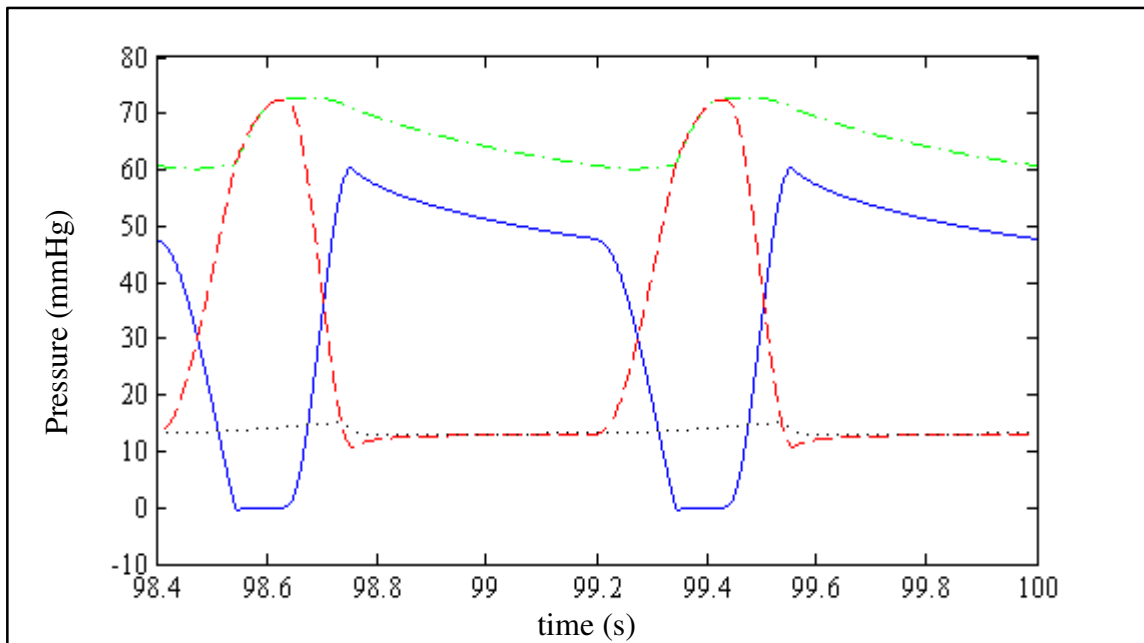


Figure 4.51. Pressure difference across the pump (continuous line), left atrial pressure (dotted line), left ventricular pressure (dashed line) and aortic pressure (chain line) at 1380 rpm operating speed

Maximum pressure difference across the pump is 60.3 mmHg and minimum pressure difference across the pump is -0.3 mmHg. Maximum left atrial pressure is 15 mmHg and minimum left atrial pressure is 12.8 mmHg. Maximum left ventricular pressure is 72.5 mmHg and minimum left ventricular pressure is 10.8 mmHg. Left ventricular pressure is above the threshold suction resistance value defined in Equation 4.3. Therefore pump inlet pressure is the same as left ventricular pressure. Maximum aortic pressure is 72.8 mmHg and minimum aortic pressure is 60.2 mmHg at 1380 rpm pump operating speed.

Left ventricular and left atrial volumes are shown in Figure 4.52 at 1380 rpm operating speed.

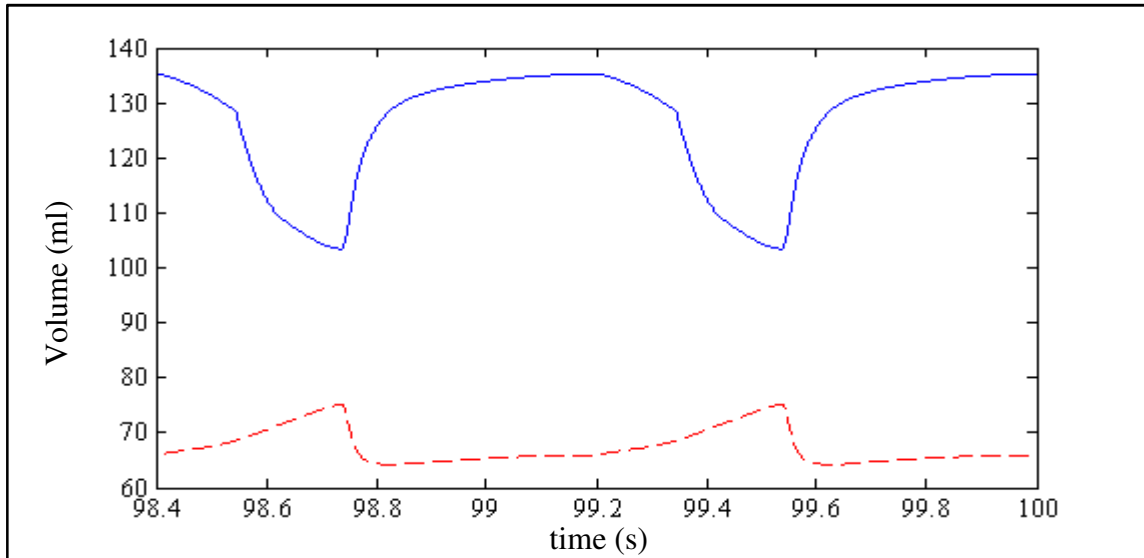


Figure 4.52 Left ventricular volume (continuous line) and left atrial volume (dashed line) at 1380 rpm pump operating speed

End diastolic volume of left ventricle is 135.3 ml, end systolic volume of left ventricle is 103.4 ml and stroke volume of left ventricle is 31.9 ml. Maximum volume of left atrium is 75.3 ml and minimum volume at left atrium is 64.2 ml at 1380 rpm operating speed.

Pump flow rate, mitral valve flow rate and aortic valve flow rate at 1380 rpm operating speed are shown in Figure 4.53.

At 1380 rpm operating speed regurgitation in pump flow disappears. In other words, aortic pressure cannot exceed the pressure difference across the pump over a cardiac cycle. Also at 1380 operating speed heart and heart pump operates together. The lowest value of pump flow is shown in Figure 4.54.

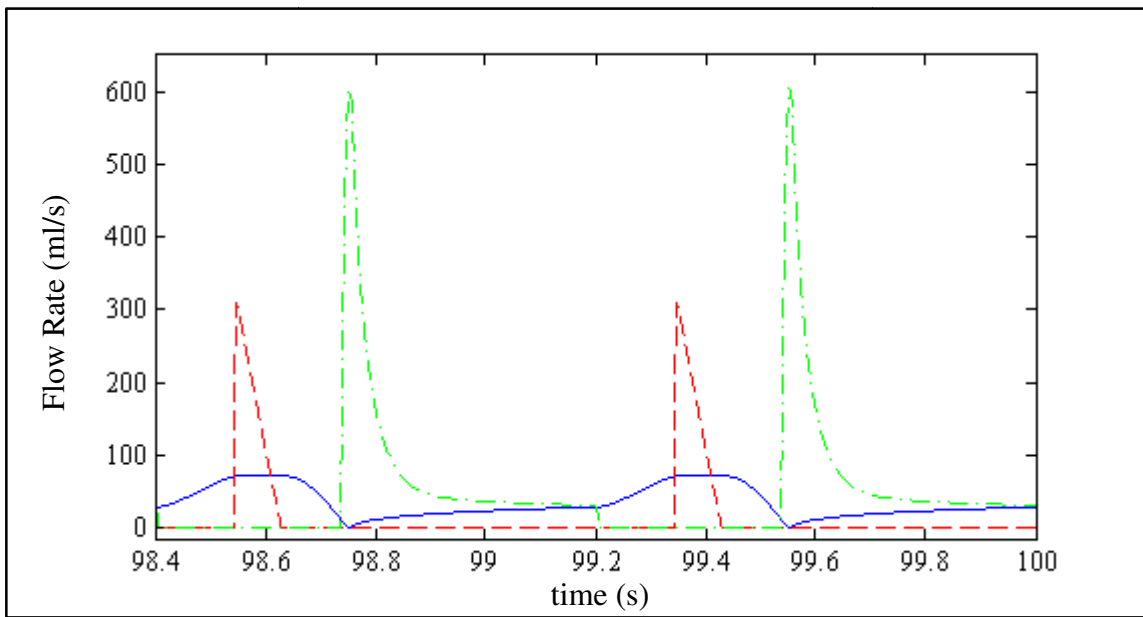


Figure 4.53. Pump flow rate (continuous line), mitral valve flow rate (chain line) and aortic valve flow rate (dashed line) at 1380 rpm operating speed

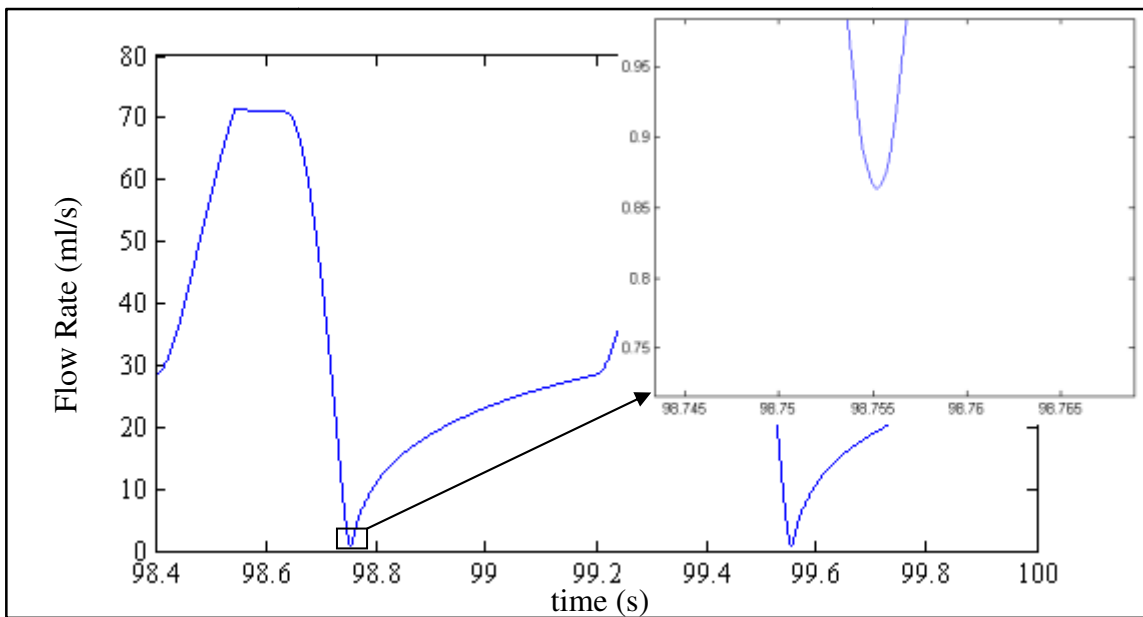


Figure 4.54. Pump flow rate at 1380 rpm operating speed

As shown in Figure 4.54 the lowest value of pump flow is very close to zero. If the rotation speed of the pump is decreased slightly, regurgitation in pump flow will start again. Also cardiac output is 3.10 l/min at 1380 rpm operating speed. Pressure pulsatility

index is 2.02 and flow pulsatility index is 1.95 at this speed. Results that are explained above are shown in Table 4.11.

Table 4.11. Simulation results for 1380 rpm operating speed

Parameter	Max. Value	Min. Value	Parameter	Max. Value	Min. Value
ΔP_{pump} (mmHg)	60.3	-0.3	V_{la} (ml)	75.3	64.2
P_{in} (mmHg)	72.5	10.8	V_{lv} (ml)	135.3	103.4
P_{la} (mmHg)	15	12.8	Stroke V_{lv} (ml)	31.9	
P_{lv} (mmHg)	72.5	10.8	CO (l/min)	3.10	
P_{ao} (mmHg)	72.8	60.2			

4.4.3. Simulation Results at 1500 rpm Operating Speed

Operating speed of Heart Turcica centrifugal V13 was adjusted to 1500 rpm and simulations were performed at 1500 rpm constant operating speed. Pressure difference across the pump, left atrial pressure, left ventricular pressure and aortic pressure are shown in Figure 4.55.

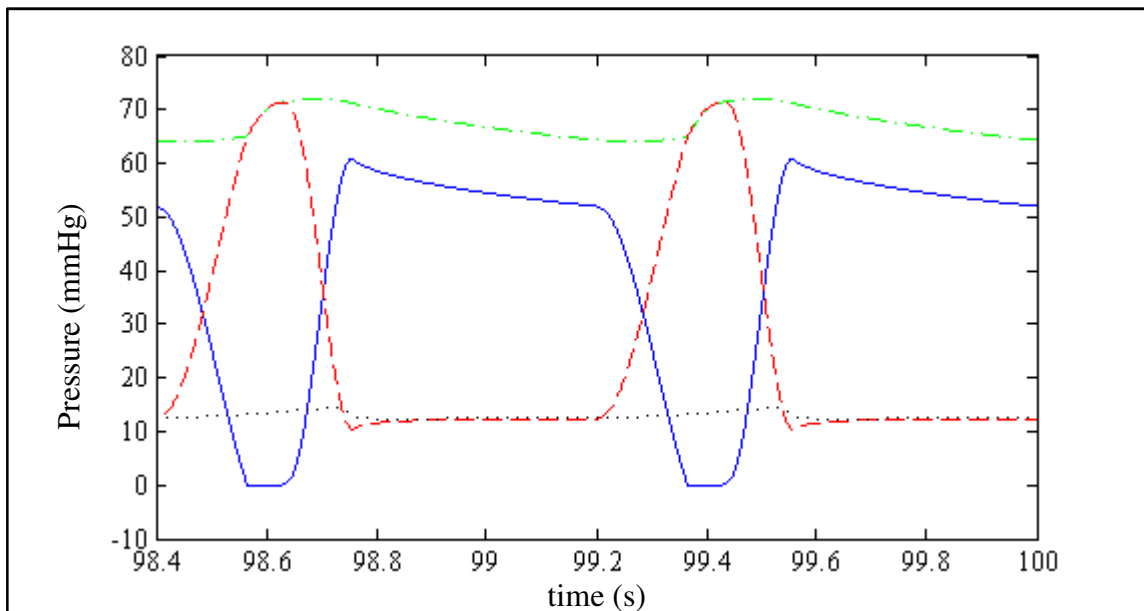


Figure 4.55. Pressure difference across the pump (continuous line), left atrial pressure (dotted line), left ventricular pressure (dashed line) and aortic pressure (chain line) at 1500 rpm operating speed

Maximum pressure difference across the pump is 60.7 mmHg and minimum pressure difference across the pump is -0.2 mmHg. Maximum left atrial pressure is 14.4 mmHg and minimum left atrial pressure is 12.3 mmHg. Maximum left ventricular pressure is 71.4 mmHg and minimum left ventricular pressure is 10.4 mmHg. Left ventricular pressure is above the threshold suction resistance value that defined in Equation 4.3. Therefore pump inlet pressure is same with left ventricular pressure. Maximum aortic pressure is 72.1 mmHg and minimum aortic pressure is 63.9 mmHg at 1500 rpm pump operating speed.

Left ventricular and left atrial volumes are shown in Figure 4.56 at 1500 rpm operating speed.

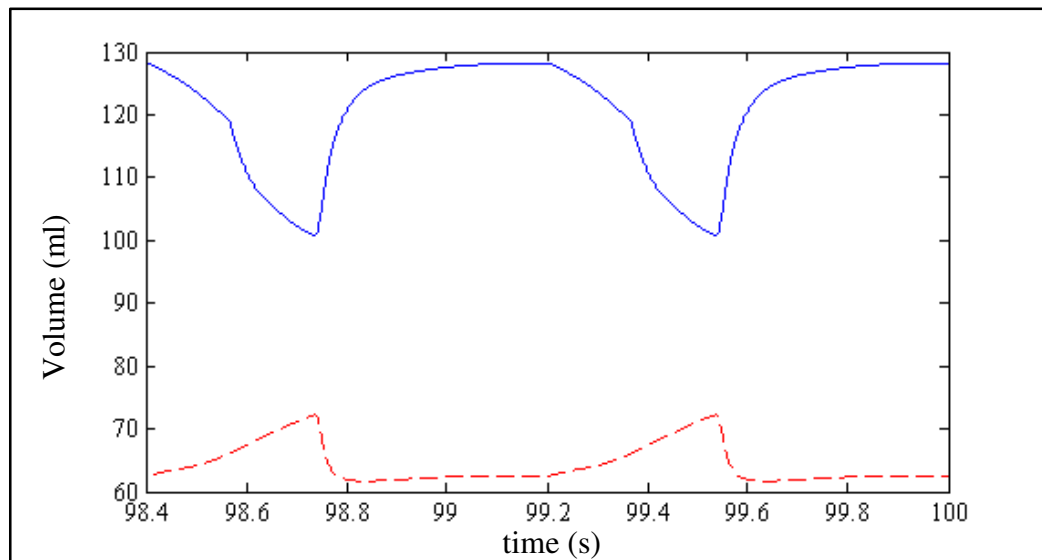


Figure 4.56 Left ventricular volume (continuous line) and left atrial volume (dashed line) at 1500 rpm pump operating speed

End diastolic volume of left ventricle is 128.2 ml, end systolic volume of left ventricle is 100.8 ml and stroke volume of left ventricle is 27.4 ml. Maximum volume of left atrium is 72.3 ml and minimum volume at left atrium is 61.7 ml at 1500 rpm operating speed.

Pump flow rate, mitral valve flow rate and aortic valve flow rate at 1500 rpm operating speed are shown in Figure 4.57.

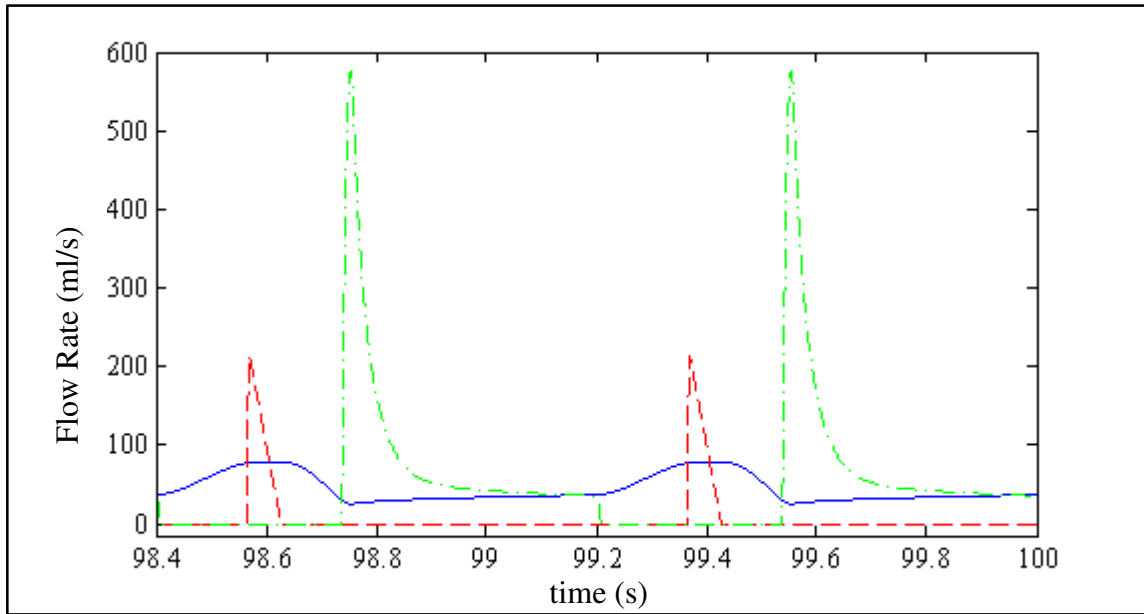


Figure 4.57. Pump flow rate (continuous line), mitral valve flow rate (chain line) and aortic valve flow rate (dashed line) at 1500 rpm operating speed

At 1500 rpm operating speed there is no regurgitation in pump flow. In other words aortic pressure cannot exceed difference across the pump over a cardiac cycle. Also heart and heart pump operates together. Cardiac output at 1500 operating speed is 3.20 l/min. Pressure pulsatility index is 2.01 and flow pulsatility index is 1.02 at this speed. Results that are explained above are shown in Table 4.12.

Table 4.12. Simulation results for 1500 rpm operating speed

Parameter	Max. Value	Min. Value	Parameter	Max. Value	Min. Value
ΔP_{pump} (mmHg)	60.7	-0.2	V_{la} (ml)	72.3	61.7
P_{in} (mmHg)	71.4	10.4	V_{lv} (ml)	128.2	100.8
P_{la} (mmHg)	14.4	12.3	Stroke V_{lv} (ml)	27.4	
P_{lv} (mmHg)	71.4	10.4	CO (l/min)	3.20	
P_{ao} (mmHg)	72.1	63.9			

4.4.4. Simulation Results at 1638 rpm Operating Speed

Operating speed of Heart Turcica centrifugal V13 was adjusted to 1638 rpm and simulations were performed at 1638 rpm constant operating speed. Pressure difference

across the pump, left atrial pressure, left ventricular pressure and aortic pressure are shown in Figure 4.58.

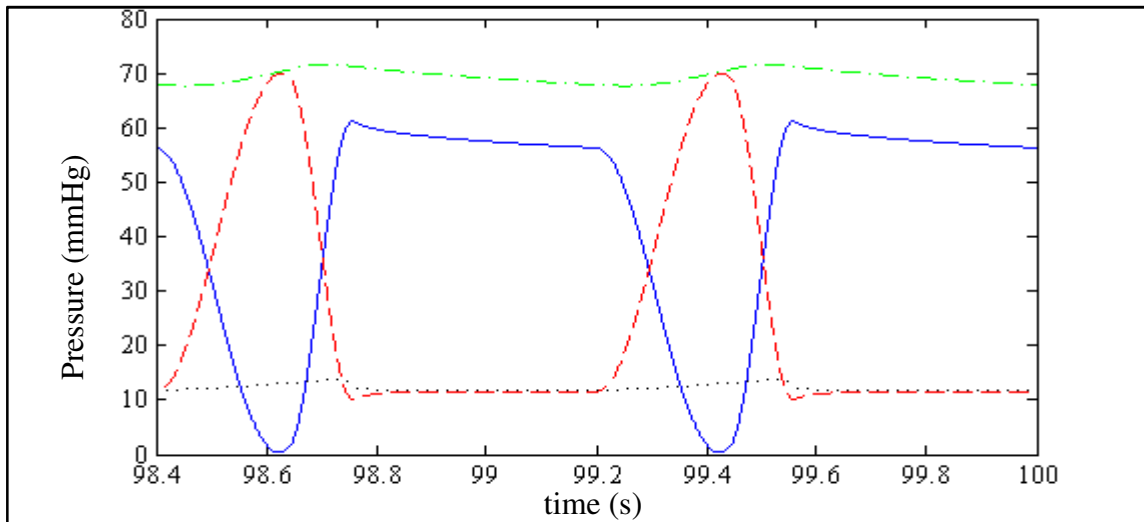


Figure 4.58. Pressure difference across the pump (continuous line), left atrial pressure (dotted line), left ventricular pressure (dashed line) and aortic pressure (chain line) at 1638 rpm operating speed

Maximum pressure difference across the pump is 61.2 mmHg and minimum pressure difference across the pump is 0.3 mmHg. Maximum left atrial pressure is 13.8 mmHg and minimum left atrial pressure is 11.8 mmHg. Maximum left ventricular pressure is 69.9 mmHg and minimum left ventricular pressure is 10 mmHg. Left ventricular pressure is above the threshold suction resistance value defined in Equation 4.3. Therefore pump inlet pressure is the same as left ventricular pressure. Maximum aortic pressure is 71.6 mmHg and minimum aortic pressure is 67.7 mmHg at 1638 rpm pump operating speed.

At 1638 rpm operating speed, flow through aortic valve disappears. In other words, left ventricular pressure is not sufficient to open the aortic valve. Therefore 1638 rpm is accepted as boundary operating speed between ventricular ejection state and aortic valve non-opening state. The comparison of left ventricular pressure and aortic pressure at 1638 rpm is shown in Figure 4.59.

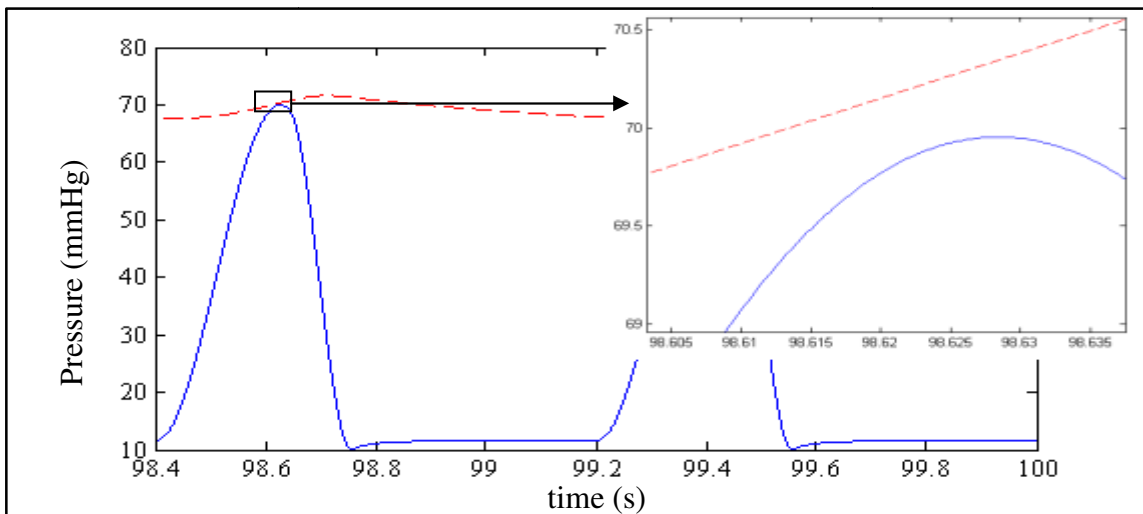


Figure 4.59. Left ventricular pressure (continuous line), aortic pressure (dashed line) at 1638 rpm operating speed

Left ventricular and left atrial volumes are shown in Figure 4.60 at 1638 rpm operating speed.

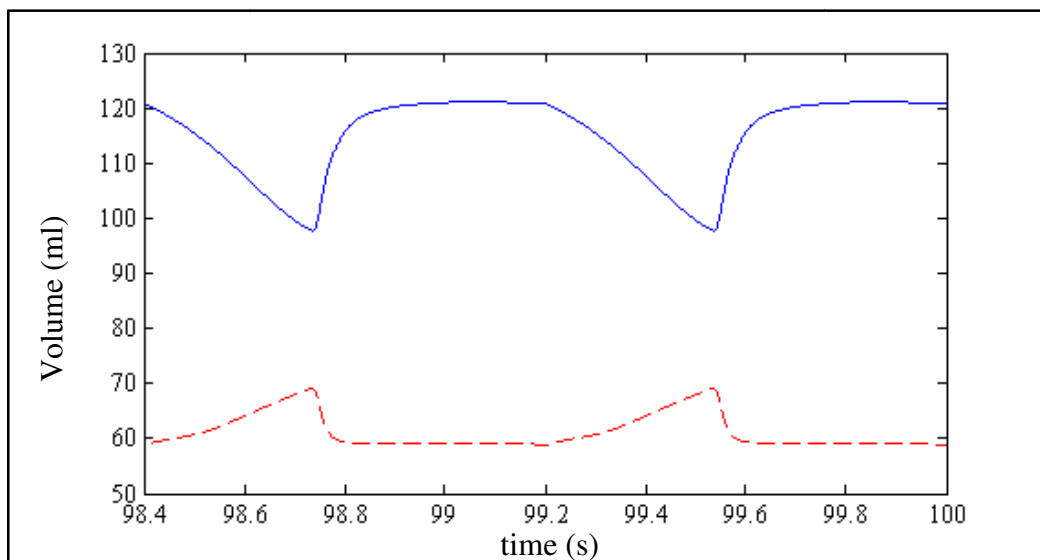


Figure 4.60 Left ventricular volume (continuous line) and left atrial volume (dashed line) at 1638 rpm pump operating speed

End diastolic volume of left ventricle is 121.1 ml, end systolic volume of left ventricle is 97.7 ml and stroke volume of left ventricle is 23.4 ml. Maximum volume of left

atrium is 69.1 ml and minimum volume at left atrium is 58.9 ml at 1638 rpm operating speed.

Pump flow rate, mitral valve flow rate and aortic valve flow rate at 1638 rpm operating speed are shown in Figure 4.61.

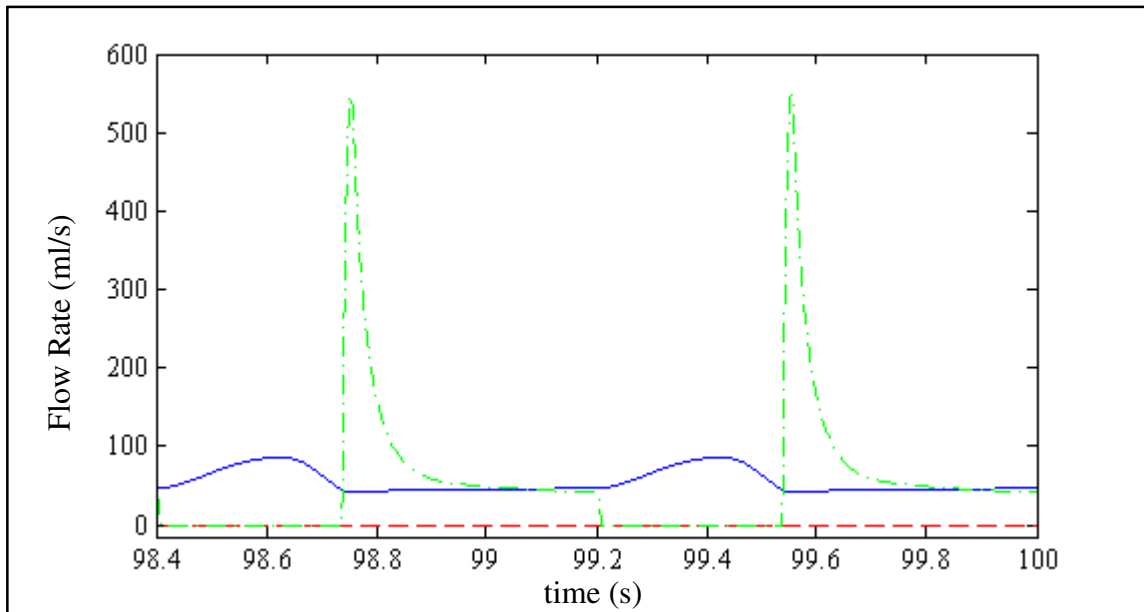


Figure 4.61. Pump flow rate (continuous line), mitral valve flow rate (chain line) and aortic valve flow rate (dashed line) at 1638 rpm operating speed

At 1638 rpm operating speed there is no regurgitation in pump flow. In other words aortic pressure is not higher than the pressure difference across the pump over a cardiac cycle. Heart and heart pump are not operating together due to relatively low pressure in the left ventricle. Cardiac output at 1638 operating speed is 3.30 l/min. Pressure pulsatility index is 1.98 and flow pulsatility index is 0.69 at this speed. Results that are explained above are shown in Table 4.13.

Table 4.13. Simulation results for 1638 rpm operating speed

Parameter	Max. Value	Min. Value	Parameter	Max. Value	Min. Value
ΔP_{pump} (mmHg)	61.2	0.3	V_{la} (ml)	69.1	58.9
P_{in} (mmHg)	69.9	10	V_{lv} (ml)	121.1	97.7
P_{la} (mmHg)	13.8	11.8	Stroke V_{lv} (ml)	23.4	
P_{lv} (mmHg)	69.9	10	CO (l/min)	3.30	
P_{ao} (mmHg)	71.6	67.7			

4.4.5. Simulation Results at 1900 rpm Operating Speed

Operating speed of Heart Turcica centrifugal V13 was adjusted to 1900 rpm and simulations were performed at this constant operating speed. Pressure difference across the pump, left atrial pressure, left ventricular pressure and aortic pressure are shown in Figure 4.62.

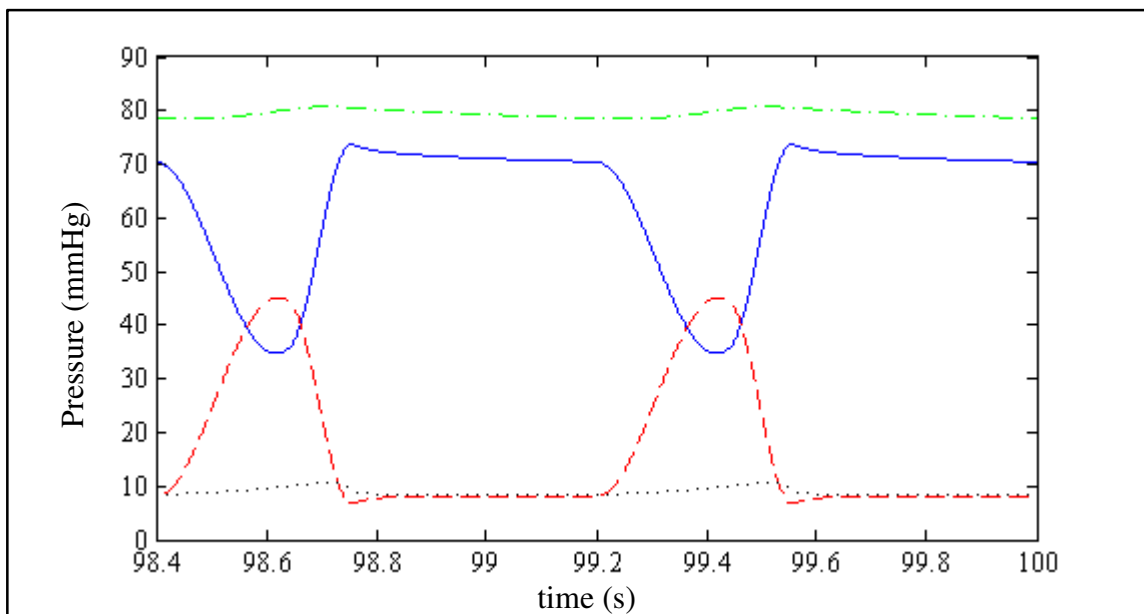


Figure 4.62. Pressure difference across the pump (continuous line), left atrial pressure (dotted line), left ventricular pressure (dashed line) and aortic pressure (chain line) at 1900 rpm operating speed

Maximum pressure difference across the pump is 73.8 mmHg and minimum pressure difference across the pump is 34.7 mmHg. Maximum left atrial pressure is 10.7 mmHg and

minimum left atrial pressure is 8.3 mmHg. Maximum left ventricular pressure is 45.2 mmHg and minimum left ventricular pressure is 6.7 mmHg. Left ventricular pressure is above the threshold suction resistance value defined in Equation 4.3. Therefore pump inlet pressure is the same as left ventricular pressure. Maximum aortic pressure is 80.7 mmHg and minimum aortic pressure is 78.4 mmHg at 1900 rpm pump operating speed.

Left ventricular and left atrial volumes are shown in Figure 4.63 at 1900 rpm operating speed.

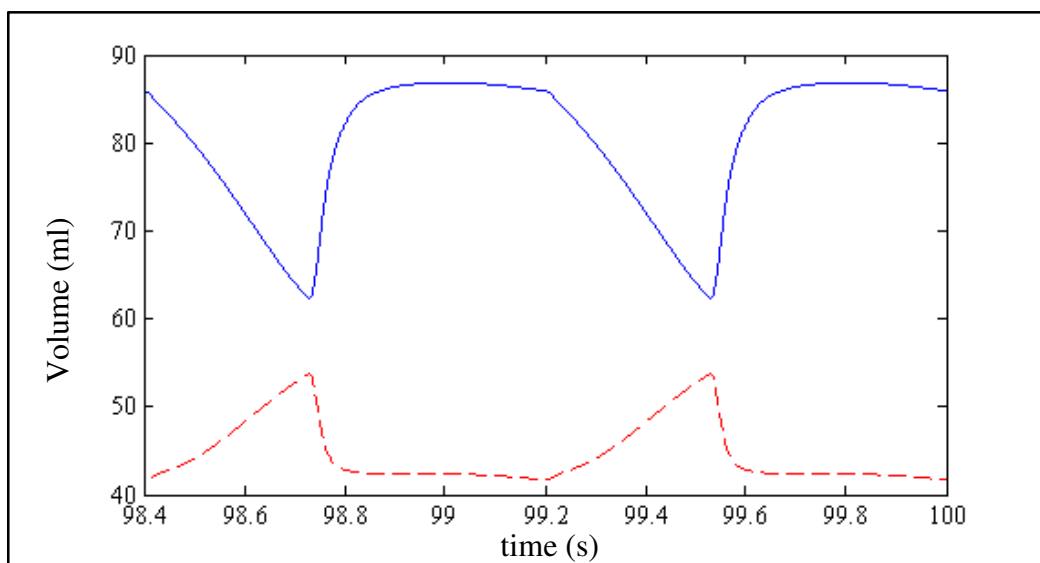


Figure 4.63 Left ventricular volume (continuous line) and left atrial volume (dashed line) at 1900 rpm pump operating speed

End diastolic volume of left ventricle is 86.8 ml, end systolic volume of left ventricle is 62.2 ml and stroke volume of left ventricle is 24.6 ml. Maximum volume of left atrium is 53.8 ml and minimum volume at left atrium is 41.7 ml at 1900 rpm operating speed.

Pump flow rate, mitral valve flow rate and aortic valve flow rate at 1900 rpm operating speed are shown in Figure 4.64.

At 1900 rpm operating speed there is no regurgitation in pump flow. In other words aortic pressure cannot exceed the pressure difference across the pump over a cardiac cycle. Also heart and heart pump are not operating together due to relatively low pressure in left

ventricle. Cardiac output at 1900 operating speed is 3.87 l/min. Pressure pulsatility index is 0.72 and flow pulsatility index is 0.37 at this speed. Results explained above are shown in Table 4.14.

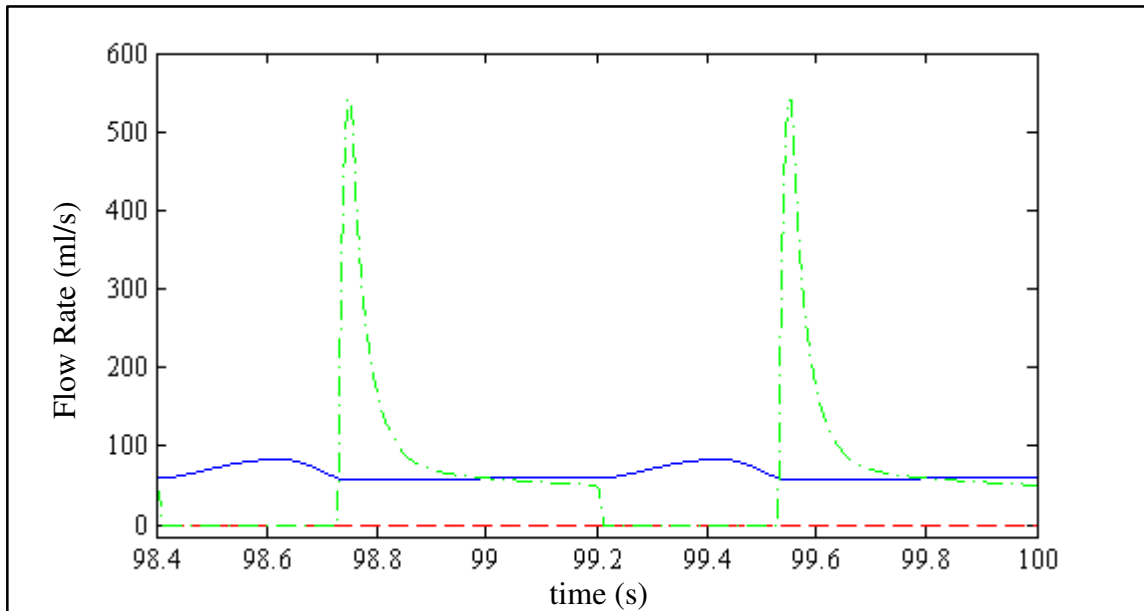


Figure 4.64. Pump flow rate (continuous line), mitral valve flow rate (chain line) and aortic valve flow rate (dashed line) at 1900 rpm operating speed

Table 4.14. Simulation results for 1900 rpm operating speed

Parameter	Max. Value	Min. Value	Parameter	Max. Value	Min. Value
ΔP_{pump} (mmHg)	73.8	34.7	V_{la} (ml)	53.8	41.7
P_{in} (mmHg)	45.2	6.7	V_{lv} (ml)	86.8	62.2
P_{la} (mmHg)	10.7	8.3	Stroke V_{lv} (ml)	24.6	
P_{lv} (mmHg)	45.2	6.7	CO (l/min)	3.87	
P_{ao} (mmHg)	80.7	78.4			

4.4.6. Simulation Results at 2140 rpm Operating Speed

Operating speed of Heart Turcica centrifugal V13 was adjusted to 2140 rpm and simulations were performed at that constant operating speed. Pressure difference across the pump, left atrial pressure, left ventricular pressure and aortic pressure are shown in Figure 4.65.

Maximum pressure difference across the pump is 85.8 mmHg and minimum pressure difference across the pump is 65 mmHg. Maximum left atrial pressure is 8.2 mmHg and minimum left atrial pressure is 5.5 mmHg. Maximum left ventricular pressure is 24.7 mmHg and minimum left ventricular pressure is 4.1 mmHg. Left ventricular pressure is above the threshold suction resistance value defined in Equation 4.3. Therefore pump inlet pressure is the same as left ventricular pressure. Maximum aortic pressure is 90.1 mmHg and minimum aortic pressure is 89 mmHg at 2140 rpm pump operating speed. To provide perfusion minimum systolic aortic pressure must be 90 mmHg. Therefore minimum operating speed of Heart Turcica centrifugal V13 has to be set to 2140 rpm.

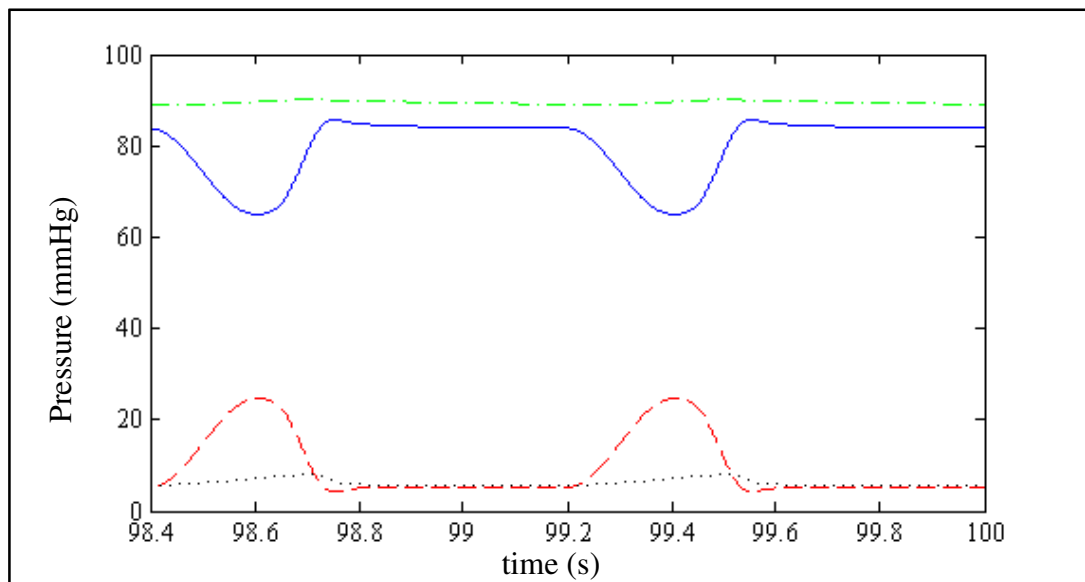


Figure 4.65. Pressure difference across the pump (continuous line), left atrial pressure (dotted line), left ventricular pressure (dashed line) and aortic pressure (chain line) at 2140 rpm operating speed

Left ventricular and left atrial volumes are shown in Figure 4.66 at 2140 rpm operating speed.

End diastolic volume of left ventricle is 58.6 ml, end systolic volume of left ventricle is 33 ml and stroke volume of left ventricle is 25.6 ml. Maximum volume of left atrium is 41 ml and minimum volume at left atrium is 27.6 ml at 2140 rpm operating speed.

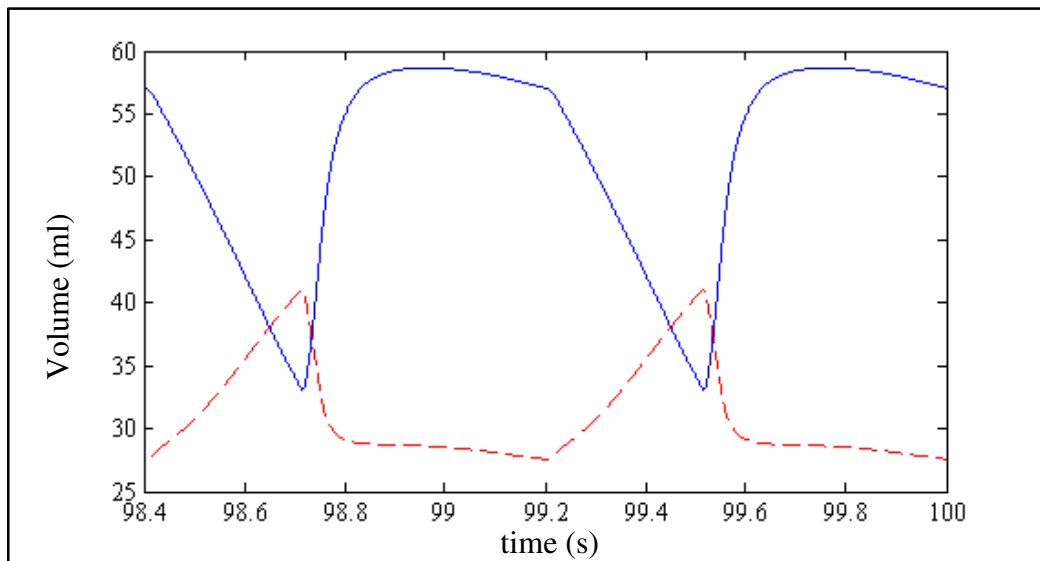


Figure 4.66 Left ventricular volume (continuous line) and left atrial volume (dashed line) at 2140 rpm pump operating speed

Pump flow rate, mitral valve flow rate and aortic valve flow rate at 2140 rpm operating speed are shown in Figure 4.67.

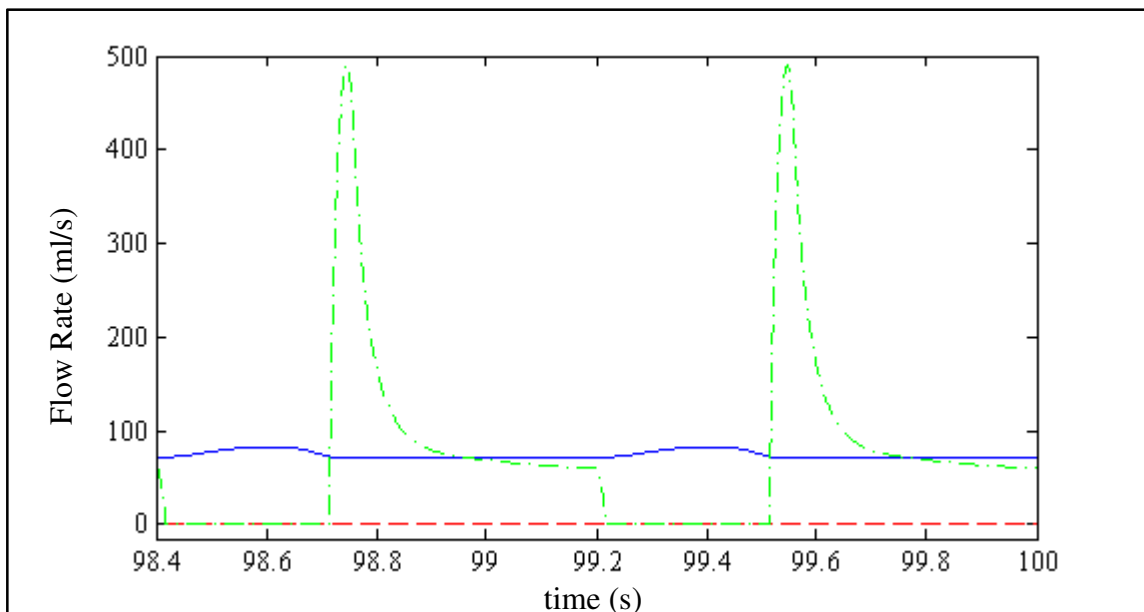


Figure 4.67. Pump flow rate (continuous line), mitral valve flow rate (chain line) and aortic valve flow rate (dashed line) at 2140 rpm operating speed

At 2140 rpm operating speed there is no regurgitation in pump flow. In other words aortic pressure cannot exceed the pressure difference across the pump over a cardiac cycle. Also heart and heart pump are not operating together due to low pressure in left ventricle. Cardiac output at 2140 operating speed is 4.45 l/min. Pressure pulsatility index is 0.27 and flow pulsatility index is 0.16 at this speed. Results explained above are shown in Table 4.15.

Table 4.15. Simulation results for 2140 rpm operating speed

Parameter	Max. Value	Min. Value	Parameter	Max. Value	Min. Value
ΔP_{pump} (mmHg)	85.8	65	V_{la} (ml)	41	27.6
P_{in} (mmHg)	24.7	4.1	V_{lv} (ml)	56.6	33
P_{la} (mmHg)	8.2	5.5	Stroke V_{lv} (ml)	25.6	
P_{lv} (mmHg)	24.7	4.1	CO (l/min)	4.45	
P_{ao} (mmHg)	90.1	89			

4.4.7. Simulation Results at 2350 rpm Operating Speed

Operating speed of Heart Turcica centrifugal V13 was adjusted to 2350 rpm and simulations were performed at that constant speed. Pressure difference across the pump, left atrial pressure, left ventricular pressure and aortic pressure are shown in Figure 4.68.

Maximum pressure difference across the pump is 96.7 mmHg and minimum pressure difference across the pump is 89.1 mmHg. Maximum left atrial pressure is 5.8 mmHg and minimum left atrial pressure is 3.4 mmHg. Maximum left ventricular pressure is 9.8 mmHg and minimum left ventricular pressure is 2.4 mmHg. Left ventricular pressure is above the threshold suction resistance value defined in Equation 4.3. Therefore pump inlet pressure is the same as left ventricular pressure. Maximum aortic pressure is 99.1 mmHg and minimum aortic pressure is 98.8 mmHg at 2350 rpm pump operating speed.

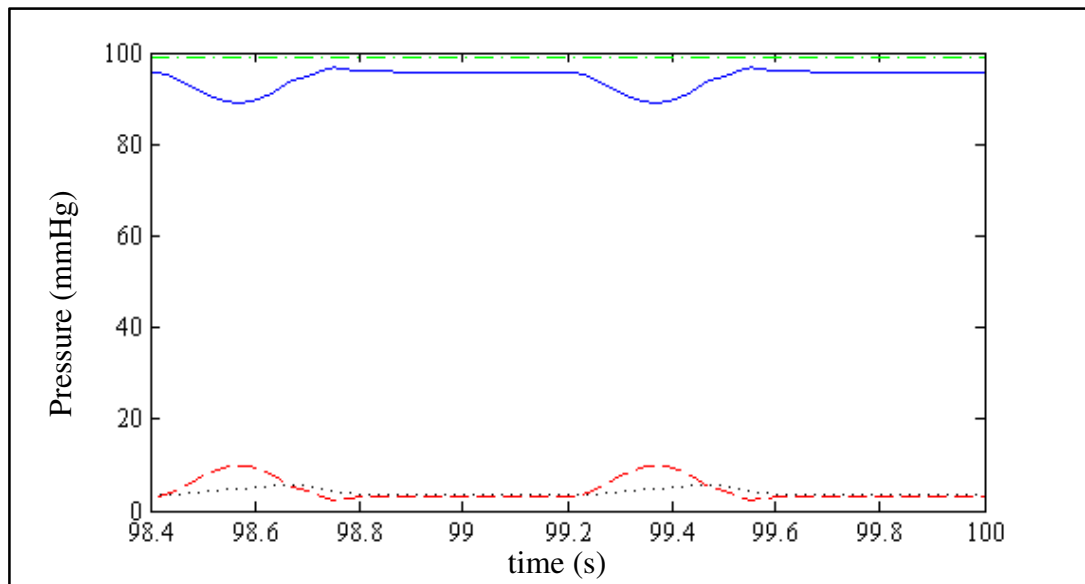


Figure 4.68. Pressure difference across the pump (continuous line), left atrial pressure (dotted line), left ventricular pressure (dashed line) and aortic pressure (chain line) at 2350 rpm operating speed

Left ventricular and left atrial volumes are shown in Figure 4.69 at 2350 rpm operating speed.

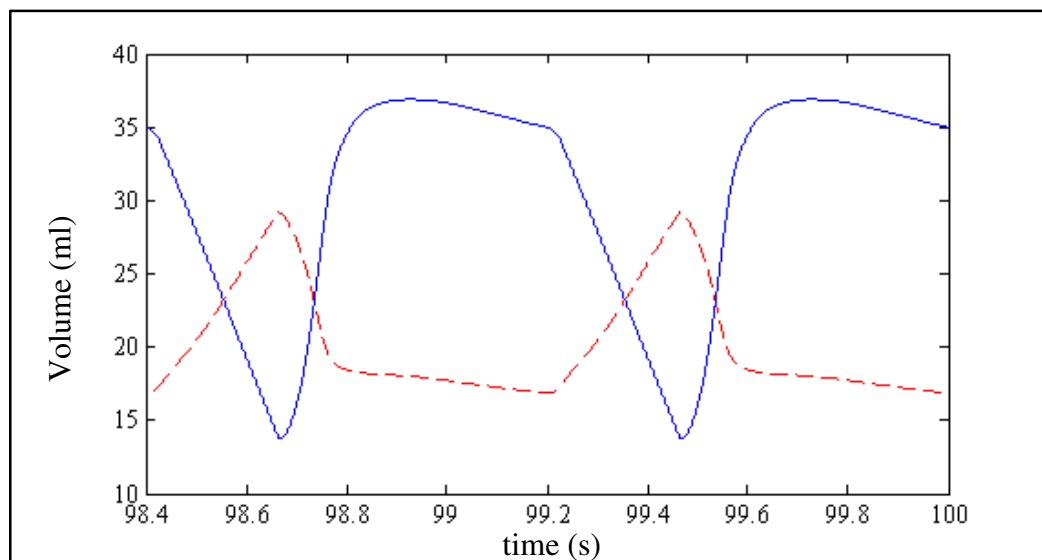


Figure 4.69 Left ventricular volume (continuous line) and left atrial volume (dashed line) at 2350 rpm pump operating speed

End diastolic volume of left ventricle is 36.9 ml, end systolic volume of left ventricle is 13.7 ml and stroke volume of left ventricle is 23.2 ml. Maximum volume of left atrium is 29.2 ml and minimum volume at left atrium is 16.8 ml at 2350 rpm operating speed.

Pump flow rate, mitral valve flow rate and aortic valve flow rate at 2350 rpm operating speed are shown in Figure 4.70.

At 2350 rpm operating speed there is no regurgitation in pump flow. In other words aortic pressure cannot exceed the pressure difference across the pump over a cardiac cycle. Also heart and heart pump are not operating together due to low pressure in left ventricle. Cardiac output at 2350 operating speed is 5.01 l/min. Pressure pulsatility index is 0.08 and flow pulsatility index is 0.05 at this speed. Results that are explained above are shown in Table 4.16.

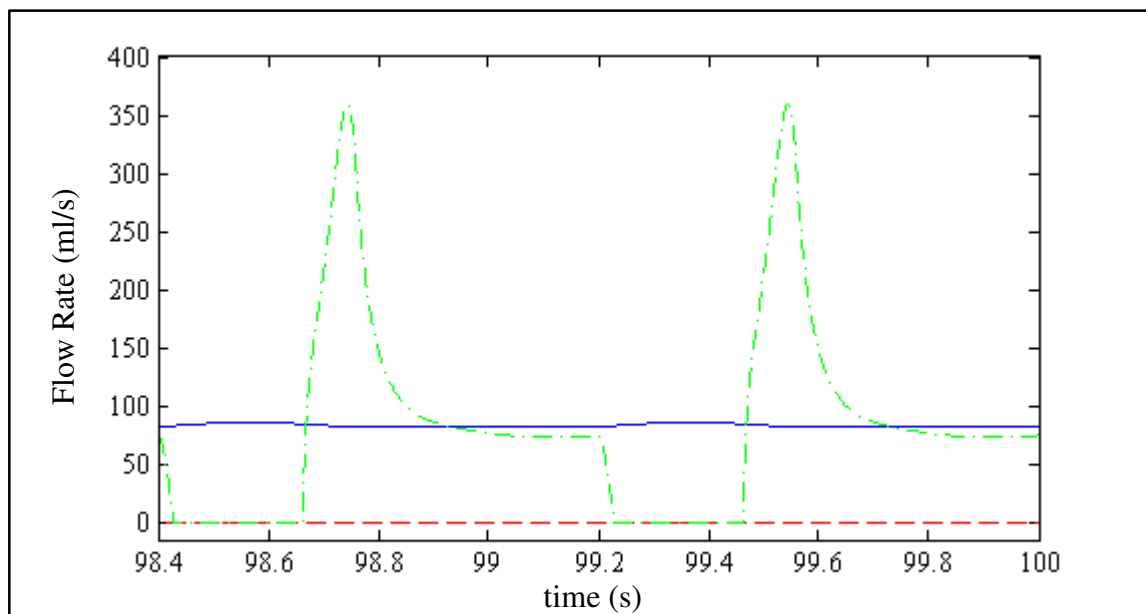


Figure 4.70. Pump flow rate (continuous line), mitral valve flow rate (chain line) and aortic valve flow rate (dashed line) at 2350 rpm operating speed

Table 4.16. Simulation results for 2350 rpm operating speed

Parameter	Max. Value	Min. Value	Parameter	Max. Value	Min. Value
ΔP_{pump} (mmHg)	96.7	89.1	V_{la} (ml)	29.2	16.8
P_{in} (mmHg)	9.8	2.4	V_{lv} (ml)	57.6	33
P_{la} (mmHg)	5.8	3.4	Stroke V_{lv} (ml)	23.2	
P_{lv} (mmHg)	9.8	2.4	CO (l/min)	5.01	
P_{ao} (mmHg)	99.1	98.8			

4.4.8. Simulation Results at 2542 rpm Operating Speed

Operating speed of Heart Turcica centrifugal V13 was adjusted to 2542 rpm and simulations were performed at this constant speed. Pressure difference across the pump, left atrial pressure, left ventricular pressure and aortic pressure are shown in Figure 4.71.

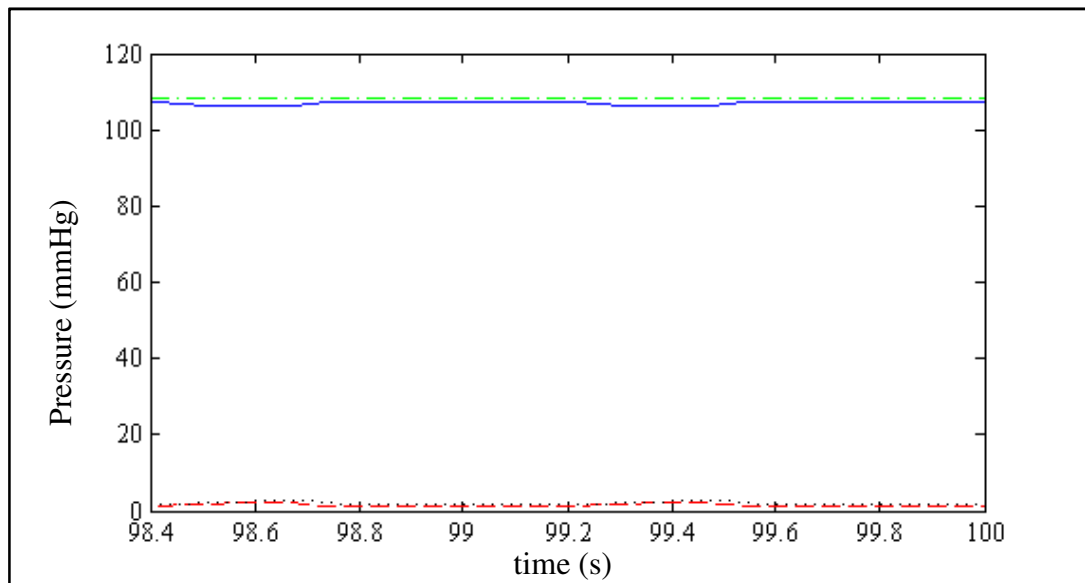


Figure 4.71. Pressure difference across the pump (continuous line), left atrial pressure (dotted line), left ventricular pressure (dashed line) and aortic pressure (chain line) at 2542 rpm operating speed

Maximum pressure difference across the pump is 107.5 mmHg and minimum pressure difference across the pump is 106.3 mmHg. Maximum left atrial pressure is 2.7 mmHg and minimum left atrial pressure is 1.5 mmHg. Maximum left ventricular pressure is 2.1 mmHg and minimum left ventricular pressure is 1 mmHg. Left ventricular pressure

is above the threshold suction resistance value defined in Equation 4.3. Therefore pump inlet pressure is the same as left ventricular pressure. Maximum aortic pressure is 108.5 mmHg and minimum aortic pressure is 108.4 mmHg at 2542 rpm pump operating speed. According to these results, if the pump speed slightly increased suction effect will occur in the left ventricle.

Left ventricular and left atrial volumes are shown in Figure 4.72 at 2542 rpm operating speed.

End diastolic volume of left ventricle is 18.4 ml, end systolic volume of left ventricle is 8.1 ml and stroke volume of left ventricle is 10.3 ml. Maximum volume of left atrium is 13.3 ml and minimum volume at left atrium is 7.7 ml at 2542 rpm operating speed.

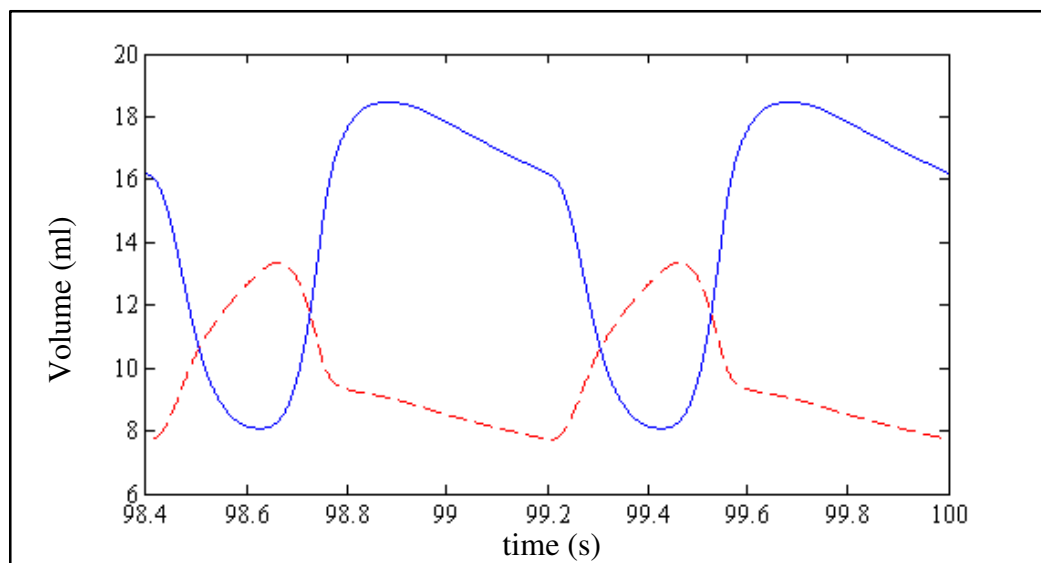


Figure 4.72 Left ventricular volume (continuous line) and left atrial volume (dashed line) at 2542 rpm pump operating speed

Pump flow rate, mitral valve flow rate and aortic valve flow rate at 2542 rpm operating speed are shown in Figure 4.73.

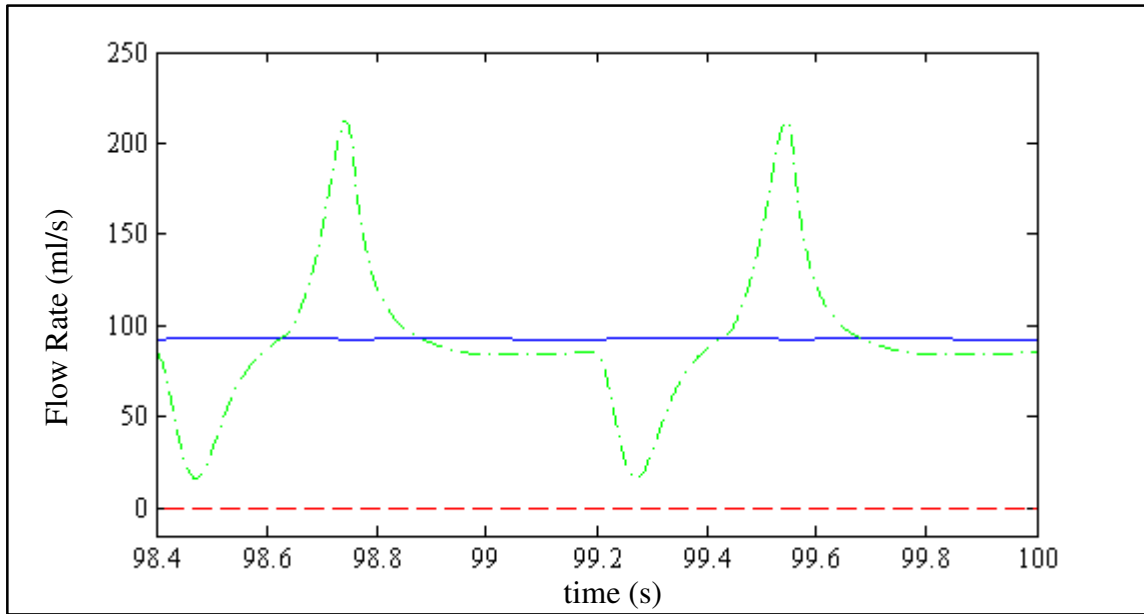


Figure 4.73. Pump flow rate (continuous line), mitral valve flow rate (chain line) and aortic valve flow rate (dashed line) at 2542 rpm operating speed

At 2542 rpm operating speed there is no regurgitation in pump flow. In other words aortic pressure cannot exceed the pressure difference across the pump over a cardiac cycle. Also heart and heart pump are not operating together due to low pressure in left ventricle. At 2542 rpm operating speed mitral valve remains open due to relatively lower pressure in left ventricle. In other words pressure in left ventricle is lower than left atrial pressure over a cardiac cycle. Cardiac output at 2542 operating speed is 5.57 l/min. Pressure pulsatility index is 0.01 and flow pulsatility index is 0.006 at this speed. Results that are explained above are shown in Table 4.17.

Table 4.17. Simulation results for 2542 rpm operating speed

Parameter	Max. Value	Min. Value	Parameter	Max. Value	Min. Value
ΔP_{pump} (mmHg)	107.5	106.3	V_{la} (ml)	13.3	7.7
P_{in} (mmHg)	2.1	1.01	V_{lv} (ml)	18.4	8.1
P_{la} (mmHg)	2.7	1.5	Stroke V_{lv} (ml)	10.3	
P_{lv} (mmHg)	2.1	1.01	CO (l/min)	5.57	
P_{ao} (mmHg)	108.5	108.4			

4.4.9. Simulation Results at 2600 rpm Operating Speed

Operating speed of Heart Turcica centrifugal was adjusted to 2600 rpm and simulations were performed at this constant speed. Left atrial pressure and left ventricular pressure are shown in Figure 4.77.

Left atrial maximum pressure is 2.2 mmHg and left atrial minimum pressure is 1.3 mmHg. Left ventricular maximum pressure is 1.7 mmHg and left ventricular minimum pressure is 0.85 mmHg at 2600 rpm operating speed.

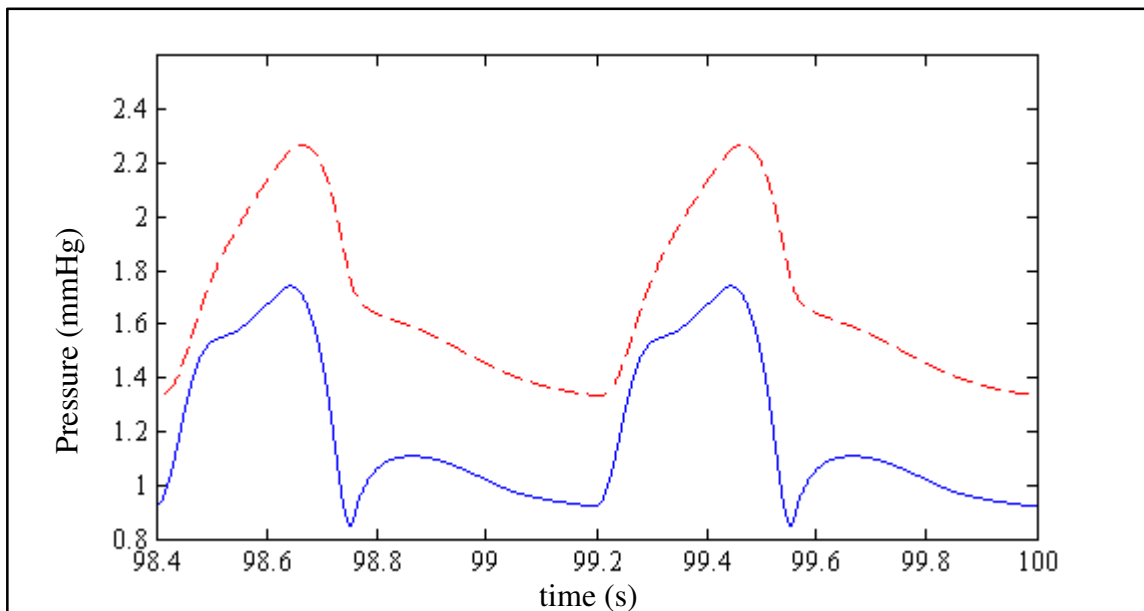


Figure 4.77. Left ventricular pressure (continuous line), left atrial pressure (dashed line) at 2600 rpm operating speed

Pump inlet pressure at 2600 rpm operating speed is shown in Figure 4.78.

Maximum pump inlet pressure is 1.7 mmHg and minimum pump inlet pressure is -38.2 mmHg. Pump inlet pressure is not negative over whole cardiac cycle. This result shows that partial ventricular suction occurs in left ventricle.

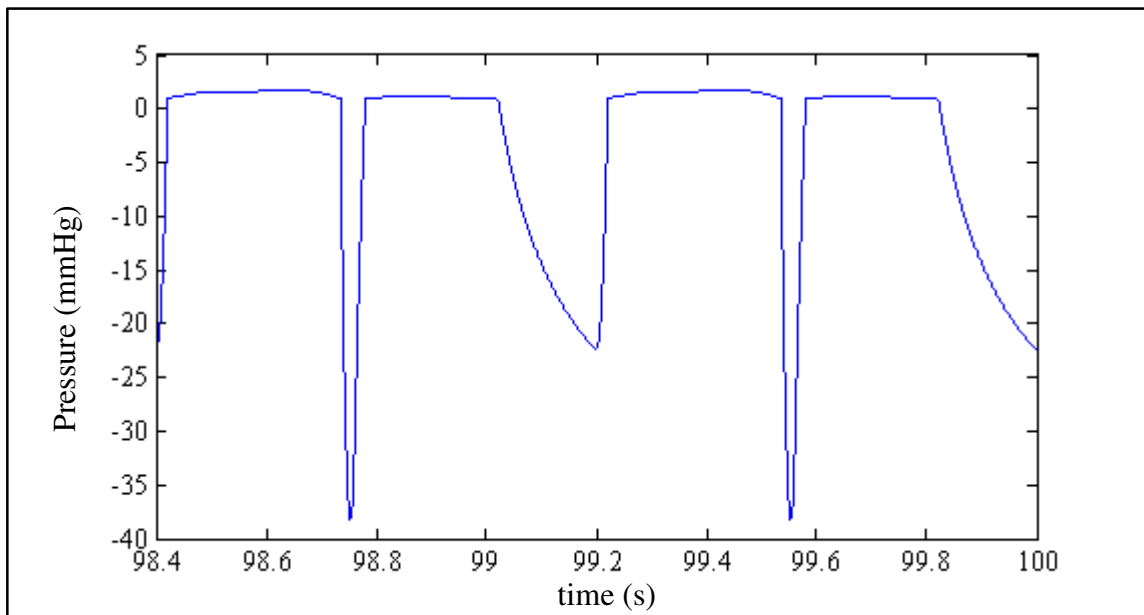


Figure 4.78. Pump inlet pressure at 2600 rpm pump operating speed

Pressure difference across the pump and aortic pressure are shown in Figure 4.79.

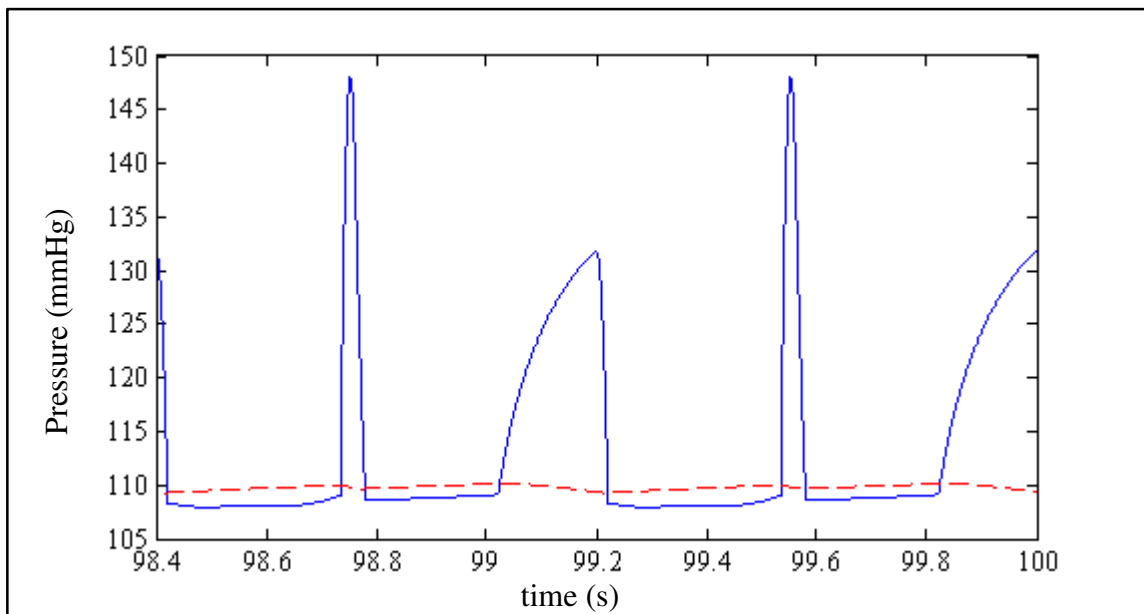


Figure 4.79. Pressure difference across the pump (continuous line), aortic pressure (dashed line) at 2600 rpm operating speed

Maximum pressure difference across the pump is 148.1 mmHg and minimum pressure difference across the pump is 107.9 mmHg. Maximum aortic pressure is 110.1 mmHg and 109.3 mmHg.

Left ventricular and left atrial volumes are shown in Figure 4.80 at 2600 rpm operating speed.

End diastolic volume of left ventricle is 16.1 ml, end systolic volume of left ventricle is 7.5 ml and stroke volume of left ventricle is 8.6 ml. Maximum volume of left atrium is 11.3 ml and minimum volume at left atrium is 6.6 ml at 2600 rpm operating speed.

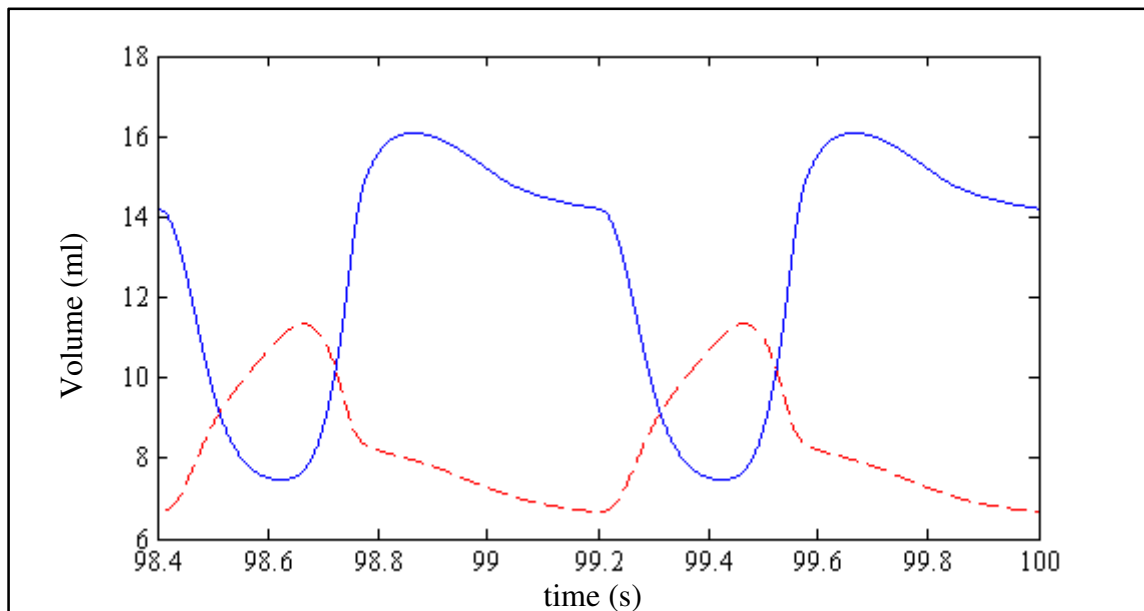


Figure 4.80. Left ventricular volume (continuous line) and left atrial volume (dashed line) at 2600 rpm pump operating speed

Pump flow rate, mitral valve flow rate and aortic valve flow rate at 2600 rpm operating speed are shown in Figure 4.81.

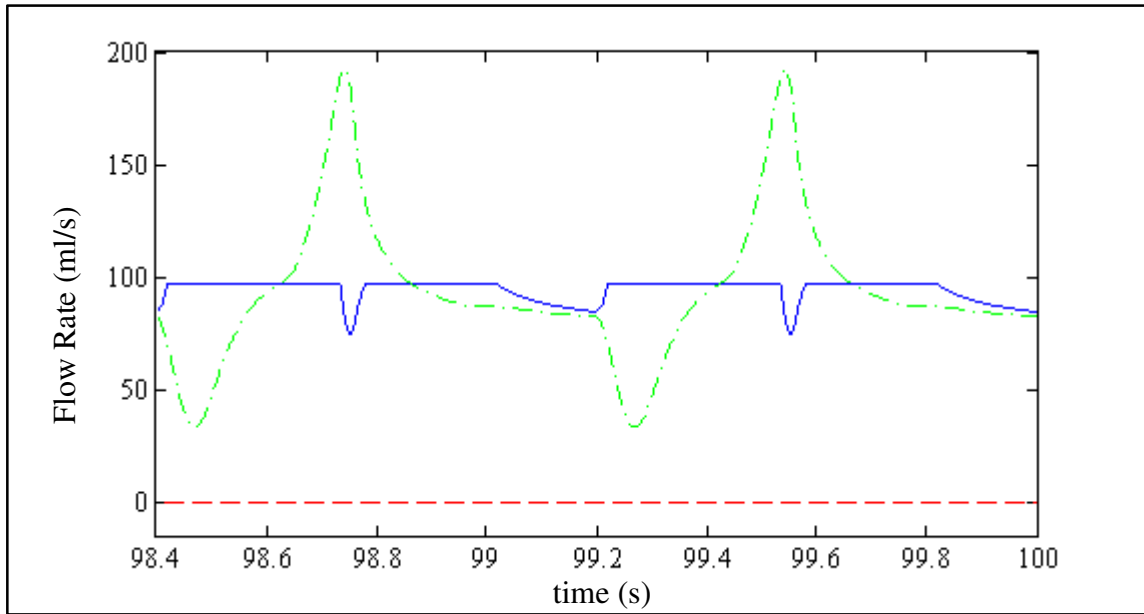


Figure 4.81. Pump flow rate (continuous line), mitral valve flow rate (chain line) and aortic valve flow rate (dashed line) at 2600 rpm operating speed

At 2600 rpm operating speed mitral valve remains open due to relatively lower pressure in left ventricle. In other words pressure in left ventricle is lower than left atrial pressure over a cardiac cycle. Cardiac output at 2600 operating speed is 5.65 l/min. Pressure pulsatility index is 0.31 and flow pulsatility index is 0.26 at this speed. Results that are explained above are shown in Table 4.18.

Table 4.18. Simulation results for 2600 rpm operating speed

Parameter	Max. Value	Min. Value	Parameter	Max. Value	Min. Value
ΔP_{pump} (mmHg)	148.1	107.9	V_{la} (ml)	11.3	6.6
P_{in} (mmHg)	1.7	-38.2	V_{lv} (ml)	16.1	7.5
P_{la} (mmHg)	2.2	1.3	Stroke V_{lv} (ml)	8.6	
P_{lv} (mmHg)	1.7	0.85	CO (l/min)	5.65	
P_{ao} (mmHg)	110.1	109.3			

As shown in the results in suction condition the shape of pump flow, pressure difference across the pump. In other words distortion occurs due to suction. Also pulsatility appears again that has been disappeared with increasing operating speed.

Left ventricular pressure-volume loops are good indicators to explain the help of the left ventricular assist devices to left ventricle. Left ventricular pressure-volume loops from 1250 rpm to 2600 rpm that explained above are shown in Figure 4.82.

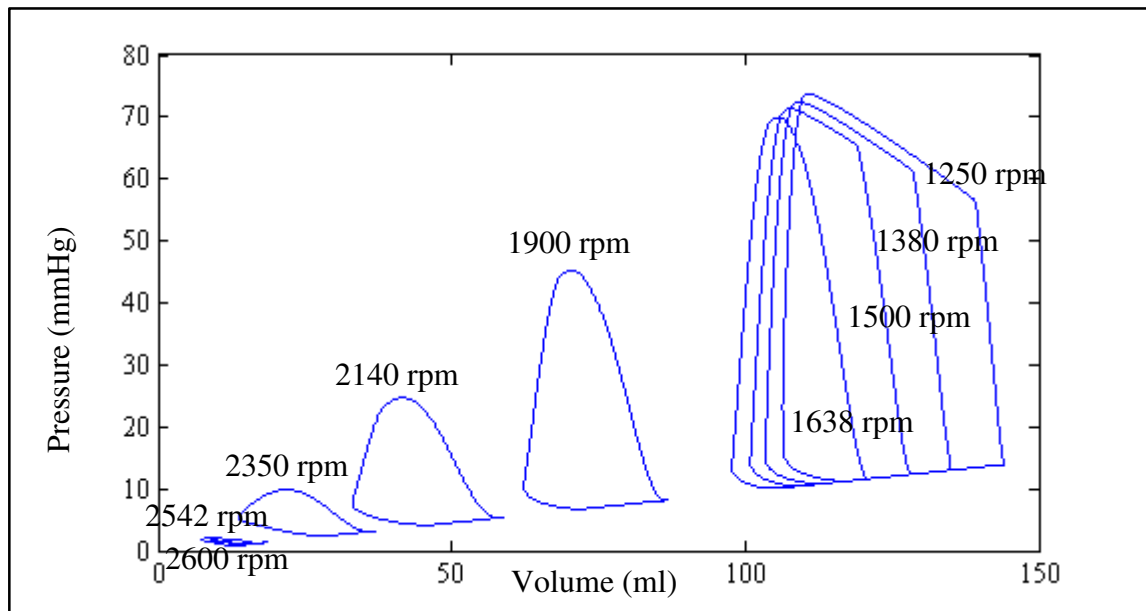


Figure 4.82. Left ventricular pressure – volume loops from 1250 rpm to 2600 rpm

According to the results, area of the left ventricular pressure-volume loop is getting smaller with increasing pump operating speeds. In other words external work of the left ventricle is decreasing.

Also pressure – flow rate diagram of Heart Turcica centrifugal V13 shows the effect of increasing pump operating speed. Pressure – flow rate diagram of Heart Turcica axial from 1250 rpm to 2600 rpm is shown in Figure 4.83.

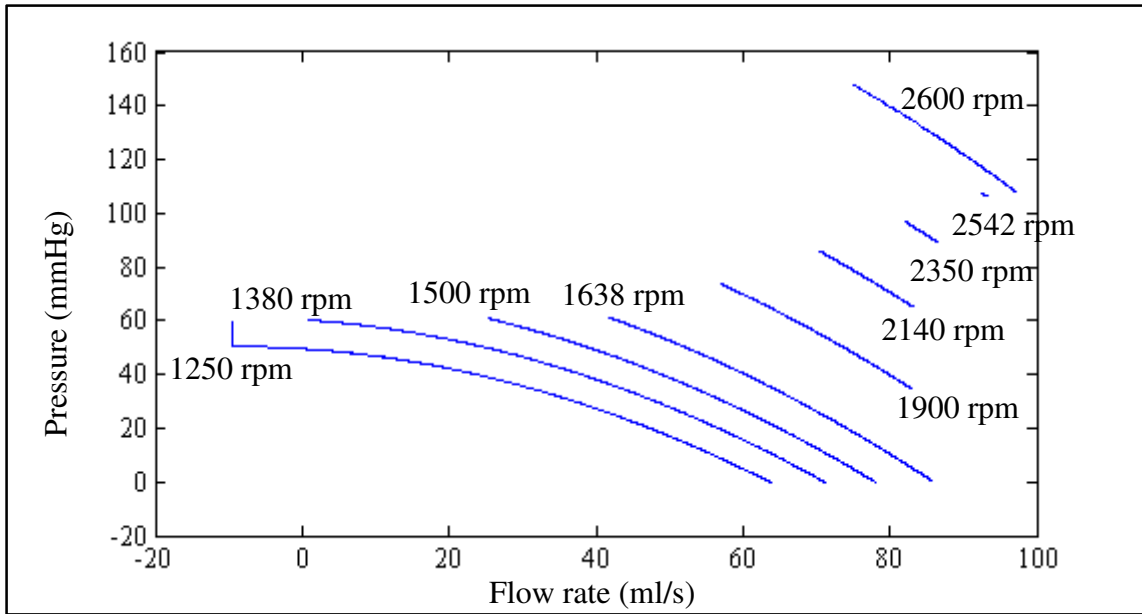


Figure 4.83. Heart Turcica centrifugal V13 pressure-flow rate diagram from 1250 rpm to 2600 rpm

As mentioned above increasing pump operating speed causes pulsatility to disappear in pump flow rate and pressure difference across the pump. After suction initiation pulsatility is appear again in these variables. In other words, increasing pump operating speed provides shorter pressure-flow rate curves in non-suction conditions. But in suction conditions, longer pressure-flow rate curves are obtained again.

Pulsatility indexes are also good indicators of increasing operating speed. Pressure pulsatility index and flow pulsatility index with respect pump rotation speed are shown in Figure 4.84 and 4.85 respectively.

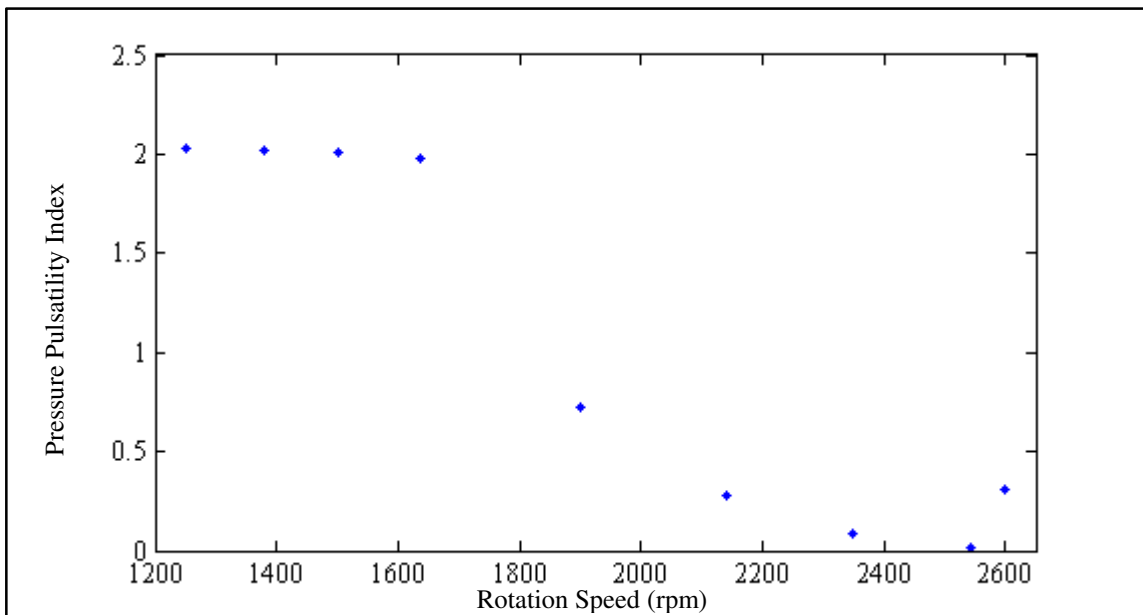


Figure 4.84. Heart Turcica centrifugal V13 pressure pulsatility index from 1250 rpm to 2600 rpm

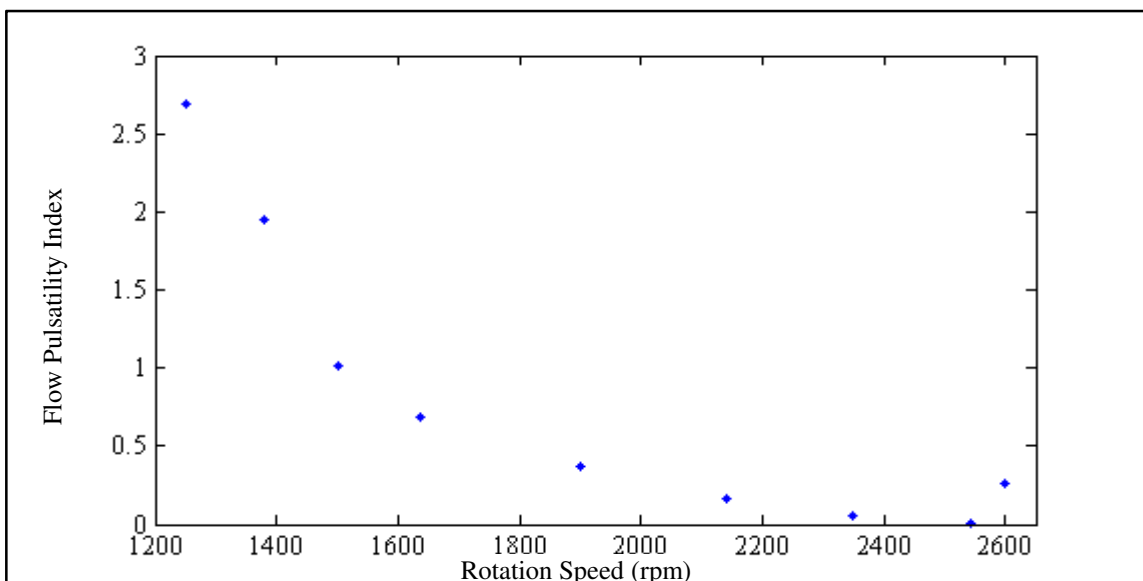


Figure 4.85. Heart Turcica centrifugal V13 flow pulsatility index from 1250 rpm to 2600 rpm

As shown in the results pressure pulsatility index and flow pulsatility index decrease with increasing pump rotation speed. Suction initiation makes increase the pulsatility indexes again.

4.5. DISCUSSION

In this chapter simulations are made for constant rotation speeds of heart pumps and these speeds are assessed with respect to physiologically significant pumping states that have been caused.

As shown in the results for axial heart pump aortic valve closure occurs nearly at 7565 rpm rotation speed. Regurgitant pump flow disappears nearly at 9250 rpm rotation speed. These results indicate that regurgitant pump flow occurs during the ventricle ejection state and aortic valve non-opening state. The heart pump cannot support the cardiovascular system completely in regurgitant pump flow condition. Therefore regurgitant pump flow must be avoided. According to the simulation results, minimum operating speed of Heart Turcica axial is nearly 10000 rpm. At 10000 rpm operating speed systolic blood pressure is 89.9 mmHg and cardiac output is 4.19 l/min. Suction state occurs nearly at 12000 rpm rotation speed. If the heart pump operates above 12000 rpm rotation speed, suction that has deleterious effects on the cardiovascular system will occur. According to these results Heart Turcica axial must operate between 10000 rpm and 12000 rpm rotation speeds.

In relatively lower rotation speeds pulsatility is seen in pump flow, pressure difference across the pump, aortic pressure, pump inlet pressure and motor current. Increasing rotation speed increases the blood flow in the pump. Therefore increasing rotation speed decreases pulsatility in the variables mentioned above. Pulsatility appears again with suction initiation. Also suction occurrence causes the pump inlet pressure decrease to below zero. Increasing rotation speed causes the left ventricular pressure to decrease below left atrial pressure. In this condition mitral valve remains open and blood flow through mitral valve becomes continuous. But in suction condition mitral valve closes again.

Left ventricular pressure-volume loop area is getting smaller with increasing heart pump speed. In other words external work of the left ventricle decreases with increasing pump speed. As mentioned above increasing pump speed causes the pulsatility in pump flow and pressure difference across the pump decreases. In this condition pressure-flow

rate curves of the pump get shorter. In suction condition longer pressure-flow rate curves are obtained.

Regurgitant pump flow is disappeared at nearly 1380 rpm operating speed in Heart Turcica centrifugal. Also at nearly 1638 rpm operating speed aortic valve closes over the whole cardiac cycle. According to these simulation results regurgitant pump flow state occurs at rotation speed lower than 1380 rpm. Ventricle ejection state occurs between 1380 rpm and 1638 rpm operating speeds. Simulation results show that minimum operating speed is 2140 rpm for Heart Turcica centrifugal. At 2140 rpm operating speed systolic aortic blood pressure is 90.1 mmHg and cardiac output is 4.45 l/min. Suction occurs at the rotation speeds that above 2542 rpm. In Heart Turcica centrifugal suction does not occur over the whole cardiac cycle.

Pulsatility index variation with respect to pump rotation speed is a good indicator of detecting suction. As shown in the results suction initiation increases the pulsatility indexes. Therefore pulsatility indexes can used to develop control strategies to prevent suction effect.

5. CONTROL STUDIES OF HEART TURCICA AXIAL

In this chapter physiological control of Heart Turcica axial was considered to achieve perfusion and provide sufficient blood flow. In order to make physiological control pressure difference across the pump and pump flow rate were controlled.

5.1. CONTROL OF PRESSURE DIFFERENCE ACROSS THE PUMP

In order to control pressure difference across Heart Turcica axial PI control was applied between pressure difference error and pump electrical current input. Proportional gains and integral gain were adjusted to 0.01. These values are numerically stable largest values. Simulations were performed for several reference pressure difference values but only important results are explained in this section of the thesis. Block diagram of the pressure difference control across Heart Turcica Axial is shown in Figure 5.1.

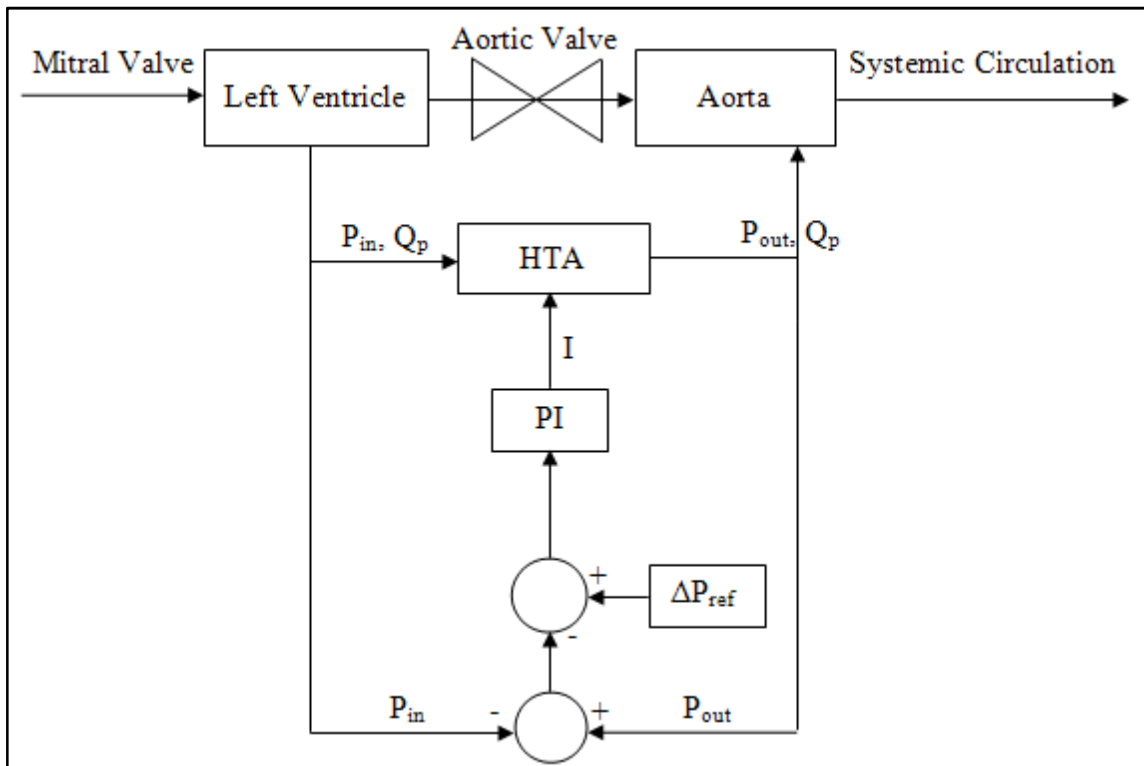


Figure 5.1. Block diagram of the pressure difference control across Heart Turcica axial

5.1.1. Simulation Results for 65 mmHg Reference Pressure Difference

Reference pressure difference value was adjusted to 65 mmHg and simulations were performed. Pressure difference across the pump, left atrial pressure, left ventricular pressure and aortic pressure are shown in Figure 5.2.

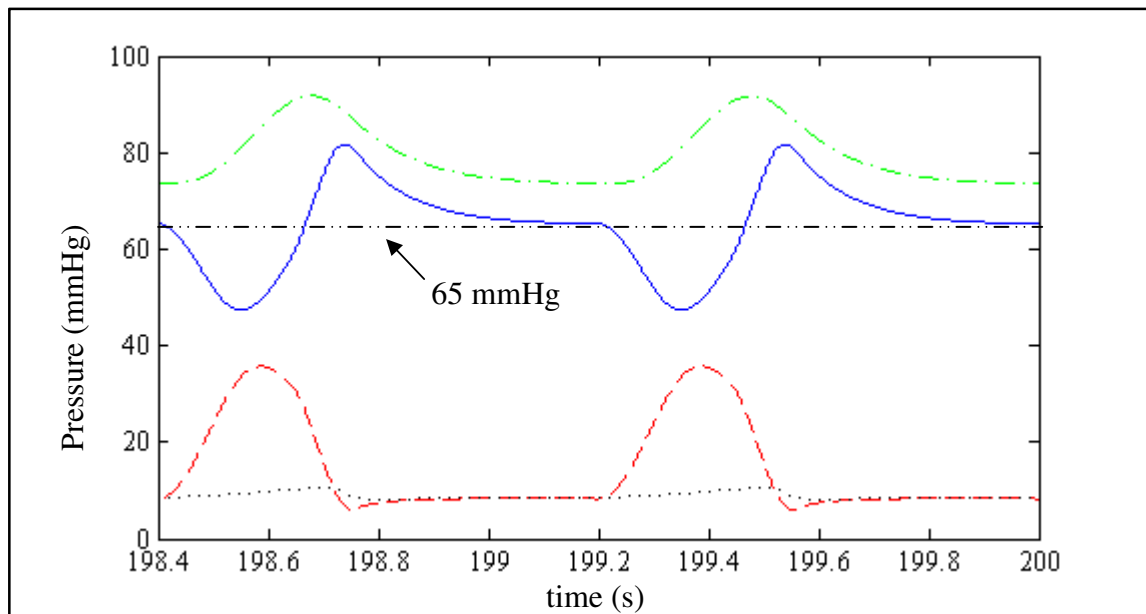


Figure 5.2. Pressure difference across the pump (continuous line), left atrial pressure (dotted line), left ventricular pressure (dashed line) and aortic pressure (chain line) for 65 mmHg reference pressure difference value

Maximum pressure difference across the pump is 81.6 mmHg and minimum pressure difference across the pump is 47.4 mmHg. Maximum left atrial pressure is 10.8 mmHg and minimum left atrial pressure is 8.1 mmHg. Maximum left ventricular pressure is 35.7 mmHg and minimum left ventricular pressure is 6 mmHg. Left ventricular pressure is above the threshold suction resistance value defined by Equation 4.3. Therefore pump inlet pressure is the same as left ventricular pressure. Maximum aortic pressure is 91.7 mmHg and minimum aortic pressure is 73.5 mmHg for 65 mmHg reference pressure value.

Left ventricular and left atrial volumes are shown in Figure 5.3 for 65 mmHg reference pressure difference value.

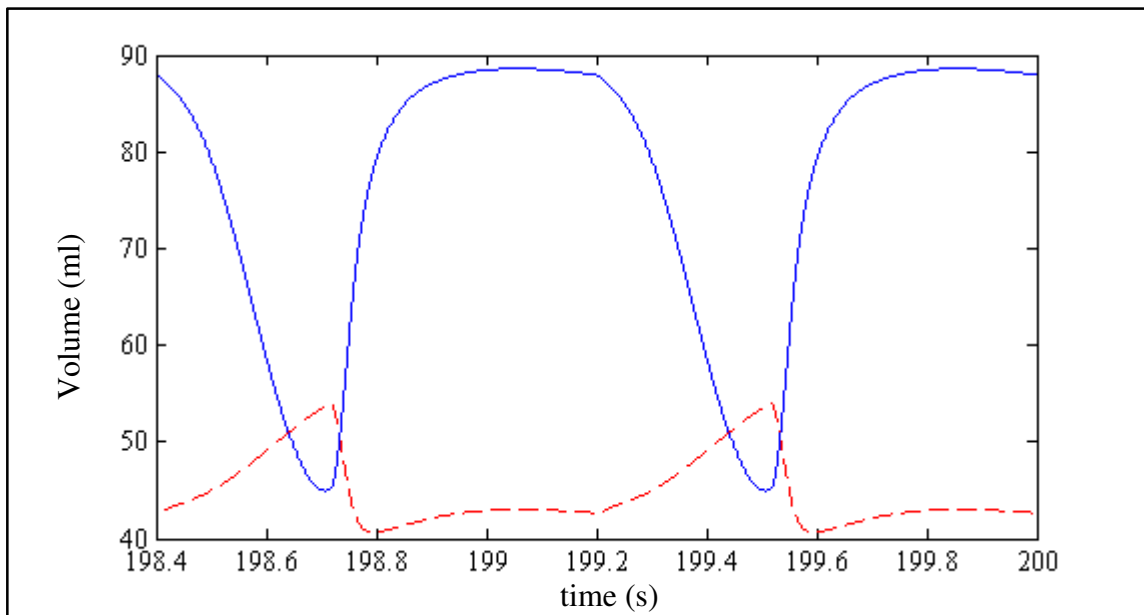


Figure 5.3. Left ventricular volume (continuous line), left atrial volume (dashed line) for 65 mmHg reference pressure difference value

End diastolic volume of left ventricle is 88.6 ml, end systolic volume of left ventricle is 45 ml and stroke volume of left ventricle is 43.6 ml Maximum volume of left atrium is 54.1 ml and minimum volume at left atrium is 40.7 ml for 65 mmHg reference pressure difference value.

Pump flow rate, mitral valve flow rate and aortic valve flow rate for 65 mmHg reference pressure difference value are shown in Figure 5.4.

For 65 mmHg reference pressure difference value heart and Heart Turcica Axial are not operating together. In other words blood flow through aortic valve disappears due to aortic valve closure. Also pump flow regurgitates due to relatively high aortic pressure in diastolic phase.

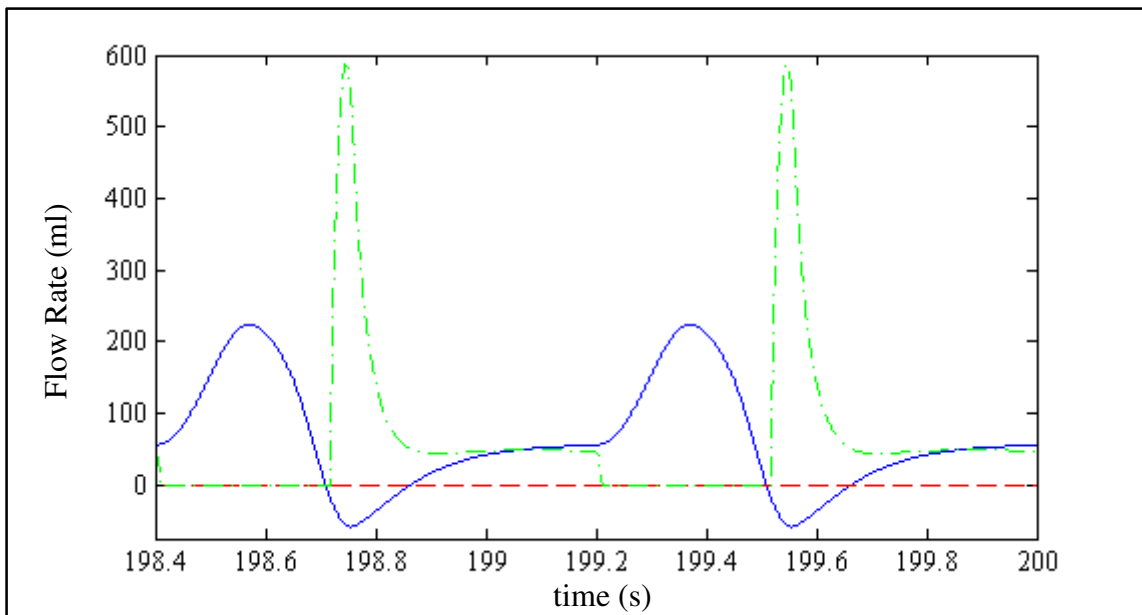


Figure 5.4. Pump flow rate (continuous line), mitral valve flow rate (chain line) and aortic valve flow rate (dashed line) for 65 mmHg reference pressure difference value

Rotation speed for 65 mmHg reference pressure value is shown Figure 5.5.

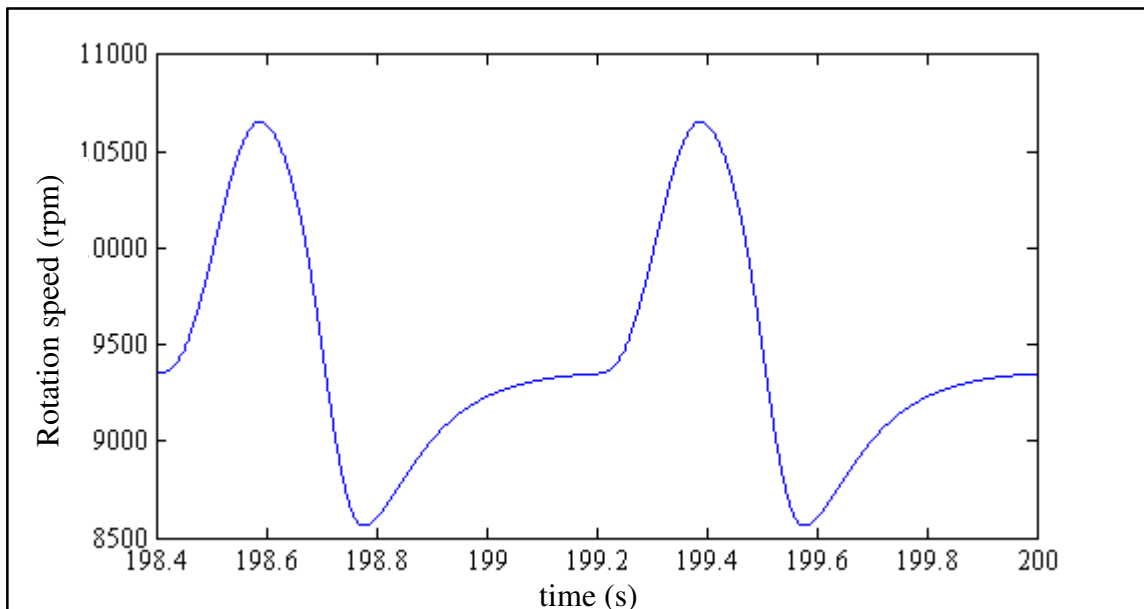


Figure 5.5. Rotation speed for 65 mmHg reference pressure difference value

Maximum rotation speed is 10657 rpm and minimum rotation speed is 8562 rpm for

65 mmHg reference pressure difference value.

Motor current for 65 mmHg reference pressure value is shown Figure 5.6.

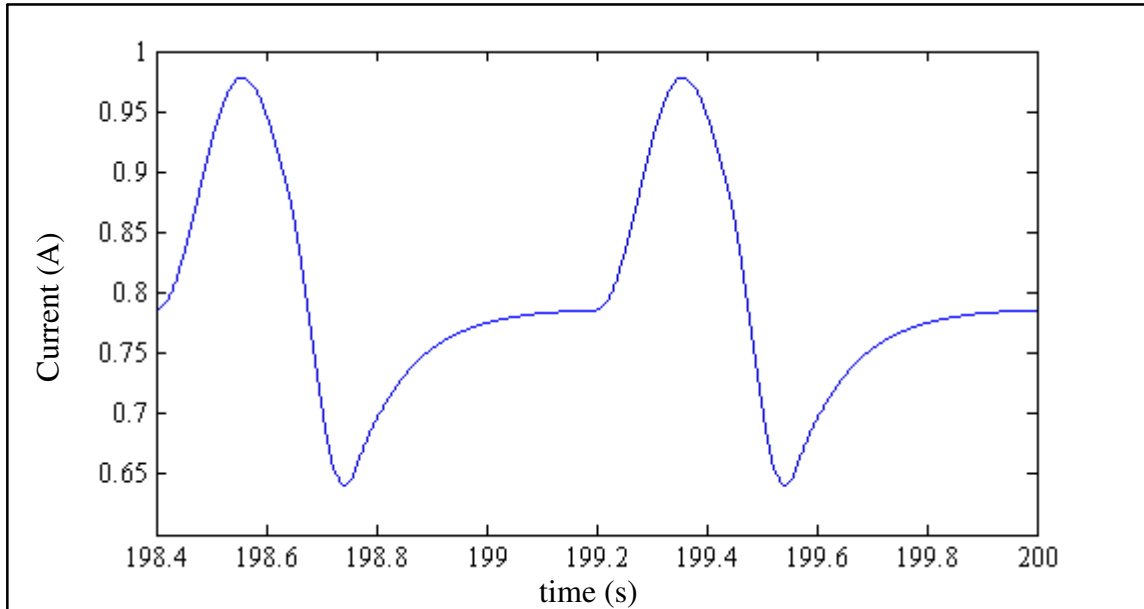


Figure 5.6. Motor current for 65 mmHg reference pressure difference value

Maximum motor current is 0.978 A and minimum motor current is 0.641 A for 65 mmHg reference pressure difference value. Total cardiac output is 3.88 l/min. Results that are explained above are shown in Table 5.1.

Table 5.1. Simulation results for 65 mmHg reference pressure difference value.

Parameter	Max. Value	Min. Value	Parameter	Max. Value	Min. Value
ΔP_{pump} (mmHg)	81.6	47.4	V_{Iv} (ml)	88.6	45
P_{in} (mmHg)	35.7	6	Stroke V_{Iv} (ml)	43.6	
P_{la} (mmHg)	10.8	8.1	CO (l/min)	3.88	
P_{Iv} (mmHg)	35.7	6	Rot. Speed (rpm)	10657	8562.7
P_{ao} (mmHg)	91.7	73.5	I_{motor} (A)	0.978	0.641
V_{la} (ml)	54.1	40.7			

5.1.2. Simulation Results for 75 mmHg Reference Pressure Difference

Reference pressure difference value was adjusted to 75 mmHg and simulations were performed. Pressure difference across the pump, left atrial pressure, left ventricular pressure and aortic pressure are shown in Figure 5.7.

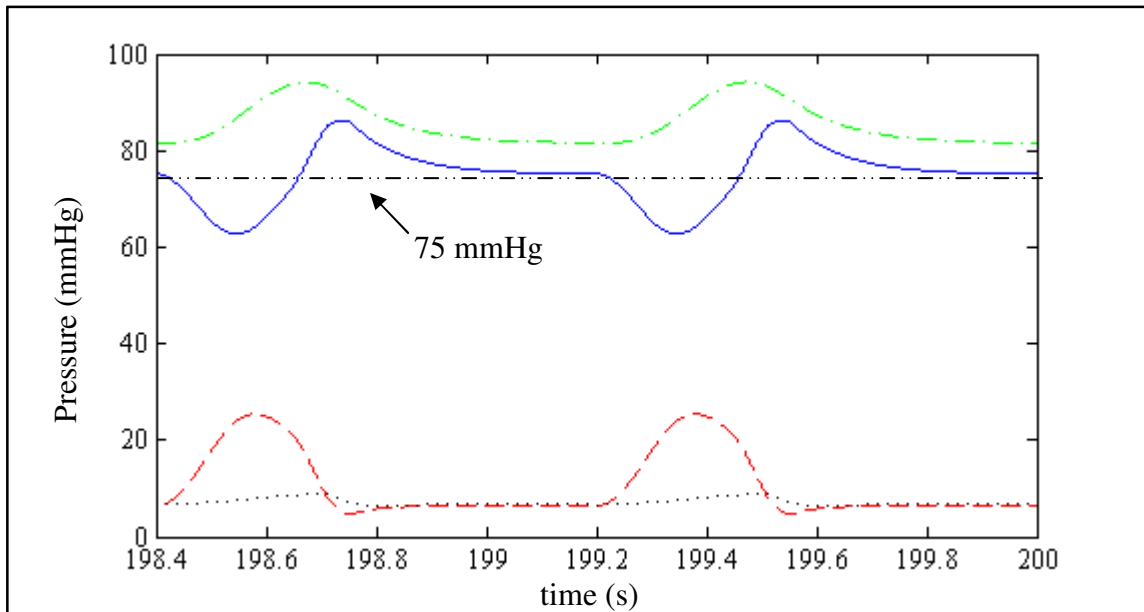


Figure 5.7. Pressure difference across the pump (continuous line), left atrial pressure (dotted line), left ventricular pressure (dashed line) and aortic pressure (chain line) for 75 mmHg reference pressure difference value

Maximum pressure difference across the pump is 86.3 mmHg and minimum pressure difference across the pump is 62.7 mmHg. Maximum left atrial pressure is 9.1 mmHg and minimum left atrial pressure is 6.5 mmHg. Maximum left ventricular pressure is 25.4 mmHg and minimum left ventricular pressure is 4.6 mmHg. Left ventricular pressure is above the threshold suction resistance value defined by Equation 4.3. Therefore pump inlet pressure is the same as left ventricular pressure. Maximum aortic pressure is 94.2 mmHg and minimum aortic pressure is 81.5 mmHg for 75 mmHg reference pressure value.

Left ventricular and left atrial volumes are shown in Figure 5.8 for 75 mmHg reference pressure difference value.

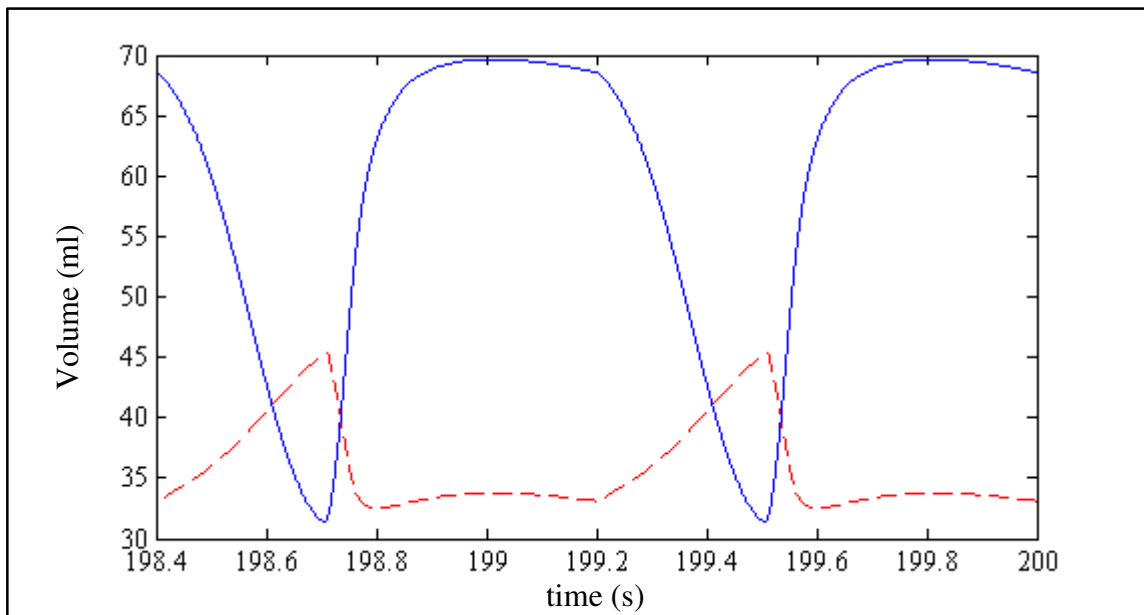


Figure 5.8. Left ventricular volume (continuous line), left atrial volume (dashed line) for 75 mmHg reference pressure difference value

End diastolic volume of left ventricle is 69.6 ml, end systolic volume of left ventricle is 31.3 ml and stroke volume of left ventricle is 38.3 ml Maximum volume of left atrium is 45.4 ml and minimum volume at left atrium is 31.3 ml for 75 mmHg reference pressure difference value.

Pump flow rate, mitral valve flow rate and aortic valve flow rate for 75 mmHg reference pressure difference value are shown in Figure 5.9.

For 75 mmHg reference pressure difference value heart and Heart Turcica Axial are not operating together. In other words blood flow through aortic valve disappears due to aortic valve closure. Also pump flow regurgitates due to relatively high aortic pressure in diastolic phase.

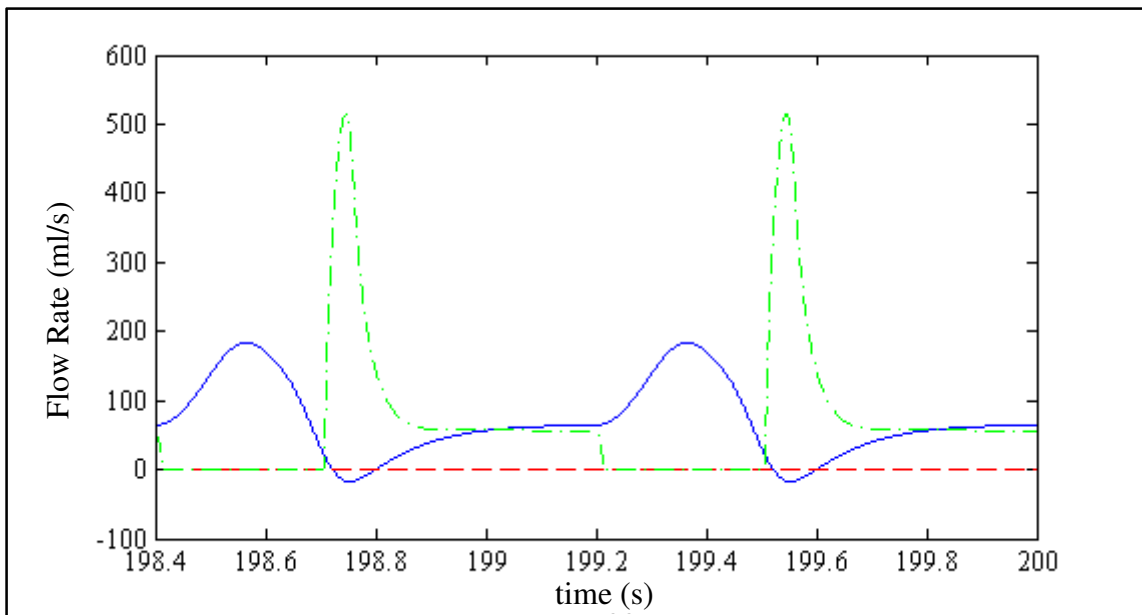


Figure 5.9. Pump flow rate (continuous line), mitral valve flow rate (chain line) and aortic valve flow rate (dashed line) for 75 mmHg reference pressure difference value

Rotation speed for 75 mmHg reference pressure difference value is shown Figure 5.10.

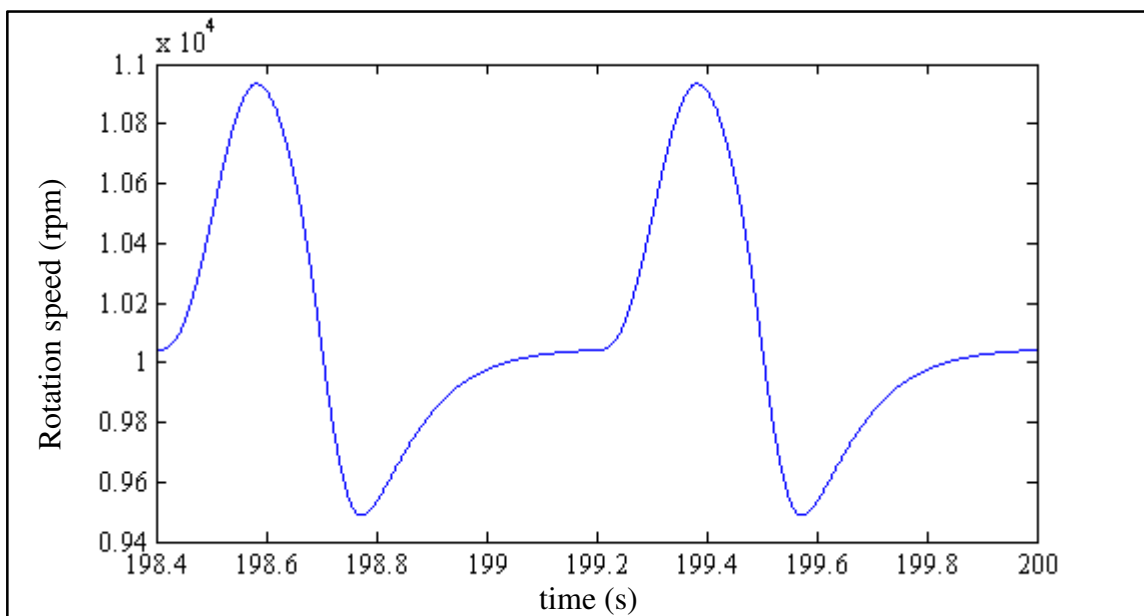


Figure 5.10. Rotation speed for 75 mmHg reference pressure difference value

Maximum rotation speed is 10934 rpm and minimum rotation speed is 9487 rpm for 75 mmHg reference pressure difference value.

Motor current for 75 mmHg reference pressure difference value is shown Figure 5.11.

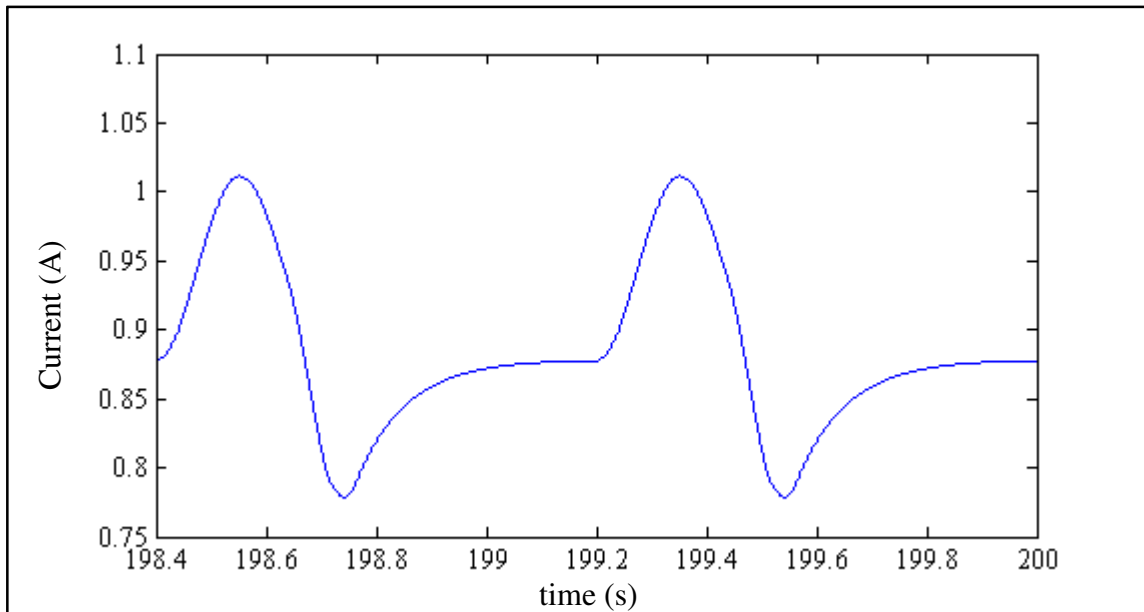


Figure 5.11. Motor current for 75 mmHg reference pressure difference value

Maximum motor current is 1.011 A and minimum motor current is 0.778 A for 75 mmHg reference pressure difference value. Total cardiac output is 4.23 l/min for 75 mmHg reference pressure difference value. Results that are explained above are shown in Table 5.2.

Table 5.2. Simulation results for 75 mmHg reference pressure difference value.

Parameter	Max. Value	Min. Value	Parameter	Max. Value	Min. Value
ΔP_{pump} (mmHg)	86.3	62.7	V_{lv} (ml)	69.6	31.3
P_{in} (mmHg)	25.4	4.6	Stroke V_{lv} (ml)	38.3	
P_{la} (mmHg)	9.1	6.5	CO (l/min)	4.23	
P_{lv} (mmHg)	25.4	4.6	Rot. Speed (rpm)	10934	9487.3
P_{ao} (mmHg)	94.2	81.5	I_{motor} (A)	1.011	0.778
V_{la} (ml)	45.4	38.3			

5.1.3. Simulation Results for 85 mmHg Reference Pressure Difference

Reference pressure difference value was adjusted to 85 mmHg and simulations were performed. Pressure difference across the pump, left atrial pressure, left ventricular pressure and aortic pressure are shown in Figure 5.12.

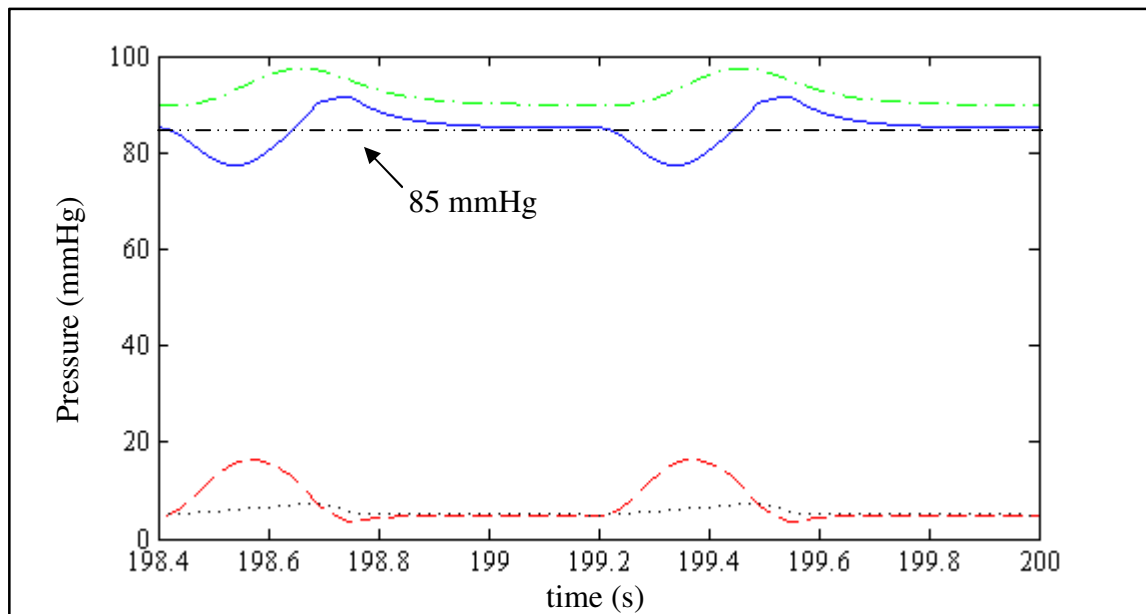


Figure 5.12. Pressure difference across the pump (continuous line), left atrial pressure (dotted line), left ventricular pressure (dashed line) and aortic pressure (chain line) for 85 mmHg reference pressure value

Maximum pressure difference across the pump is 91.5 mmHg and minimum pressure difference across the pump is 77.3 mmHg. Maximum left atrial pressure is 7.5 mmHg and minimum left atrial pressure is 4.9 mmHg. Maximum left ventricular pressure is 16.4 mmHg and minimum left ventricular pressure is 3.4 mmHg. Left ventricular pressure is above the threshold suction resistance value defined by Equation 4.3. Therefore pump inlet pressure is the same as left ventricular pressure. Maximum aortic pressure is 97.4 mmHg and minimum aortic pressure is 89.8 mmHg for 85 mmHg reference pressure value.

Left ventricular and left atrial volumes are shown in Figure 5.13 for 85 mmHg reference pressure difference value.

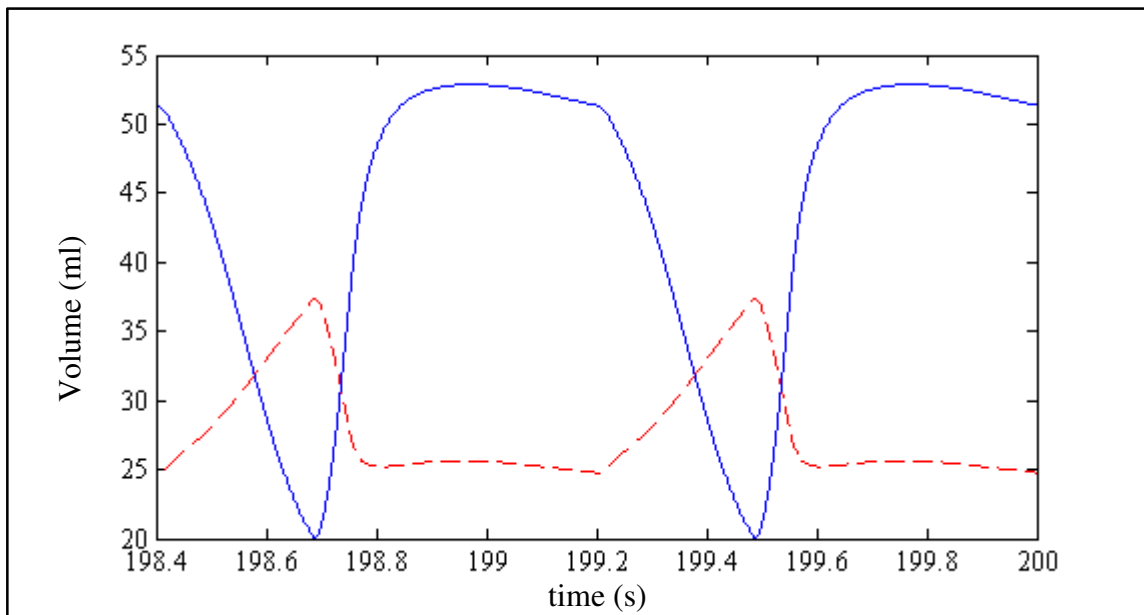


Figure 5.13. Left ventricular volume (continuous line), left atrial volume (dashed line) for 85 mmHg reference pressure difference value

End diastolic volume of left ventricle is 52.8 ml, end systolic volume of left ventricle is 20 ml and stroke volume of left ventricle is 32.8 ml Maximum volume of left atrium is 37.41 ml and minimum volume at left atrium is 24.8 ml for 85 mmHg reference pressure difference value.

Pump flow rate, mitral valve flow rate and aortic valve flow rate for 85 mmHg reference pressure difference value are shown in Figure 5.14.

For 85 mmHg reference pressure difference value heart and Heart Turcica Axial are not operating together. In other words blood flow through aortic valve is disappeared due to aortic valve closure. Also pump flow does not regurgitate due to relatively high aortic pressure in diastolic phase.

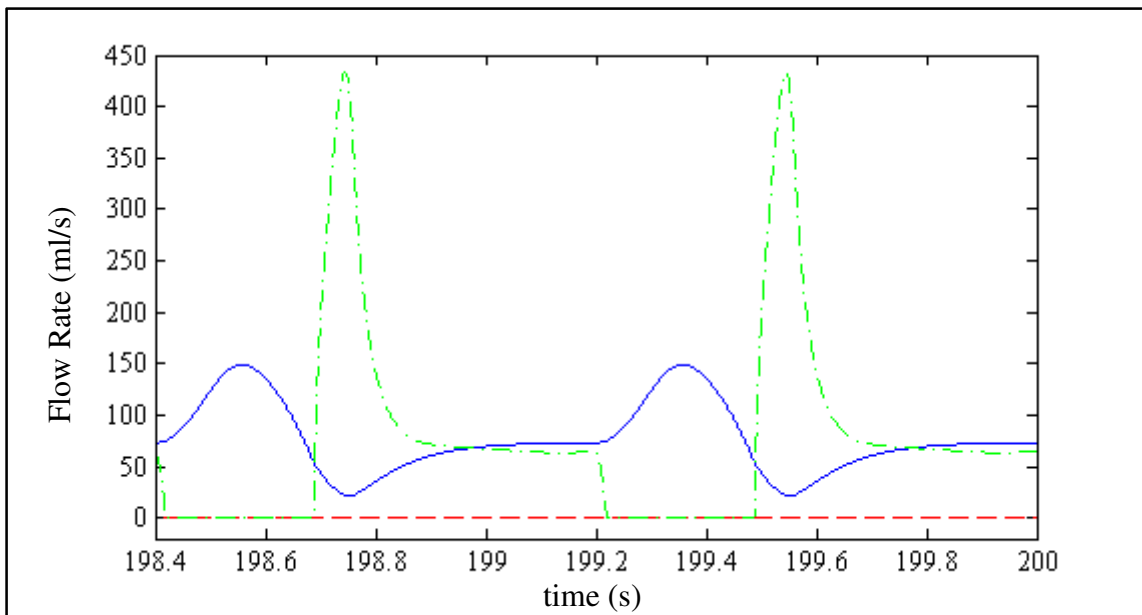


Figure 5.14. Pump flow rate (continuous line), mitral valve flow rate (chain line) and aortic valve flow rate (dashed line) for 85 mmHg reference pressure difference value

Rotation speed for 85 mmHg reference pressure difference value is shown Figure 5.15.

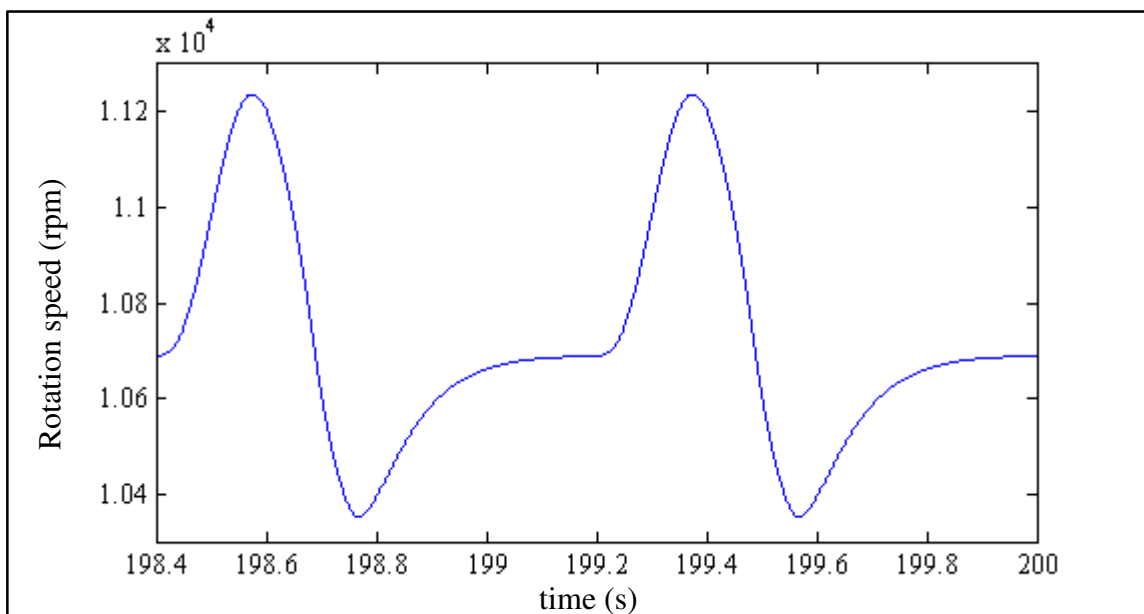


Figure 5.15. Rotation speed for 85 mmHg reference pressure difference value

Maximum rotation speed is 11237 rpm and minimum rotation speed is 10351 rpm for 85 mmHg reference pressure difference value.

Motor current for 85 mmHg reference pressure difference value is shown Figure 5.16.

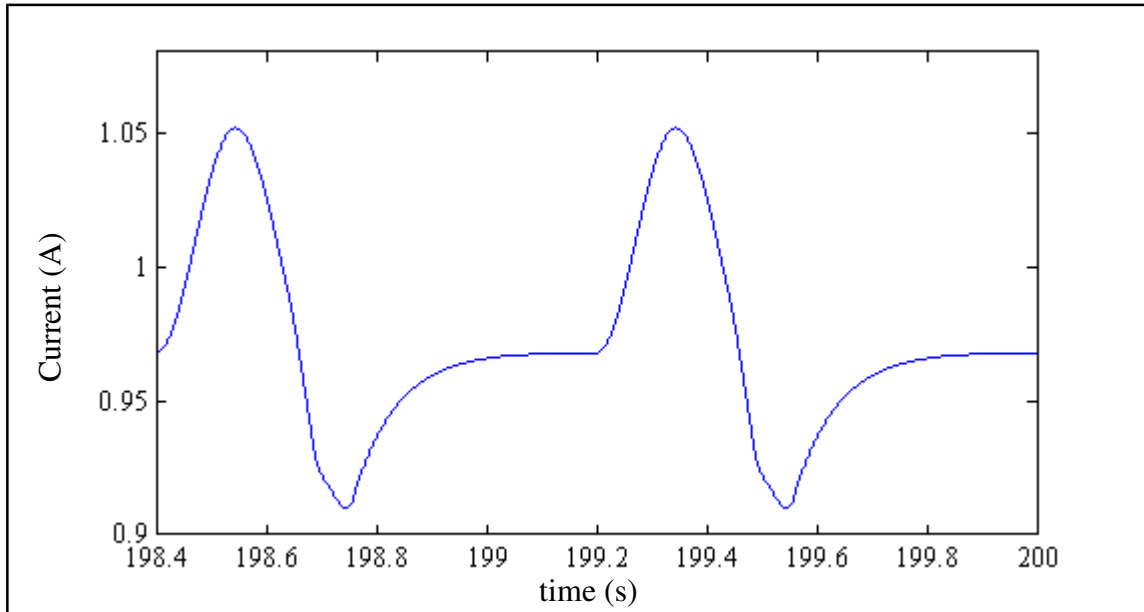


Figure 5.16. Motor current for 85 mmHg reference pressure difference value

Maximum motor current is 1.051 A and minimum motor current is 0.910 A for 85 mmHg reference pressure difference value. Total cardiac output is 4.61 l/min for 85 mmHg reference pressure value. Results that are explained above are shown in Table 5.3.

Table 5.3. Simulation results for 85 mmHg reference pressure difference value.

Parameter	Max. Value	Min. Value	Parameter	Max. Value	Min. Value
ΔP_{pump} (mmHg)	91.5	77.3	V_{lv} (ml)	52.8	20
P_{in} (mmHg)	16.4	3.4	Stroke V_{lv} (ml)	32.8	
P_{la} (mmHg)	7.5	4.9	CO (l/min)	4.61	
P_{lv} (mmHg)	16.4	3.4	Rot. Speed (rpm)	11237	10351
P_{ao} (mmHg)	97.4	89.8	I_{motor} (A)	1.051	0.910
V_{la} (ml)	37.4	24.8			

5.1.4. Simulation Results for 95 mmHg Reference Pressure Difference

Reference pressure difference value was adjusted to 95 mmHg and simulations were performed. Pressure difference across the pump, left atrial pressure, left ventricular pressure and aortic pressure are shown in Figure 5.17.

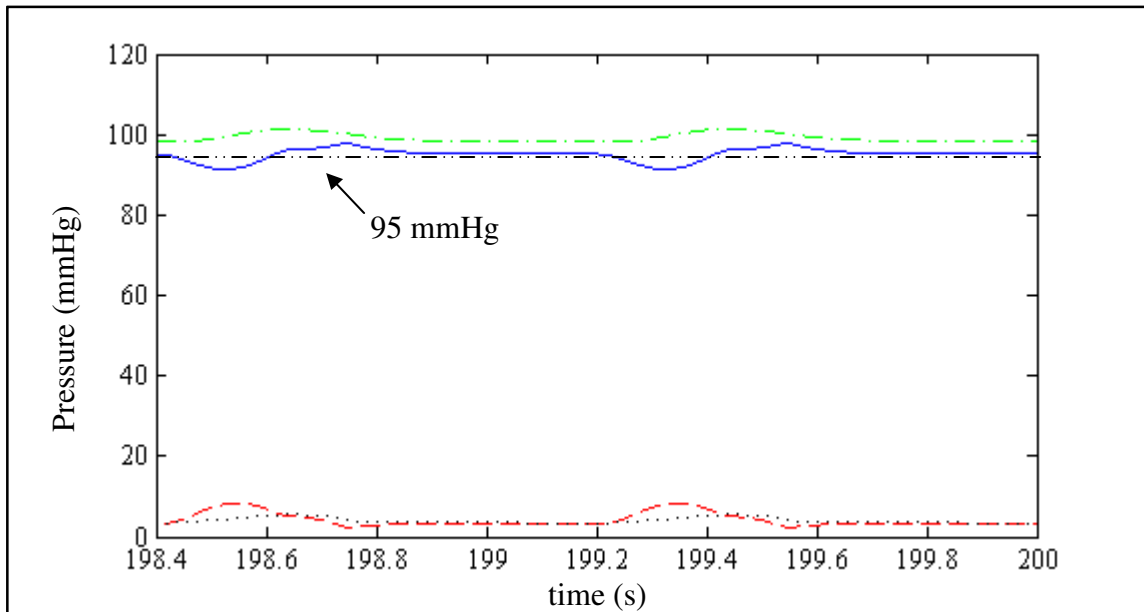


Figure 5.17. Pressure difference across the pump (continuous line), left atrial pressure (dotted line), left ventricular pressure (dashed line) and aortic pressure (chain line) for 95 mmHg reference pressure difference value

Maximum pressure difference across the pump is 97.7 mmHg and minimum pressure difference across the pump is 91.3 mmHg. Maximum left atrial pressure is 5.5 mmHg and minimum left atrial pressure is 3.3 mmHg. Maximum left ventricular pressure is 8.4 mmHg and minimum left ventricular pressure is 2.3 mmHg. Left ventricular pressure is above the threshold suction resistance value that defined in Equation 4.3. Therefore pump inlet pressure is same with left ventricular pressure. Maximum aortic pressure is 101.3 mmHg and minimum aortic pressure is 98.1 mmHg for 95 mmHg reference pressure value.

Left ventricular and left atrial volumes are shown in Figure 5.18 for 95 mmHg reference pressure difference value.

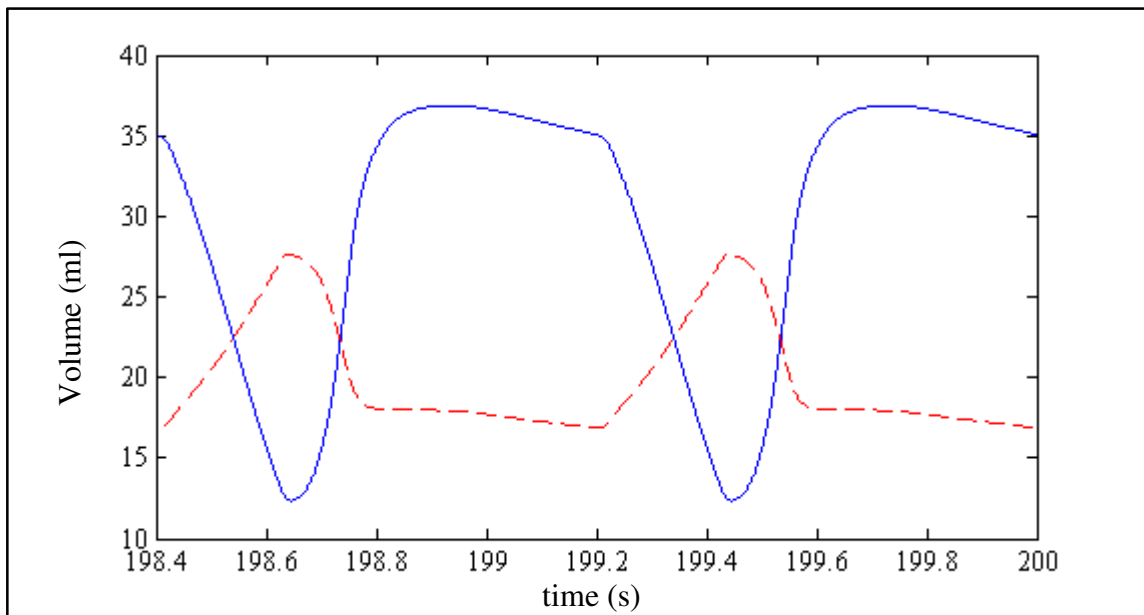


Figure 5.18. Left ventricular volume (continuous line), left atrial volume (dashed line) for 95 mmHg reference pressure difference value

End diastolic volume of left ventricle is 36.9 ml, end systolic volume of left ventricle is 12.3 ml and stroke volume of left ventricle is 24.6 ml Maximum volume of left atrium is 27.6 ml and minimum volume at left atrium is 16.9 ml for 95 mmHg reference pressure difference value.

Pump flow rate, mitral valve flow rate and aortic valve flow rate for 95 mmHg reference pressure difference value are shown in Figure 5.19.

For 95 mmHg reference pressure value heart and Heart Turcica Axial are not operating together. In other words blood flow through aortic valve is disappeared due to aortic valve closure. Also pump flow does not regurgitate due to relatively high aortic pressure in diastolic phase.

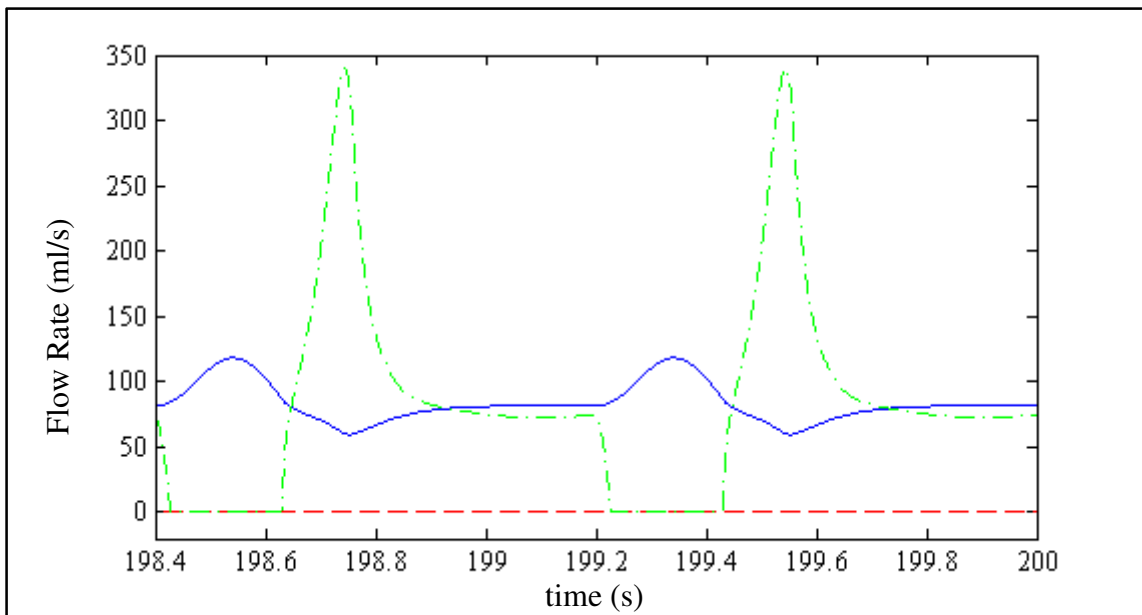


Figure 5.19. Pump flow rate (continuous line), mitral valve flow rate (chain line) and aortic valve flow rate (dashed line) for 95 mmHg reference pressure difference value

Rotation speed for 95 mmHg reference pressure difference value is shown Figure 5.20.

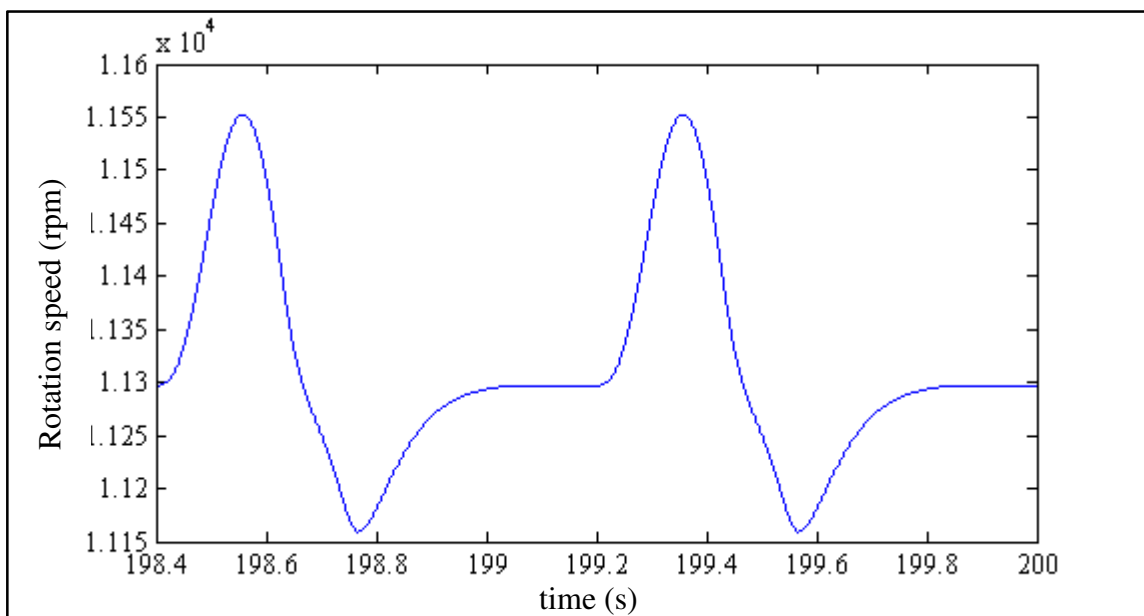


Figure 5.20. Rotation speed for 95 mmHg reference pressure difference value

Maximum rotation speed is 11553 rpm and minimum rotation speed is 11159 rpm for 95 mmHg reference pressure difference value.

Motor current for 95 mmHg reference pressure difference value is shown Figure 5.21.

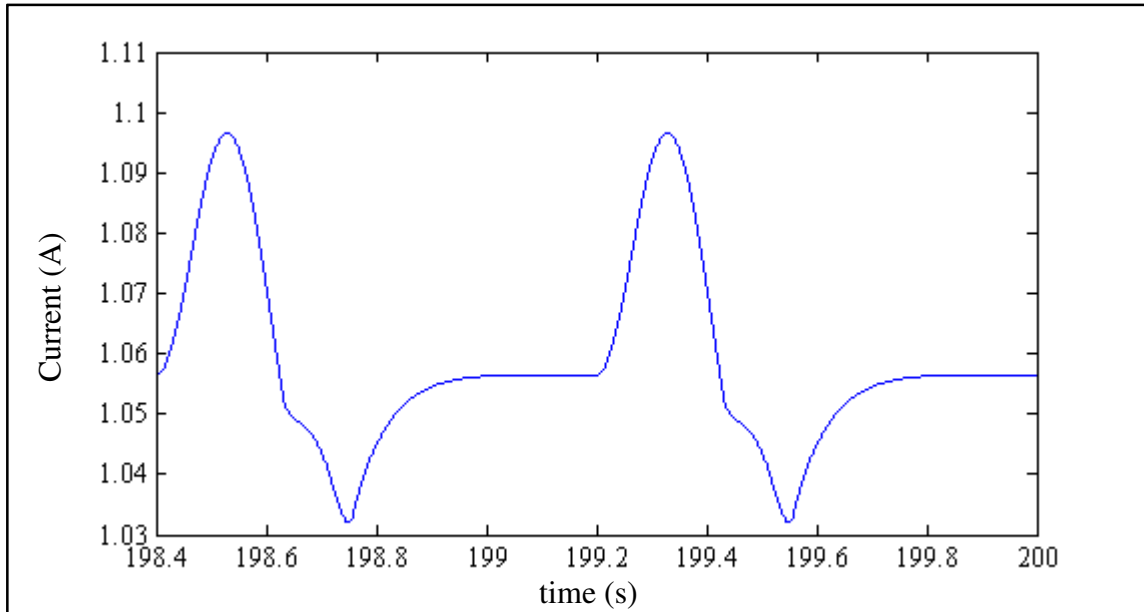


Figure 5.21. Motor current for 95 mmHg reference pressure difference value

Maximum motor current is 1.096 A and minimum motor current is 1.032 A for 95 mmHg reference pressure value. Total cardiac output is 5.02 l/min for 95 mmHg reference pressure value. These results are similar to constant rotation speed control strategy. Results that are explained above are shown in Table 5.4.

Table 5.4. Simulation results for 95 mmHg reference pressure difference value.

Parameter	Max. Value	Min. Value	Parameter	Max. Value	Min. Value
ΔP_{pump} (mmHg)	97.7	91.3	V_{lv} (ml)	36.9	12.3
P_{in} (mmHg)	8.4	2.3	Stroke V_{lv} (ml)	24.6	
P_{la} (mmHg)	5.5	3.3	CO (l/min)	5.02	
P_{lv} (mmHg)	8.4	2.3	Rot. Speed (rpm)	11553	11159
P_{ao} (mmHg)	101.3	98.1	I_{motor} (A)	1.096	1.032
V_{la} (ml)	27.6	16.9			

Left ventricular pressure – volume loops are good indicators to explain the contribution of the left ventricular assist devices to left ventricle. Left ventricular pressure-volume loops from 65 mmHg to 95 mmHg reference pressure difference with 10 mmHg increments that are explained above are shown in Figure 5.22.

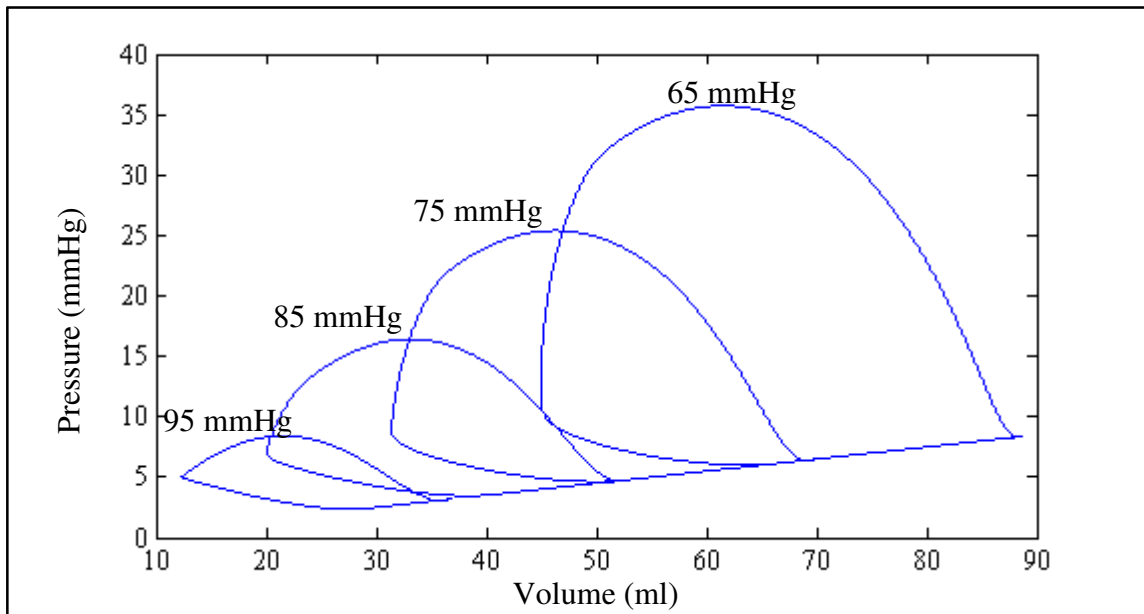


Figure 5.22. Left ventricular pressure – volume loops from 65 mmHg to 95 mmHg with 10 mmHg increments

According to the results area of the left ventricular pressure – volume loop is getting smaller with increasing reference pressure difference. In other words external work of the left ventricle is decreasing.

Also pressure – flow rate diagram of Heart Turcica Axial is shows the effect of increasing reference pressure difference. Pressure – flow rate diagram of Heart Turcica Axial from 65 mmHg to 95 mmHg with reference pressure difference 10 mmHg increments shown in Figure 5.23.

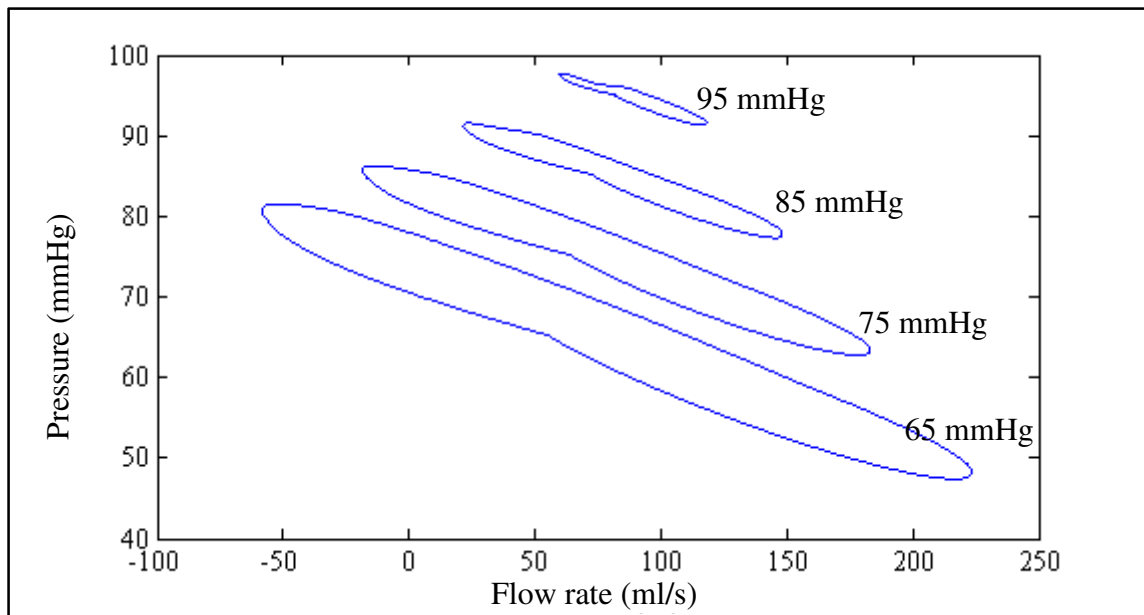


Figure 5.23. Heart Turcica Axial pressure–flow rate diagram from 65 mmHg to 95 mmHg reference pressure difference with 10 mmHg increments

As shown in the results increasing reference pressure difference across the pump causes a shrinkage of the pressure-flow rate loop area. In other words the effect of heart on the heart pump decreases.

5.2. CONTROL OF PUMP FLOW RATE

Proportional-integral (PI) control was applied between the pump flow rate error and the motor current of Heart Turcica Axial. Proportional and integral gains were adjusted to 0.1. These values are numerically stable largest values. Simulations were performed for several reference flow rate values but only important results are explained in this section of thesis. Block diagram of the flow rate control through Heart Turcica Axial is shown in Figure 5.2.

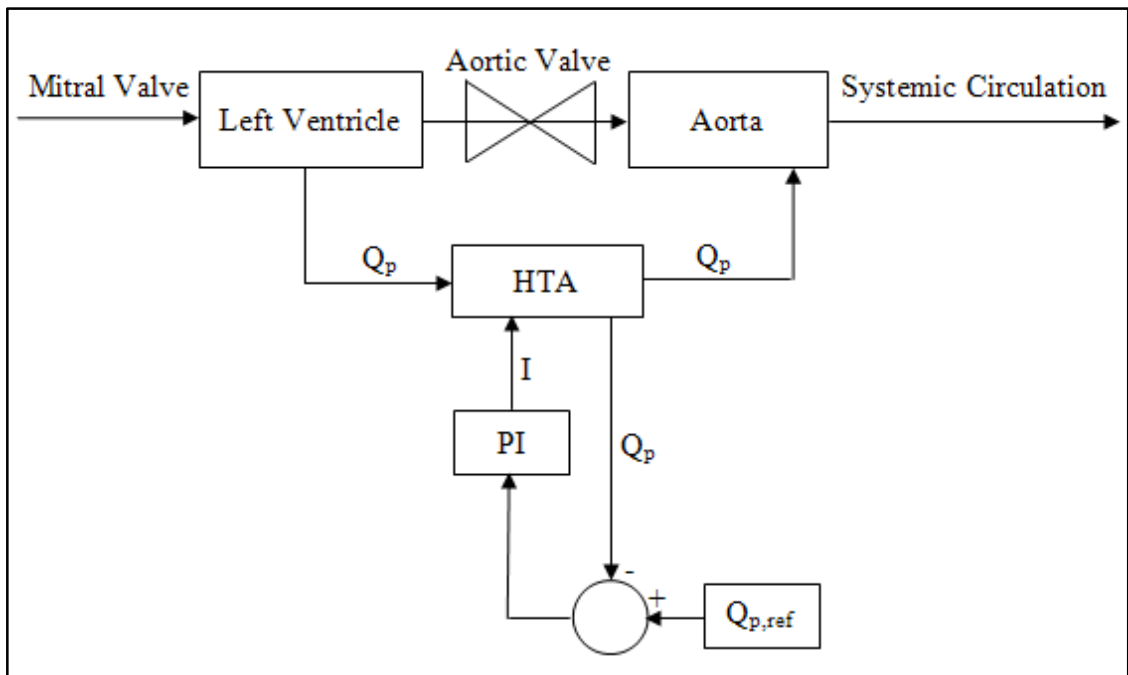


Figure 5.24. Block diagram of the flow rate control through Heart Turcica Axial

5.2.1. Simulation Results for 50 ml/s Reference Flow Rate

Reference pump flow rate value was adjusted to 50 ml/s and simulations were performed. Pressure difference across the pump, left atrial pressure, left ventricular pressure and aortic pressure are shown in Figure 5.28.

Maximum pressure difference across the pump is 59.7 mmHg and minimum pressure difference across the pump is -0.1 mmHg. Maximum left atrial pressure is 13.9 mmHg and minimum left atrial pressure is 11.9 mmHg. Maximum left ventricular pressure is 70.7 mmHg and minimum left ventricular pressure is 10.3 mmHg. Left ventricular pressure is above the threshold suction resistance value defined by Equation 4.3. Therefore pump inlet pressure is the same as left ventricular pressure. Maximum aortic pressure is 70.7 mmHg and minimum aortic pressure is 67.8 mmHg for 50 ml/s reference pump flow rate value.

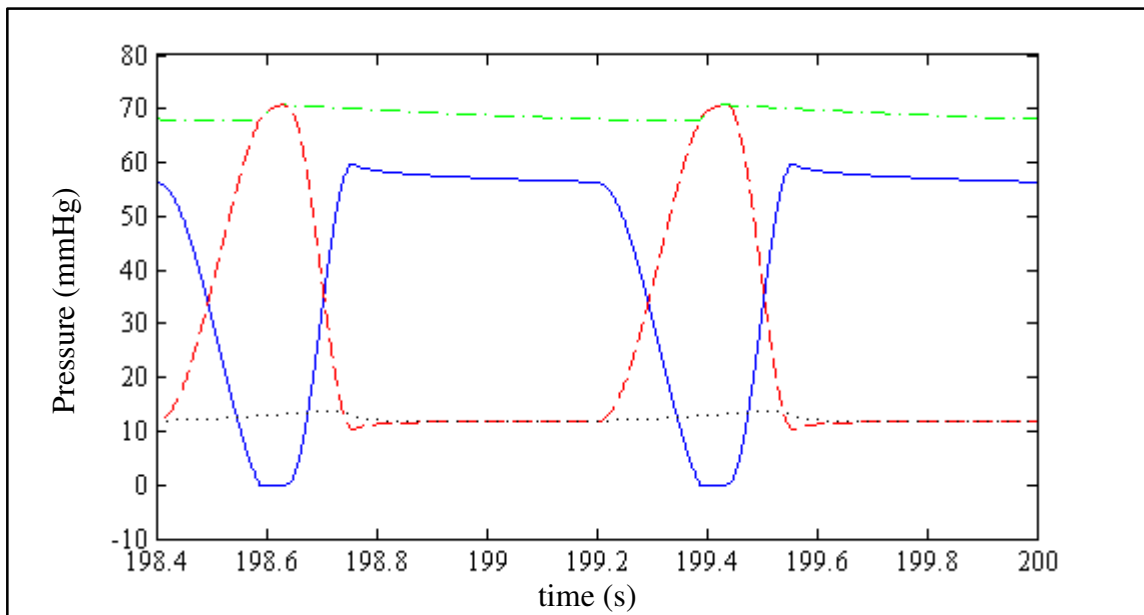


Figure 5.25. Pressure difference across the pump (continuous line), left atrial pressure (dotted line), left ventricular pressure (dashed line) and aortic pressure (chain line) for 50 ml/s reference pump flow rate value

Left ventricular and left atrial volumes are shown in Figure 5.29 for 50 ml reference pump flow rate value.

End diastolic volume of left ventricle is 122.5 ml, end systolic volume of left ventricle is 100 ml and stroke volume of left ventricle is 22.5 ml Maximum volume of left atrium is 69.7 ml and minimum volume at left atrium is 59.5 ml for 50 ml/s reference pump flow rate value.

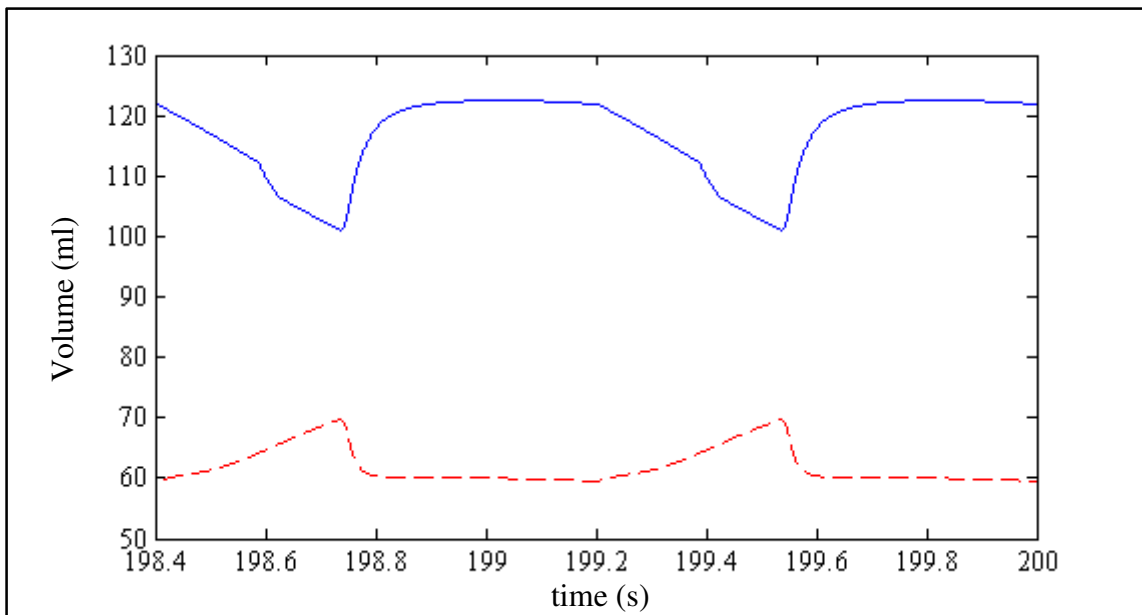


Figure 5.26. Left ventricular volume (continuous line), left atrial volume (dashed line) for 50 ml/s reference pump flow rate value.

Pump flow rate, mitral valve flow rate and aortic valve flow rate for 50 ml reference pump flow rate value are shown in Figure 5.30.

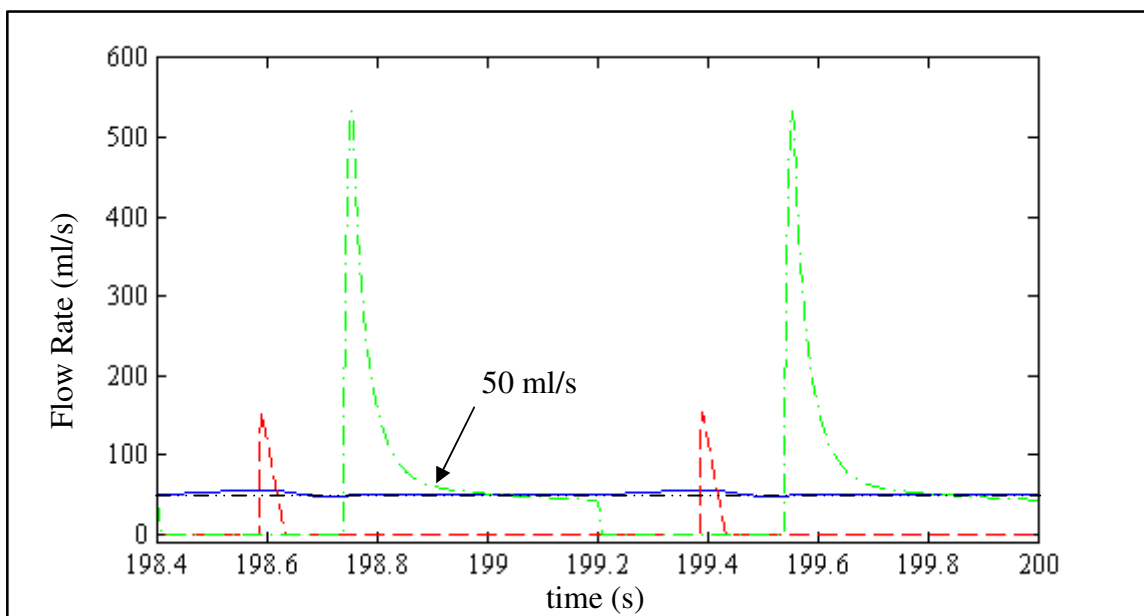


Figure 5.27. Pump flow rate (continuous line), mitral valve flow rate (chain line) and aortic valve flow rate (dashed line) for 50 ml/s reference pump flow rate value

For 50 ml/s reference pump flow rate value heart and Heart Turcica Axial are operating together. Also pump flow does not regurgitate due to relatively low aortic pressure in diastolic phase.

Rotation speed for 50 ml/s reference pump flow rate value is shown Figure 5.31.

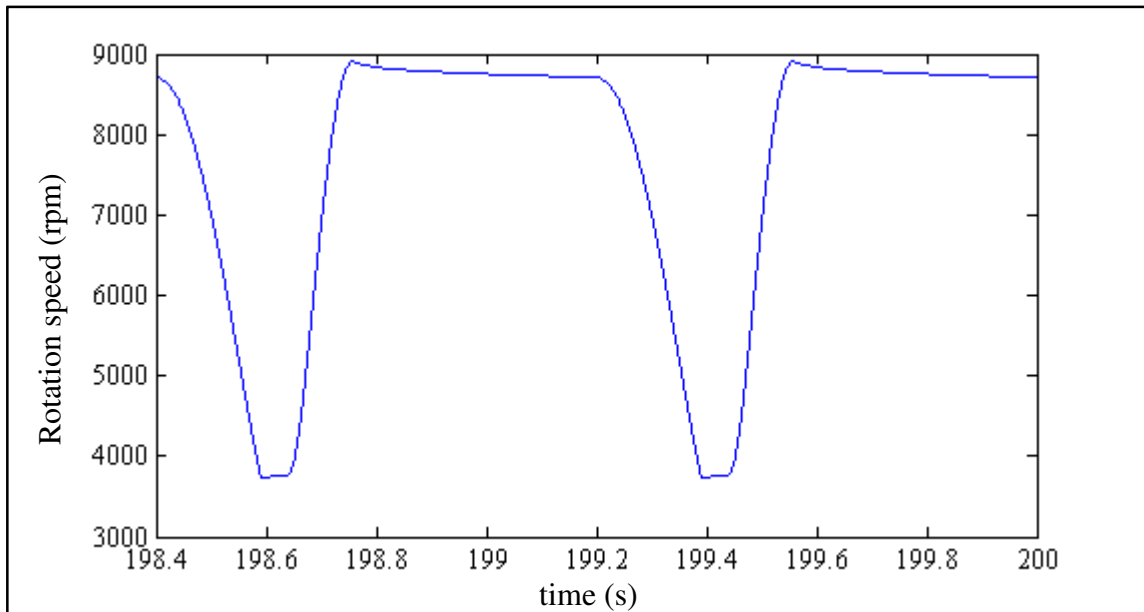


Figure 5.28. Rotation speed for 50 ml reference pump flow rate value

Maximum rotation speed is 3742 rpm and minimum rotation speed is 8908 rpm for 50 ml/s reference pump flow rate value.

Motor current for 50 ml/s reference pump flow rate value is shown Figure 5.32.

Maximum motor current is 0.843 A and minimum motor current is 0.080 A for 50 ml reference pump flow rate value. Total cardiac output is 3.28 l/min for 50 ml/s reference pump flow rate value. Results that are explained above are shown in Table 5.6.

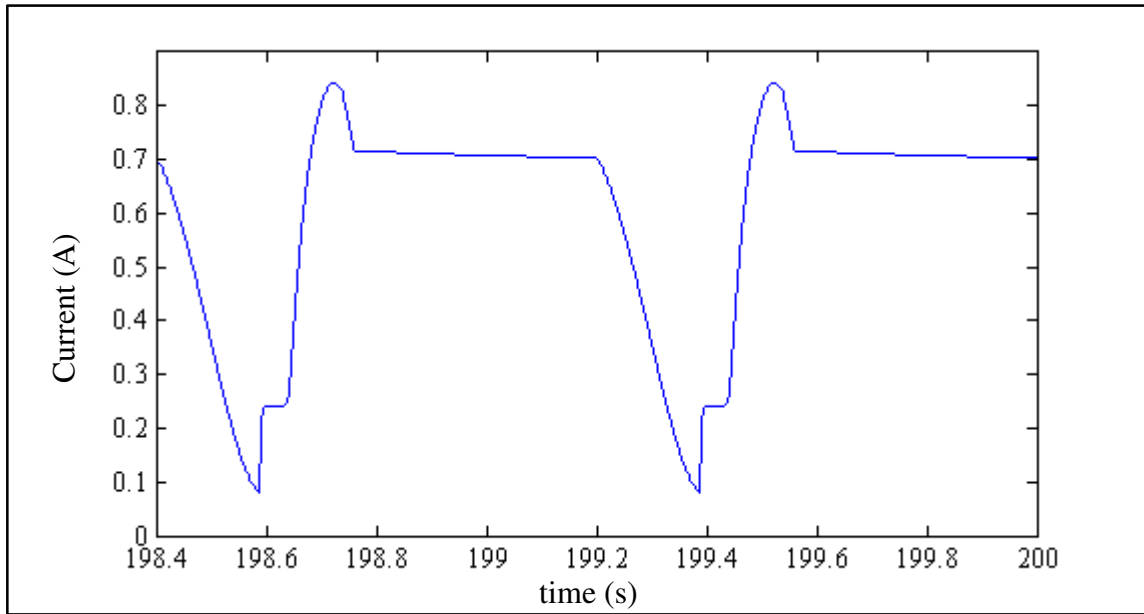


Figure 5.29. Motor current 50 ml/s reference pump flow rate value

Table 5.6. Simulation results for 50 ml/s reference pump flow rate value

Parameter	Max. Value	Min. Value	Parameter	Max. Value	Min. Value
ΔP_{pump} (mmHg)	59.7	-0.1	V_{lv} (ml)	122.5	100
P_{in} (mmHg)	70.7	10.3	Stroke V_{lv} (ml)	22.5	
P_{la} (mmHg)	13.9	11.9	CO (l/min)	3.28	
P_{lv} (mmHg)	70.7	10.3	Rot. Speed (rpm)	3742	8908.9
P_{ao} (mmHg)	70.7	67.8	I_{motor} (A)	0.843	0.080
V_{la} (ml)	69.7	59.5			

5.2.2. Simulation Results for 60 ml/s Reference Flow Rate

Reference pump flow rate value was adjusted 60 ml/s and simulations were performed. Pressure difference across the pump, left atrial pressure, left ventricular pressure and aortic pressure are shown in Figure 5.33.

Maximum pressure difference across the pump is 66.2 mmHg and minimum pressure difference across the pump is 16.8 mmHg. Maximum left atrial pressure is 12.2 mmHg and minimum left atrial pressure is 9.9 mmHg. Maximum left ventricular pressure is 57.9 mmHg and minimum left ventricular pressure is 8.4 mmHg. Left ventricular pressure is

above the threshold suction resistance value defined by Equation 4.3. Therefore pump inlet pressure is the same as left ventricular pressure. Maximum aortic pressure is 74.8 mmHg and minimum aortic pressure is 74.4 mmHg for 60 ml/s reference pump flow rate value.

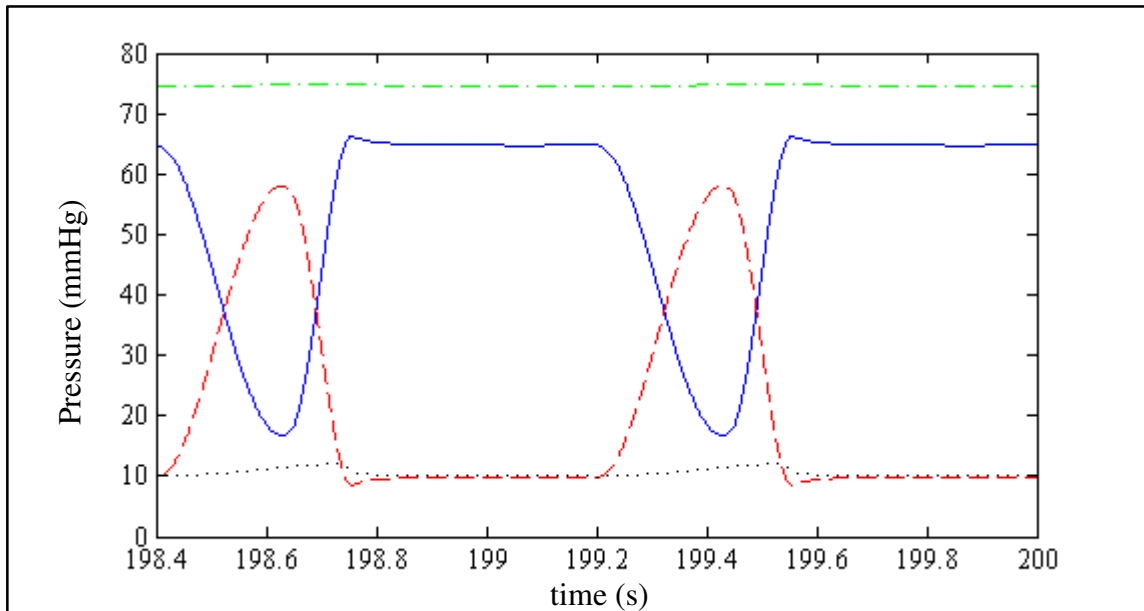


Figure 5.30. Pressure difference across the pump (continuous line), left atrial pressure (dotted line), left ventricular pressure (dashed line) and aortic pressure (chain line) for 60 ml/s ml reference pump flow rate value

Left ventricular and left atrial volumes are shown in Figure 5.34 for 60 ml/s reference pump flow rate value.

End diastolic volume of left ventricle is 103.2 ml, end systolic volume of left ventricle is 81.8 ml and stroke volume of left ventricle is 21.4 ml Maximum volume of left atrium is 61 ml and minimum volume at left atrium is 49.7 ml for 60 ml/s reference pump flow rate value.

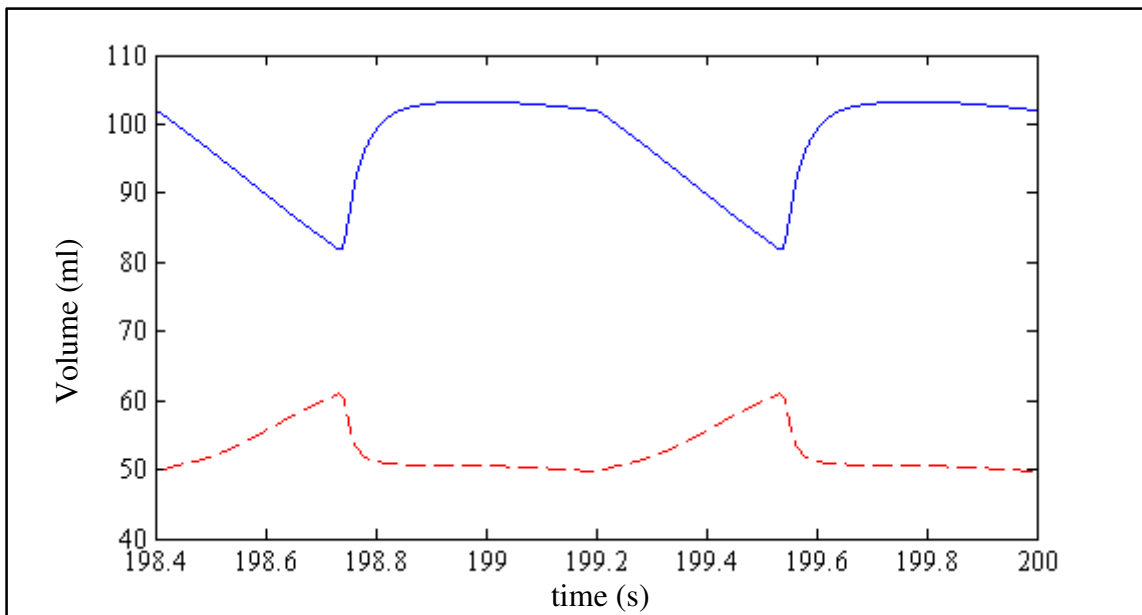


Figure 5.31. Left ventricular volume (continuous line), left atrial volume (dashed line) for 60 ml/s reference pump flow rate value.

Pump flow rate, mitral valve flow rate and aortic valve flow rate for 60 ml/s reference pump flow rate value are shown in Figure 5.35.

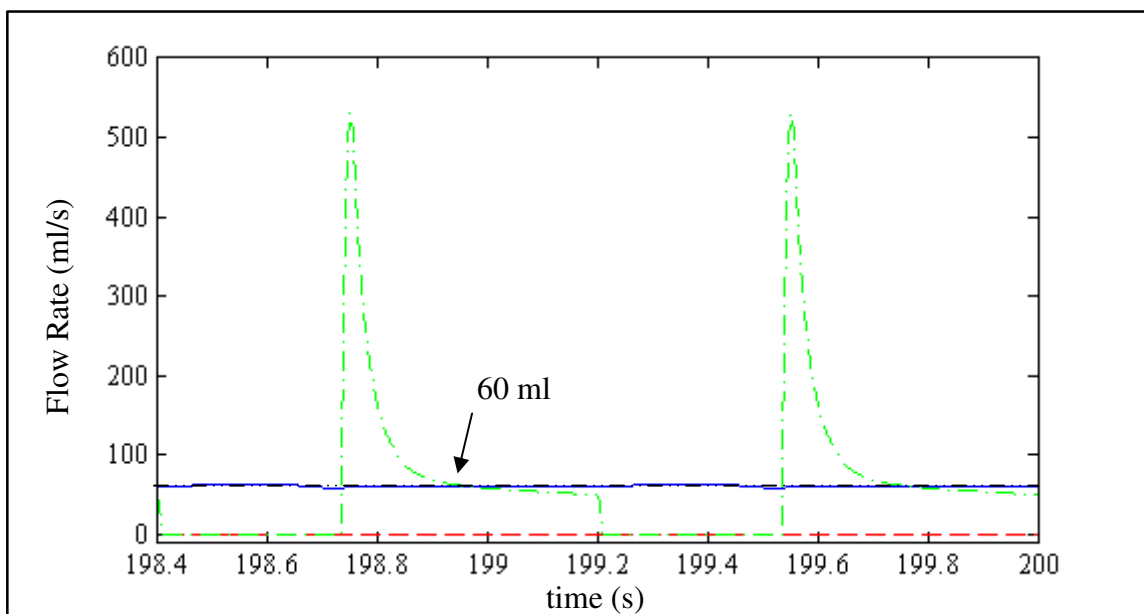


Figure 5.32. Pump flow rate (continuous line), mitral valve flow rate (chain line) and aortic valve flow rate (dashed line) for 60 ml/s reference pump flow rate value

For 60 ml/s reference pump flow rate value heart and Heart Turcica Axial are not operating together. Also pump flow does not regurgitate due to relatively low aortic pressure in diastolic phase.

Rotation speed for 60 ml/s reference pump flow rate value is shown Figure 5.36.

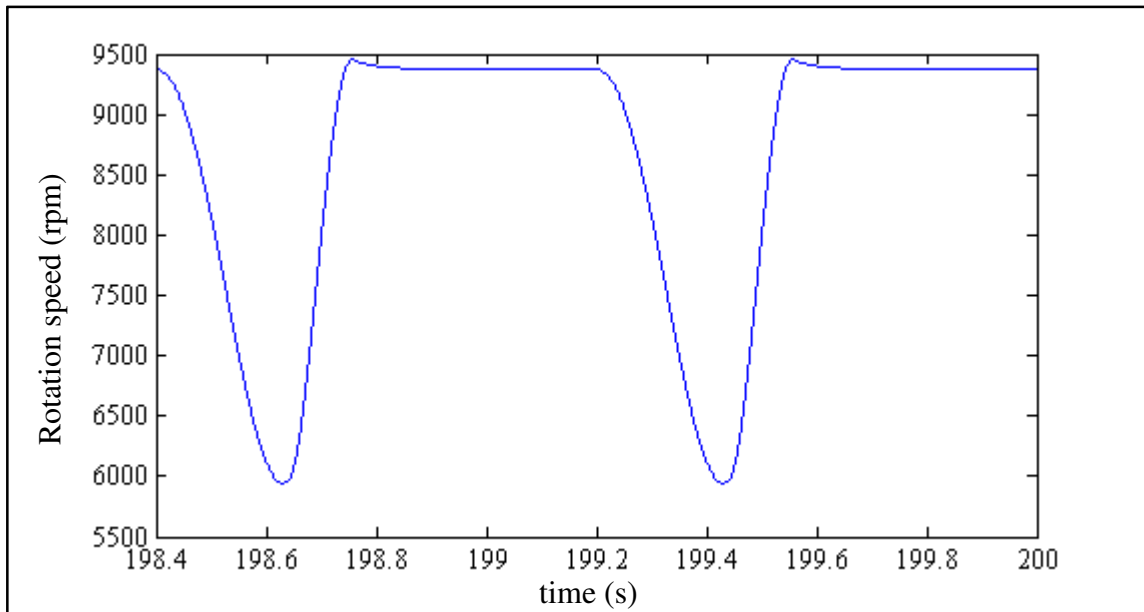


Figure 5.33. Rotation speed for 60 ml reference pump flow rate value

Maximum rotation speed is 5946 rpm and minimum rotation speed is 9456 rpm for 60 ml/s reference pump flow rate value.

Motor current for 60 ml/s reference pump flow rate value is shown Figure 5.37.

Maximum motor current is 0.882 A and minimum motor current is 0.371 A for 60 ml/s reference pump flow rate value. Total cardiac output is 3.60 l/min for 60 ml/s reference pump flow rate value. Results that are explained above are shown in Table 5.7.

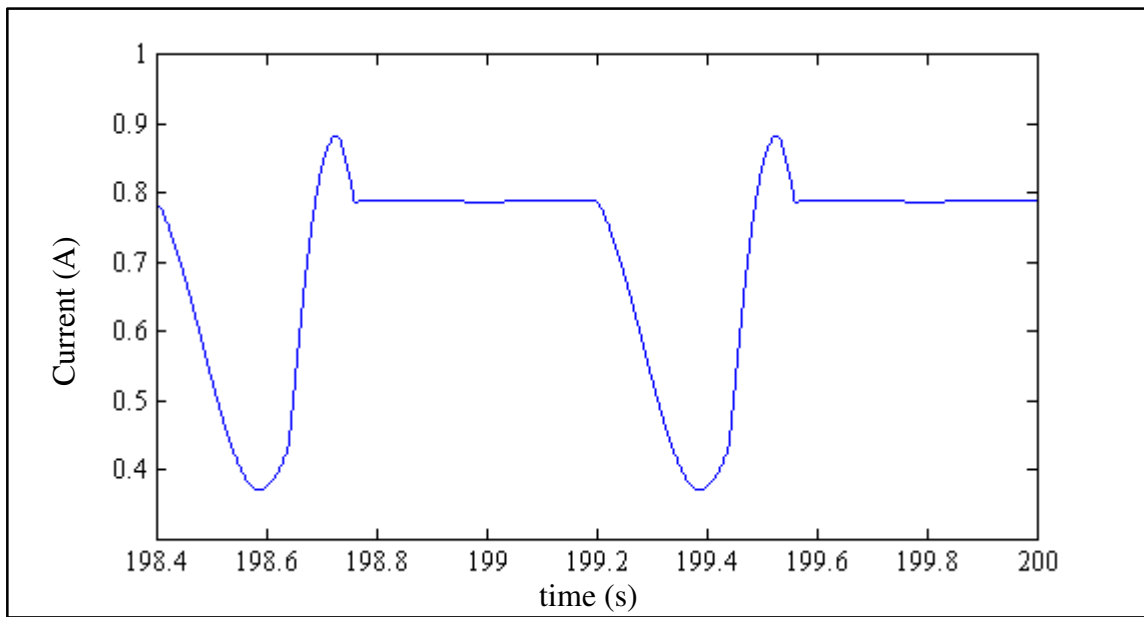


Figure 5.34. Motor current for 60 ml/s reference pump flow rate value

Table 5.7. Simulation results for 60 ml/s reference pump flow rate value

Parameter	Max. Value	Min. Value	Parameter	Max. Value	Min. Value
ΔP_{pump} (mmHg)	66.2	16.8	V_{lv} (ml)	103.2	81.8
P_{in} (mmHg)	57.9	8.4	Stroke V_{lv} (ml)	21.4	
P_{la} (mmHg)	12.21	8.9	CO (l/min)	3.60	
P_{lv} (mmHg)	57.9	8.4	Rot. Speed (rpm)	5946	9456.4
P_{ao} (mmHg)	74.8	74.4	I_{motor} (A)	0.882	0.371
V_{la} (ml)	61	49.7			

Left ventricular pressure-volume loops are good indicators to explain the help of the left ventricular assist devices to left ventricle. Left ventricular pressure–volume loops of 50 ml reference pump flow rate and 60 ml/s reference pump flow rate that are explained above shown in Figure 5.35.

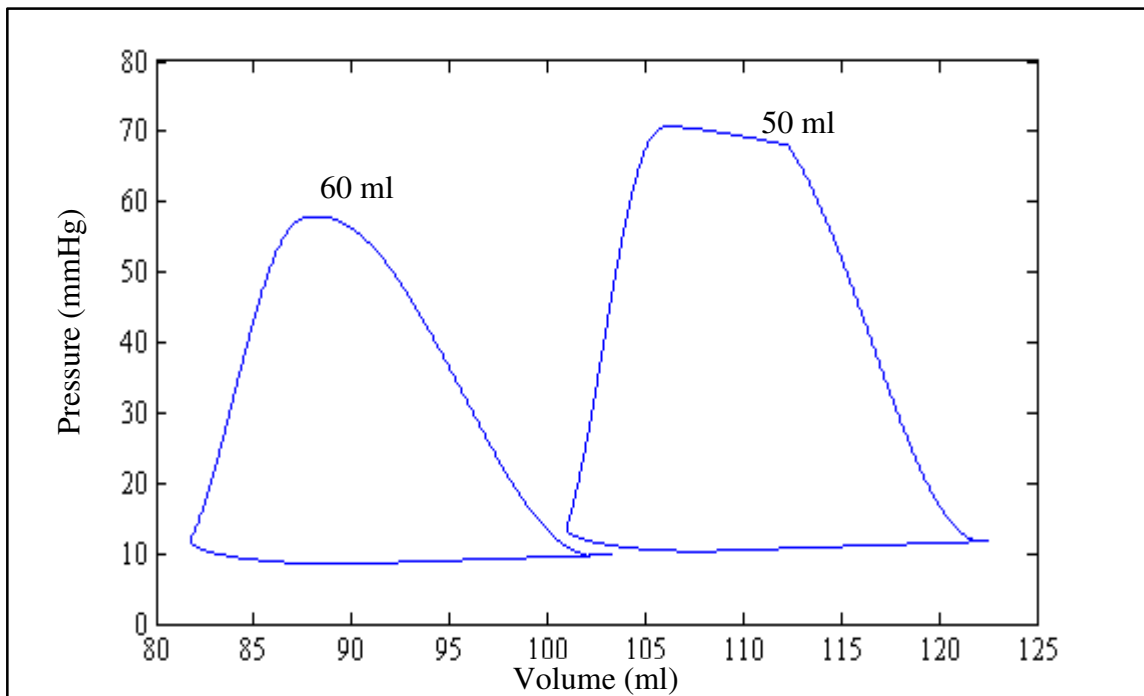


Figure 5.35. Left ventricular pressure–volume loops of 50 ml reference pump flow rate and 60 ml reference pump flow rate

According to the results area of the left ventricular pressure – volume loop is getting smaller with increasing reference flow rate. In other words external work of the left ventricle is decreasing.

Also pressure–flow rate diagram of Heart Turcica Axial is shows the effect of increasing reference flow rate. Pressure – flow rate diagram of Heart Turcica Axial from of 50 ml reference pump flow rate and 60 ml reference pump flow rate are shown in Figure 5.36.

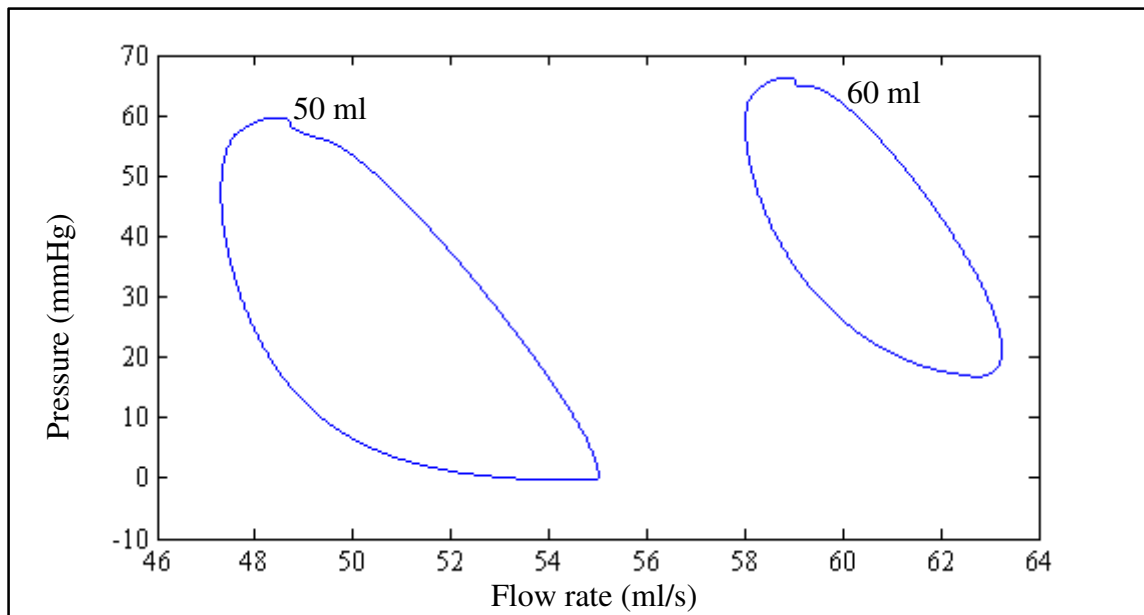


Figure 5.36. Heart Turcica Axial pressure–flow rate diagram of 50 ml reference pump flow rate and 60 ml reference pump flow rate

5.3. DISCUSSION

In order to use a heart pump bridge to recovery left ventricle must operate with heart pump. Otherwise micro thrombosis and other deleterious effects develop on the aortic valve and recovery may not be possible. As shown in the results in this section both of the proposed control strategies do not provide left ventricle operation by itself. Also in rotation speed control strategy aortic valve closes over a cardiac cycle due to high aortic pressure to provide perfusion. If a control strategy could be developed that provides flow through aortic valve in systolic phase and provides perfusion over a cardiac cycle heart pumps can be used to bridge to recovery. In this section preliminary studies have been shown in order to develop such a control strategy.

As shown in the results increasing reference pump flow rate values cause the pressure-flow rate loop area to get smaller. In other words the effect of heart on the heart pump decreases.

6. CONCLUSION AND FUTURE WORKS

In this thesis numerical modeling of human cardiovascular system and cardiovascular system assisted with two types of heart pumps are studied. Simulations were performed for the combined model of the diseased human cardiovascular system and heart pumps to assess the optimum operating intervals of the heart pumps.

Diseased human cardiovascular system model used is a dilated heart model. For the various conditions that occur in the heart disease pump operating speed interval should be adjusted accordingly. For these conditions different diseased cardiovascular system models can be developed. In other words specific models of patients can be developed to assess appropriate treatment strategies.

The following main results have been obtained from simulations of Heart Turcica Axial. In Heart Turcica axial aortic valve closes at 7565 rpm rotation speed due to relatively high aortic pressure. At the rotation speeds higher than this speed only heart pump operates. The regurgitant pump flow disappears at 9250 rpm rotation speed. Minimum operating speed is 10000 rpm for the numerical human cardiovascular system model used in this thesis. At this speed systolic aortic pressure is 89.9 mmHg and cardiac output is 4.19 l/min. Maximum operating speed is nearly 12000 rpm for Heart Turcica axial in this numerical human cardiovascular model. Rotation speeds higher than this speed causes suction effect in the left ventricle.

The following results have been obtained for Heart Turcica centrifugal V13. In Heart Turcica centrifugal V13 regurgitant pump flow disappears at 1380 rpm rotation speed. Aortic valve closes at 1638 rpm rotation speed due to relatively high aortic pressure. In other words heart and Heart Turcica centrifugal V13 operates together between these speeds. Minimum operating speed is 2140 rpm for the numerical human cardiovascular system model used in this thesis. At this speed systolic aortic pressure is 90.1 mmHg and cardiac output is 4.45 l/min. Maximum operating speed is nearly 2542 rpm for Heart Turcica centrifugal V13 in this numerical human cardiovascular model. Rotation speeds higher than this speed causes suction effect in the left ventricle.

For the modeling of Heart Turcica axial CFD analysis results were used. To obtain more accurate results, simulations have to be validated by the experimental results.

The aim of the pressure difference control strategy across the pump is to provide sufficient blood pressure and to prevent suction effect in the left ventricle. In pressure difference control strategy rotation speed of the pump is variable. Also aortic valve remains closed in this control strategy in relatively high reference pressure difference values. To avoid this condition pump flow rate is controlled. Also in pump flow rate control strategy aortic valve closure occurs in relatively high flow rate values and systolic aortic pressure does not increase above 90 mmHg.

By using a coupled model of diseased human cardiovascular system model and heart pumps, more advanced control strategies can be developed. Development of suitable control strategies will lead to widely use of heart pumps as a bridge to recovery method. Also control strategies can be developed to detect and prevent the suction effect. Development of such control strategies can be cited as the future work.

REFERENCES

1. Hosenpud, J. D. and B. H. Greenberg (editors), *Congestive Heart Failure*, Lippincott Williams & Wilkins, Philadelphia, 2006.
2. Zipes, D. P, P. Libby, R. O. Bonow and E. Braunwald, *Braunwald's Heart Disease: A Textbook of Cardiovascular Medicine*, Elsevier Saunders, Philadelphia, 2005.
3. Ferreira, A. L. S, *A Rule-Based Controller Based on Suction Detection for Rotary Blood Pumps*, Ph.D. Thesis, University of Pittsburgh, 2007.
4. Mason, D. G, A. K. Hilton and R. F. Salamosen, "*Reliable Suction Detection for Patients with Rotary Blood Pumps*", *ASAIO Journal*, Vol. 54, pp. 359-366, August 2008.
5. Chen, S. H., *Baroreflex-Based Physiological Control of a Left Ventricular Assist Device*, Ph.D. Thesis, University of Pittsburgh, 2006.
6. Shim, E. B, J. Y. Sah and C. H. Youn, "*Mathematical Modeling of Cardiovascular System Dynamics Using a Lumped Parameter Method*", *Japanese Journal of Physiology*, Vol. 54, pp. 545-553, December 2004.
7. Mauro, U, "*Interaction Between Carotid Baroregulation and the Pulsating Heart: A Mathematical Model*", *American Journal of Physiology (Heart and Circulation Physiology)*, Vol. 275, pp. 1733-1747, November 1998.
8. Mauro, U, "*A Mathematical Model of the Carotid Baroregulation in Pulsating Conditions*", *IEEE Transactions on Biomedical Engineering*, Vol. 46, pp. 382-392, April 1999.
9. Lu, K., W. Clark, F. H. Ghorbel, D. L. Ware and A. Bidani, "*A Human Cardiopulmonary System Model Applied to the Analysis of the Valsalva Maneuver*",

- American Journal of Physiology (Heart and Circulation Physiology), Vol. 281, pp, 2661-2679, December 2001.
10. Heldt, T, E. B. Shim, R. D. Kamm and R. G. Mark, "*Computational Modeling of Cardiovascular Response to Orthostatic Stress*", Journal of Applied Physiology, Vol. 92, pp. 1239-1254, March 2002.
 11. Podnar t, F. Runovc, I Milisav and M Kordas, "*Simulation of Some Short Term Control Mechanisms in Cardiovascular Physiology*", Computers in Biology and Medicine, Vol. 34, pp. 35-49, January 2004.
 12. Smith, B. W, S. Andreassen, G. M. Shaw, P. L. Jensen, S. E. Rees and J. G. Chase, "*Simulation of Cardiovascular System Diseases by Including the Autonomic Nervous System Into a Minimal Model*", Computer Methods and Programs in Biomedicine, vol. 86, pp. 153-160, May 2007.
 13. Smith, B. W, J. G. Chase, R. I. Nokes, G. M. Shaw and G. Wake, "*Minimal Haemodynamic System Model Including Ventricular Interaction and Valve Dynamics*", Medical Engineering & Physics, Vol. 26, pp. 131-139, March 2004.
 14. Ottesen, J. T. and M. Danielsen, "*Modeling Ventricular Contraction with Heart Rate Changes*", Journal of Theoretical Biology, Vol. 222, pp. 337-346. June 2003.
 15. Danielsen M. and J. T. Ottesen, "*Describing the Pumping Heart as a Pressure Source*", Journal of Theoretical Biology, Vol. 212, pp. 71-81. September 2001.
 16. Korakianitis, T. and Y. Shi, "*A Concentrated Parameter Model for the Human Cardiovascular System Including Heart Valve Dynamics and Atrioventricular Interaction*", Medical Engineering & Physics, Vol. 28, pp. 613-628, September 2006.
 17. Shi, Y, T. Korakianitis and C. Bowles, "*Numerical Simulation of Cardiovascular Dynamics with Different Types of VAD Assistance*", Journal of Biomechanics, Vol. 40, pp. 2919-2933, April 2007.

18. Li, X, J. Bai and P. He, "*Simulation Study of the Hemopump as a Cardiac Assist Device*", Medical & Biological Engineering & Computing, Vol. 40, pp. 344-353, May 2002.
19. He, P, J. Bai, X. Li, "*Optimum Control of the Hemopump as a Left Ventricular Assist Device*", Medical & Biological Engineering & Computing, Vol. 43, pp. 136-141, February 2005.
20. Bertram, C. D., "*Measurement for Implantable Rotary Blood Pumps*", Physiological Measurement, Vol. 26, pp. 99-117, August 2005.
21. Choi, S, J. R. Boston, D. Thomas and J. Antaki, "*Modeling and Identification of an Axial Flow Blood Pump*", Proceedings of the American Control Conference, Albuquerque, 4 June-6 June 1997, Vol. 6, pp. 3714-3715, IEEE, 2002.
22. Ayre, P.J. and N. H. Lovell, "*Identifying Physiologically Significant Pumping States In Implantable Rotary Blood Pumps Using Non-Invasive System Observers*", Proceedings of the 25th Annual International Conference of the IEEE EMBS, Cancun, 17 Septemeber-21 September 2003, Vol. 1, pp. 439-442, IEEE, 2004.
23. Karantonis, D. M, N. H. Lovell, P. J. Ayre, D. G. Mason and S. H. Cloherty, "*Identification and Classification of Physiologically Significant Pumping States in an Implantable Rotary Blood Pump*", Artificial Organs, Vol. 30, pp. 671-679, September 2006.
24. Karantonis, D. M, S. H. Cloherty, D. G. Mason, R. F. Salomosen, P. J. Ayre and N. H. Lovell, "*Automated Non-invasive Detection of Pumping States in an Implantable Rotary Blood Pump*", Proceedings of the 28th Annual International Conference of the IEEE EMBS, New York City, 30 August-3 September 2006, Vol. 1, pp. 5386-5389, IEEE, 2006.
25. Karantonis, D. M, N. H. Lovell, P. J. Ayre, D. G. Mason and S. H. Cloherty, "*Classification of Physiologically Significant Pumping States in Implantable Rotary*

- Blood Pump: Effects of Cardiac Rhythm Disturbances*", Artificial Organs, Vol. 31, pp. 476-479, June 2007.
26. Karantonis, D. M, D. G. Mason, R. F. Salomosen, P. J. Ayre, S. H. Cloherty and N. H. Lovell, "*Classification of Physiologically Significant Pumping States in an Implantable Rotary Blood Pump: Patient Trial Results*", ASAIO Journal, Vol. 53, pp. 617-622, October 2007.
 27. Baloa, L. A, D. Liu, J. R. Boston, M. A. Simaan and J. F. Antaki, "*Control of Rotary Heart Assist Devices*", Proceedings of the American Control Conference, Chicago, 28 June-30 June 2000, Vol. 5, pp. 2982-2986, IEEE, 2002.
 28. Choi, S, "*Suction Detection in Left Ventricular Assist System: Data fusion Approach*", International Journal of Control, Automation and Systems, Vol. 1, pp. 368-375, September 2003.
 29. Choi, S, J. R. Boston and J. F. Antaki, "*An Investigation of the Pump Operating Characteristics as a Novel Control Index foe LVAD Control*", International Journal of Control, Automation and Systems, Vol. 3, pp. 100-108, March 2005.
 30. Choi, S, J. R. Boston and J. F. Antaki, "*Hemodynamic Controller for Left Ventricular Assist Device Based on Pulsatility Ratio*", Artificial Organs, Vol. 31, pp. 1144-125, February 2007.
 31. Choi, S, J. F. Antaki, J. R. Boston and D. Thomas, "*A Sensorless Approach to Control of a Turbodynamic Left Ventricular Assist System*", IEEE Transactions on Control Systems Technology, Vol. 9, pp. 473-482, May 2001.
 32. Chen, S, J. F. Antaki, M. A. Simaan and J. R. Boston, "*Physiological Control of Left Ventricular Assist Devices Based on Gradient of Flow*", American Control Conference, Portland, 8 June-10 June 2005, Vol. 6, pp. 3829-3834, IEEE, 2005.
 33. Vollkron, M, H. Schima, L. Huber and G. Wieselthaler, "*Interaction of the*

Cardiovascular System with an Implanted Rotary Assist Device: Simulation Study with a Refined Computer Model", Artificial Organs, Vol. 26, pp. 349-359, April 2002.

34. Vollkron, M, H. Schima, L. Huber, R Benkowski, G. Morello and G. Wieselthaler, "*Development of a Suction Detection System for Axial Blood Pumps*", Artificial Organs, Vol.28, pp. 709-716, July 2004.
35. Vollkron, M, H. Schima, L. Huber, R Benkowski, G. Morello and G. Wieselthaler, "*Development of a Reliable Autonomic Speed Control System for Rotary Blood Pumps*", The Journal of Heart and Lung Transplantation, Vol. 24, pp. 1878-1885, November 2005.
36. Vollkron, M, H. Schima, L. Huber, R Benkowski, G. Morello and G. Wieselthaler, "*Advanced Suction detection for an Axial Flow Pump*", Artificial Organs, Vol. 30, pp. 665-670, September 2006.
37. Giridharan, G. A. and M. Skliar, "*Control Strategy for Maintaining Physiological Perfusion with Rotary Blood Pumps*", Artificial Organs, Vol. 27, pp. 639-648, July 2003.
38. Giridharan, G. A. and M. Skliar, "*Physiological Control of Blood Pumps Without Implantable Sensors*", American Control Conference, Portland, 4 June-6 June 2003, Vol. 1, pp. 471-476, IEEE, 2003.
39. Giridharan, G, G. Pantalos S. Koenig, K. Gillars and M. Skliar, "*Achieving Physiologic Perfusion with Ventricular Assist Device: Comparison of Control Strategies*", American Control Conference, Portland, 8 June-10 June 2005, Vol. 6, pp. 3823-3828, IEEE, 2005.
40. Oshikawa, M, K. Araki, G. Endo, H. Anai and M. Sato, "*Sensorless Controlling Method for a Continuous Flow Left Ventricular Assist Device*", Artificial Organs, Vol. 24, pp. 600-605, August 2000.

41. Ohuchi, K, D. Kikugawa, K. Takahashi, M. Uemura, M. Nakamura, T. Murakami, T. Sakamoto and S. Takatani, "*Control Strategy for Rotary Blood Pumps*", *Artificial Organs*", Vol. 25, pp. 366-370, June 2001.
42. Iijima, T, T. Inamoto, M. Nogawa and S. Takatani, "*Control of Centrifugal Blood Pump Based on the Motor Current*", *Artificial Organs*, Vol. 21, pp. 655-660, July 1997.
43. Kikugawa, D., "*Evaluation of cardiac Function During Left Ventricular Assist by a Centrifugal Blood Pump*", *Artificial Organs*, Vol. 24, pp. 632-635, August 2000.
44. Arndt, A, P. Nüsser, K. Graichen, J. Müller and Bernhard Lampe, "*Physiological Control of a Rotary Blood Pump With Selectable Therapeutic Options: Control of Pulsatility Gradient*", *Artificial Organs*, Vol. 32, pp. 761-771, October 2008.
45. Fu, M and L. Xu, "*Computer Simulation of Sensorless Fuzzy Control of a Rotary Blood Pump to Assure Normal Physiology*", *ASAIO Journal*, Vol. 46, pp. 273-278, June 2000.
46. Casas, F, A Orozco, W.A. Smith, J.A. D. Abreu-Garcia and J. Durkin, "*A Fuzzy System Cardio Pulmonary Bypass Rotary Blood Pump Controller*", *Expert System with Applications*, Vol. 26, pp. 357-361, April 2004.
47. Casas, F, N. Ahmed and A. Reeves, "*Minimal Sensor Count Approach to Fuzzy Logic Rotary Blood Pump Flow Control*", *ASAIO Journal*, Vol. 53, pp. 140-146, April 2007.
48. Klabunde, R. E., *Cardiovascular Physiology Concepts*, Lippincott Williams & Wilkins, Philadelphia, 2004.
49. Guyton, A. C. and J. E. Hall, *Textbook of Medical Physiology*, Elsevier Saunders, Philadelphia, 2006.
50. Sheffer, L, W. P. Santamore and O. Barnea, "*Cardiovascular Simulation Toolbox*",

Cardiovascular Engineering, Vol. 7, pp. 81-88, June 2007.

51. Darowski, M, C. D. Lazzari, G. Ferrari, F. Clemente and M. Guaragno, "*The Influence of Simultaneous Intra-Aortic Balloon Pumping and Mechanical Ventilation on Hemodynamic Parameters Numerical Simulation*", *Frontiers of Medical and Biological Engineering*, Vol. 9, pp. 155-174, 1999.
52. Ferreira, A, S. Chen, M. A. Simaan, J. R. Boston J. F. Antaki, "*A Nonlinear State-Space Model of a Combined Cardiovascular System and a Rotary Blood Pump*", 44th IEEE Conference on Decision and Control, Seville, 12 December-15 December 2005, Vol. 1, pp. 897-902, IEEE, 2006.
53. Lazzari, C. D, and M. Darowski, *Cardiopulmonary Mechanical Interaction Modeling and Simulation*, Institute of Biocybernetics and Biomedical Engineering Polish Academy of Sciences, Warsaw, 2002.
54. Lazzari, C. D, M. Darowski, G. Ferrari, F. Clemente and M. Guaragno, "*Computer Simulation of Haemodynamic Parameters Changes with Left Ventricle Assist Device and Mechanical Ventilation*", *Computer in Biology and Medicine*, Vol. 30, pp. 55-69, December 2000.
55. Samar, Z., *Cardiovascular Parameter Estimation Using a Computational Model*, M. Sc. Thesis, Massachusetts Institute of Technology, 2005.
56. Lazzari, C. D, M. Darowski, G. Ferrari, D. M. Pisanelli and G. Tosti, "*Modeling in the Study of Interaction of Hemopump Device and Artificial Ventilation*", *Computer in Biology and Medicine*, Vol. 36, pp. 1235-1251, November 2006.
57. Faulhaber Complementary Catalogue

REFERENCES NOT CITED

Wrong Diagnosis, Congestive Heart Failure available on web site
http://www.wrongdiagnosis.com/c/congestive_heart_failure/basics.htm, 2009